Exploring Structural and Chemical Reactivity of γ-Amino Acids in the Design of Peptide Foldamers and Small Molecule Peptidomimetics

A thesis
Submitted in partial fulfillment of the requirements
Of the degree of
Doctor of Philosophy

By

K. Veeresh

ID: 20143295

Indian Institute of Science Education and Research, Pune

Dedicated to My family and Teachers……

CERTIFICATE

This is to certify that the work incorporated in the thesis entitled "**Exploring Structural and Chemical Reactivity of γ-Amino Acids in the Design of Peptide Foldamers and Small Molecule Peptidomimetics**" submitted by **K. Veeresh** carried out by the candidate at the Indian Institute of Science Education and Research (IISER), Pune, under my supervision. The work presented here or any part of it has not been included in any other thesis submitted previously for the award of any degree or diploma from any other University or Institution.

Date: 20/11/2020

Dr. Hosahudya N. Gopi
(Research Supervisor)
Professor, IISER-Pune
Pune-411008, India

Declaration

I hereby declare that the thesis entitled "**Exploring Structural and Chemical Reactivity of γ-Amino Acids in the Design of Peptide Foldamers and Small Molecule Peptidomimetics**" submitted for the degree of Doctor of Philosophy in Chemistry at Indian Institute of Science Education and Research (IISER), Pune has not been submitted by me to any other University or Institution. This work was carried out at Indian Institute of Science Education and Research (IISER), Pune, India under the supervision of Dr. Hosahudya N. Gopi.

Date: 20/11/2020

K. Veeresh

K. Veeresh

ID: 20143295

Senior Research Fellow

Dept. of Chemistry, IISER-Pune

Pune-411008

Acknowledgment

First I would like to thank my thesis supervisor Dr. Hosahudya N. Gopi for his unconditional support throughout six years to conduct my research. He is a prolific and brilliant chemist. He is by far the hardest working person I know. His commitment to work, punctuality, motivating students and constant support at their difficult times and many more qualities I always admire at. I am fortunate to work with him.

Special thanks to Dr. D. Srinivasa Reddy and Dr. Hotha Srinivas for being my RAC committee members. Their valuable suggestions and critics always encouraged me to pursue in the right direction. I would like to acknowledge Dr. S. Raghothama from IISc, Bangalore for building the NMR structure models, Dr. N. Voyer from Laval University, Canada for ion channel activity studies and I am very much thankful to all chemistry faculties, technicians and admin staff of IISER-Pune for their numerous supports.

I am lucky to have wonderful labmates. I would extend my sincere thanks to all of them. Dr. M. Ganesh, Dr. Sandip V. Jadhav and Dr. Schitanand M. Mali, Dr. Rajkumar Misra, Dr. Sushil Benke for their support and guidance. They are very helpful from the beginning of my Ph.D and I am lucky to have such colleagues. I would like to thank all my current labmates Aninditha, Rahi Reja, Puneeth, Manjeet, Sachin, Saikath Patan, Panda Brothers (Souvik Roy, Souvik Panda), Vivek Kumar, Abhijith, Rajit, Sanjit and Nithun Raj for keeping cheerful atmosphere in the lab during my doctoral research.

From my first year, I am fortunate to have many good friends and teammates from the Alchemist cricket team. I thank all my teammates Manoharan, Vijaykanth, Algar Raja, Ravi Kumar, Shiva, Triayambak (captain), Bala, Thamarai, Dharma Raja for their continued support, help and creating a cheerful atmosphere outside the lab. We had great fun during IPL Cricket, watching movies, scientific discussions etc.

I would also like to express my deepest gratitude to my family. My family has been encouraging, supportive and shown belief in me and my work. Without them I wouldn't have a chance to be at IISER-Pune. My Brother Kuruva Beerappa is a role model in life. He took all my responsibilities and sacrificed a lot to support me and my younger brothers and sisters. Without him my PhD wouldn't have been possible. I never forget their support in my lifetime.

K. Veeresh

Contents

Chapter 4: Design of β-Sheet Mimetic and β-Double Helix from (*E*)-Vinylogous Amino Acid Oligomers

Chapter 5: Design of Crown Ether Embedded γαα-Hybrid Peptide Foldamer Ion Channels

Abbreviations

Ac_2O = Acetic anhydride

ACN = Acetonitrile

AcOH = Acetic acid

Aib = α-Amino isobutyric acid

aq. = Aqueous

Bn = Benzyl

Boc = tert-Butoxycarbonyl

$(Boc)_2O$ = Boc anhydride

^tBu = tertiary Butyl

Calcd. = Calculated

Cbz = Bezyloxycarbonyl

Cbz-Cl = Benzyl chloroformate

CCDC no. = Cambridge Crystallographic Data Centre number

CD = Circular Dichroism

COSY = **CO**rrelation **S**pectroscop**Y**

CIF = Crystallographic Information File

dγ = dehydro gamma

dr = Diastereomeric ratio

DBU = 1,8-Diazabicyclo[5.4.0]undec-7-ene

DCC = N, N' –Dicyclohexylcarbodiimide

DCM = Dichloromethane

DiPEA = Diisopropylethyl Amine

DMAP = 4-Dimethylaminopyridine

DMF = Dimethylformamide

DMSO = Dimethylsulfoxide

EtOH = Ethanol

Et = Ethyl

EtOAc = Ethyl acetate

Fmoc = 9-Fluorenylmethoxycarbonyl

Fmoc-OSu = N-(9-Fluorenylmethoxycarbonyloxy) succinimide

g = gram

h = hours

HBTU = 2-(1H-benzotriazol-1-yl)-1, 1, 3, 3-tetramethyluronium hexafluorophosphate

H-bond = Hydrogen bond

HOBt = Hydroxybenzotriazole

HCl = Hydrochloric acid

IR = Infrared spectroscopy

IBX = 2-Idoxybenzoic acid

LAH = Lithium Aluminium Hydride

M = Molar

MALDI-TOF/TOF = Matrix-Assisted Laser Desorption/Ionization-Time of Flight

MBHA = Methyl bezydrylamine

Me = Methyl

MeOH = Methanol

mg = Milligram

min = Minutes

µL = Micro liter

mL = Milliliter

mM = Millimolar

mmol = millimoles

m.p = Melting Point

MS = Mass Spectroscopy

N = Normal

NHS = N-hydroxy succinimide

NMP = N-methyl pyrrolidone

NMR = Nuclear Magnetic Resonance

NOE = Nuclear Overhauser Effect

ORTEP = Oak Ridge Thermal-Ellipsoid Plot Program

PG = Protecting Group

ppm = Parts per million

Py = Pyridine

R_f = Retention factor

R_t = Retention time

ROESY = **R**otating-frame nuclear **O**verhauser **E**ffect correlation **S**pectroscop**Y**

RP- HPLC = Reversed Phase-High Performance Liquid Chromatography

RT = Room Temperature

TFA = Trifluoroacetic acid

THF = Tetrahydrofuran

UV = Ultraviolet–Visible Spectroscopy

TOCSY = **TO**tal **C**orrelation **S**pectroscop**Y**

*Z*dγ = Z-dehydro gamma

Abstract

The progress in the field of foldamers constructed from the unnatural amino acid building blocks revealed that the folding phenomenon is not restricted to proteins. The advancement in the foldamer research has opened doors to various remarkable structures available to the oligomers of non-natural amino acids. Perhaps, β-and γ-peptides are among the most extensively studied unnatural oligomers. In addition to the various types of synthetic unnatural γ-amino acids, a variety of backbone functionalized, relatively unexplored γ-amino acids have been frequently found in many biologically active peptide natural products. In our previous studies, we have shown the utility of naturally occurring *E*-vinylogous γ-amino acids in the design of β-hairpins, β-double helices, β-meanders, and multi-stranded β-sheets. In the present study, we have examined the conformational properties and chemical reactivity of α,β-unsaturated γ-amino acids and their utility in the design of novel peptide foldamers, small molecule peptidomimetics and β-double helices. We have demonstrated the direct transformation of unusual planar α,γ-hybrid peptides composed of alternating α- and *E*-vinylogous γ-amino acids into 12-helical structures through a base mediated α,β→β,γ double bond migration. Further, we have shown the transformation of *E*-vinylogous amino amides into new γ-lactams through a molecular rearrangement involving consecutive multiple double bond migrations. Moreover, we have examined the impact of dialkyl substituents (Thorpe–Ingold effect) in the design of β-sheet mimetics versus β-double helices from the homo-oligomers of *E*-vinylogous γ-amino acids. In addition to the geometrically constrained γ-amino acids, we have also examined conformations of saturated γ-amino acids in α,γ-hybrid peptide sequences. We have designed and studied the conformations of γαα-hybrid peptides embedded with crown-ethers and studied their ion transporting activities. Overall, the chemistry and conformational properties of unsaturated γ-amino acids reported here open wide opportunities to further explore them as building blocks for the foldamers design as well as templates to perform various organic reactions on peptides.

List of publications

1. Veeresh, K.; Gopi. H. N. Design of Helical Peptide Foldamers through α,β → β,γ Double-Bond Migration. *Org. Lett.* **2019,** *21*, 4500.
2. Veeresh, K.; Ganesh Kumar, M.; Nalawade, S.; Nithun, R. V.; Gopi. H. N. Direct Transformation of N-Protected α,β-Unsaturated γ-Amino Amides into γ-Lactams through a Base-Mediated Molecular Rearrangement. *J. Org. Chem.* **2019,** *84*, 15145.
3. Veeresh, K.; Singh, M.; Gopi. H. N. Impact of substituent effects on the design of β-sheet mimetics and β-double helices from (*E*)-vinylogous γ-amino acid oligomers. *Org. Biomol. Chem.* **2019,** *17*, 9226.
4. Veeresh, K.; Otis, F.; George, G.; Krishnamurthy, K.; Raghothama, S.; Voyerand, N.; Gopi. H. N.; Crown Ethers embedded γαα-hybrid peptide ion channel foldamers. *Manuscript submitted* **2020**.
5. Misra, R.; Saseendran, A.; George, G.; Veeresh, K.; Raja, K. M. P.; Raghothama, S.; Hofmann, H. J.; Gopi. H. N. Structural Dimorphismof Achiral α,γ-Hybrid Peptide Foldamers: Coexistence of 12- and 15/17-Helices. *Chem. Eur. J.* **2017,** *23*, 3764.
6. Ganesh Kumar, M.; Thombare, V. J.; Katariya, M. M.; Veeresh, K.; Raja, K. M. P.; Gopi, H. N. Non-classical Helices with *cis* Carbon–Carbon Double Bonds in the Backbone: Structural Features of α,γ-Hybrid Peptide Foldamers. *Angew. Chem. Int. Ed*. **2016**, *55*, 7847.
7. Singh, M.; Veeresh, K.; Gopi. H. N. Lactamisation of Vinylogous amino acids via active esters. *Manuscript under Preparation* **2020.**

CHAPTER 1

Introduction to Protein Secondary Structures and Their Mimics

1. Introduction

All the living organisms majorly contain four different biomolecules in their composition, namely nucleic acids, lipids, carbohydrates, and proteins. Proteins are the polymers of standard L-amino acids. In proteins, amino acids are connected with each other through peptide bonds, hence the proteins are also called polypeptides. By different permutation and combination of about 20 different L-amino acids and by varying length of the polypeptide chain, living organisms brings a diversity into proteins three-dimensional structures to perform variety of biological functions, such as enzyme catalysis, transport of molecules, cell signaling, energy source, muscle contraction, host defense against infections and etc.[1] Three-dimensional structure is an essential requirement for the biological function of protein. Often protein misfolding to other conformation leads misfolding diseases such as Marfan syndrome, Creutzfeldt–Jakob disease and other prion diseases, Alzheimer's disease, Parkinson's disease, amyloidosis, cystic fibrosis, type II diabetes, Gaucher's disease and wide range of other disorders.[2] To understand the protein function and therapeutic approaches for the diseases associated with proteins, understanding the native three-dimensional structure of proteins is an essential requirement.

1.1. Protein structure

Protein's three-dimensional structure is very complex. The protein structure can be divided into four different levels namely 1) Primary 2) Secondary 3) Tertiary and 4) Quaternary structure. The four different levels of protein structures are schematically represented in Figure **1**.

1) Primary structure: The primary structure gives information about the linear sequence of amino acids present in the polypeptide chain. The sequence of amino acids is represented with a single letter code of amino acids. These polypeptide chains spontaneously fold into three-dimensional secondary structures.

2) Secondary structure: Proteins majorly fold into three different secondary conformations namely i) helices, ii) β-sheets and iii) reverse turns. In the seminal work done by Linus Pauling and colleagues first described the structures of α-helix and β-sheet. These secondary structures are identified by the definite hydrogen bonding pattern between the *NH* and *CO* groups of the polypeptide chain. In protein structures, different secondary structural elements connect with

each other by loops of various lengths. The loops connecting two adjacent anti-parallel β-strands in protein structure are called reverse turn.

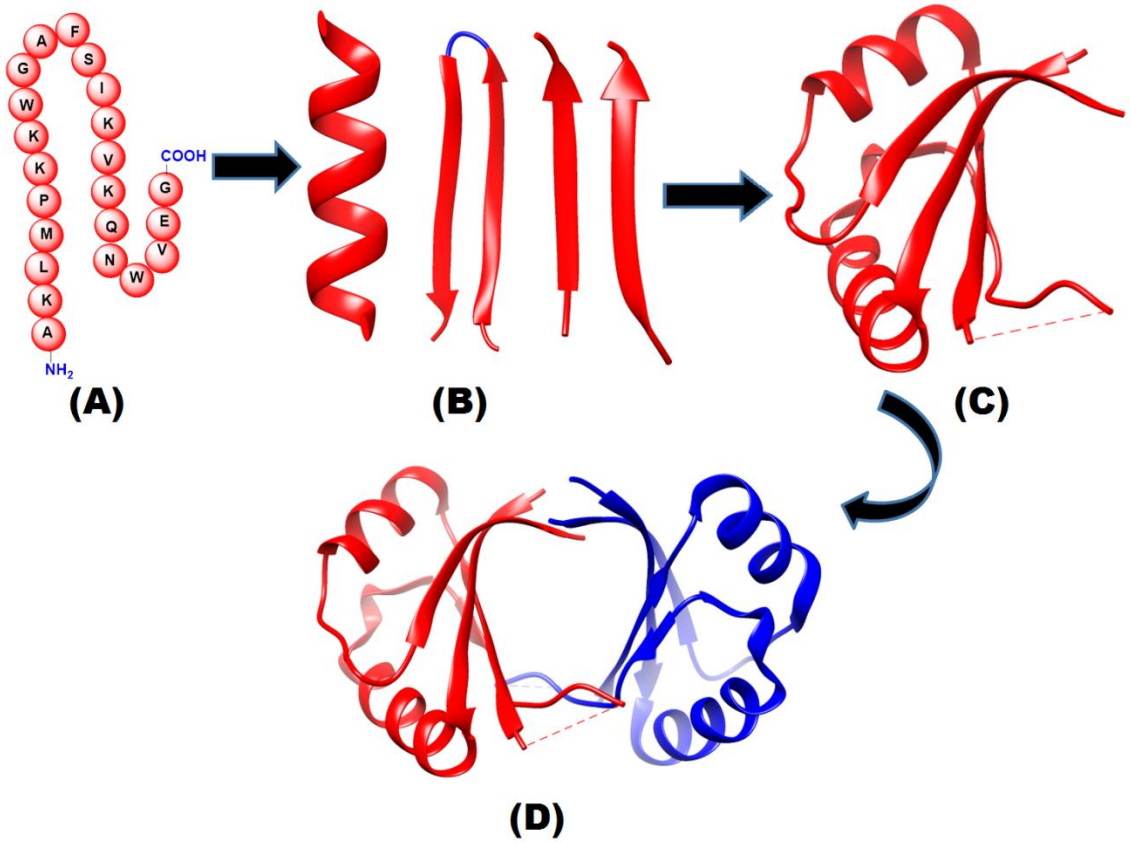

Figure 1: Schematic representation of the structural organization of protein in four different levels (A) Primary structure (B) Secondary structures (C) Tertiary structures (D) Quaternary structure

In the year 1963, G. N. Ramachandran and colleagues[3] developed a [ϕ, ψ] plot (Ramachandran plot or Ramachandran diagram) to visualize the stereochemically allowed dihedral angles ψ against ϕ of amino acids in the secondary structures of polypeptides. Dihedral angles ψ and ϕ of amino acids in the polypeptide backbone are depicted in Figure **2A**. and the Ramachandran plot for different protein secondary structures are shown in Figure **2C**. Brief descriptions regarding secondary structures are given below.

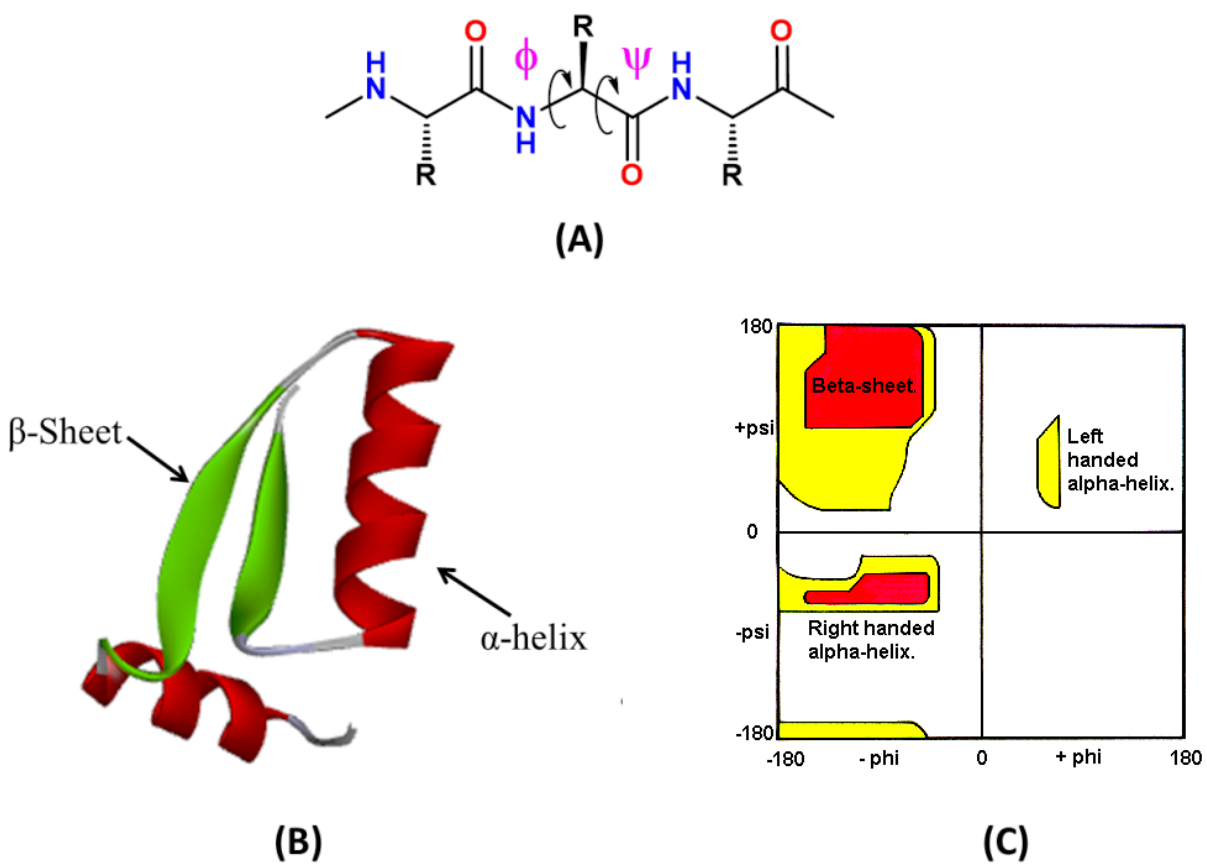

Figure 2: (A) Torsional angles ϕ and ψ on peptide backbone, (B) Secondary structural elements of protein shown in ribbon model (PDB ID: 1H75) and (C) Ramachandran plot, showing the torsional angles of different secondary structures.

i) Helices: Helices are one of the major secondary structures of proteins. The main stabilizing energy of these helical structures comes from the intermolecular hydrogen bonding formed between *CO* and *NH* groups of polypeptide backbone (CO⋯⋯HN). Based on the number atoms in the hydrogen-bonded pseudo-cycle and the number of residues per helical turn, these helical structures are classified into 2.2_7-helix (or γ-helix), 3.0_{10}, 3.6_{13} (or α-helix) and 4.4_{16}-helix (or π-helix). α-Helix is the most common secondary structure found in proteins and predominant over all other types of secondary structures. The structure of α-helix was proposed in 1951 by Linus Pauling.[4] α-helix is right-handed screw-like structure (right-handedness and left-handedness are symbolized by (*P*) and (*M*), respectively) which is stabilized by 13-membered intramolecular hydrogen bond pseudo-cycles (i.e., contains 13-atoms in a hydrogen bond cycle and also called as C_{13}-hydrogen bonding) and contains 3.6 amino acid residues per helical turn. These C_{13}-

hydrogen bonds involve the *CO* group of *i* amino acid and the *NH* group of (*i+4*) amino acid (*i*←*i+4*) of the polypeptide backbone. Generally, α-helix is represented as 3.6_{13}-(*P*)-helix and the average torsion angles ϕ and ψ values of peptide backbone -60° and -45°, respectively fall in left down quadrant of the Ramachandran plot. Unlike α-helical structures, 3.0_{10}-helical structures (or 3.0_{10}-(*P*)-helix) are not common in proteins. The 3.0_{10}-helical structures are stabilized by 10-membered hydrogen bonding pseudo-cycles which involves the *CO* group of *i* amino acid and *NH* group of (*i+3*) amino acids (*i*←*i+3*) of polypeptide backbone and contains 3 amino acid residues per helical turn. The average torsion values ϕ and ψ are -49° and -26°, respectively. Similarly, π-helix is symbolized as 4.4_{16}-(*P*)-helix (ϕ = -55°, ψ = -70°) and γ-helix as 2.2_{7}-helix (ϕ = -70°, ψ = 70°). The hydrogen-bonding pattern of all the helical structures are is schematically represented in Scheme **1**.

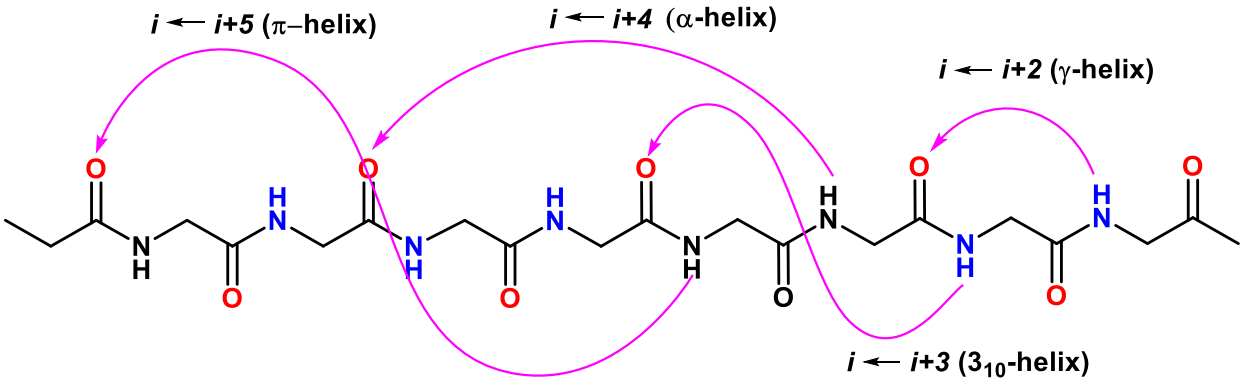

Scheme 1: Schematic representation of the hydrogen bonding pattern in different helices of proteins.

ii) β-Sheets or β-pleated sheets: β-Sheets are the second majorly found structural elements found in proteins after the helices. These structures are the extended conformations of polypeptide chains with all the peptide bonds in the same plane. The extended β-sheet structure was proposed in 1930 by William Astbury. However, the precised version of the β-sheet structure was reported by Linus Pauling and Robert Corey in 1951.[5] The *C=O* and *N-H* groups of the backbone are oriented in the perpendicular direction to the chain axis and therefore are available to participate in *inter*-strand hydrogen-bonding with neighboring protein chains. Based on the directionality of polypeptide chains arranged in β-pleated sheets, they are classified into (i) parallel β-sheets, in which the neighboring chains are arranged in a parallel manner and (ii)

anti-parallel β-sheets, in which the neighboring chains are arranged in an anti-parallel manner connected by hydrogen-bonds. The structures of parallel and anti-parallel sheets are schematically represented in Scheme **2**. Parallel β-sheets usually adopts less extended structures (ϕ = -119°, ψ = 113°), whereas anti-parallel β-sheets adapts greater extended structures (ϕ = -135°, ψ = 139°). The torsion values of both the parallel and anti-parallel β-sheets fall in the upper left quadrant of the Ramachandran plot.

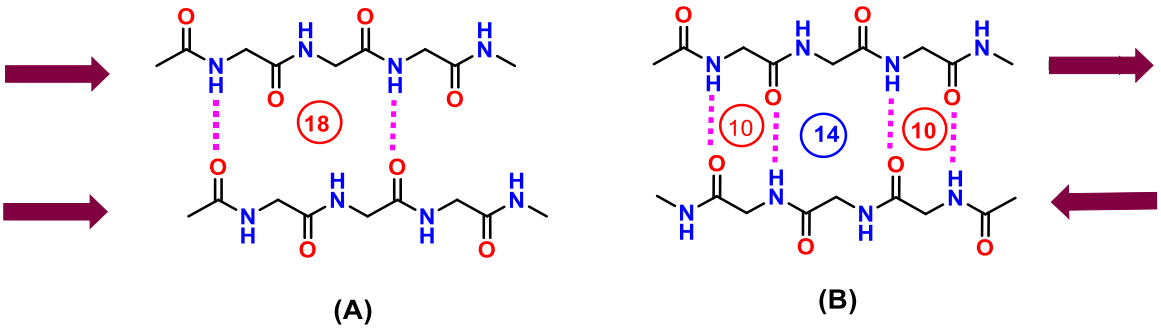

Scheme 2: Showing the hydrogen bonding pattern and directionality of polypeptides chains in β-sheet structures, **(A)** Parallel β-sheets and **(B)** Anti-parallel β-sheets.

iii) Reverse turns: Reverse turns are a type of secondary structure that causes a change in the direction of the polypeptide chain. Based on the number of residues involved in the reverse turn of the polypeptide chain, reverse turns are classified into γ-turn (3 amino acid residues), β-turn (4 amino acid residues), α-turn (5 amino acid residues) and π-turn (6 amino acid residues). Among all the reverse turns β-turns are predominantly found in protein structures. Based on the ϕ and ψ angles of middle two residues (i.e., *i+1* and *i+2*) residues, β-turns are further divided into type I, II and III and their mirror images as type I', II' and III' turns respectively.[6]

3) Tertiary structures: Tertiary structure is the complete three-dimensional folding of the polypeptide chain. All the secondary elements (helix, sheets, and turns) of the polypeptide with the help of unstructured loops folds into compact and energy minimized three-dimensional structures. The folding of the tertiary structure is driven by different electrostatic interactions such as π-π stacking, ionic interactions, and hydrophobic interactions.

4) Quaternary structure: Only proteins containing multiple polypeptides chains (multi-subunit proteins) will have a quaternary structure. In multi-subunit proteins, an individual tertiary

structure of polypeptide chains come close to each other and bind with electrostatic interaction to form a quaternary structure.

1.2. Mimics of protein secondary structures

In order to understand the structure and function of protein, many chemists used different types of non-natural building blocks to mimic the protein structure. Mimicking the protein secondary structure with abiotic oligomers gives the opportunity to develop functional macromolecules and to transcend nature by developing the molecules with superior biological activity. These abiotic oligomers can offer novel structures with greater affinity as biological ligands in protein-protein interaction inhibition, improved enzymatic and thermodynamic stable as well.

In this context, a variety of abiotic amino acids (unnatural amino acids) and organic templates have been explored as building blocks in the construction of protein secondary structures. Among the structures of various abiotic amino acids and organic templates, oligomers of β- and γ-amino acid are the most widely studied.[7]

1.2.1. Foldamers of β-amino acid

β-Amino acids are homologated species of naturally occurring α-amino acids. Oligomers constructed from β-amino acids are called β-peptides. Homologation of α-amino acid generates an extra methylene group in between amine and carboxyl groups of α-amino acids. These extra methylene group of β-amino acids gives an additional torsional angle θ, along with the Φ and Ψ of α-amino acids. The torsional variables of β-amino acids are shown in Scheme **3**. Depending on the position of the side chain, β-amino acids are classified as β^3- and β^2-amino acids. Some of the different β-amino acids reported in the literature are shown in Scheme **3**. In comparison to α-peptides, *β*-peptides and higher homologue oligomers were proved to have greater proteolytic stability and greater half-life time *in vivo* conditions.[8] The proteolytic stability of *β*-oligomers and higher homologue oligomers makes them attractive towards peptide-based drug discovery research. From the past two decades, β-peptides are emerging as promising tools in the construction of protein secondary structure mimetics.

In the year 1996, Seebach introduced chiral acyclic β-peptides and investigated the conformational properties and enzymatic stability.[9] In the same time period, Gellman and coworkers introduced cyclically constrained β-amino acids ACHC and ACPC with definite stereochemistry.[10] In addition, Sharma *et al.* extensively investigated the structures of β-peptide oligomers generated from carbo-β-amino acids.[11] Reiser and colleagues designated novel β-peptide structures using the cyclic β-amino acids.[12] Further, Fulop *et al.*[13] and Aitken *et al.*[14] introduced different cyclic β-amino acids to the design of β-peptide secondary structures.

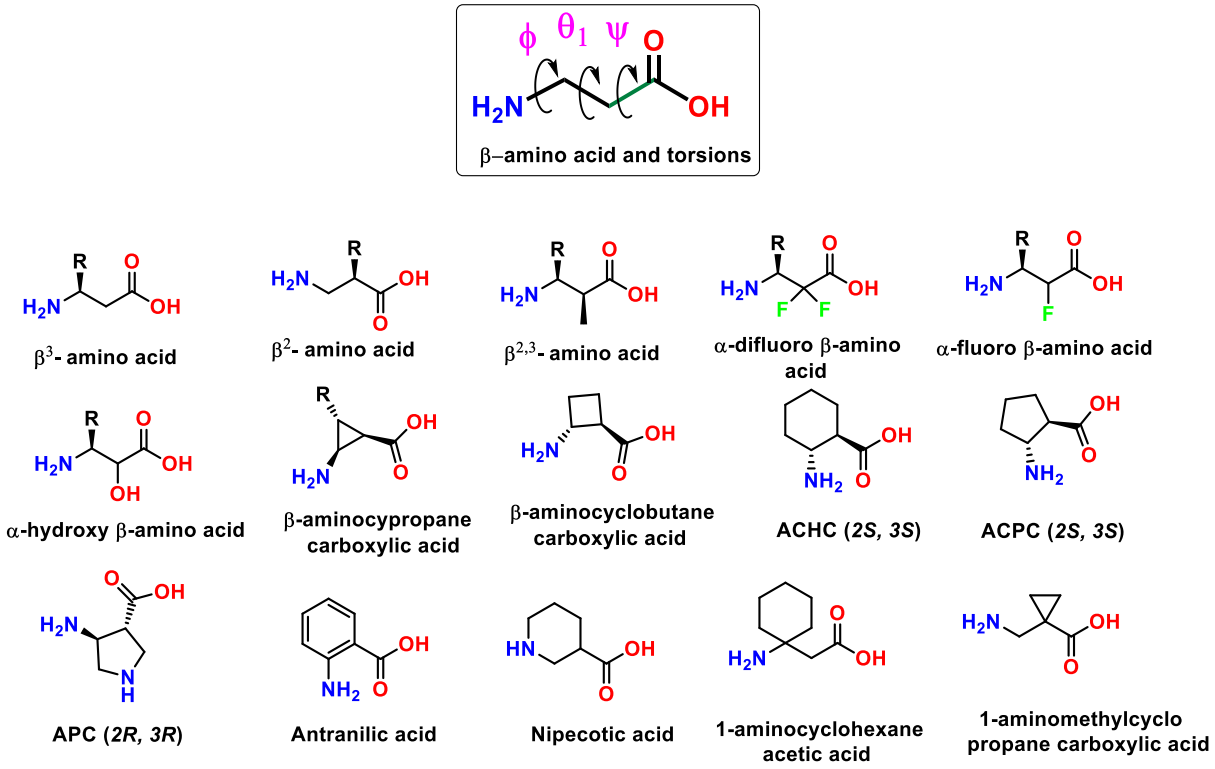

Scheme 3: General structure along with torsional variables of β-amino acid is showed and the structures of different β-amino acids used in the design of foldamers are given.

Similar to α-amino acid sequences, β-amino acid sequences also folds into well-organized secondary structures, such as sheets, turns, and helices, but secondary structures formed by β-peptide and higher homologue peptides completely differ from the secondary structures of α-peptides. Based on the hydrogen bonding pattern the helical structures produced by the β-peptides are classified as C_{14}-, C_{12}-, C_{10}- and C_8-helices.[15-17] These β-peptide helical structures differ from each other not only in hydrogen-bonding pattern also in their polarities

with respect to their *C* and *N*-termini. The C_8- and C_{12}-helices have a hydrogen bond direction (C←N), which is the same as that observed in α-peptides, whereas in the C_{10}- and C_{14}-helical structures the hydrogen bond directions (N←C) are reversed. The β-peptides helical folding patterns can be controlled by manipulating the substitution pattern on the β-amino-acids. The β-amino acid residues with a single side chain at β-position (β^3-residues) tend to adopt 14-helical structures.[9] Constrained β-amino acids, such as *trans*-2-aminocyclohexanecarboxylic acid (ACHC) displayed a much stronger 14-helical structure when compared β^3-residues.[10] The homooligomers of β-amino acids with a five-membered ring (ACPC) and four-membered ring (β-amino cyclobutane carboxylic acid) folded into 12-helix secondary structures.[11] The helical structures of β-peptides are shown in Figure **3**. The structural diversity of the helices increases upon progressing from α- to β- to γ-peptides.

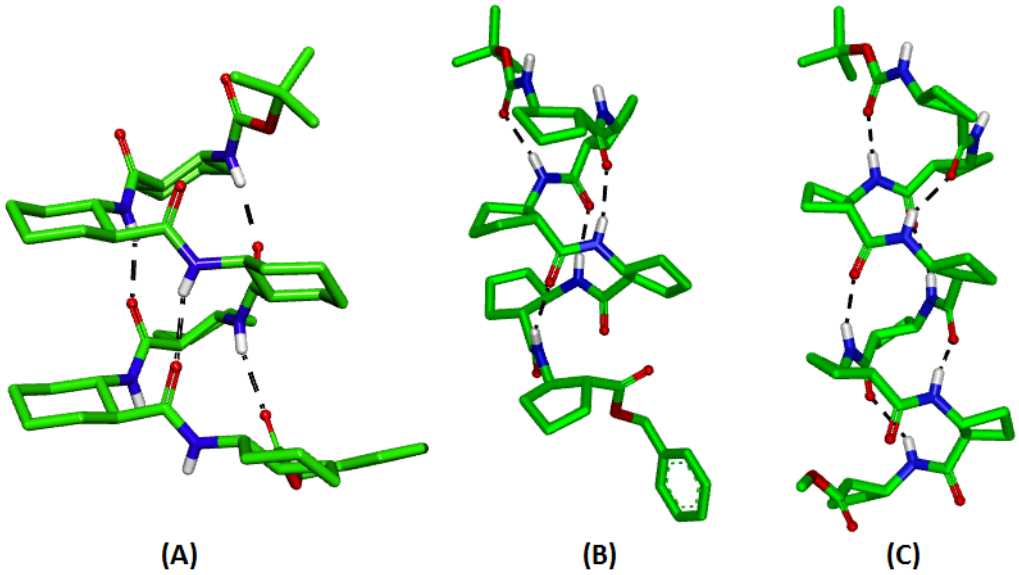

Figure 3: Helical conformation of β-peptides, (A) 14-helix formed from the *trans*-ACHA β-amino acid, (B) 12-helix formed from *trans*-ACPC β-amino acid (C) 12-helix formed from cyclobutane β-amino acid

In their initial attempt, Balaram and colleagues developed the hybrid peptide structures by inserting β-amino acids and higher homologous amino acids into α-peptide helices and β-hairpin structures.[18a, 18b] The concept of hybrid peptides was further explored by others.[18c-18f] The hybrid peptides composed of α- and other β- and γ-amino acids displayed various different

hydrogen-bonded helical structures compared to the homooligomers of β- and γ-amino acids. Using the concept of hybrid peptides it is possible to design a variety of helical structures by simply varying the patterns of amino acid sequence.

Gellman and co-workers studied the conformations of shorter peptide sequences of α, β-hybrid peptides containing constrained *trans*-ACPC amino acids (*trans*-2-aminocyclopentane carboxylic acid and its derivatives), and proved their folding ability to form both C_{11}-helix and $C_{14/15}$-helical structures.[19a, 19b] Further, Amblard *et al*. studied the conformations of tri-substituted β-amino acid ((S)-ABOC) containing α,β-hybrids and proved that the shorter sequences adopt $C_{9/11}$-helical conformation in solid state and longer sequences tend to adopts $C_{18/16}$-helical conformation in solid-state.[19c] In addition, Gellman and co-workers established the $C_{11/11/12}$ and $C_{10/11/11}$-helical conformations of 1:2 and 2:1 α,β-hybrid peptides, respectively.[19d] Fulop and colleagues studied the stereochemical patternings in α,β-hybrid peptides, which lead to a new helical structures.[19e] Consistent results have also been obtained from the studies of Sharma and co-workers.[19f-19i] In addition to these secondary structural mimetics, Gellman and co-workers reported helix bundle quaternary structures in hybrid α/β-peptide foldamers.[19j,19k]

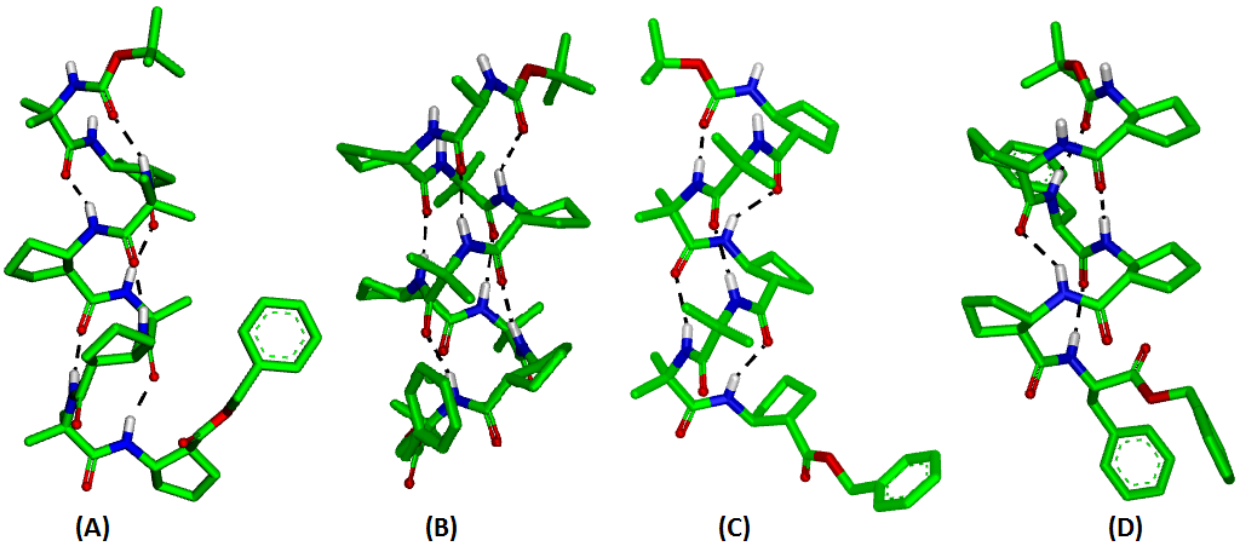

Figure 4: α,β-Hybrid peptide helical structures (A) 11-helical structure of α,β-hybrid peptide constructed from Aib and ACPC amino acids (B) 14/15-helical structure of α,β-hybrid peptide constructed from Ala, ACPC and Aib amino acids (C) 12/11/11 helical structure of 1:2, α/β-hybrid peptides (D) 10/11/11 helical structure of 2:1 α/β-hybrid peptide.

1.2.2. Biological activity of β-peptide foldamers

As these hybrid peptides offer greater biological stability over the natural peptides, the conformational properties of these foldamers have been exploited in the design of biologically active sequences such as antimicrobials,[20] cancer-cell growth inhibitors,[21] human somatostatin hormone analogs,[22] p53-hDM2 protein-protein interaction inhibitors,[23] protein binding ligands for HIV-gp41,[24] human cytomegalovirus (HCMV) fusion inhibitors[25]etc. Nylon-3, a β-amino acid polymer displayed selective and potent activity against planktonic forms of different fungal species.[26a] In addition, these peptides also showed good inhibitory profile against biofilm formation of *Candida Albicans*.[26b]

1.2.3. Foldamers of γ-amino acid

Double homologation of α-amino acid produces γ-amino acids. The structures of different γ-amino acids are shown in Scheme **4**. Double homologation inserts two additional $–CH_2–$ groups between the amine and carboxyl group of α-amino acid. The two additional torsional variables introduced by these two methylene groups are defined by θ_1 and θ_2 along with regular ϕ and ψ of α-amino acid. Unlike β-amino acids, foldamers of γ-amino acids are not much explored, it may be due to the difficulties in the synthesis of enantiopure γ-amino acid monomers.

However, in the year 1998, Seebach and Hanessian groups independently reported the 14-helical conformations of homooligomers of mono-substituted γ^4-amino acids and di-substituted $\gamma^{2,4}$-amino acids in the solution state.[27,28] Later on Seebach and colleagues reported crystal evidence for the 14-helical conformation of γ-homooligomers using tri-substituted $\gamma^{2,3,4}$-amino acids.[29] Further, Hofmann and colleagues performed ab initio MO theory calculations on oligomers of unsubstituted γ-amino acids and mono-substituted (methyl substitution on α, β or γ) γ-amino acids. They predicted the folding propensity γ-amino acids oligomers into 14-helical and 9-helical conformations.[30] As predicted by Hofmann, 9-helical conformation was observed in the oligomers of symmetrically β, β-disubstituted γ-amino acid gabapentin (Gpn).[31] The helical structures of γ-peptides are shown in Figure **5**.

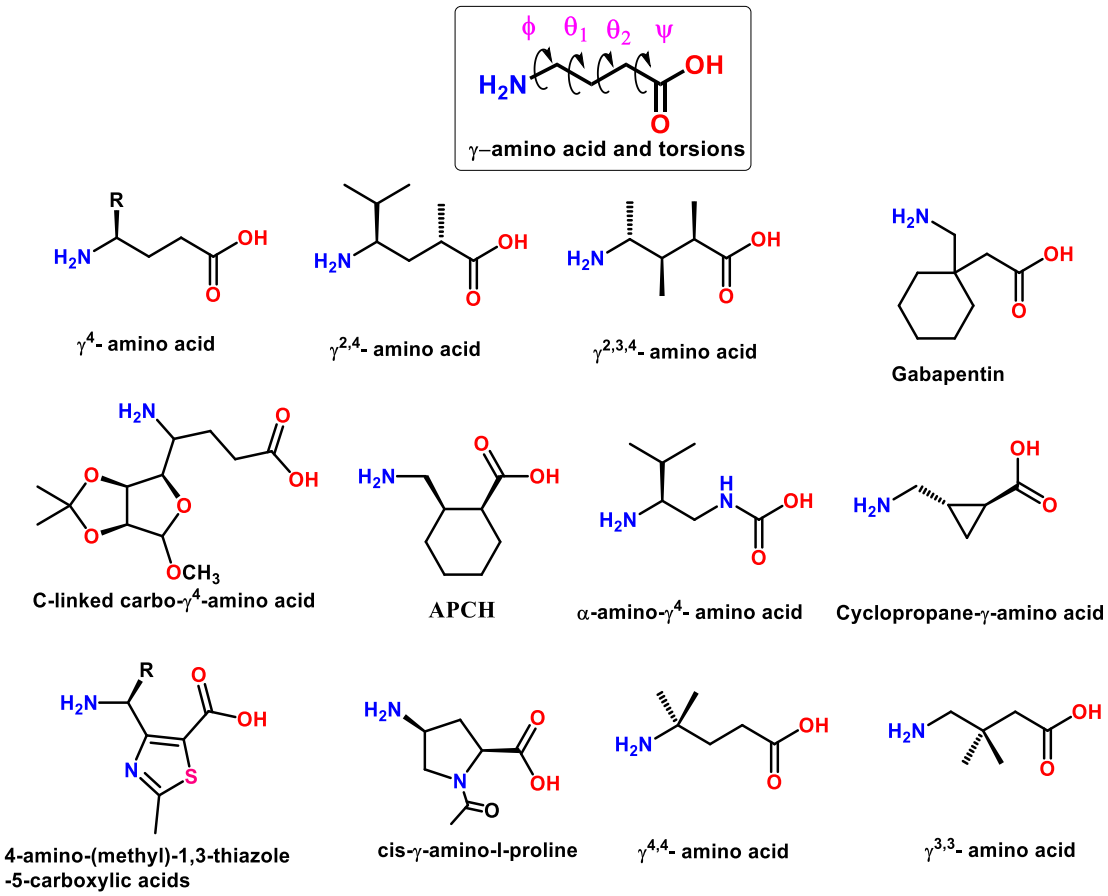

Scheme 4: The list of different γ-amino acids utilized in the design foldamers and the torsional variables of γ- amino acid are depicted.

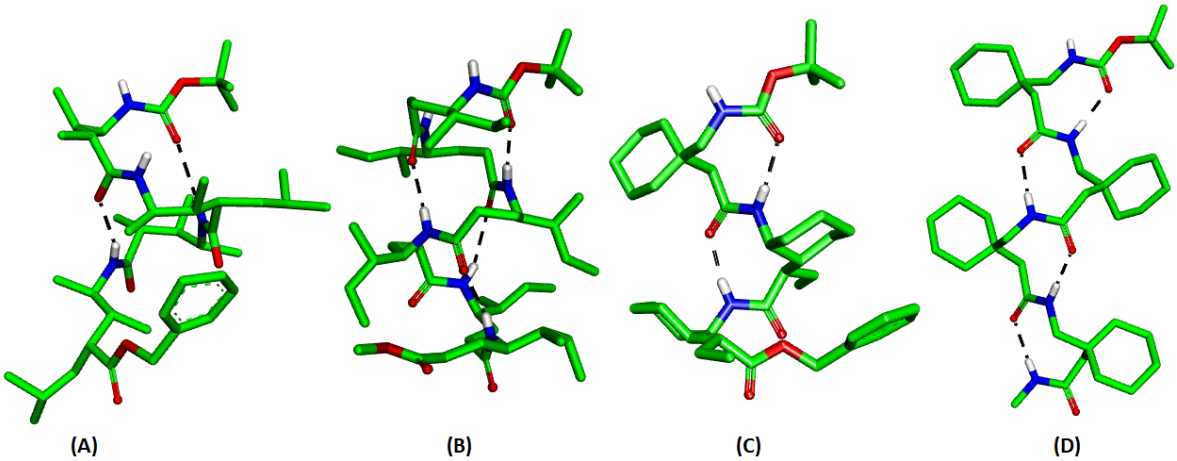

Figure 5: Helical structures of γ-amino acid homooligomers (A) C_{14}-helix of $\gamma^{2,3,4}$-amino acid homooligomer (B) C_{14}-helix of γ^{4}-amino acid homooligomer (C) C_{14}-helix of cyclic constrained γ-amino acid homooligomer (D) C_{9}-helix of gabapentin homooligomer.

Further, the α,γ-hybrid peptides composed of gabapentin displayed 12-helical and a combination of 12 and 10 H-bonding helical conformations.[32] In continuation, Sharma and colleagues reported the conformations of γ-peptides derived from dipeptide repeats with alternating C-linked carbo-γ^4-amino acids and γ-aminobutyric acid. These peptides have proved to adopt a left-handed helical conformation in $CDCl_3$ solvent.[33] Further, using cyclically constrained γ-amino acid Gellman and colleagues reported a verity of helical conformations from the single crystals and solution state studies.[34] Further, using $\gamma^{2,3}$-cyclopropane amino acids Smith and colleagues reported extended sheet conformations of γ-peptides with bifurcated hydrogen-bonding pattern.[35] Guichard and colleagues introduced a new class of *N*, *N*′-linked oligourea (γ-peptide lineage) γ-peptides, where they replaced α-carbon (C) atom of γ-amino acid with nitrogen (N) atom and designed a variety of oligourea peptidomimetics.[36] Single crystals conformational analysis of the oligourea peptides revealed that they adopted 14-helical conformations. Further, Royo and co-workers synthesized *cis*-γ-amino-L-proline containing γ-peptides and postulated C_9-ribbon structure in H_2O on the basis of NOE connectivities.[37] Recently, Millard and colleagues introduced thiazole ring containing constrained γ-amino acid to design homooligomers and studied their conformational properties. The results showed that these homooligomers adopt a well-defined 9-helix structure in solution, as well as in solid-state.[38] We have recently reported the coexistence of 12-helix and 15/17-helical structure of α,γ-hybrid nonapeptide composed of alternative 4-aminoisocaproic acid (Aic, doubly homologated Aib) and α-aminoisobutyric acid (Aib). Surprisingly the shorter versions of these peptides (tetra and hepta) showed only 12-helical conformations.[39] The structures of γ-amino acids developed in the design of foldamers are shown in Scheme **4**. The helical structures obtained from various γ-amino acids are shown in Figure **6**.

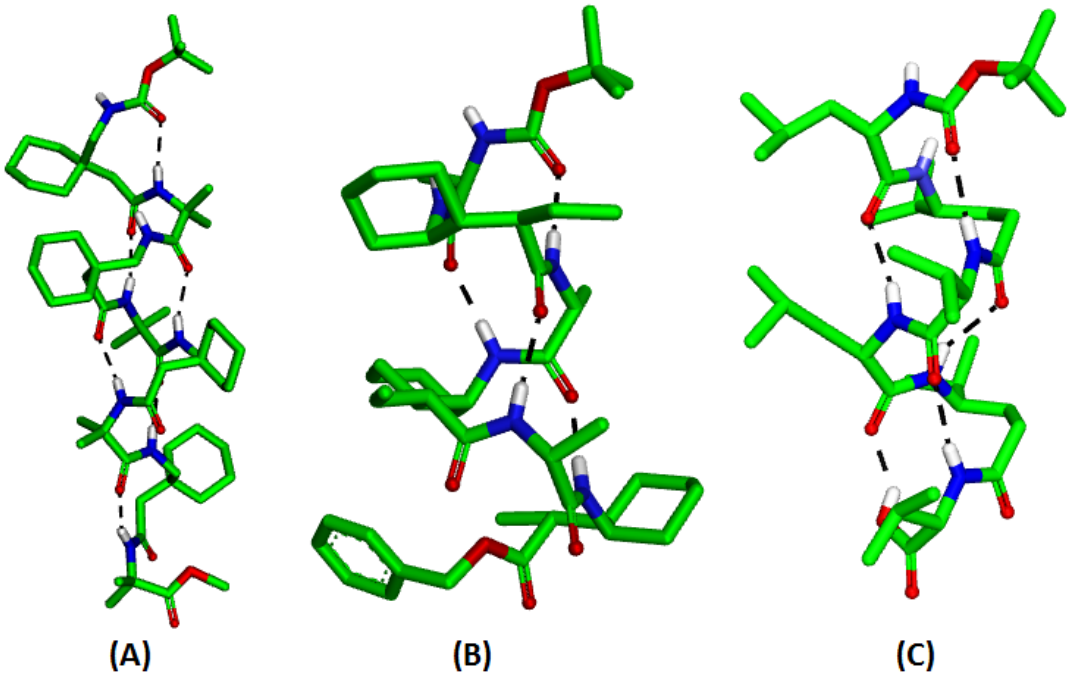

Figure 6: Helical structures of α,γ -hybrid peptides (A) 12-helical structure of α,γ-hybrid peptide composed of Aib and Gpn amino acids (B) 12-helical structure of α,γ-hybrid peptide composed of Ala, and EtACHA amino acids (C) 10/12 helical structures of α,γ,α-hybrid peptide composed of Leu and γ-Val.

1.2.4. Foldamers of α,β-unsaturated γ-amino acids

α,β-Unsaturated γ-amino acids (vinylogous amino acids) are non-ribosomal amino acids found in many natural peptide products like Cyclotheonamides (A, B, C, D, E) which are potent inhibitors for serine protease and bovine β-trypsin,[40] Luminmycins (A, B, C) which are active proteasome inhibitors, Gallinamide A which is an anti-malarial agents,[41] and Miraziridine A which acts as inhibitors for variety of proteases like trypsin-like protease, papain-like cysteine protease, and pepsin-like aspartyl protease.[42] The structures of these natural peptide products are shown in Scheme **5**. Inspired by the excellent biological activity and of these vinylogous amino acid containing peptides many synthetic chemists designed vinylogous amino acid based peptide inhibitors for serine and cysteine proteases. The structures of these inhibitors are shown in Scheme **6**.[43]

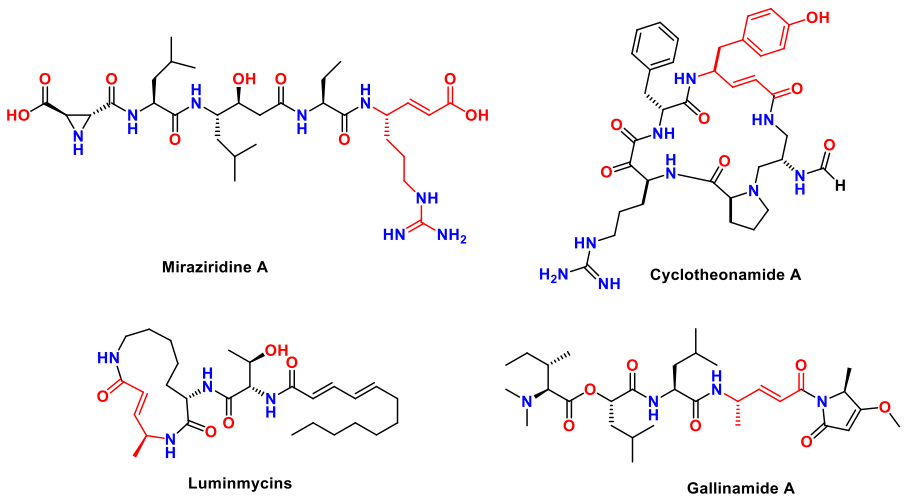

Scheme 5: Chemical structures of naturally available cyclic and linear peptides containing α,β-unsaturated γ-amino acid.

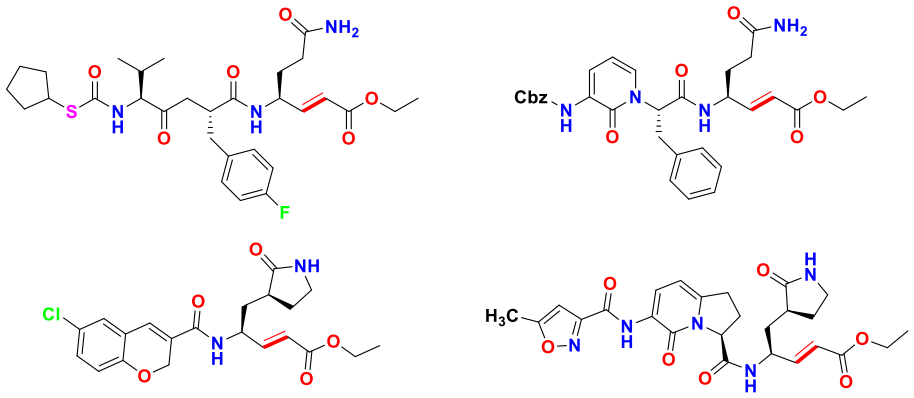

Scheme 6: α,β-unsaturated γ-amino acids containing synthetic protease inhibitors.

In 1992, Schreiber and colleagues reported that the dipeptides of (*E*)-vinylogous amino acids crystal structures and suggested that these kinds of shorter oligomers form an extended β-sheet type of structure.[44] Followed by Chakraborty and colleagues utilized (*E*)-vinylogous proline acids to induce turn in construction of hairpin structures.[45] Further, Claude and coworkers reported 9-helical conformations of (*Z*)-vinylogous amino acid dipeptides.[46] At the same time, Hofmann and colleagues reported ab initio MO theory calculations on oligomers of (*E*)- and (*Z*)-vinylogous homooligomers.[47] These studies suggested that the higher oligomers of (*E*)-vinylogous amino acids favor helices with larger hydrogen-bonded cycles from 14- to 27-membered. On the other hand, (*Z*)-vinylogous amino acid oligomers favor the smaller hydrogen-

bonded cycles such as 9 and 12-helices. The helical structures obtained from ab initio MO theory calculations are shown in Figure **7**. These studies also suggested that the larger hydrogen-bonded helical structures of (*E*)-vinylogous amino acids have an inner diameter large enough to pass the ions and molecules.

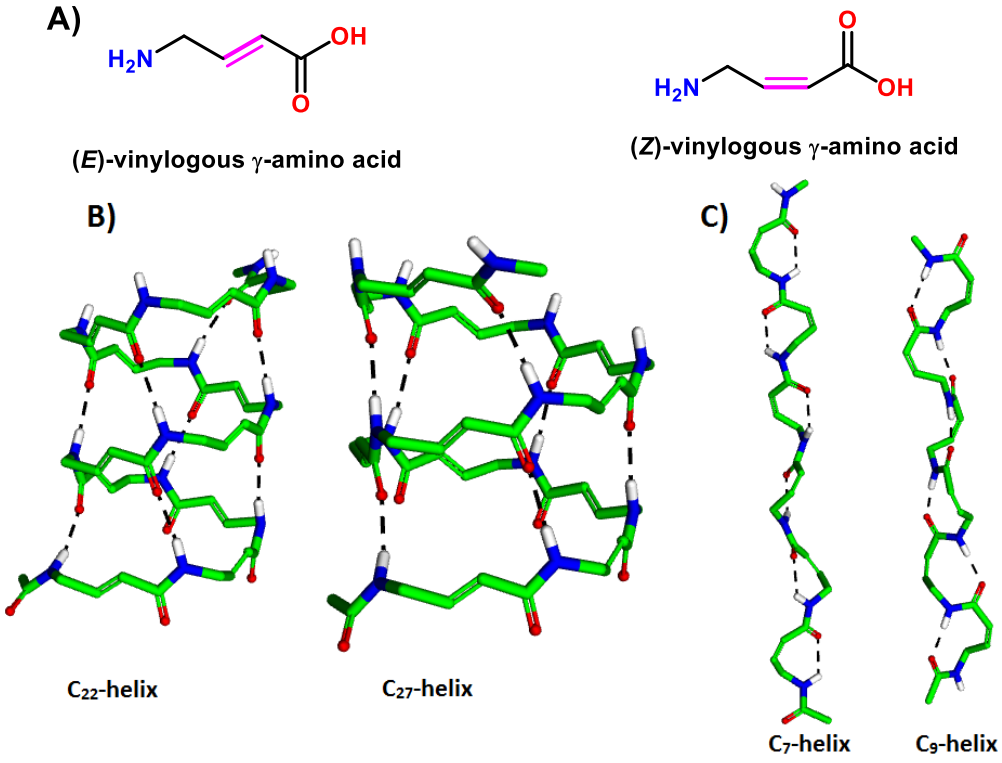

Figure 7: (A) Chemical structures of (*E*)- and (*Z*)-vinylogous γ-amino acids (B) Theoretically predicted stable structures of (*E*)-vinylogous γ-amino acids homooligomers, C_{22}- and C_{27}-helices (C) Theoretically predicted stable structures of (*Z*)-vinylogous γ-amino acids homooligomers, C_7- and C_9-helices.

In our previous studies, we have shown the utility of naturally occurring (*E*)-vinylogous γ-amino acids in the design of stable β-hairpins structures by inserting the (*E*)-vinylogous γ-amino acids at the facing positions of anti-parallel β-sheets.[48] In addition to the β-hairpins, we have also designed miniature β-meanders,[49] and multiple β-sheet structures.[50] Recently we also reported β-double-helical structures using homo-oligomers of 4,4-gem-dimethyl α,β-unsaturated γ-amino acid.[51] Further, we have also utilized (*Z*)-vinylogous γ-amino acids in the construction of α,γ-hybrid peptide 12-helical structures.[52] Crystal structures of various α,β-unsaturated γ-amino acid

foldamers are shown in Figure **8**. In the present study, we have examined the conformational properties and chemical reactivity of α,β-unsaturated γ-amino acids and their utility in the design of novel peptide foldamers, small molecule peptidomimetics, and β-double helices.

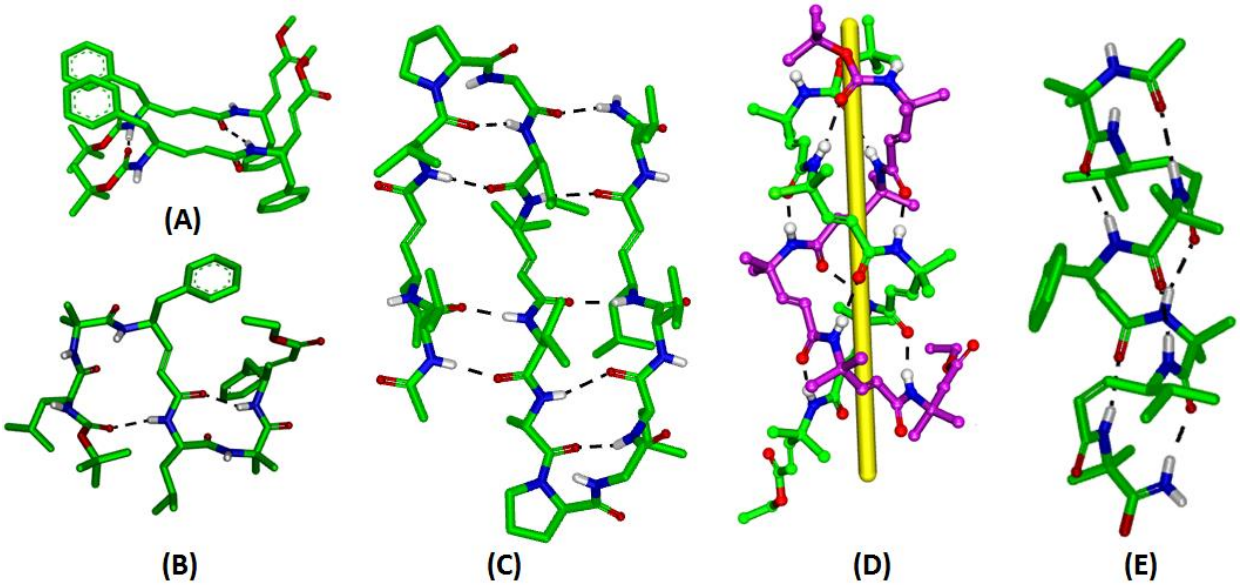

Figure 8: Foldamers of vinylogous γ-amino acids (A) Extended sheet structures of (*E*)-vinylogous γ-Phe dipeptide (B) β-meanders type super secondary structures of ααγ-hybrid peptide of (*E*)-vinylogous γ-Phe, Aib and Leu (C) Stable multi-stranded β-sheets containing (*E*)-vinylogous amino acids (D) β-double helical structures of (*E*)-vinylogous $\gamma^{4,4}$-amino acid homooligomer (E) C_{12}-helical structures of α,γ- hybrid peptides containing (*Z*)-vinylogous γ^{4}-amino acids.

2. References

1. a) Buxbaum, E. (**2007**), *Fundamentals of protein structure and function,* Vol. 31, 2nd ed., New York: Springer. b) Linderstrom-Lang, K. U.; Schellman, J. A. (**1959**), *The Enzymes*, (P. D. Boyer, Ed.), *Vol. 1*, 2nd ed., pp. 443-510. Academic Press, New York.
2. Chaudhuri, T. K.; Paul, S. *FEBS J.* **2006**, *273*, 1331.
3. Ramachandran, G. N.; Sasisekaran, V. *Advan. Protein Chem*. **1968**, *23*, 283.
4. Pauling, L.; Corey, R. B.; Branson, R. *Proc. Nat. Acad. Sci. USA*, **1951**, *37*, 205.
5. Pauling, L.; Corey, R. B. *Proc. Nat. Acad. Sci. USA* **1951**, *37*, 729.
6. Venkatachalam, C. M. *Biopolymers* **1968**, *6*, 1425.

7. (a) Seebach, D.; Gardiner, J. *Acc. Chem. Res.* **2008**, *41*, 1366. (b) Horne, W. S.; Gellmann, S. H. *Acc. Chem. Res*., **2008**, *41*, 1399.
8. (a) Frackenpohl , J.; Arvidsson , P. I.; Schreiber , J. V.; Seebach , D. *ChemBioChem* **2001**, *2*, 445. (b) Goodman, C. M.; Choi, S.; Shandler, S.; DeGrado, W.F. *Nat. Chem. Biol*. **2007**, *3*, 252.
9. Hintermann, T.; Gademann, K.; Jaun, B.; Seebach, D. *Helv. Chim. Acta*, **1998**, *81*, 983.
10. (a) Appella, D. H.; Christianson, L. A.; Klein, D. A.; Richards, M. A.; Powell, D. R.; Gellman, S. H. *J. Am. Chem. Soc.*, **1999**, *121*, 7574. (b) Appella, D. H.; Christianson, L. A.; Karle, I. L.; Powell, D. R.; Gellman, S. H. *J. Am. Chem. Soc.*, **1999**, *121*, 6206. (c) Appella, D. H.; Christianson, L. A.; Karle, I. L.; Powell, D. R.; Gellman, S. H. *J. Am. Chem. Soc*., **1996**, *118*, 13071.
11. (a) Sharma, G. V. M.; Reddy, V. G.; Chander, A. S.; Reddy, K. R. *Tetrahedron: Asymmetry* **2002**, *13*, 21. (b) Sharma, G. V. M.; Reddy, K. R.; Krishna, P. R.; Sankar, A. R.; Narsimulu, K.; Kumar, S. K.; Jayaprakash, P.; Jagannadh, B.; Kunwar, A. C. *J. Am. Chem. Soc*. **2003**, *125*, 13670; (c) Sharma, G. V. M.; Reddy, K. R.; Krishna, P. R.; Sankar, A. R.; Jayaprakash, P.; Jagannadh, B.; Kunwar, A. C. *Angew. Chem., Int. Ed*. **2004**, *43*, 3961.
12. (a) Pilsl, L. K. A.; Reiser, O. *Amino Acids* **2011**, *41*, 709. (b) De Pol, S.; Zorn, C; Klein, C. D.; Zerbe, O.; Reiser, O. *Angew. Chem., Int. Ed*. **2004**, *43*, 511.
13. (a) Hetenyi, A.; Mandity, I. M.; Martinek, T. A.; Toth, G. K.; Fulop, F. *J. Am. Chem. Soc*. **2005**, *127*, 547. (b) Mandity, I. M.; Weber, E.; Martinek, T. A.; Olajos, G.; Toth, G. K.; Vass E.; Fulop, F. *Angew. Chem., Int. Ed*. **2009**, *48*, 2171. (c) Martinek, T. A.; Toth, G. K.; Vass, E.; Hollosi, M.; Fulop, F. *Angew. Chem., Int. Ed*. **2002**, *41*, 1718. (d) Martinek, T. A.; Mandity, I. M.; Fulop, L.; Toth, G. K.; Vass, E.; Hollosi, M.; Forro, E.; Fulop, F. *J. Am. Chem. Soc*. **2006**, *128*, 13539.
14. Fernandes, C.; Faure, S.; Pereira, E.; Thery, V.; Declerck, V.; Guillot, R.; Aitken, D. J. *Org. Lett*. **2010**, *12*, 3606.
15. (a) Gellman, S. H. *Acc. Chem. Res.* **1998**, *31*, 173. (b) Hill, D. J.; Mio, M. J.; Prince, R. B.; Hughes, T. S.; Moore, J. S. *Chem. Rev*. **2001**, *101*, 3893. (c) Cheng, R. P.; Gellman, S. H.; DeGrado, W. F. *Chem. Rev*. **2001**, *101*, 3219. (d) Venkatraman, J.; Shankaramma, S. C.; Balaram, P. *Chem. Rev*. **2001**, *101*, 3131. (e) Seebach, D.; Beck, A. K.; Bierbaum, D. J.

Chem. Biodiversity **2004**, *1*, 1111. (f) Hecht, S.; Huc, I. *Foldamers: Structure, Properties and Applications*; Wiley-VCH: Weinheim, **2007**. (g) Seebach, D.; Gardiner, J. *Acc. Chem. Res.* **2008**, *41*, 1366. (h) Cummings, C. G.; Hamilton, A. D. *Curr. Opin. Chem. Biol*. **2010**, *14*, 341.

16. (a) Petersson, E. J.; Schepartz, A. *J. Am. Chem. Soc*. **2008**, *130*, 821. (b) Price, J. L.; Horne, W. S.; Gellman, S. H. *J. Am. Chem. Soc*. **2010**, *132*, 12378.
17. (a) Arvidsson, P. I.; Rueping, M.; Seebach, D. *Chem. Commun*. **2001**, 649. (b) Appella, D. H.; Christianson, L. A.; Klein, D. A.; Powell, D. R.; Huang, X. L.; Barchi J. J.; Gellman, S. H. *Nature* **1997**, *387*, 381. (c) Seebach, D.; Schreiber, V. J.; Abele, S.; Daura, X.; Gunsteren, F. W. *Helv. Chim. Acta* **2000**, *83*, 34. (d) Daura, X.; Bakowies, D.; Seebach, D.; Fleischhauer, J.; van Gunsteren, W. F.; Kruger, P. *Eur. Biophys. J*. **2003**, *32*, 661. (e) Hetenyi, A.; Mandity, I. M.; Martinek, T. A.; Toth, G. K.; Fulop, F. *J. Am. Chem. Soc*. **2005**, *127*, 547. (f) Threlfall, R. ; Davies, A. ; Howarth, N.M. ; Fisher, J. ; Cosstick, R. *Chem. Commun*. **2008**, 585. (g) Rua, F.; Boussert, S.; Parella, T.; Diez-Perez, I.; Branchadell, V.; Giralt, E.; Ortuno, R. M. *Org. Lett*. **2007**, *9*, 3643. (h) Arvidsson, P. I.; Ryder, N. S.; Weiss, H. M.; Gross, G.; Kretz, O.; Woessner, R.; Seebach, D. *ChemBioChem* **2003**, *4*, 1345. (i) Mandity, I. M.; Weber, E.; Martinek, T. A.; Olajos, G.; Toth, G. K.; Vass E.; Fulop, F. *Angew. Chem., Int. Ed*. **2009**, *48*, 2171. (j) Seebach, D.; Abele, S.; Gademann, K.; Jaun, B. *Angew. Chem., Int. Ed*. **1999**, *38*, 1595. (k) Martinek, T. A.; Toth, G. K.; Vass, E.; Hollosi, M.; Fulop, F. *Angew. Chem., Int. Ed*. **2002**, *41*, 1718. (l) Martinek, T. A.; Mandity, I. M.; Fulop, L.; Toth, G. K.; Vass, E.; Hollosi, M.; Forro, E.; Fulop, F. *J. Am. Chem. Soc*. **2006**, *128*, 13539.
18. (a) Roy, R. S.; Karle, I. L.; Raghothama, S.; Balaram, P. *Proc. Natl. Acad. Sci. USA* **2004**, *101*, 16478. (b) Karle, I. L.; Pramanik, A.; Banerjee, A.; Bhattacharjya, S.; Balaram, P. *J. Am. Chem. Soc.* **1997**, *119*, 9087. (c) De Pol, S.; Zorn, C.; Klein, C. D.; Zerbe, O.; Reiser, O. *Angew. Chem., Int. Ed.* **2004**, *43*, 511–514. (d) Hayen, A.; Schmitt, M. A.; Ngassa, F. N.; Thomasson, K. A.; Gellman, S. H. *Angew. Chem., Int. Ed.* **2004**, *43*, 505–510. (e) Schmitt, M. A.; Choi, S. H.; Guzei, I. A.; Gellman, S. H. *J. Am. Chem. Soc.* **2005**, *127*, 13130-13131. (f) Schmitt, M. A.; Choi, S. H.; Guzei, I. A.; Gellman, S. H. *J. Am. Chem. Soc.* **2006**, *128*, 4538-4539.

19. (a) Hayen, A.; Schmitt, M. A.; Ngassa, F. N.; Thomasson, K. A.; Gellman, S. H. *Angew. Chem., Int. Ed*. **2004**, *43*, 505. (b) Choi, S. H.; Guzei, I. A.; Spencer, L. C.; Gellman, S. H. *J. Am. Chem. Soc*. **2008**, *130*, 6544. (c) Legrand, B.; Andre, C.; Moulat, L.; Wenger, E.; Didierjean, C.; Aubert, E.; Averlant-Petit, M. C.; Martinez, J.; Calmes, M.; Amblard, M. *Angew. Chem., Int. Ed*. **2014**, *53*, 13131. (d) Schmitt, M. A.; Choi, S. H.; Guzei, I. A.; Gellman, S. H. *J. Am. Chem. Soc*. **2006**, *128*, 4538. (e) Mándity, I. M.; Weber, E.; Martinek, T. A.; Olajos, G.; Tóth, G. K.; Vass, E.; Fülöp, F. *Angew. Chem., Int. Ed*. **2009**, *48*, 2171. (f) Sharma, G. V. M.; Reddy, K. R.; Krishna, P.R.; Sankar, A. R.; Narasimulu, K.; Kumar, S. K.; Jayaprakash, P.; Jagannadh, B.; Kunwar, A. C. *J. Amer. Chem. Soc*. **2003**, *125*, 13670. (g) Sharma, G. V. M.; Reddy, K. R.; Krishna, P. R.; Sankar, A. R.; Jayaprakash, P.; Jagannadh, B.; Kunwar, A. C. *Angew. Chem., Int. Ed. Engl*. **2004**, *43*, 3961. (h) Sharma, G. V. M.; Nagendar, P.; Krishna, P. R.; Ramakrishna K. V. S.; Jayaprakash, P.; Kunwar, A. C. *Angew. Chem., Int. Ed. Engl*. **2005**, *44*, 5878. (i) Sharma, G. V. M.; Subash, V.; Narasimulu, K.; Sankar, A. R.; Kunwar, A. C. *Angew. Chem. Int. Ed. Engl*. **2006**, *45*, 8207. (j)Horne, W. S.; Price, J. L.; Keck, J. L.; Gellman, S. H. *J. Am. Chem. Soc*. **2007**, *129*, 4178. (k) Giuliano, M. W.; Horne, W. S.; Gellman, S. H. *J. Am. Chem. Soc*. **2009**, *131*, 9860.

20. (a) Hamuro, Y.; Schneider, J. P.; DeGrado, W. F. *J. Am. Chem. Soc*. **1999**, *121*, 12200. (b) Karlsson, A. J.; Pomerantz, W. C.; Weisblum, B.; Gellman, S. H.; Palecek, S. P. *J. Am. Chem. Soc*. **2006**, *128*, 12630.

21. Gademann, K.; Seebach, D. *Helv. Chim. Acta* **2001**, *84*, 2924.

22. (a) Gademann, K.; Ernst, M.; Hoyer, D.; Seebach, D. *Angew. Chem. Int. Ed*. **1999**, *38*, 1223. (b) Gademann, K.; Ernst, M.; Seebach, D.; Hoyer, D. *Helv. Chim. Acta* **2000**, *83*, 16. (c) Gademann, K.; Kimmerlin, T.; Hoyer, D.; Seebach, D. *J. Med. Chem*. **2001**, *44*, 2460.

23. Kritzer, J. A.; Lear, J. D.; Hodsdon, M. E.; Schepartz, A. *J. Am. Chem. Soc*. **2004**, *126*, 9468.

24. Stephens, O. M.; Kim, S.; Welch, B. D.; Hodsdon, M. E.; Kay, M. S.; Schepartz, A. *J. Am. Chem. Soc*. **2005**, *127*, 13126.

25. English, E. P.; Chumanov, R. S.; Gellman, S. H.; Compton, T. *J. Biol. Chem.* **2006**, *281*, 2661.

26. (a) Liu, R.; Chen, X.; Falk, S. P.; Mowery, B. P.; Karlsson, A. J.; Weisblum, B.; Palecek, S. P.; Masters, K. S.; Gellman, S. H. *J. Am. Chem. Soc*. **2014**, *136*, 4333. (b) Liu, R.; Chen, X.; Falk, S. P.; Masters, K. S.; Weisblum, B.; Gellman, S. H. *J. Am. Chem. Soc*. **2015**, *137*, 2183.

27. Hintermann, T.; Gademann, K.; Jaun, B.; Seebach, D. *Helv. Chim. Acta.* **1998**, *81*, 893.
28. Hanessian, S.; Luo, X.; Schaum, R.; Michnick, S. *J. Am. Chem. Soc.* **1998**, *120*, 8569.
29. Seebach, D.; Brenner, M.; Rueping, M.; Schweizer, B.; Jaun, B. *Chem. Commun.* **2001**, 0, 207.
30. (a) Baldauf, C.; Gunther, R.; Hofmann, H. J. *Helv. Chim. Acta*. **2003**, *86*, 2573. (b) Baldauf, C.; Gunther, R.; Hofmann, H. -J. *J. Org. Chem.* **2006**, *71*, 1200.
31. Vasudev, P. G.; Shamala, N.; Ananda, K.; Balaram, P. *Angew. Chem., Int. Ed*. **2005**, *44*, 4972.
32. Vasudev, P. G.; Chatterjee, S.; Shamala, N.; Balaram, P. *Acc. Chem. Res*. **2009**, *42*, 1628.
33. (a) Sharma, G. V. M.; Jayaprakash, P.; Narsimulu, K.; Sankar, A. R.; Reddy, K. R.; Kunwar, A. C. *Angew. Chem. Int. Ed.* **2006**, *45*, 2944. (b) Sharma, G. V. M.; Reddy, K. R.; Krishna, P.R.; Sankar, A. R.; Narasimulu, K.; Kumar, S. K.; Jayaprakash, P.; Jagannadh, B.; Kunwar, A. C. *J. Amer. Chem. Soc*. **2003**, *125*, 13670. (c) Sharma, G. V. M.; Subash, V.; Narasimulu, K.; Sankar, A. R.; Kunwar, A. C. *Angew. Chem. Int. Ed. Engl*. **2006**, *45*, 8207. (d) G. V. M. Sharma.; Thodupunuri, P.; Sirisha, K.; Basha, S. J.; Reddy, P. G.; Sarma, A. V. S. J. *Org. Chem. 2014*, 79, 8614.
34. (a) Giuliano, M. W.; Maynard, S. J.; Almeida, A. M.; Guo, L.; Guzei, L. A.; Spencer, L. C.; Gellman, S. H. *J. Am. Chem. Soc*. **2014**, *136*, 15046. (b) Fisher, B. F.; Guo, L.; Dolinar, B. S.; Guzei, L. A.; Gellman, S. H. *J. Am. Chem. Soc*. **2015**, *137*, 6484.
35. Khurram, M.; Qureshi, N.; Smith, M. D. *Chem. Commun*. **2006**, 5006.
36. (a) Pendem, N.; Nelli, Y. R.; Douat, C.; Fischer, L.; Laguerre, M.; Ennifar, E.; Kauffman, B.; Guichard, G. *Angew. Chem. Int. Ed*. **2013**, *52*, 4147. (b) Collie, G. W.; Pulka-Ziach, K.; Lombardo, C. M.; Fremaux, J.; Rosu, F.; Decossas, M.; Mauran, L.; Lambert,O.; Gabelica, V.; Mackereth, C. D.; Guichard, G. *Nature Chemistry* **2015**, *7*, 871.
37. Farrera-Sinfreu, J.; Zaccaro, L.; Vidal, D.; Salvatella, X.; Giralt, E.; Pons, M.; Albericio, F.; Royo, M.; *J. Am. Chem. Soc*. **2004**, *126*, 6048.

38. Mathieu, L.; Legrand, B.; Deng, C.; Vezenkov, L.; Wenger, E.; Didierjean, C.; Amblard, M.; Averlant-Petit, M. C.; Masurier, N.; Lisowski, V.; Martinez, J.; Maillard, L. T. *Angew. Chem. Int. Ed*. **2013**, *52*, 6006.
39. Misra, R.; Saseendran, A.; George, G.; Veeresh, K.; Raja, K. M. P.; Raghothama, S.; Hofmann, H. J.; Gopi, H. N. *Chem. Eur. J.* **2017**, 23, 3764.
40. Hagihara, M.; Schreiber, S. L. *J. Am. Chem. Soc*. **1992**, *114*, 6570.
41. Linington, R. G.; Clark, B. R.; Trimble, E. E.; Almanza, A.; Uren, L.-D.; Kyle, D. E.; Gerwick, W. H. *J. Nat. Prod*. **2009**, *72*, 14.
42. Nakao, Y.; Fujita, M.; Warabi, K.; Matsunaga, S.; Fusetani, N. *J. Am. Chem. Soc*. **2000**, *122*, 10462.
43. (a) Hanzlik, R. P.; Thompson, S. A. *J. Med. Chem*. **1984**, *27*, 711. (b) Bastiaans, H. M. M.; Van der Baan, J. L.; Ottenheijm, H. C. J. *J. Org. Chem*. **1997**, *62*, 3880. (c) Liu, S.; Hanzlik, R. P. *J. Med*. *Chem*. **1992**, *35*, 1067. (d) Kong, J-S.; Venkatraman, S.; Furness, K.; Nimkar, S.; Shepherd, T. A.; Wang, Q. M.; Aube, J.; Hanzlik, R. P. *J. Med. Chem*. **1998**, *41*, 2579. (e) Schaschke, N.; Sommerhoff, C. P. *ChemMedChem* **2010**, *5*, 367.
44. Hagihara, M.; Anthony, N. J.; Stout, T. J.; Clardy, J.; Schreiber, S. L. *J. Am. Chem. Soc*. **1992**, *114*, 6568.
45. Chakraborty, T. K.; Ghosh, A.; Kumar, S. K.; Kunwar, A. C. *J. Org. Chem*. **2003**, *68*, 6459.
46. (a) Grison, C.; Coutrot, P.; Ge´neve, S.; Didierjean, C.; Marraud, M. *J. Org. Chem*. **2005**, *70*, 10753. (b) Grison, C.; Ge´neve, S.; Halbin, E.; Coutrot, P. *Tetrahedron* **2001**, *57*, 4903.
47. Baldauf, C.; Gunther, R.; Hofmann, H.-J. *J. Org. Chem*. **2005**, *70*, 5351.
48. Bandyopadhyay, A.; Mali, S. M.; Lunawat, P.; Raja, K. M. P.; Gopi, H. N. *Org. Lett*. **2011**, *13*, 4482.
49. Bandyopadhyay, A.; Gopi, H. N. *Org. Lett*. **2012**, *14*, 2770.
50. Bandyopadhyay, A.; Misra. R.; Gopi, H. N. *Chem. Commun.* **2016**, *52*, 4938.
51. Misra, R.; Dey, S.; Reja, R. M.; Gopi, H. N. *Angew. Chem.* **2018**, *130*, 1069.
52. Ganesh Kumar, M.; Thombare, V. J.; Katariya, M. M.; Veeresh, K.; Raja, K. M. P.; Gopi, H. N. *Angew. Chem.* **2016**, *128*, 7978.

CHAPTER 2

Design of Helical Peptide Foldamers through α,β→β,γ Double Bond Migration

The original work of this chapter has been published in the "Organic Letters" journal. Here, we adopted the text from Ref. Veeresh, K.; Gopi, H. N. *Org. Lett.* **2019**, *2*, 4500. with permission from the American Chemical Society. A copy of the permission letter attached at the end of the chapter.

1. Introduction

Proteins spontaneously fold into functionally important, well-defined three-dimensional structures. The growth in the field of foldamers constructed from the non-natural amino acid building blocks shown that the folding phenomenon is not only restricted to proteins.[1] The progress in the foldamers research has opened doors to various structures available to the oligomers of non-natural amino acids. Perhaps, β- and γ-peptides are the most extensively studied among unnatural oligomers.[2,3] In addition to β- and γ-peptides, hybrid peptides sequences $(\alpha\beta)_n$,[4] $(\alpha\gamma)_n$[5] and $(\beta\gamma)_n$[6] have shown to adopt well-defined helical conformations similar to the protein secondary structures, however with different hydrogen bond pseudo cycles. To achieve the targeted helical structures, diverse unnatural building blocks were invented. Most often, the targeted helical structures were achieved by the usage of pre-organized amino acid building blocks.[7]

We have been interested in understanding the chemical reactivity and conformations of α,β-unsaturated γ-amino acids. In our previous studies, we demonstrated the transformation of an unusual planar structure of a α,γ-hybrid peptide composed of alternating α- and *E*-vinylogous amino acid residues into α,γ-hybrid peptide 12-helix through catalytic hydrogenation.[8] In this case, the double bond reduction released the geometrical constraints of α,β-unsaturated γ-amino acids to accommodate them into 12-helix. Further, using *E*-vinylogous amino acids (Scheme **1a**) we have designed stable β-hairpins,[9] three-stranded β-sheets,[10] and miniature β-meander mimetic.[11] Recently, using achiral *E*-vinylogous $\gamma^{4,4}$ dimethyl amino acid (Scheme **1e**) we have reported the design of double-helical peptide foldamers.[12] Schreiber et al. demonstrated the extend sheet type structures of oligopeptides constructed from the *E*-vinylogous amino acids (Scheme **1a** and **1b**).[13] Further proline *E*-vinylogous amino acids (Scheme **1c** and **1d**) have been utilized to generate a β-turn.[14] Maillard and co-workers reported the C_9-helical structures of new thiazole-based γ-amino acid containing homo-oligomers (Scheme **1g**).[15] Whereas α/γ-hybrid peptides containing *Z*-vinylogous residues (Scheme **1f**) showed well-folded C_{12}-helical structures.[16] These studies revealed the incapability of *E*-vinylogous residues to fit into a helix. In contrast to *E*-vinylogous residue, *Z*-vinylogous residue nicely fits into a well-folded helical structures.[15,16] In line with these studies, we sought to investigate the possibilities of α,β→β,γ

double bond migration in the α,γ-hybrid peptides composed of *E*-vinylogous amino acids and the consequence of such migration on the peptide conformation and chemical reactivity.

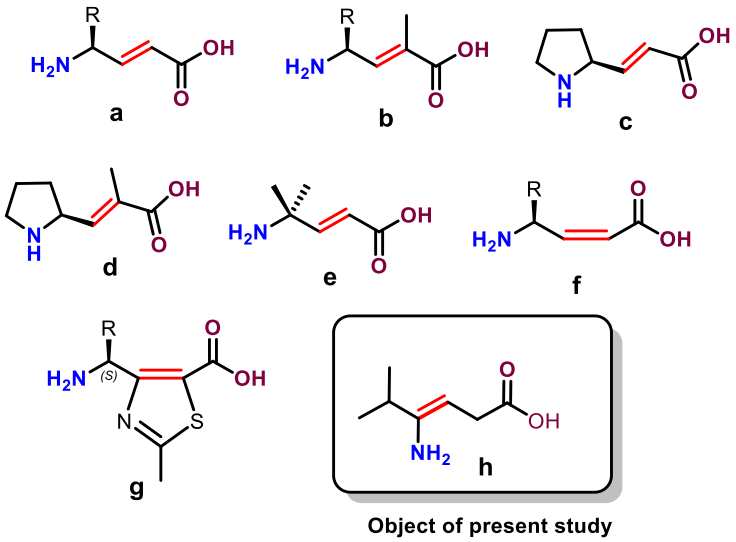

Scheme 1: *E*- and *Z*-vinylogous amino acids used in the synthesis of foldamers.

2. Aim and rationale of the present work

The biosynthesis process of natural polyketides such as corallopyronins (A, A', B and C), myxopyronins (A and B), bacillaene, ansamitocin P2, and rhizoxin D involve series of enzymatic reactions.[17] The synthetic steps involved in the biosynthesis of corallopyronin is schematically shown in scheme **2**. One of the intermediate steps of the polyketide biosynthesis involves the migration of double bonds from α,β→β,γ position on the intermediate compound, *E*-vinylogous amino acid. The α,β→β,γ double bond migration step is carried out by the dehydratase enzyme. The enzyme uses histidine residue as a proton donor and still unknown base residue as a proton acceptor.[17a] The α,β→β,γ double bond migration step in the synthesis of corallopyronins is shown in Scheme **3**. As we have been working on unnatural *E*-vinylogous amino acids (α,β-unsaturated γ-amino acids foldamers) we sought to investigate the possibilities of such double bond migration *in vitro* conditions, on the α,γ-hybrid peptides composed of *E*-vinylogous amino acids and the consequence of such migration on the peptide conformation and reactivity.

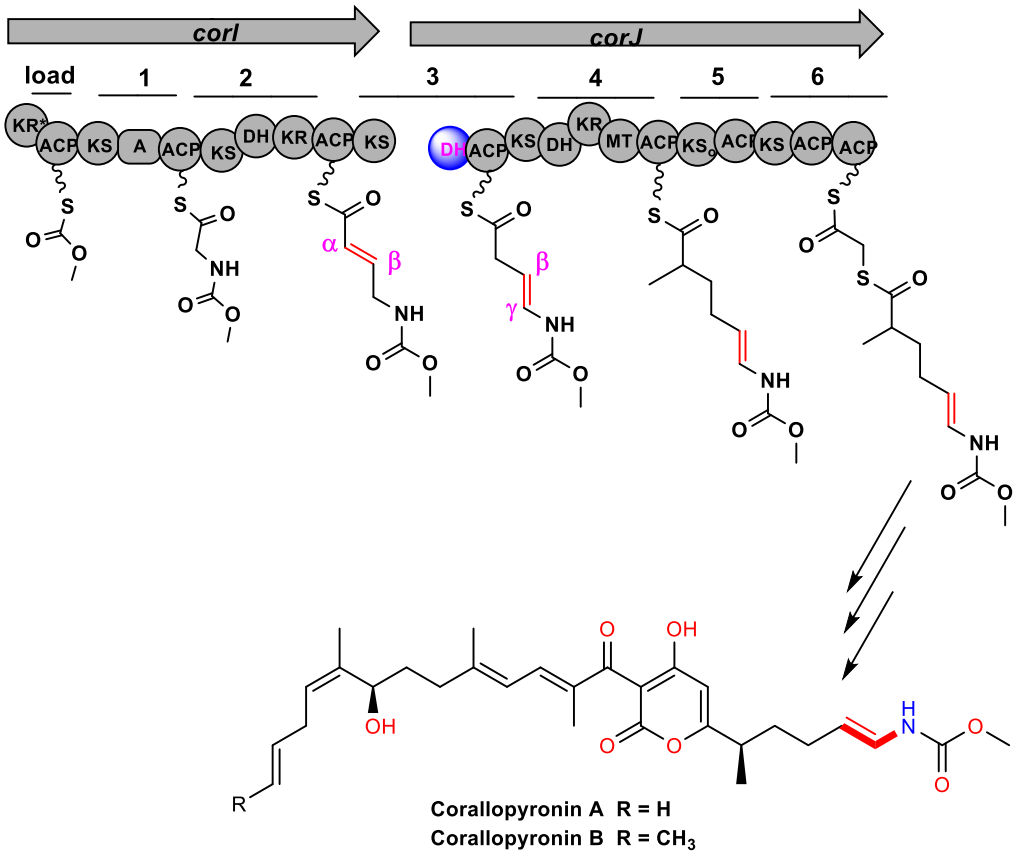

Scheme 2: Schematic representation of synthetic steps involved in the biosynthesis of corallopyronin. The α,β→β,γ double bond migration catalyzed by dehydratase enzyme is highlighted with a red color.

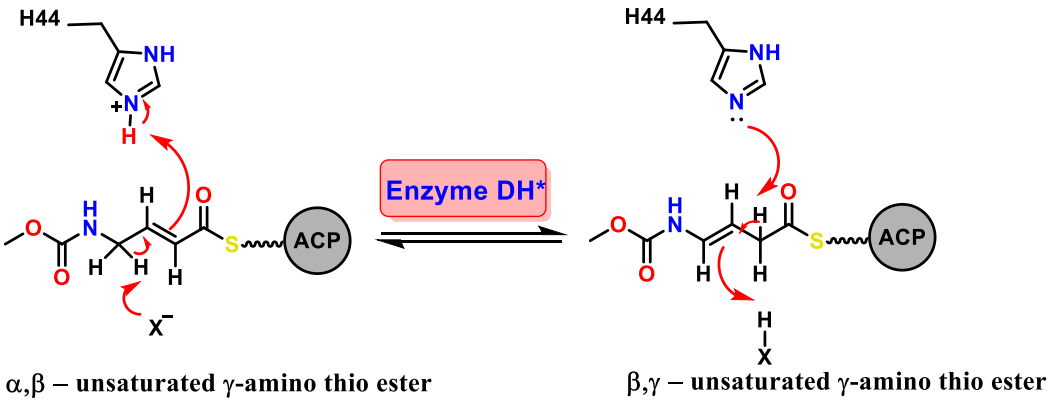

Scheme 3: Dehydratase enzyme-catalyzed α,β→β,γ double bond migration. The 44th residue histidine of dehydratase acts as a proton donor and still unknown base residue as acceptor.

3. Results and discussion

3.1 Synthesis of peptides P1 to P4

In order to examine the α,β→β,γ double bond migration and to study the structural changes of such double bond migration on peptide conformation, we have designed hybrid peptides **P1** to **P4** composed of α- and *E*-vinylogous amino acids. *N*-Terminal of these peptides was protected with the Boc and *C*-terminal with the benzylamine group. The amino acid sequences of the peptides are shown in Scheme **4**.

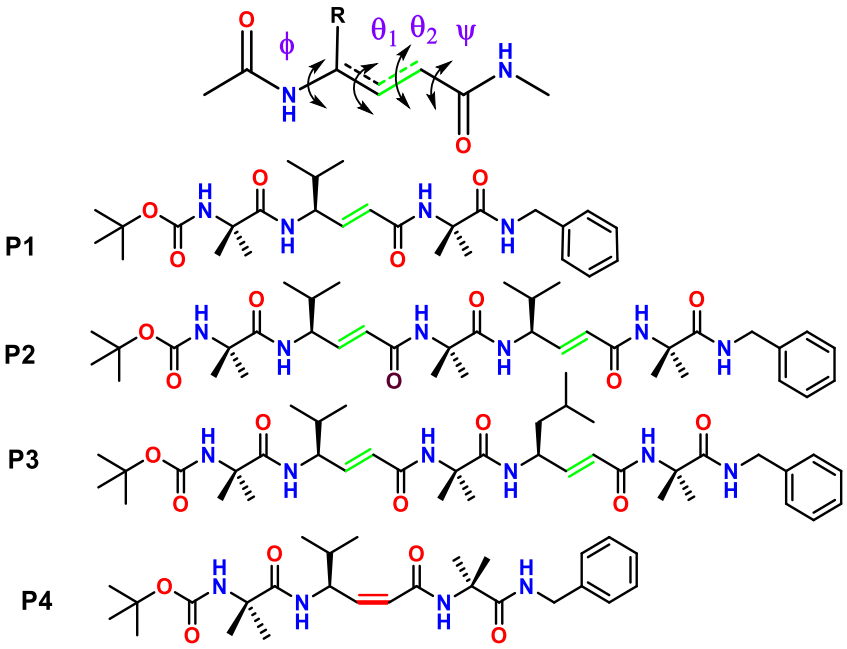

Scheme 4: Sequences of hybrid peptides composed of α- and α,β-unsaturated γ-amino acids.

Synthesis of peptides **P1** to **P4** was carried out through the conventional solution-phase method. The *tert*-butyloxycarbonyl group was used for N-terminus protection and the C-terminus was protected with the ethyl ester group. Deprotections were carried out with trifluoroacetic acid and aqueous *1N* sodium hydroxide solution for N- and C-termini, respectively. Couplings were mediated by HBTU. The α,β-unsaturated γ-amino acids BocHN-*E*-$d^{2,3}$γLeu-OEt, BocHN-E-$d^{2,3}$γVal-OEt and BocHN-*Z*-$d^{2,3}$γVal-OEt were synthesized starting from the N-Boc-Amino aldehyde through Wittig reaction as reported earlier.[18,16] The synthetic strategy for this peptides **P1** to **P3** is given in Scheme **5**. To synthesize peptide **P1,** starting materials, Boc-Aib-benzylamine (**1A**) was prepared by coupling the Boc-Aib acid with benzylamine and dipeptide

of Boc-Aib-E-d^{2,3}γVal-OEt (**Pb**) was prepared by coupling the Boc-Aib acid and H_2N-*E*-d^{2,3}γVal-OEt. The tripeptide Boc-Aib-*E*-d^{2,3}γVal-Aib-benzylamine (**P1)** was prepared by coupling the Boc-Aib-E-d^{2,3}γVal-OH (**Pb-acid**) with H_2N-Aib-benzylamine. The tripeptide Boc-Aib-*Z*-d^{2,3}γVal-Aib-benzylamine (**P4**) was prepared using a similar strategy. Finally the pentapeptides **P2** and was synthesized by coupling the Boc-Aib-E-d^{2,3}γVal-Aib-OH with H_2N-Aib-E-d^{2,3}γVal-Aib-benzylamine. A similar strategy was used to synthesize pentapeptide **P3.** Finally, these peptides **P1** to **P4** were purified through column chromatography.

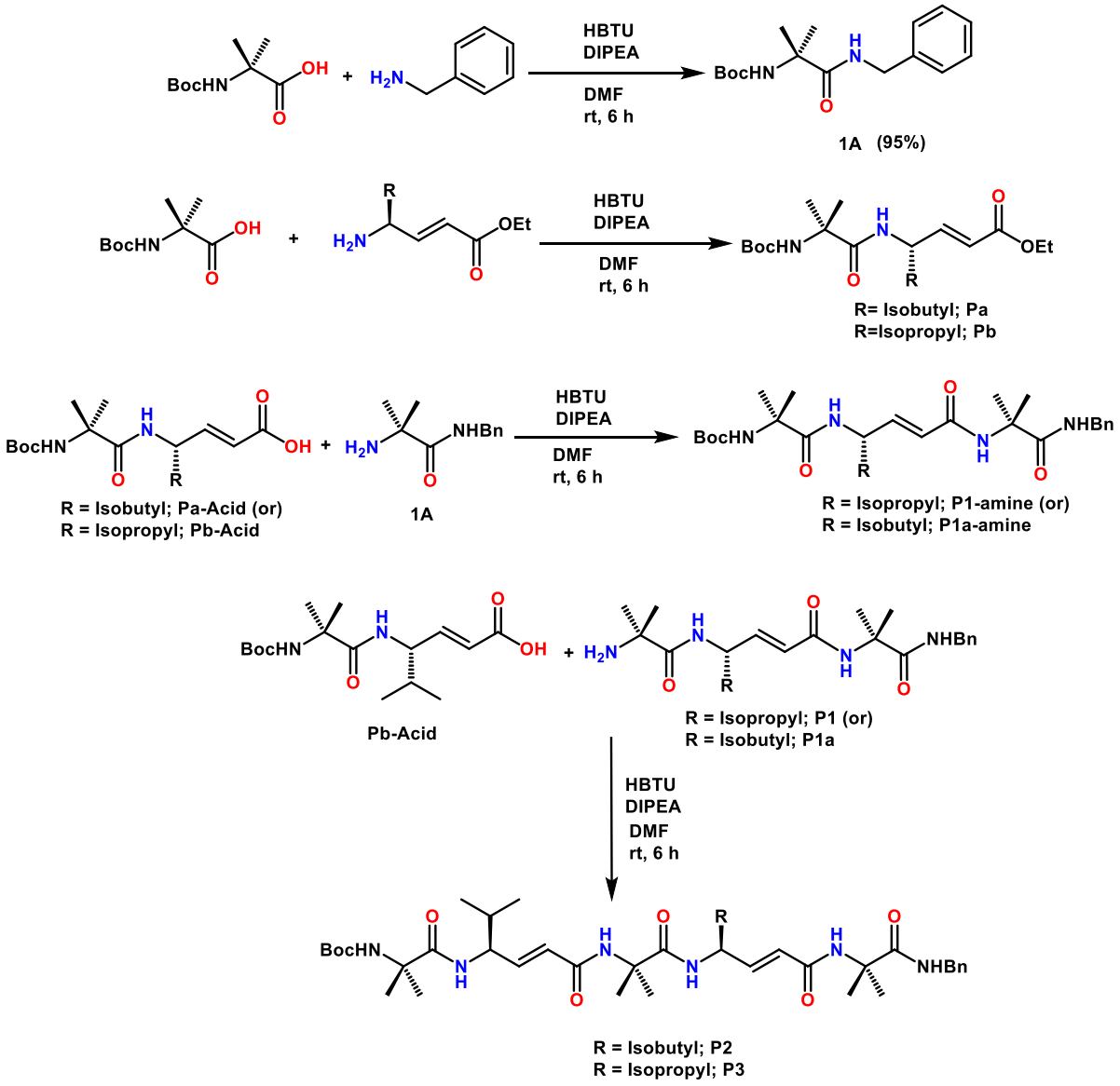

Scheme 5: Schematic representation of synthetic strategy for the synthesis of **P1** to **P3**.

3.2. α,β→β,γ Double bond migration and conformational analysis

To know about the possibilities of double bond migration, we first subjected short tripeptide P1 for the base treatment. As we observed low yields and longer reaction time in 1*N* NaOH, we chose to use KO^{t}Bu as a base and the reaction was monitored by TLC. The complete disappearance of the starting material was observed within 4 h at room temperature. The schematic representation of the double bond migration of peptide P1 is shown in Scheme **6**. The double bond migrated product **P1'** was isolated in excellent yield (93%) and subjected for NMR analysis. The ^{1}H NMR reveals the disappearance of characteristic trans double bond protons and Cγ H signal. In addition, a new triplet at around δ 5.34 ppm and a doublet at *δ* 2.01 ppm observed in the ^{1}H-NMR spectrum indicating double bond migration in the product. To gain structural insights of both **P1** and **P1'** we subjected them for crystallization in various solvent combinations.

Both **P1** and **P1'** gave single crystals from the slow evaporation of aqueous methanol containing peptides and their X-ray diffraction structures are shown in Figure **1**. Peptide **P1** adopted an unusual planar conformation in single crystals.[8] In sharp contrast to this unusual planar structure of **P1**, peptide **P1'** adopted a helical structure in single crystals. The helical structure is stabilized by two consecutive *intra*-molecular 12-membered hydrogen bonds (12-helix) between *i* and *i+3* residues. Similar to other α,γ-hybrid peptide 12-helices, the two *N*-terminal amide NH groups and *C*-terminal two CO groups are involved in the head-to-tail intermolecular hydrogen bonding with other helices in the crystal packing. Two molecules in the crystal asymmetric unit adopted opposite helical handedness indicating achiral nature of **P1'**. The local conformations of unsaturated γ-residues can be measured using torsion variables ϕ (N-C$^\gamma$), θ$_1$ (C$^\gamma$-C$^\beta$), θ$_2$ (C$^\beta$-C$^\alpha$) and ψ (C$^\alpha$-C') as shown in Scheme **4**.

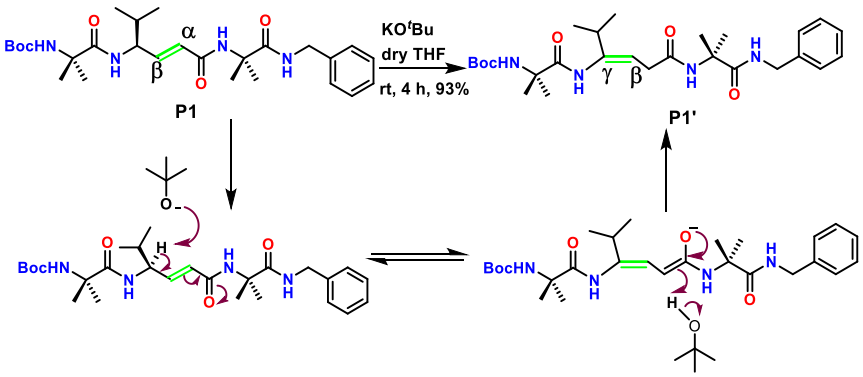

Scheme 6: α,β→β,γ Double bond migration in **P1** and possible mechanism.

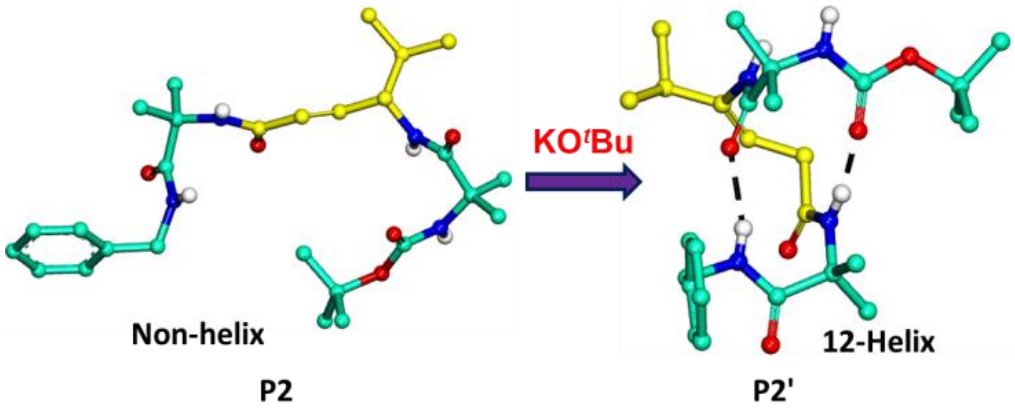

Figure 1: X-ray crystal structure of **P1** and **P1'**. The structural analysis suggested that the transformation of non-helical structure **P1** to 12-helical structure **P1'** upon treatment with KO^{t}Bu.

The torsion parameters of peptide **P1** and **P1'** are tabulated in Table **1**. The bond length of C^{γ}-C^{β} in **P1'** (1.32 Å) was found to be the same as that of C^{β}-C^{α} bond in **P1**. Instructively, the stereochemistry of the double bond in the product **P1'** was found to be *Z*. The peptide **P1'** attained the helical conformation with *Z* C-C double bond at β,γ-position. However, we previously reported the 12-helical conformations of α,γ-hybrid peptides composed of *Z*-vinylogous amino acids with *Z* C-C double bond at α,β-position.[16] Both these results suggested that *Z* C-C double bond can be accommodated into the 12-helix either at α,β-position or β,γ-position without deviating overall 12-helical fold. Being *Z* double bond, it attained the torsion value θ_1 close to 0°. The other torsion variables ϕ, θ_2 and ψ attained the values -86°, 110° and -119°, respectively. The Aib residues attained torsion values similar to α-helix conformation.[19] The possible mechanism of the double bond migration upon treatment of the base is shown in Scheme **6**. We speculate that the abstraction of acidic $C^{\gamma}H$ leads to the migration of negative charge to α,β-unsaturated carbonyl group. The stable negative charge at α-position subsequently abstract a proton from the *tert*-butanol to give β,γ-unsaturated γ-amino acid derivative.

Table 1: Torsional angle values of peptide **P1** and **P1'**

Peptide	Residue	ϕ (°)	θ_1(°)	θ_2(°)	ψ(°)
Peptide P1	Aib(1)	-54.9	-	-	-46.7
	(*S,E*)d$^{2,3}\gamma$Val (2)	-135.7	118.7	177.7	-159
	Aib (3)	61.5	-	-	168.3
Peptide P1'	Aib (1)	-58.5	-	-	-53.6
	(*Z*)d$^{3,4}\gamma$Val (2)	-86.2	-0.27	110.3	-118.9
	Aib (3)	-60.1	-	-	-31.8

To understand whether the base mediated double bond migration is specific to **P1** or it can be applied to other peptides that contain more than one unsaturated amino acids, we have designed two pentapeptides **P2** and **P3** (Scheme **4**). Similar to **P1**, both pentapeptides **P2** and **P3** were treated with base to achieve two double bonds migrated products **P2'** and **P3'**, respectively. The schematic representation of the transformation of **P2** and **P3** to the corresponding **P2'** and **P3'**, respectively is shown in Scheme **7**. The ^{1}H and ^{13}C NMR studies of **P2'** and **P3'** revealed the migration of two individual double bonds from α,β→β,γ position in both the peptides. In order to understand their unambiguous conformations, both peptides were subjected to crystallization and their single-crystal X-ray diffraction structures are shown in Figure **2**.

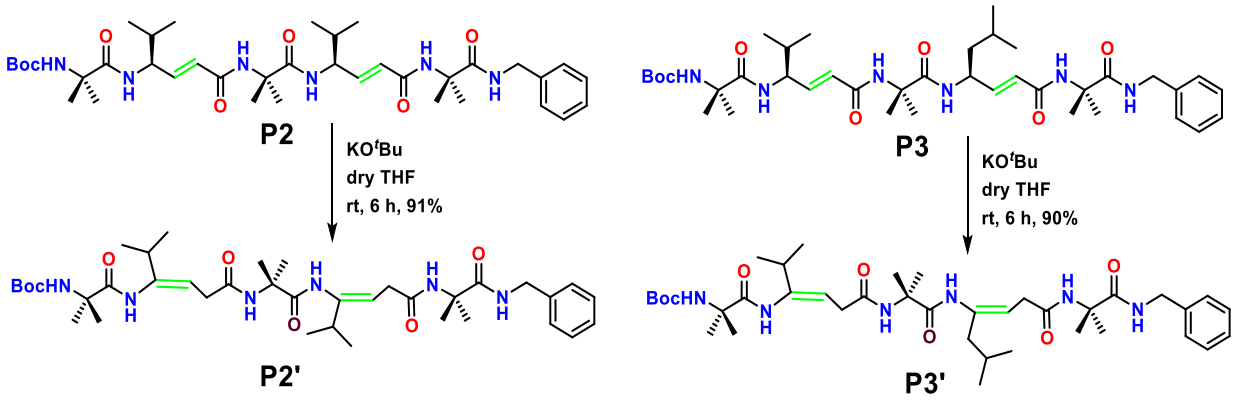

Scheme 7: The α,β→β,γ double bond migration in pentapeptides **P2** and **P3**

The crystal structure of **P2'** reveals that it adopted a 12-helix conformation in single crystals similar to **P1'**. Between the two peptide molecules observed in the asymmetric unit, one peptide adopted a (*P*)-helix and others adopted an (*M*)-helix conformation, indicating achiral nature of

the peptide **P2'**. The helical structure of the **P2'** is stabilized by four continuous 12-membered *intra*-molecular hydrogen bonds between the residues *i* and *i+3*. The hydrogen bond parameters are tabulated in Table **3**. The structural analysis revealed that the double bonds were migrated from α,β→β,γ position in both unsaturated γ-residues in the peptide sequence. Instructively, the two new double bonds at β,γ position adopted *Z*-stereochemistry. Both γ-residues with *Z*-double bond at β,γ- position are nicely accommodated into the 12-helix with similar backbone conformations as observed in the peptide **P1'**. The torsion parameters of peptide **P2'** and **P3'** backbones are tabulated in Table **2**. Similar to **P2'**, the base treatment of **P3** leads to the double bonds migrated product **P3'**. The single-crystal X-ray diffraction analysis of **P3'** suggests that it adopted the 12-helical conformation in single crystals similar to **P2'**. The helical structure is stabilized by four *intra*-molecular 12-membered H-bonds. Both *intra*-molecular hydrogen bonds and the stability of 12-helix probably dictate the *Z*-stereochemistry of the double bonds during the migration. The whole process is very clean and no side products were obtained in the reaction.

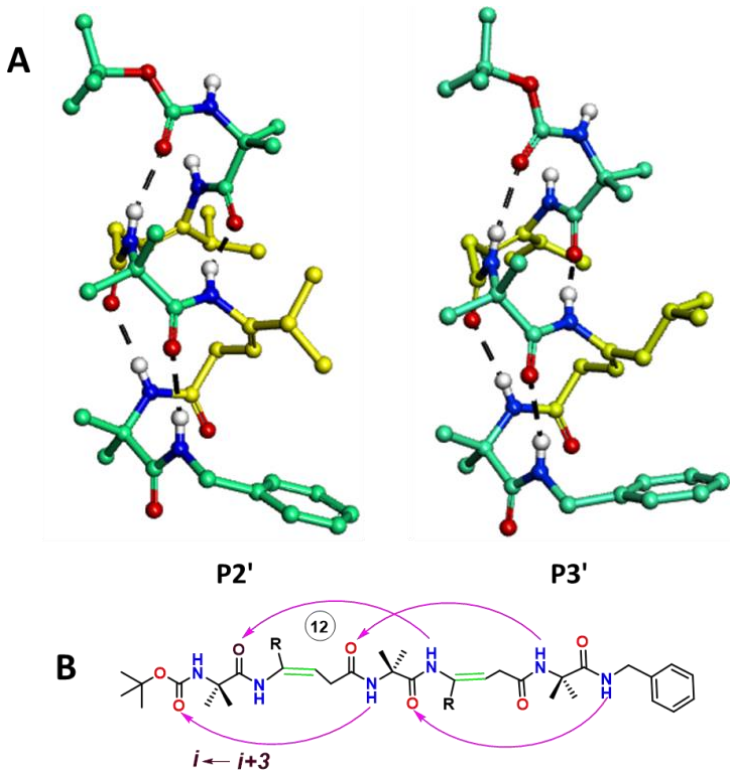

Figure 2: A) Single-crystal X-ray diffraction structures of **P2'** and **P3'**. B) Schematic representation of *intra*-molecular hydrogen bonding pattern in 12-helices.

Table 2: Backbone torsion angles of **P2'** and **P3'** 12-helices.

Peptide	Residue	ϕ (°)	θ_1(°)	θ_2(°)	ψ(°)
Peptide P2'	Aib (1)	55.4			52.9
	*(Z)*d^{3,4}γVal (2)	86.1	-0.5	-108.2	123.9
	Aib (3)	57.3			36.8
	*(Z)*d^{3,4}γVal (2)	103.4	-1.5	-100.5	99.11
	Aib (5)	52.4			46.86
Peptide P3'	Aib (1)	65.7			45.5
	*(Z)*d^{3,4}γVal (2)	62.1	5.1	-105.0	137.2
	Aib (3)	59.2			35.0
	*(Z)*d^{3,4}γLeu (4)	109.7	-7.8	-95.2	99.0
	Aib (5)	51.4			44.3

Table 3. Hydrogen bond parameters of the peptides **P1'**, **P2'** and **P3'** 12-helices.

Acceptor (A)	Donor (D)	D…A (Å)	DH….A (Å)	∠NH…O (deg)	∠CO...H (deg)
Peptide P2'					
BocCO	HNAib(3)	2.86	2.03	162.29	157.49
Aib(1)CO	HN*(Z)*d^{3,4}γVal(4)	2.82	2.03	152.62	141.39
HN*(Z)*d^{3,4}γVal(2)	HNAib(5)	2.84	1.99	169.18	144.81
Aib(3)CO	HNBn	2.96	2.13	161.22	132.11
Peptide P3'					
BocCO	HNAib(3)	3.05	2.20	164.49	156.42
Aib(1)CO	HN*(Z)*d^{3,4}γLeu(4)	2.74	1.95	152.53	144.86
HN*(Z)*d^{3,4}γVal(2)	HNAib(5)	2.91	2.06	170.89	145.36
Aib(3)CO	HNBn	2.99	2.18	156.10	126.28

Further, we examined the solution conformations of these peptides in $CDCl_3$ using 2D NMR. The analysis of the ROESY spectrum of **P3'** revealed the presence of strong sequential $NH_i \leftrightarrow NH_{i+1}$ (d_{NN}) NOEs along the peptide sequence except between the NH2 and NH3 (See in Figure **3**). The distances between the $NH_i \leftrightarrow NH_{i+1}$ are consistent with the distance observed in the crystal structure. Moreover, except NH1 and NH2 no drastic changes in the chemical shift values were observed for other amide protons upon DMSO titration, indicating their involvement in the *intra*-molecular hydrogen bonding. The observed NOEs pattern between $NH_i \leftrightarrow NH_{i+1}$ protons along with the DMSO titration experiment (See in Figure **4**) revealed that peptide **P3'** adopted a stable 12-helix conformations in solution.

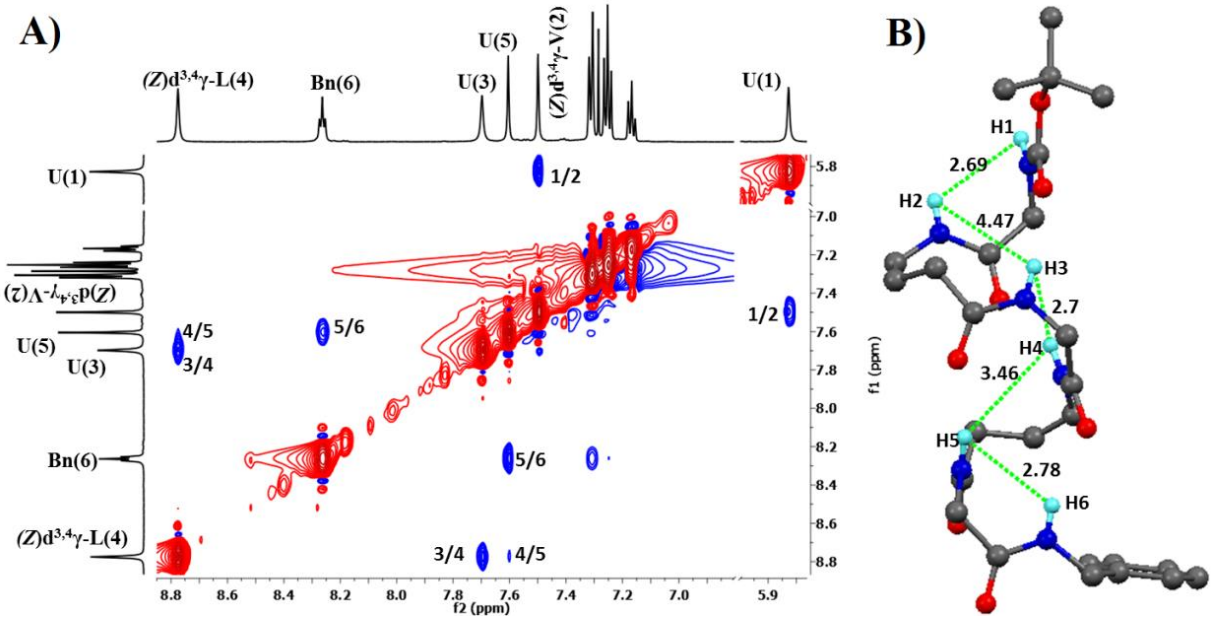

Figure 3: A) Partial ROESY spectrum of **P3'**showing sequential NOEs of NH (*i*) ↔ NH (*i+1*). The sequence of NH protons was assigned based on NOE interactions. B) Crystal structure of **P3'** depicting the NH (*i*) ↔ NH (*i+1*) distance to correlate with observed NOEs.

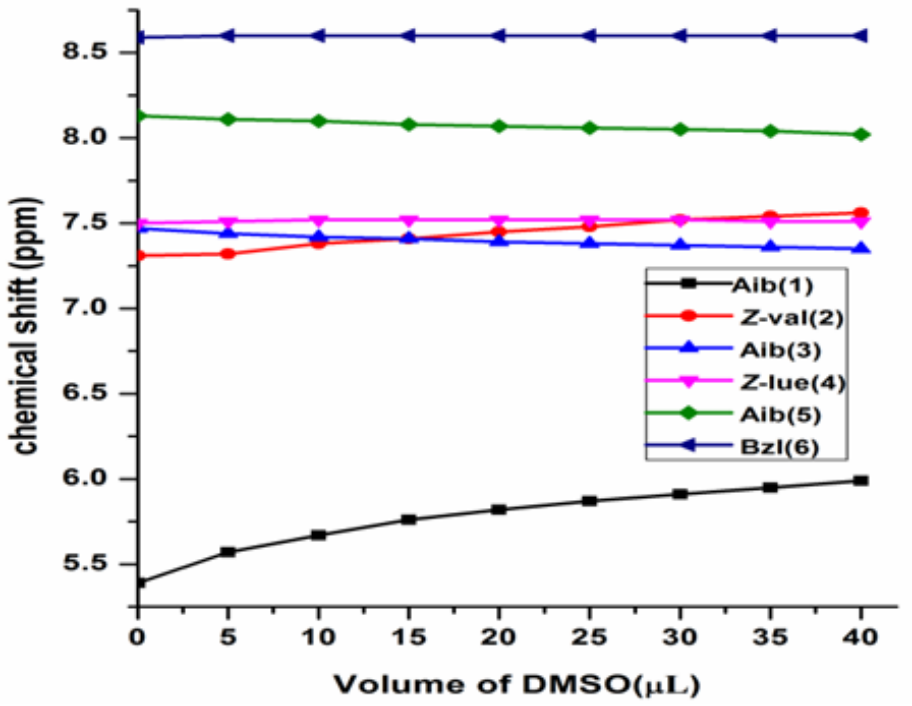

Figure 4: DMSO-d_6 titration of Peptide **P3'** in the $CDCl_3$ solvent.

3.3. α,β→β,γ Double bond migration on (*Z*)-vinylogous amino acids containing helical peptides

Double bond migration transforms the unusual planer structures of α and E-vinylogous γ-amino acid containing α,γ-hybrid peptides into C_{12}-helical structures, we wanted to study the double bond migration possibility in α and *(Z)*-vinylogous γ-amino acids containing α,γ-hybrid peptide, which are known to form a C_{12}-helical structures.[16] We have designed simple tripeptide **P4** which is the analog of **P1**. Synthesis of the **P4** was carried out following the synthetic strategy of the **P1**, used BocHN-Z-d^{2,3}γVal-OEt in place of BocHN-E-d^{2,3}γVal-OEt. Crystallization of **P4** revealed its C_{12}-helical structure, which is consistent with our previous studies on *(Z)*-α,β-unsaturated γ-amino acids containing α,γ-hybrid peptide.[16] Peptide **P4** was treated with base to test the α,β→β,γ double bond migration possibility. Upon treatment with KO^{t}Bu complete transformation of **P4** to **P1'** was observed. The overall process of α,β→β,γ double bond migration in α and *(Z)*-vinylogous γ-amino acids containing α,γ-hybrid peptide transforms the helical conformation into a different helical conformation without disturbing the hydrogen bonding pattern of the peptide backbone. The difference between the conformations of **P4** and **P1'** 12-helices is visualized from torsion angles of **P4** and **P1'**, which are tabulated in Table **4**. The complete transformation process is shown in Scheme **8**.

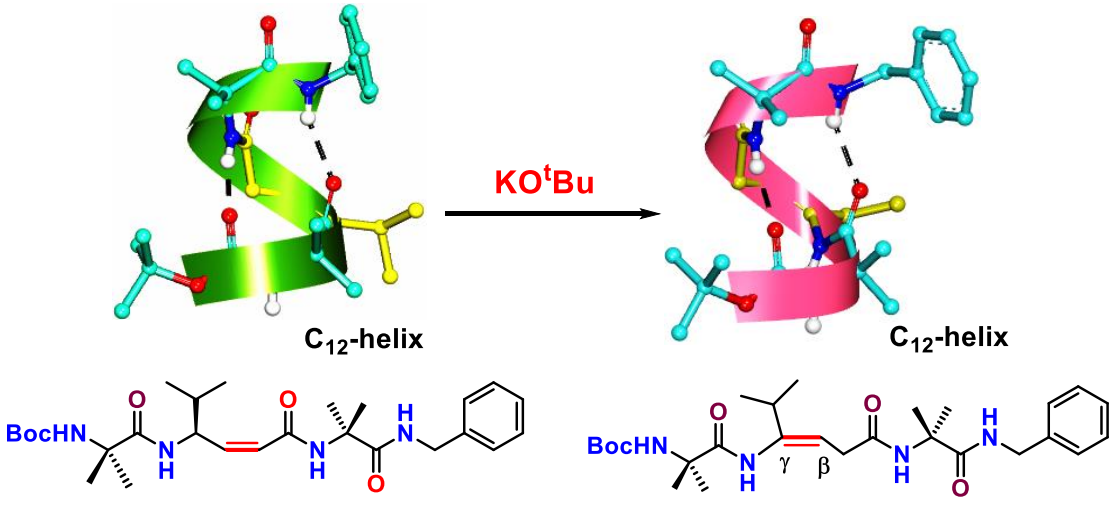

Scheme 8: α,β→β,γ Double bond migration and conformational changes in *(Z)*-α,β-unsaturated γ-amino acids containing α,γ-Hybrid Peptide.

Table 4: Backbone torsion angles of **P4** and **P1'** 12-helices.

Peptide	Residue	ϕ (°)	θ_1(°)	θ_2(°)	ψ(°)
Peptide P4	Aib (1)	-54.67	-	-	-42.52
	(*S,Z*)d^{2,3} γVal (2)	-126.84	100.70	-0.12	-118.95
	Aib (3)	-59.84	-	-	-44.37
Peptide P1'	Aib (1)	-58.5	-	-	-53.6
	*(Z)*d^{3,4}γVal (2)	-86.2	-0.27	110.3	-118.9
	Aib (3)	-60.1	-	-	-31.8

3.4. Analogy of 12-helical conformations with existing α,γ-hybrid peptide 12-helical structures

Recently we and others demonstrated the stable 12-helix conformations from α,γ-hybrid peptides composed of various types of γ-amino acids.[5,20] The list of the γ-amino acids used in the design of α,γ-hybrid peptide 12-helices is given in Table **5**. Except the 4,4-dialkyl γ-amino acids ($\gamma^{4,4}$-amino acids) and *Z*-vinylogous amino acids, other γ-amino acids adopted *gauche*, *gauche* backbone conformations along the C^{γ}-C^{β} and C^{β}-C^{α} bonds, respectively. The 4,4-dialkyl amino acids showed -55 and 140 along the C^{γ}-C^{β} and C^{β}-C^{α} bond, (respectively) [5a] while *Z*-vinylogous γ-amino acids showed 100 and 0 along the C^{γ}-C^{β} and C^{β}-C^{α} bond, respectively.[16] The γ^4-amino acids in the 12-helices presented here adopted entirely different backbone conformation than the list of amino acids given in Table **5**. The *in situ* generated *Z*-β,γ-unsaturated γ-amino acids showed 0 and 104 along the C^{γ}-C^{β} and C^{β}-C^{α} bonds, respectively. Overall these results demonstrated the structural plasticity of 12-helices. The 12-helical conformation is capable of accommodating a variety of γ-amino acids with different local conformations without deviating its overall helical structure. A two-dimensional ϕ and ψ map representing the torsion variables of various γ-amino acids in the 12-helices is shown in Figure **5**.

Table 5: Torsion angles of different γ-amino acids in α,γ-hybrid peptide foldamers[‡]

Peptide	Φ	θ_1	θ_2	Ψ
γ^4-AA12[20b]	-125±6	50±3	62±3	-118±9
$\gamma^{4,4}$-AA[5a]	-54±9	-55±5	140±10	-104±18
$\gamma^{3,3}$-AA[20d]	-125±4	57±5	65±8	-120±11
$\gamma^{2,3,4}$-AA (Cyclic)[20g]	141±9	-56±3	-52±3	111±5
$\gamma^{2,3}$-AA (Cyclic)[20g]	-129±10	55 ±3	55±2	-120±10
$\gamma^{3,4}$-AA[20a]	-120±4	51±6	64±3	-127±3
(Z)$d^{2,3}$ γ^4-AA[16]	-119±10	100±5	0±3	-178±4
(Z)$d^{3,4}$ γ^4-AA (Present Work)	89±27	0±8	-104±9	115±16

[‡] the torsion angles are derived from the X-ray structures

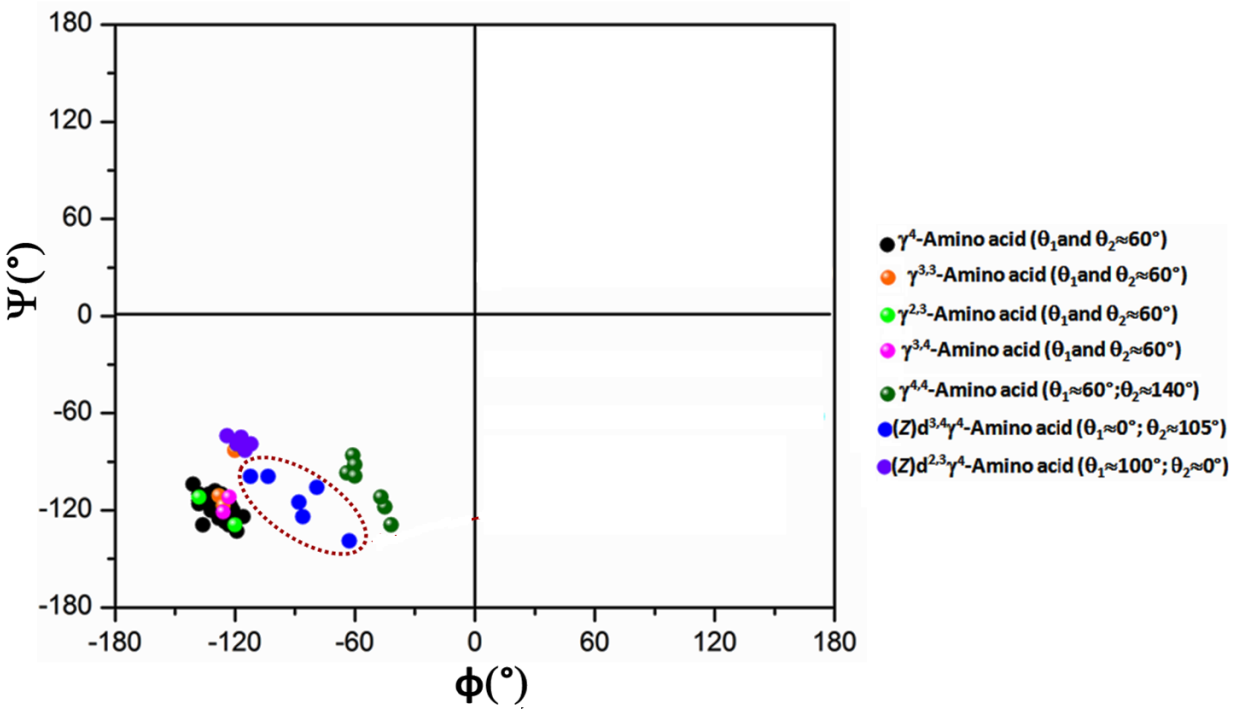

Figure 5: A two-dimensional ϕ and ψ map representing the torsion variables of various γ-amino acids in the 12-helices. The torsion variables of double bond migrated γ-amino acids are highlighted with dotted circle.

3.5. Chemical reactivity of the peptides

3.5.1. Mild acid hydrolysable peptides

As the new 12-helices (**P1'**, **P2'** and **P3'**) consists of γ-amino acids with backbone enamides, we hypothesized that these 12-helices can be sensitive to the protic acids. In order to understand the chemical reactivity of these new 12-helices, we treated the peptide **P1'** solution in THF with dilute HCl (10 % v/v). The peptide slowly brakes down into Boc-Aib-amide and γ-keto-acid protected Aib amide **P6**. The schematic representation of the reaction is shown in Scheme **4**. The reaction is monitored by both HPLC and disappearance of the starting peptide **P1'** and the appearance of **P5** with time is shown in Scheme **9**. Compound **P5** was isolated after the workup of the reaction and analyzed by NMR, MALDI-TOF and X-ray crystallography. As proteases or side-chain specific reagents[21] have been used to site-specifically cleave the peptide bonds, this is the first report showing the cleavage of peptides using dilute HCl. However, the cleavage happens here between the N-C$^{\gamma}$ bond and not the peptide bond.

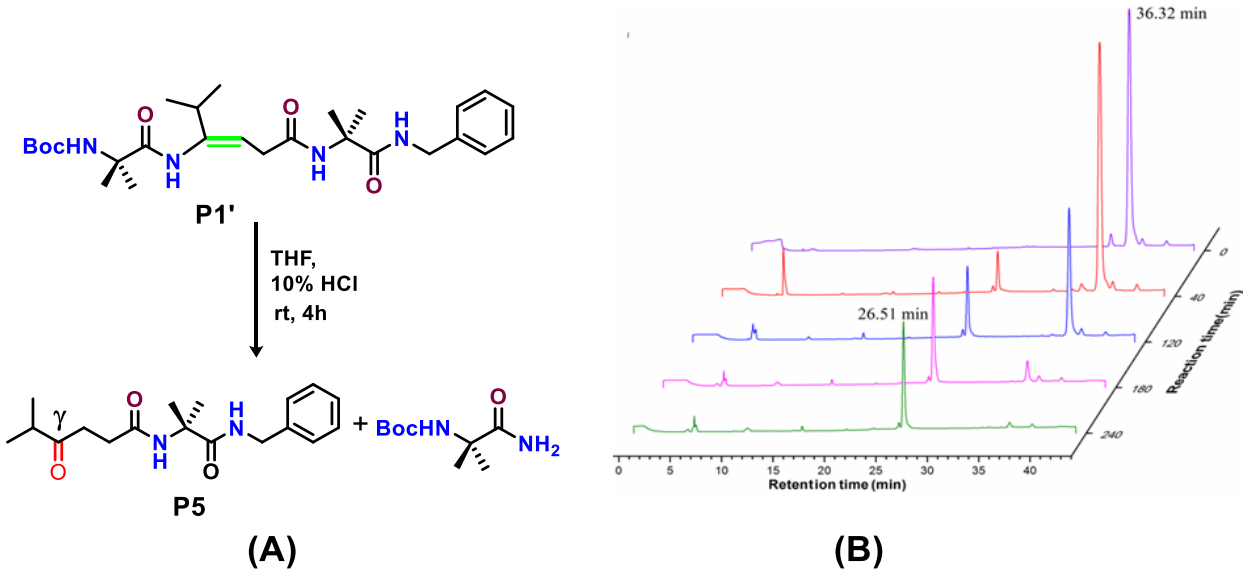

Scheme 9: (A) Acid mediated hydrolysis of **P1'** (B) HPLC reaction profile of **P1'** hydrolysis, the disappearance of the starting peptide **P1'** (retention time 36.32 min) and the appearance of **P5** (retention time 26.51 min) with time is shown.

3.5.2. Stable enamide epoxide peptides

Peptides containing epoxide functionality on the backbone are known to be medicinally important as protease inhibitors namely HIV-protease[22] and cysteine protease inhibitors.[23] The structures of these inhibitors are shown in Scheme **10B**. As the peptides, **P1'** to **P3'** contains double bond in their backbone we wanted to functionalize these peptides by epoxidation. We selected **P1'** and treated with m-CPBA reagent in dry DCM solvent. Treatment of **P1'** with m-CPBA produced stable enamide epoxide containing peptide **P6** in good yield. The epoxidation of peptide **P1'** is shown in Scheme **10A**. The peptide **P6** was characterized by NMR and MALDI-TOF. The result suggests that these kinds of peptides are chemically reactive and can be further functionalized.

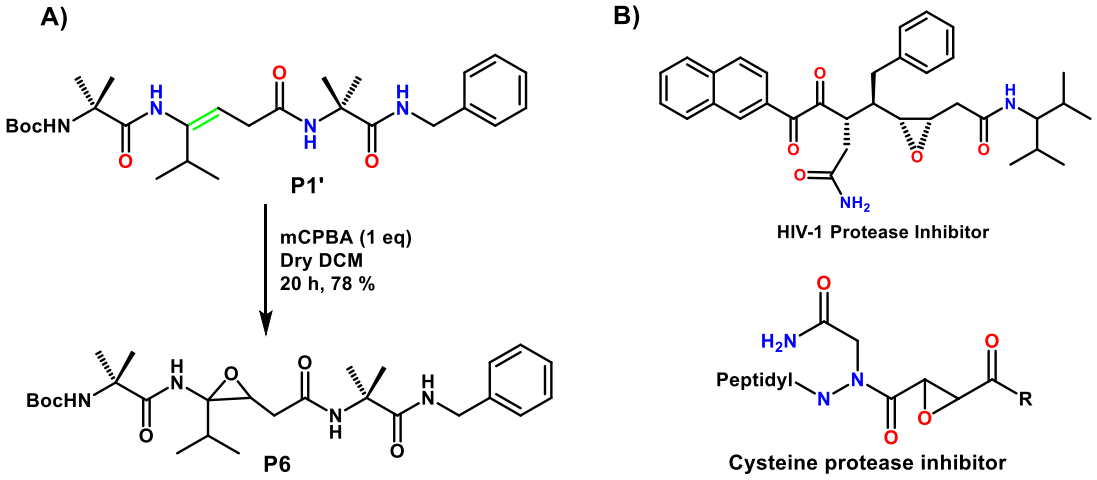

Scheme 10: A) Schematic representation of peptide **P1'** epoxidation B) Chemical structures of peptide epoxides against proteases reported in the literature.

4. Conclusion

In conclusion, we demonstrated the migration of double bonds from α,β→β,γ in hybrid peptides composed of α- and *E*-vinylogous amino acids. The double bond migrated peptides adopted 12-helical structures. In the process of double bond migration, *E*-α,β-unsaturated γ-amino acid residues transformed into *Z*-β,γ-unsaturated γ-amino acid residues. The new γ-amino acid residues adopted entirely new backbone conformation to accommodate into the 12-helix, indicating the structural plasticity of α,γ-hybrid peptide 12-helices composed of 1:1 alternating Aib and γ-residues. The α,β→β,γ double bond migrations phenomenon is not only restricted to

E-α,β-unsaturated γ-amino acid residues containing peptides, also possible to transform *Z*-α,β-unsaturated γ-amino acid residues containing α,γ-hybrid peptide 12-helices into a different 12-helical structures. More importantly, these hybrid peptide helices are unstable towards the protic acids and slowly degrade into amino acid derivatives. Further chemical reactivity of the enamide group of these peptides was used to synthesize epoxide-containing peptides. Though there are many reports in the literature dealing with the migration of double bonds in *E*-vinylogous amino acids in the natural products biosynthesis, this is the first report demonstrating the migration of double bonds and stereochemistry of the migrated double bonds. Overall, the work reported here providing fundamental information on the double bond migrations, conformations of double bond migrated products, structural plasticity of the 12-helix and stability of these new 12-helices.

5. Experimental

General experimental details

All amino acids, TFA, HBTU, HOBt, and DMF were purchased from the commercially available sources. Ethyl acetate and pet-ether (60-80°C) were distilled prior to use. Column chromatography was performed through silica gel .^{1}H NMR were recorded in deuterated solvent on 400 MHz (for ^{13}C, 100 MHz) spectrometer.

Synthetic procedures for peptides

The *N*-protected α,β-unsaturated γ- amino esters (BocHN-(*S*,*E*)d^{2,3}γVal-OEt and BocHN-(*S*,*E*)d^{2,3}γLeu-OEt) were prepared by the previously reported procedures.[24] Peptide synthesis was carried out by the conventional solution-phase synthetic procedure.[25] Boc and ethyl ester protecting groups were used to protect *N*- terminus and *C*- terminus of the peptides, respectively. The Boc group was deprotected by treating with1:1 (v/v) mixture of DCM/TFA and ethyl ester was deprotected by alkaline hydrolysis. The synthetic details of peptides are given below. The purification of final peptides was carried out through silica gel column chromatography using ethyl acetate and petroleum ether solvent gradient as eluent.

A) Synthesis of BocHN-Aib-NH-benzyl (1A)

Boc-Aib-OH (2.923 g, 10 mmol) and HBTU (3.792 g, 10 mmol) were dissolved in 7 mL of DMF, to this solution DIPEA (5.2 mL, 30 mmol) was added. After stirring the reaction mixture for about 5 min at ice-cooled temperature, benzylamine (3.932 mL, 36 mmol) was added. The

reaction mixture was stirred overnight at room temperature. After completion of the reaction (monitored by TLC), work up was done by diluting the reaction mixture with ethyl acetate (150 mL), followed by successive washings with 10% Na_2SO_4 (3 × 50 mL), 10% HCl (3× 50 mL) and brine solution (3 × 50 mL). The organic layer was dried over anhydrous sodium sulfate and concentrated under reduced pressure. The obtained crude compound was dissolved in a minimal amount of ethyl acetate and precipitated out by adding petroleum ether to get a pure, white solid compound.

White solid, Yield = 2.77 g (95%) **^{1}H NMR** (400 MHz, $CDCl_3$) δ 7.39 – 7.13 (m, 5H), 6.77 (s, 1H), 4.91 (s, 1H), 4.44 (d, *J* = 5.6 Hz, 2H), 1.50 (s, 6H), 1.39 (s, 9H).**^{13}C NMR** (100 MHz, $CDCl_3$) δ 174.5, 154.7, 138.4, 128.8, 128.6, 127.8, 127.7, 127.3, 56.9, 43.7, 42.2, 28.3, 25.8. **HRMS** m/z calculated [M+Na] is 315.1684 found 315.1687.

B) Synthesis of peptide Pa and Pb

1) BocHN-Aib-(*S*,*E*)-d^{2,3}γVal-OEt (**Pa**)

2) BocHN-Aib-(*S*,*E*)-d^{2,3}γLeu-OEt (**Pb**)

1) **Boc-group deprotection:** The BocHN-d^{2,3}γXxx-OEt (10 mmol) was treated with a 1:1 (v/v) mixture of DCM/TFA (20 mL). The reaction was stirred for about 30 min. at room temperature. After completion of the reaction (monitored by TLC), the solution was evaporated under reduced pressure. In order to remove excess TFA, the mixture was co-evaporated with DCM thrice. The obtained TFA.H_2N-d^{2,3}γXxx-OEt was utilized for the coupling.

2) **Coupling:** The BocHN-Aib-OH (2.923 g, 10 mmol) and HBTU (3.792 g, 10 mmol) were dissolved in 7 mL of DMF. To this solution, DIPEA (6.93 mL, 40 mmol) was added. After stirring the reaction mixture for 5 min at ice-cooled temperature, this solution is added to a pre-cooled TFA.H_2N-d^{2,3}γXxx-OEt (10 mmol) which was obtained from Boc-group deprotection of BocHN-d^{2,3}γXxx-OEt. The reaction mixture was stirred at room temperature overnight. After the reaction completion (monitored by TLC), the workup was done by following section **A** procedure. The obtained crude compound was dissolved in a minimal amount of ethyl acetate and precipitated out by adding petroleum ether to get white solid peptide, which is further utilized without any further purification.

C) Synthesis of peptide P1and P1a

3) BocHN-Aib-(*S*,*E*)-d^{2,3}γVal- NHBn (**P1**)

4) BocHN-Aib-(*S,E*)-d^{2,3}γLeu-Aib-NHBn (**P1a**)

1) Ethyl ester deprotection: The BocHN-Aib-d^{2,3}γXxx-OEt (5 mmol) was dissolved in ethanol (50 mL) and aqueous NaOH (1*N*, 20 mL) was added drop by drop over the time of 3 min. The stirring was continued up to completion of hydrolysis. The reaction mixture was acidified with aqueous HCl (1*N*) and extracted with ethyl acetate. The organic layer was washed with brine solution and dried over anhydrous sodium sulfate. Concentration of the organic layer gave BocHN-Aib-(*S,E*)-d^{2,3}γXxx-OH, which was further utilized for peptide coupling.

2) Boc-group deprotection: Deprotection of BocHN-Aib-NHBn (1.46 g, 5 mmol) was done by following the previously mentioned procedure (Section **B**). The obtained TFA.H_2N-Aib-NHBn was further utilized for coupling.

3) Coupling: The BocHN-Aib-(*S,E*)-d^{2,3}γXxx-OH (5 mmol) and HBTU (1.89 g, 5 mmol) were dissolved in 7 mL of DMF, to this solution DIPEA (3.46 mL, 20 mmol) was added. After stirring the reaction mixture for 5 min at ice-cooled temperature, the solution was added to a pre-cooled TFA.H_2N-Aib-NHBn (1.46 g, 5 mmol), which was obtained by deprotection of BocNH-Aib-NHBn. The reaction mixture was stirred at room temperature overnight. After completion of the reaction (monitored by TLC), work up was done by following the procedure mentioned in the Section **A**. The obtained crude product was purified through silica gel column by ethyl acetate and petroleum ethers mixture as eluent.

Peptide P1

white solid, Yield = 2.26 g (90%) ^{1}H NMR (400 MHz, $CDCl_3$) δ 7.34 – 7.20 (m, 5H), 7.12 (s, 1H), 6.73 (dd, *J* = 15.2, 5.0 Hz, 1H), 6.67 (s, 1H), 6.32 (s, 1H), 6.05 (d, *J* = 15.2 Hz, 1H), 4.94 (s, 1H), 4.43 (d, *J* = 5.6 Hz, 2H), 4.40 (m, 1H), 1.93-1.84 (m, 1H), 1.58 (s, 6H), 1.49 (s, 6H), 1.42 (s, 9H), 0.91 (dd, *J* = 12.0, 6.8 Hz, 6H). ^{13}C NMR (101 MHz, $CDCl_3$) δ 174.4, 165.6, 155.1, 143.1, 138.5, 128.7, 127.6, 127.4, 124.6, 80.4, 57.7, 57.2, 55.3, 43.7, 32.1, 28.44, 26.4, 25.7, 25.5, 19.2, 18.1. MALDI/TOF-TOF mass [M+Na] calculated *m/z* 525.30 found 525.29.

Peptide P1a

white solid, Yield = 2.32 g (90 %) ^{1}H NMR (400 MHz, $CDCl_3$) δ 7.35 – 7.21 (m, 5H), 7.14 (s, 1H), 6.68 (dd, *J* = 15.2, 4.8 Hz, 1H), 6.43 (s, 1H), 6.31 (s, 1H), 6.07 (d, *J* = 15.1 Hz, 1H), 4.95 (s, 1H), 4.66 – 4.54 (m, 1H), 4.43 (d, *J* = 5.7 Hz, 1H), 1.65 (td, *J* = 13.6, 6.9 Hz, 1H), 1.58 (s, 6H), 1.49 (s, 3H), 1.47 (s, 3H), 1.42 (s, 9H), 1.40-1.37 (m, 2H) , 1. 0.91 (t, *J* = 5.8 Hz, 3H). ^{13}C NMR

(100 MHz, $CDCl_3$) δ 174.4, 174.2, 165.70, 155.0, 144.5, 138.5, 128.7, 127.5, 127.3, 123.4, 80.4, 77.4, 77.1, 76.8, 57.6, 57.0, 48.5, 43.6, 28.4, 26.3, 25.6, 25.4, 24.8, 22.9, 22.0. MALDI/TOF-TOF mass [M+Na] calculated *m/z* 539.3209 found 539.31.

D) Synthesis of pentapeptidesP2 and P3

5) BocHN-Aib-(*S*,*E*)-$d^{2,3}$γVal-Aib-(*S*,*E*)-$d^{2,3}$γVal-Aib- NHBn (**P2**)

6) BocHN-Aib-(*S*,*E*)-$d^{2,3}$γVal-Aib-(*S*,*E*)-$d^{2,3}$γLeu-Aib-NHBn (**P3**)

1) Boc-group deprotection: Boc group of the BocHN-Aib-(*S*,*E*)-$d^{2,3}$γXxx-Aib-NHBn was deprotected by following the previously mentioned (section **A**) procedure to get TFA.H_2N-Aib-(*S*,*E*)-$d^{2,3}$γXxx-Aib-NHBn, which is utilized for coupling.

2) Coupling: The BocHN-Aib-(*S*,*E*)-$d^{2,3}$γXxx-OH (3 mmol) and HBTU (1.13 g, 3 mmol) were dissolved in 5 mL of DMF, to this solution DIPEA (2.07 mL, 12 mmol) was added. After stirring the reaction mixture for 5 min at ice-cooled temperature, the solution is added to a pre-cooled TFA.H_2N-Aib-(*S*,*E*)-$d^{2,3}$γXxx-Aib-NHBn which was obtained by deprotection of BocHN-Aib-(*S*,*E*)-$d^{2,3}$γXxx-Aib-NHBn (3 mmol). The reaction mixture was stirred at room temperature overnight. After the reaction completion (monitored by TLC) workup was done by following the procedure mentioned in the section **A**. The obtained crude product was purified through the silica gel column by using ethyl acetate and petroleum ethers gradient as eluent.

Peptide P2

White solid, Yield = 1.855 g (86 %) ^{1}H NMR (400 MHz, $CDCl_3$) δ 7.35 – 7.29 (m, 2H), 7.27 - 7.20 (m, 4H), 6.97 (s, 1H), 6.81 - 6.72 (m, 3H), 6.63 (s, 1H), 6.15 (d, *J* = 15.4 Hz, 2H), 6.06 (dd, *J* = 15.3, 1.7 Hz, 2H), 5.10 (s, 1H), 4.48 - 4.36 (m, 4H), 1.96 - 1.80 (m, 2H), 1.62 - 1.57 (br, 9H), 1.56 - 1.53(br, 4H), 1.48 (br, 6H), 1.44 (d, *J* = 0.9 Hz, 11H), 0.96 – 0.88 (m, 12H).^{13}C NMR (100 MHz, $CDCl_3$) δ 174.8, 174.8, 174.2, 174.1, 166.2, 165.8, 155.2, 143.4, 143.3, 142.9, 128.7, 127.4, 127.3, 124.5, 124.3, 80.6, 77.2, 57.9, 57.5, 57.2, 55.7, 55.6, 43.7, 32.1, 32.0, 28.5, 26.4, 25.9, 25.6, 19.3, 18.2, 18.2. MALDI/TOF-TOF mas [M+Na] calculated *m/z* 735.4421 found 735.45.

Peptide P3

White solid, Yield = 1.91 g (88 %) ^{1}H NMR (400 MHz, $CDCl_3$) δ 7.32 – 7.17 (m, 5H), 6.81-6.64(m, 5H), 6.40 (bs, 1H), 6.13 (d, *J* = 15.2 Hz, 1H), 6.06 (d, *J* = 15.2 Hz, 1H), 5.03 (s, 1H), 4.57 (s, 1H), 4.41 (bs, 3H), 1.86 (bs, 1H), 1.69-1.58(m, 1H), 1.56 (s, 6H), 1.53 (s, 6H), 1.48 (s, 3H), 1.46 (s, 3H), 1.44-1.40 (m, 11H) 0.98 – 0.83 (m, 12H). ^{13}C NMR (101 MHz, $CDCl_3$) δ 174.7, 174.0, 165.9, 165.9, 161.4, 155.1, 144.2, 143.3, 138.6, 128.7, 127.4, 127.3, 124.5, 123.3, 80.9, 77.2, 60.5, 57.7, 57.6, 57.2, 55.6, 48.8, 43.6, 43.4, 34.0, 32.0, 28.5, 26.5, 26.2, 25.6, 25.4, 25.2, 25.1, 23.0, 22.0, 19.3, 18.2, 14.3. MALDI/TOF-TOF mass [M+Na] calculated *m/z* 749.457 found 749.49.

E) Synthesis of peptide **P1'**

To the mixture of **P1** (1 mmol) and potassium *tert*-butoxide (0.336 g, 3 mmol), dry THF (20 mL) was added at room temperature. The reaction mixture was stirred at room temperature for 4 h. The progress of the reaction was monitored by TLC. After completion, the crude product was purified through silica gel column chromatography using ethyl acetate and petroleum ether gradient.

Peptide **P1'**

White solid, Yield = 0.466 g (93 %) ^{1}H NMR (400 MHz, DMSO) δ 8.60 (s, 1H), 8.11 (t, *J* = 6.1 Hz, 1H), 7.70 (s, 1H), 7.29 – 7.16 (m, 5H), 7.14 (s, 1H), 5.34 (t, *J* = 7.4 Hz, 1H), 4.25 (d, *J* = 6.1 Hz, 2H), 2.76 (d, *J* = 7.4 Hz, 2H), 2.41-2.31 (m, 1H), 1.38 (s, 9H), 1.36 (s, 6H), 1.33 (s, 6H), 0.87 (d, *J* = 6.8 Hz, 6H).^{13}C NMR (100 MHz, DMSO) δ 174.1, 169.8, 154.6, 142.1, 139.9, 128.1, 126.7, 126.3, 115.5, 79.1, 55.9, 55.8, 42.2, 39.5, 34.6, 33.1, 28.2, 25.3, 25.1, 20.5. MALDI/TOF-TOF mass [M+Na] calculated *m/z* 525.30 found 525.30.

F) Synthesis of **P2'** and **P3'**.

To the mixture of **P2'** (1 mmol) and potassium *tert*-butoxide (0.67 g, 6 mmol), dry THF (20 mL) was added at room temperature. The reaction mixture was stirred at room temperature for 6 h. and reaction progress was monitored by TLC. After completion, the crude peptide was purified through silica gel column chromatography using ethyl acetate and petroleum ether. The same procedure was followed for the synthesis of peptide **P3'**.

Peptide P2'

White solid, Yield = 0.648 g (91 %)^{1}H NMR (400 MHz, $CDCl_3$) δ 8.50 (s, 1H), 8.29 (t, *J* = 6.0 Hz, 1H), 7.57 (s, 1H), 7.47 (s, 1H), 7.33 – 7.28 (m, 3H), 7.23 (t, *J* = 7.5 Hz, 2H), 7.14 (t, *J* = 7.2 Hz, 1H), 5.58 – 5.47 (m, 2H), 5.43 (s, 1H), 4.43 (d, *J* = 6.0 Hz, 2H), 2.81 (t, *J* = 7.6 Hz, 3H), 2.36 - 2.21 (m, 2H), 1.53 (s, 6H), 1.45 (d, *J* = 2.0 Hz, 12H), 1.43 (s, 9H), 0.94 (d, *J* = 6.8 Hz, 6H), 0.85 (d, *J* = 6.9 Hz, 6H).^{13}C NMR (100 MHz, $CDCl_3$) δ 175.7, 175.4, 175.1, 170.2, 155.2, 143.0, 142.3, 139.9, 128.1, 127.5, 126.4, 118.9, 118.8, 81.2, 77.2, 57.0, 56.9, 56.9, 43.4, 35.0, 34.7, 28.5, 25.6, 25.5, 25.3, 20.6. MALDI/TOF-TOF mass [M+Na] calculated *m/z* 735.4421 found 735.47.

Peptide P3'

White solid, Yield = 0.721 g (90 %)^{1}H NMR (400 MHz, $CDCl_3$) δ 8.74 (s, 1H), 8.25 (s, 1H), 7.67 (s, 1H), 7.59 (s, 1H), 7.50 (s, 1H), 7.31 (d, *J* = 7.2 Hz, 2H), 7.25 (t, *J* = 7.5 Hz, 2H), 7.16 (t, *J* = 7.2 Hz, 1H), 5.80 (s, 1H), 5.55 (t, *J* = 8.4 Hz, 1H), 5.37 (t, *J* = 8.3 Hz, 1H), 4.44 (d, *J* = 6.0 Hz, 2H), 2.81 (t, *J* = 8.8 Hz, 4H), 2.33 (sept, *J* = 6.8 Hz,1H), 1.77 (d, *J* = 7.0 Hz, 2H), 1.70-1.61(m, 2H), 1.53 (s, 6H), 1.47-1.41 (m, 21H), 0.95 (d, *J* = 6.8 Hz, 6H), 0.78 (d, *J* = 6.5 Hz, 6H).^{13}C NMR (100 MHz, $CDCl_3$) δ 175.6, 175.2, 175.0, 170.3, 170.1, 155.2, 142.1, 139.6, 137.5, 128.0, 127.5, 126.4, 121.1, 118.6, 80.7, 77.3, 77.0, 76.7, 56.8, 56.7, 56.7, 44.6, 43.2, 36.1, 35.0, 34.7, 28.3, 25.5, 25.5, 25.3, 25.1, 22.3, 20.4. MALDI/TOF-TOF mass [M+Na] calculated *m/z* 749.457 found 749.49.

G) Synthesis of P4

Peptide **P4** was synthesized following the synthetic procedure of **P1**. Here we used BocHN-Z-$d^{2,3}$γVal-OEt in the place BocHN-E-$d^{2,3}$γVal-OEt.

Characterization: White solid, Yield = 2.18 g (87 %) 1H NMR (400 MHz, DMSO-D6) δ 8.19 (s, 1H), 8.13 (s, 1H), 7.52 (d, J = 8.8 Hz, 1H), 7.27 - 7.24 (m, 4H), 7.21 – 7.14 (m, 1H), 6.82 (d, J = 32.7 Hz, 1H), 5.84 (d, J = 11.7 Hz, 1H), 5.71 (t, J = 10.2 Hz 1H), 4.91 - 4.79 (m, 1H), 4.27 (d, J = 6.1 Hz, 2H), 1.84 -1.71(m, 1H), 1.39 (s, 6H), 1.37 (s, 9H), 1.28 (d, J = 7.5 Hz, 6H), 0.8 - 0.7 (m, 6H). 13C NMR (100 MHz, DMSO-D6) δ 174.1, 174.0, 165.1, 154.2, 140.3, 140.0, 128.0, 126.8, 126.3, 124.5, 78.1, 57.7, 56.0, 55.8, 52.4, 42.3, 39.5, 31.9, 28.2, 25.5, 25.0, 19.2, 18.4. MALDI/TOF-TOF mas [M+Na] calculated m/z 525.30 found 525.29.

H) Acid hydrolysis of peptide P1'

Peptide **P1'** (200 mg, 0.4 mmol) was dissolved in THF (7 mL) and 10 % HCl (2 mL) was added. The reaction mixture was stirred for 4 h. The progress of the reaction was monitored by RP-HPLC using MeOH/H_2O solvent system. After completion of the reaction, THF was evaporated and diluted with water (15 mL). The compound was extracted with Ethyl acetate (3 ×15 mL). The combined organic layer was washed with brine solution (2 × 20) and dried over anhydrous sodium sulfate. The organic layer was concentrated to get crude compound, which was purified through a silica gel column using ethyl acetate and petroleum ether gradient.

HPLC reaction progress monitoring: Reaction mixture (200 μL) was injected into HPLC in time intervals of 40, 120, 180 and 240 min. and the compound was eluted using Methanol/water gradient through the C18 column.

Peptide P5

Characterization: White solid; Yield = 0.112 g (88 %); ^{1}H NMR (400 MHz, $CDCl_3$) δ 7.34 – 7.18 (m, 5H), 7.15 (s, 1H), 6.10 (s, 1H), 4.40 (d, *J* = 5.9 Hz, 2H), 2.80 (t, *J* = 6.0 Hz, 2H), 2.49 (hept, *J* = 6.9 Hz, 1H), 2.31 (t, *J* = 6.0 Hz, 2H), 1.54 (s, *J* = 13.2 Hz, 6H), 0.98 (d, *J* = 6.9 Hz, 6H).^{13}C NMR (101 MHz, $CDCl_3$) δ 215.3, 174.3, 172.0, 138.8, 128.6, 127.6, 127.2, 77.2, 57.6, 43.7, 40.7, 35.6, 30.8, 25.8, 18.3. HRMS m/z calculated [M+H] is 319.2022 found 319.2024.

I) Synthesis of peptide P6

Peptide **P1'** (100 mg, 0.2 mmol) was dissolved in dry DCM (5 mL) and m-chloroperoxybenzoic acid (0.0344 g, 0.2 mmol, 1eq). The reaction mixture was stirred for 20 h, the reaction mixture was concentrated under reduced pressure. The crude obtained was purified through a silica gel column by using ethyl acetate and petroleum ether gradient as eluent.

White solid, Yield = 0.08 g (78 %) ^{1}H NMR (400 MHz, DMSO-D_6) δ 8.06 (s, 1H), 8.01 (t, *J* = 5.9 Hz, 1H), 7.30 – 7.25 (m, 3H), 7.23 - 7.16 (m, 3H), 5.40 (t, *J* = 6.1 Hz, 1H), 4.24 (d, *J* = 6.1 Hz, 2H), 3.00 – 2.90 (m, 1H), 2.70 (dd, *J* = 15.6, 5.5 Hz, 1H), 2.60 (dd, *J* = 15.6, 6.7 Hz, 1H), 1.35 (d, *J* = 5.1 Hz, 15H), 1.33 (d, *J* = 3.3 Hz, 6H), 1.00 (d, *J* = 6.8 Hz, 3H), 0.94 (d, *J* = 6.8 Hz, 3H). ^{13}C NMR (100 MHz, DMSO-D_6) δ 174.4, 174.1, 168.2, 155.1, 140.3, 128.5, 127.2, 126.7, 78.6, 74.2, 56.5, 55.8, 55.7, 42.7, 40.5, 40.3, 40.1, 39.9, 39.7, 39.5, 39.3, 28.6, 25.9, 25.6, 18.6, 18.4. HRMS m/z calculated [M+K] is 557.274 found 557.294.

6. References

1. (a) Hecht, S.; Huc, I. *Foldamers: Structure, Properties and Applications*, Wiley-VCH, Weinheim, **2007**. (b) Seebach, D.; Beck, A. K.; Bierbaum, D. J. *Chem. Biodiversity* **2004**, *1*, 1111. (c) Fülöp, F.; Martinek, T. A. *Chem. Soc. Rev.* **2012**, ***41***, 687. (d) Guichard, G.; Huc, I. *Chem. Commun*. **2011**, *47*, 5933. (e) Horne, W. S.; Gellman, S. H. *Acc. Chem. Res*. **2008**, *41*, 1399. (f) Goodman, C. M.; Choi, S.; Shandler, S.; DeGrado, W. F. *Nat. Chem. Biol.* **2007**, *3*, 252 (g) Vasudev, P. G.; Chatterjee, S.; Shamala, N.; Balaram, P. *Chem. Rev*. **2011**, *111*, 657.
2. (a) Seebach, D.; Gardiner, J. *Acc. Chem. res*. **2008**, *41*, 1366-1375. (b) Gellman, S. H. *Acc. Chem. Res*. **1998**, *31*, 173.
3. (a) Hanessian, S.; Luo, X.; Schaum, R.; Michnick, S. *J. Am. Chem. Soc*. **1998**, *120*, 8569. (b) Seebach, D.; Brenner, M.; Rueping, B.; Schweizer, M.; Jaun, B. *Chem. Commun.* **2001**, 207. (c) Basuroy, K.; Dinesh, B.; Reddy, M. B. M.; Chandrappa, S.; Raghothama, S.; Shamala, N.; Balaram, P. *Org. Lett*. **2013**, *15*, 4866.
4. (a) Pilsl, L. K. A.; Reiser, O. *Amino Acids* **2011**, *41*, 709-718. (b) Sharma, G. V. M.; Nagendar, P.; Jayaprakash, P.; Krishna, P. R.; Ramakrishna, K. V. S.; Kunwar, A. C. *Angew. Chem. Int. Ed.* **2005**, *44*, 5878. (c) Schmitt, M. A.; Choi, S. H.; Guzei, I. A.; Gellman, S. H. *J. Am. Chem. Soc.* **2005**, *127*, 13130. (d) Schmitt, M. A.; Choi, S. H.; Guzei, I. A.; Gellman, S. H. *J. Am. Chem. Soc.* **2006**, *128*, 4538. (e) Choi, S. H.; Guzei, I. A.; Spencer, L. C.; Gellman, S. H. *J. Am. Chem. Soc.* **2008**, *130*, 6544. (f) Choi, S. H.; Guzei, I. A.; Gellman, S. H. *J. Am. Chem. Soc.* **2007**, *129*, 13780. (g) Lee, M.; Shim, J.; Kang, P.; Guzei, I. A.; Choi, S. H. *Angew. Chem. Int. Ed.* **2013**, *52*, 12564.
5. (a) Misra, R.; Saseendran, A.; George, G.; Veeresh, K.; Raja, K. M. P.; Raghothama, S.; Hofmann, H.-J.; Gopi, H. N. *Chem. Eur. J.* **2017**, *23*, 3764. (b) Fisher, B.; Guo, L. B.; Dolinar, S.; Guzei, I. A.; Gellman, S. H. *J. Am. Chem. Soc.* **2015**, *137*, 6484. (c) Fisher, B. F.; Gellman, S. H. *J. Am. Chem. Soc.* **2016**, *138*, 10766. (d) Sonti, R.; Dinesh, B.; Basuroy, K.; Raghothama, S.; Shamala, N.; Balaram, P. *Org. Lett.* **2014**, *16*, 1656. (e) Chatterjee, S.; Vasudev, P. G.; Ragothama, S.; Ramakrishna, C.; Shamala, N.; Balaram, P. *J. Am. Chem. Soc.* **2009**, *131*, 5956. (f) Basuroy, K.; Dinesh, B.; Shamala, N.; Balaram, P. *Angew. Chem. Int. Ed.* **2012**, *51*, 8736. (g) Guo, L.; Zhang, W.; Guzei, I. A.;

Spencer, L. C.; Gellman, S. H. *Org. Lett.* **2012**, *14*, 2582. (h) Sharma, G. V. M.; Jadhav, V. B.; Ramakrishna, K. V. S.; Jayaprakash, P.; Narsimulu, K.; Subash, V.; Kunwar, A. C. *J. Am. Chem. Soc.* **2006**, *128*, 14657. (i) Baldauf, C.; Gunther, R.; Hofmann, H.-J. *J. Org. Chem.* **2006**, *71*, 1200.

6. (a) Grison, C. M.; Robin, S.; Aitken, D. J. *Chem. Commun.* **2016**, *52*, 7802-7805. (b) Rezaei Araghi, R.; Jäckel, C.; Cölfen, H.; Salwiczek, M.; Völkel, A.; Wagner, S. C.; Wieczorek, S.; Baldauf, C.; Koksch, B. *ChemBioChem* **2010**, *11*, 335. (c) Guo, L.; Almeida, A. M.; Zhang, W.; Reidenbach, A. G.; Choi, S. H.; Guzei, I. A.; Gellman, S. H. *J. Am. Chem. Soc.* **2010**, *132*, 7868.
7. (a) Appella, D. H.; Christianson, L. A.; Karle, I. L.; Powell, D. R.; Gellman, S. H. *J. Am. Chem. Soc.* **1996**, *118*, 13071. (b) Shin, Y.-H.; Gellman, S. H. *J. Am. Chem. Soc.* 2018, **140**, 1394. (c) Fernandes, C.; Faure, S.; Pereira, E.; Thery, V.; Declerck, V.; Guillot, R.; Aitken, D. J. *Org. Lett*. **2010**, *12*, 3606. (d) Mandity, I. M.; Fulop, L.; Vass, E.; Toth, G. K.; Martinek, T. A.; Fulop, F. *Org. Lett*. **2010**, *12*, 5584.
8. Bandyopadhyay, A.; Gopi, H. N. *Org. Lett*. **2012**, *14*, 2770.
9. Bandyopadhyay, A.; Mali, S. M.; Lunawat, P.; Raja, K. M. P.; Gopi, H. N. *Org. Lett.* **2011**, *13*, 4482.
10. Bandyopadhyay, A.; Misra, R.; Gopi, H. N. *Chem. Commun.* **2016**, *52*, 4938.
11. Ganesh Kumar, M.; Benke, S. N.; Raja, K. M. P.; Gopi, H. N. Chem. Commun. **2015**, *51*, 13397.
12. Misra, R.; Dey, S.; Reja, R. M.; Gopi, H. N. *Angew. Chem. Int. Ed*. **2018**, *57*, 1057.
13. Hagihara, M.; Anthony, N. J.; Stout, T. J.; Clardy, J.; Schreiber S. L. *J. Am. Chem. Soc.* **1992**, *114*, 6568.
14. (a) Grison, C.; Coutrot, P.; Ge´neve, S.; Didierjean, C.; Marraud, M. *J. Org. Chem.* **2005**, *70*, 10753. (b) Grison, C.; Ge´neve, S.; Halbin, E.; Coutrot, P. *Tetrahedron* **2001**, *57*, 4903.
15. (a) Mathieu, L.; Legrand, B.; Deng, C.; Vezenkov, L.; Wenger, E.; Didierjean, C.; Amblard, M.; Averlant-Petit, M.-C.; Masurier, N.; Lisowski, V.; Martinez, J.; Maillard, L. T. *Angew. Chem. Int. Ed.* **2013**, *52*, 6006. (b) Grison, C.; Coutrot, P.; Géneve, S.; Didierjean, C.; Marraud, M. *J. Org. Chem.* **2005**, *70*, 10753. (c) Baldauf, C.; Gunther, R.; Hofmann, H.-J. *J. Org. Chem.* **2005**, *70*, 5351.

16. Ganesh Kumar, M.; Thombare, V. J.; Katariya, M. M.; Veeresh, K.; Raja, K. M. P.; Gopi, H. N. *Angew. Chem. Int. Ed*. **2016**, *55*, 7847.

17. (a) Lohr, F.; Jenniches, I.; Frizler, M.; Meehan, M. J.; Sylvester, M.; Schmitz, A.; Gütschow, M.; Dorrestein, P. C.; König, G. M.; Schäberle, T. F. *Chem. Sci.* **2013**, *4*, 4175. (b) Yu, T. W.; Bai, L.; Clade, D.; Hoffmann, D.; Toelzer, S.; Trinh, K. Q.; Xu, J.; Moss, S. J.; Leistner, E.; Floss, H. G. *Proc. Natl. Acad. Sci. U. S. A*. **2002**, *99*, 7968. (c) Gay, D. C.; Spear, P. J.; Keatinge-Clay, A. T. *ACS Chem. Biol*. **2014**, *9,* 2374. (d) Helfrich, E. J. N.; Piel, J. *Nat. Prod. Rep*. **2016**, *33*, 231. (e) Taft, F.; Brünjes, M.; Knobloch, T.; Floss, H. G.; Kirschning, A. *J. Am. Chem. Soc.* **2009**, *131*, 3812.

18. Ganesh Kumar, M.; Gopi, H. N. *Org. Lett.* **2015**, *17*, 4738.

19. (a) Karle, I. L.; Balaram, P. *Biochemistry* **1990**, *29*, 6747. (b) Crisma, M.; Formaggio, F.; Moretto, A.; Toniolo, C. *Biopolymers* **2006**, *84*, 3.

20. (a) Bandyopadhyay, A.; Malik, A.; Ganesh Kumar, M.; Gopi, H. N. *Org. Lett*. **2014**, *16*, 294. (b) Jadhav, S. V.; Bandyopadhyay, A.; Gopi, H. N. *Org. Biomol. Chem*. **2013**, *11*, 509 (c) Fisher, B.F.; Gellman, S.H. *J. Am.Chem. Soc.* **2016**, *138*, 10766. (d) Vasudev, P. G.; Ananda, K.; Chatterjee, S.; Aravinda, S.; Shamala, N.; Balaram, P. *J. Am. Chem. Soc.* **2007**, *129*, 4039. (e) Vasudev, P.G.; Chatterjee, S.; Ananda, K.; Shamala, N.; Balaram, P. *Angew. Chem. Int. Ed.* **2008**, *47*, 6430; *Angew. Chem.* **2008**, *120*, 6530. (f) Chatterjee, S.; Vasudev, P. G.; Ananda, K.; Raghothama, S.; Shamala, N.; Balaram, P. *J. Org. Chem.* **2008**, *73*, 6595. (g) Guo, L.; Chi, Y. G.; Almeida, A. M.; Guzei, I. A.; Parker, B. K.; Gellman, S. H. *J. Am. Chem. Soc*. **2009**, *131*, 16018. (h) Sharma, G.V.M.; Chandramouli, N.; Choudhary, M.; Nagendar, P.; Ramak-rishna, K.V.S.; Kunwar, A. C.; Schramm, P.; Hofmann, H.-J. *J. Am.Chem.Soc.* **2009**, *131*, 17335.

21. (a) Milović, N. M.; Kostić, N. M. *J. Am. Chem. Soc.* **2002**, *124*, 4759-4769. (b) Ly, H. G. T.; Fu, G.; Kondinski, A.; Bueken, B.; De Vos, D.; Parac-Vogt, T. N. *J. Am. Chem. Soc.* **2018**, *140*, 6325.

22. Lee, C. S.; Choy, N.; Park, C.; Choi, H.; Son, Y. C.; Kim, S.; Ok, J. H.; Yoon, H.; Kim, S. C.; *Bioorg. Med. Chem. Lett.* **1996**, *6*, 589.

23. Ovat, A.; Muindi, F.; Fagan, C.; Brouner, M.; Hansell, E.; Dvorák, J.; Sojka, D.; Kopácek, P.; McKerrow, J. H.; Caffrey, C. R.; Powers, J. C. *Journal of medicinal chemistry* **2009**, *52*, 7192.

24. Mali, S. M.; Bandyopadhyay, A.; Jadhav, S. V.; Ganesh Kumar, M.;Gopi, H. N. *Org. Biomol. Chem*. **2011**, *9*, 6566.
25. Bodanszky, M.; Bodanszky, A. *The Practice of Peptide Synthesis*, Springer-Verlag, Berlin, **1984**.

7. Appendix

1. Crystallographic information of peptides

All the crystals of peptides were grown by slow evaporation of solutions of methanol room temperature. The X-ray data were collected at 100 Kon diffractometer using MoK_{α} radiation (λ = 0.71073 Å). The structures were obtained by direct methods using the SHELXS-97 program.

Table 1: Crystal and diffraction parameters of peptides **P1**, **P1'**, and **P2'**.

	P1	**P1'**	**P2'**
Chemical formula	C_{27} H_{42} N_4 O_5	C_{27} H_{42} N_4 O_5	C_{38} H_{60} N_6 O_7
Molecular weight	502.656	502.656	712.9330
Crystal habit	Clear	Clear	Clear
Crystal size (nm)	0.3× 0.3× 0.3	0.3× 0.3× 0.4	0.3×0.3× 0.3
Crystallization solvent	MeOH/Wate r	MeOH/Water	MeOH/Water
Space group	P212121	P -1	P -1
a (Å)	9.483(15)	9.835(2)	11.521(2)
b (Å)	12.190(17)	17.812(3)	12.939(3)
c (Å)	24.53(3)	18.650(3)	15.958(3)
α (°)	90	81.438(5)	106.320(5)
β(°)	90	76.668(7)	94.431(5)
γ(°)	90	78.939(4)	108.235(5)
Volume (Å^3)	2835.61	3101.2(10)	2132.5(7)
Z	4	2	2
Molecules/asym.unit	1	2	1
Density (g/cm^3)(cal)	1.177	1.144	1.185
F (000)	1088.0	1158.0	824.0
Radiation	Mo K_α	Mo K_α	Mo K_α
2θ Max. (^{o})	49.992	56.02	50.056
μ mm^{-1}	0.081	0.080	0.084
Reflections (cal)	4995	14987	7544
Parameters	334	706	497
R (reflections)	0.0476(3641)	0.0651(7827)	0.0543(5335)
wR2 (Reflections)	0.1442(4995)	0.2058(13267)	0.1422(7507)
Goodness-of- fit (S)	0.878	0.939	1.036

Table S2: Crystal and diffraction parameters for peptides **P3', P4** and **P5**.

	P3'	**P4**	**P4**
Chemical formula	C_{39} H_{62} N_6 O_7	C_{27} H_{42} N_4 O_5	$C_{18}H_{26}N_2O_3$
Molecular weight	726.960	502.656	318.41
Crystal habit	Clear	clear	Clear
Crystal size (nm)	0.4×0.2× 0.3	0.4X0.2X0.3	0.3X0.3X0.3
Crystallization solvent	MeOH/Water	MeOH/Water	MeOH/Water
Space group	P -1	P21	P -1
a (Å)	16.557(9)	9.830(3)	11.740(7)
b (Å)	22.957(13)	14.384(4)	11.775(6)
c (Å)	23.243(13)	10.341(3)	14.050(8)
α (dge)	91.007(14	90	100.239(12)
β (dge)	100.512(13)	91.869(7)	90.054(14)
γ (dge)	100.436(13)	90	109.887(13)
Volume $(Å)^3$	8531(8)	1461.4(7)	1793.4(17)
Z	8	2	4
Molecules/asym.unit	4	1	2
Density (g/cm^3)(cal)	1.132	1.179	1.179
F (000)	3152.0	560.0	688.0
Radiation	Mo K_α	Mo K_α	Mo K_α
2θ Max. (^{o})		56.86	53.462
μ mm^{-1}	0.078	0.083	0.080
Reflections (cal)	31996	7361	7603
Parameters	1925	158	424
R (reflections)	0.0864(131)	0.0893(696)	0.0952(3996)
wR2 (Reflections)	0.2273(315)	0.0946(158)	0.2179(7596)
Goodness-of- fit (S)	0.960	1.172	1.470

2. ^{1}H, ^{13}C NMR and Mass Spectra of Compounds

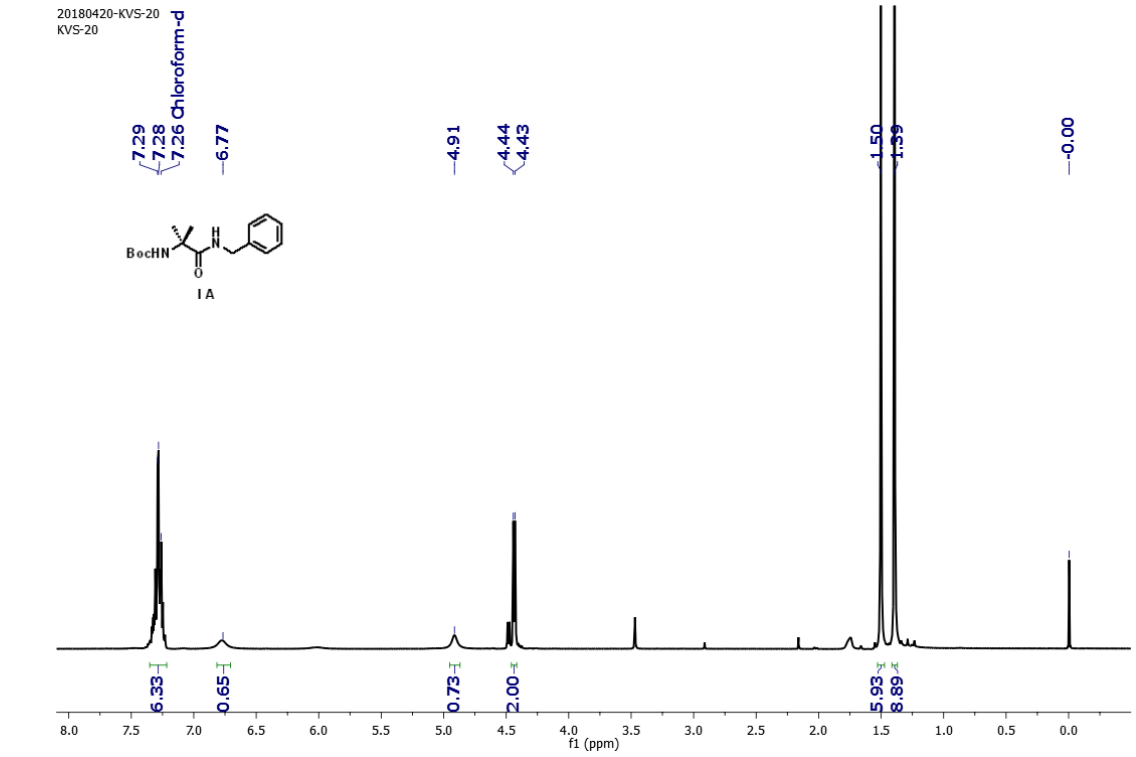

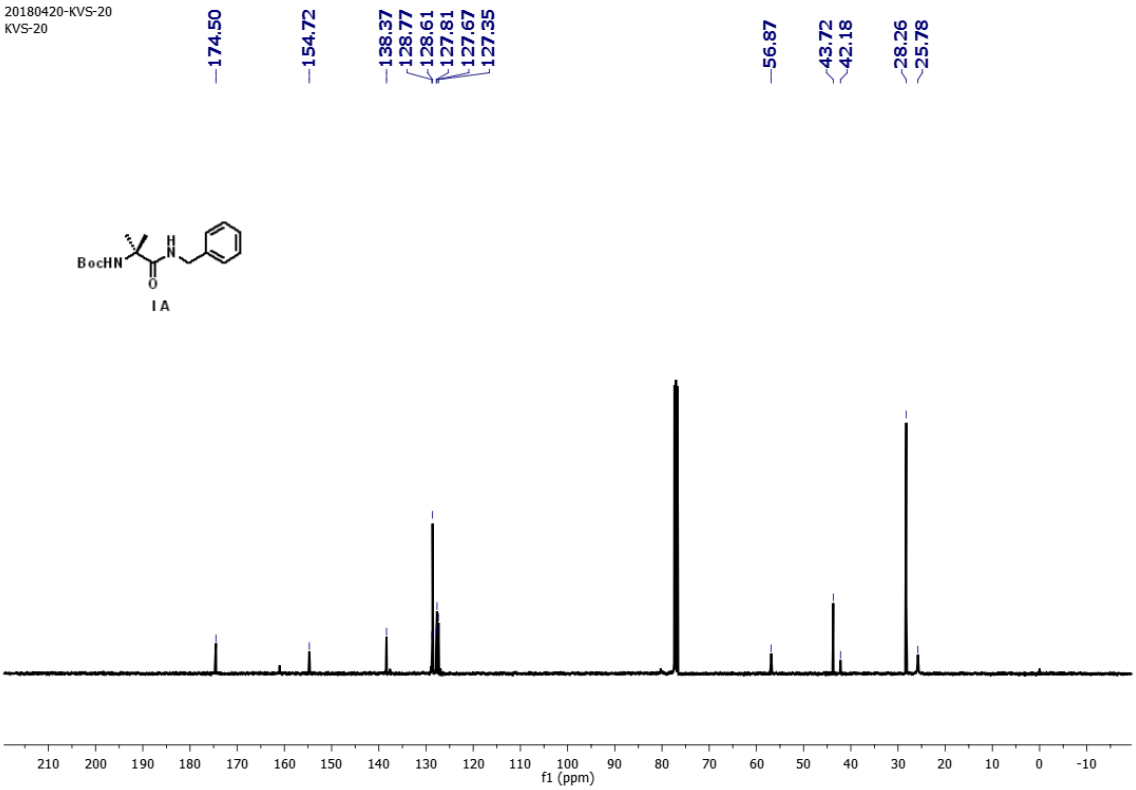

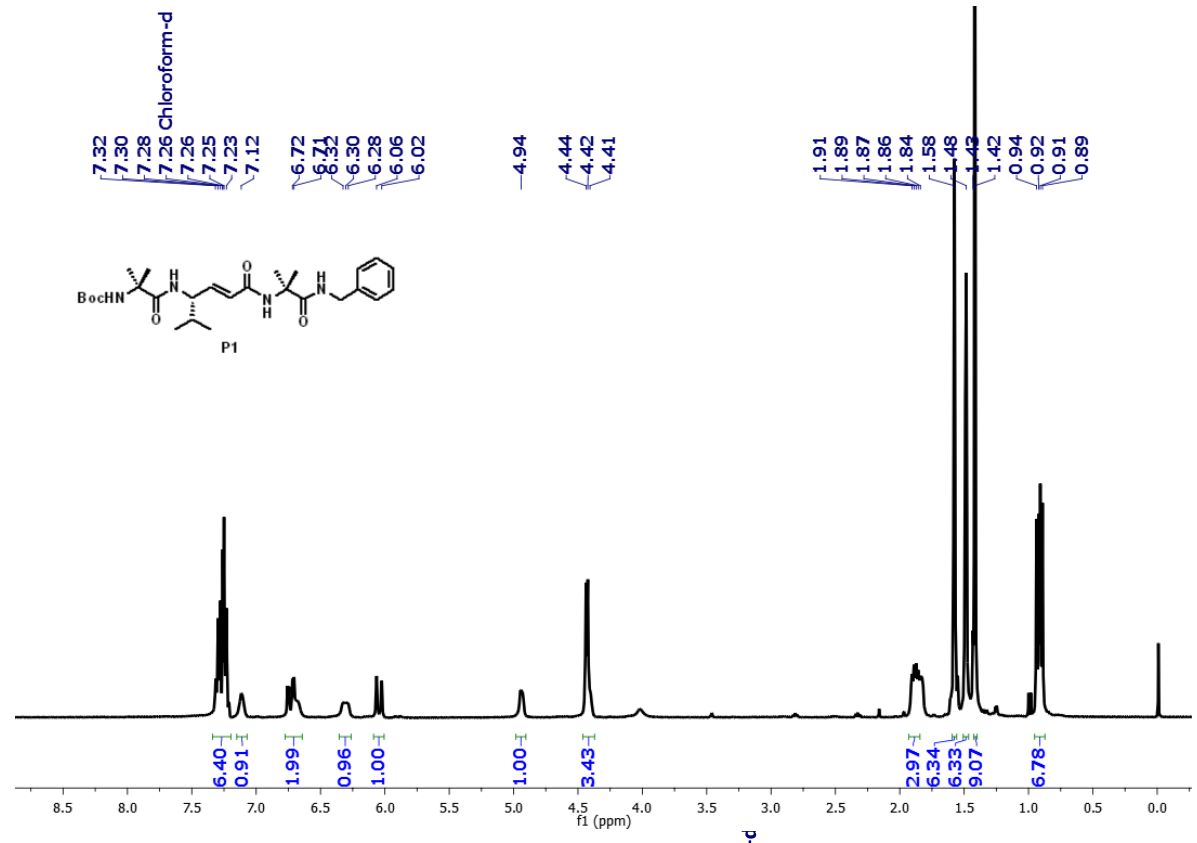
7.32
7.30
7.28
7.26 Chloroform-d
7.26
7.25
7.23
7.12
6.72
6.71
6.32
6.30
6.28
6.06
6.02
4.94
4.44
4.42
4.41
1.91
1.89
1.87
1.86
1.84
1.58
1.48
1.43
1.42
0.94
0.92
0.91
0.89
BocHN
P1
6.40
0.91
1.99
0.96
1.00
1.00
3.43
2.97
6.34
6.33
9.07
6.78
f1 (ppm)

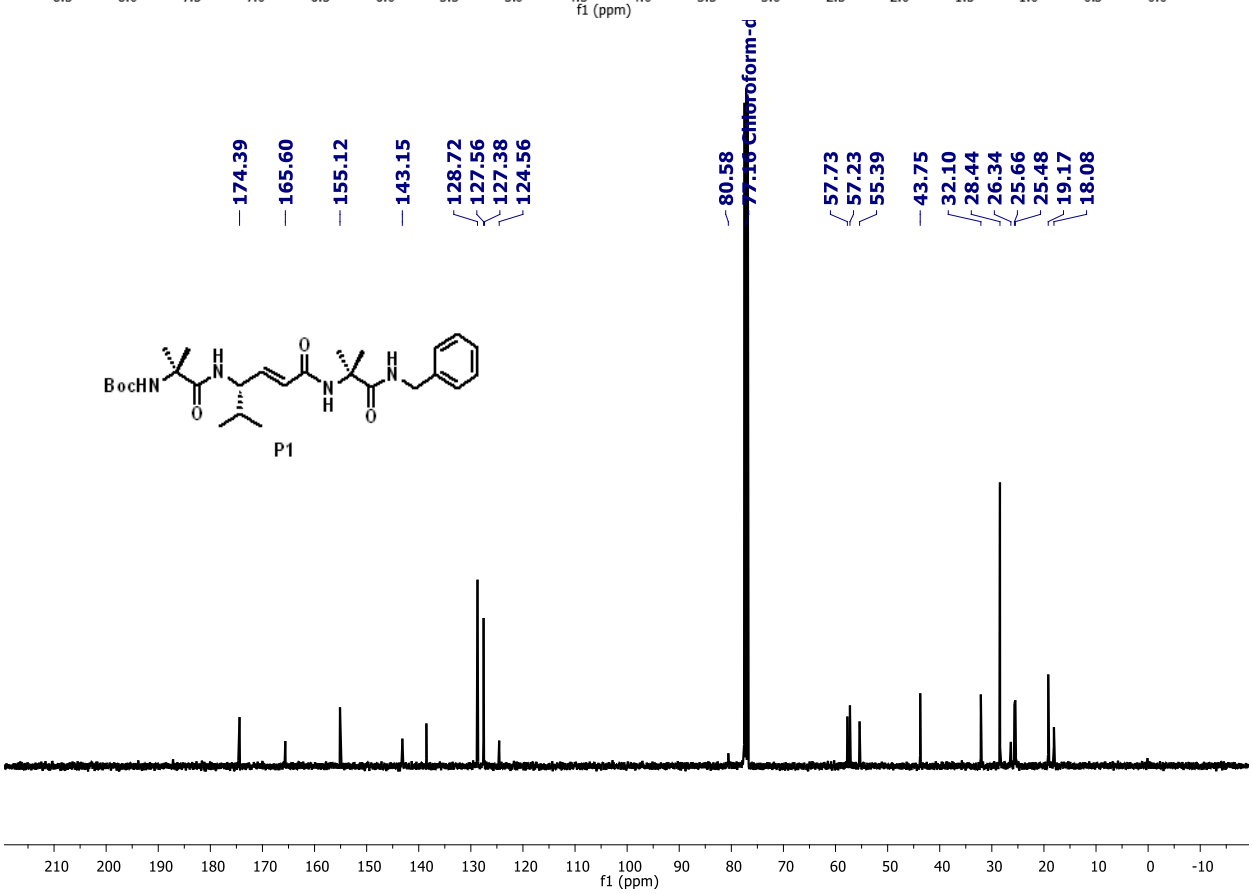
174.39
165.60
155.12
143.15
128.72
127.56
127.38
124.56
80.58
77.16 Chloroform-d
57.73
57.23
55.39
43.75
32.10
28.44
26.34
25.66
25.48
19.17
18.08
BocHN
P1
f1 (ppm)

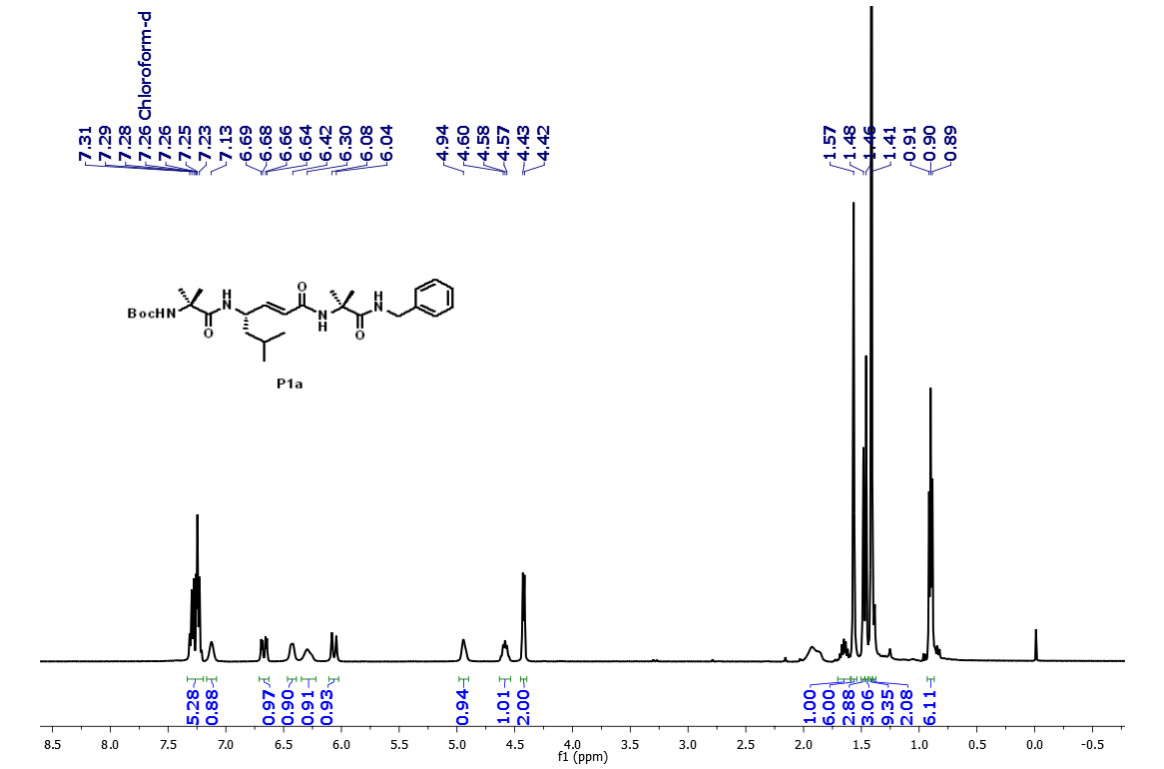
7.31
7.29
7.28
7.26 Chloroform-d
7.26
7.25
7.23
7.13
6.69
6.68
6.66
6.64
6.42
6.30
6.08
6.04
4.94
4.60
4.58
4.57
4.43
4.42
1.57
1.48
1.46
1.41
0.91
0.90
0.89
BocHN
P1a
5.28
0.88
0.97
0.90
0.91
0.93
0.94
1.01
2.00
1.00
6.00
2.88
3.06
9.35
2.08
6.11
f1 (ppm)

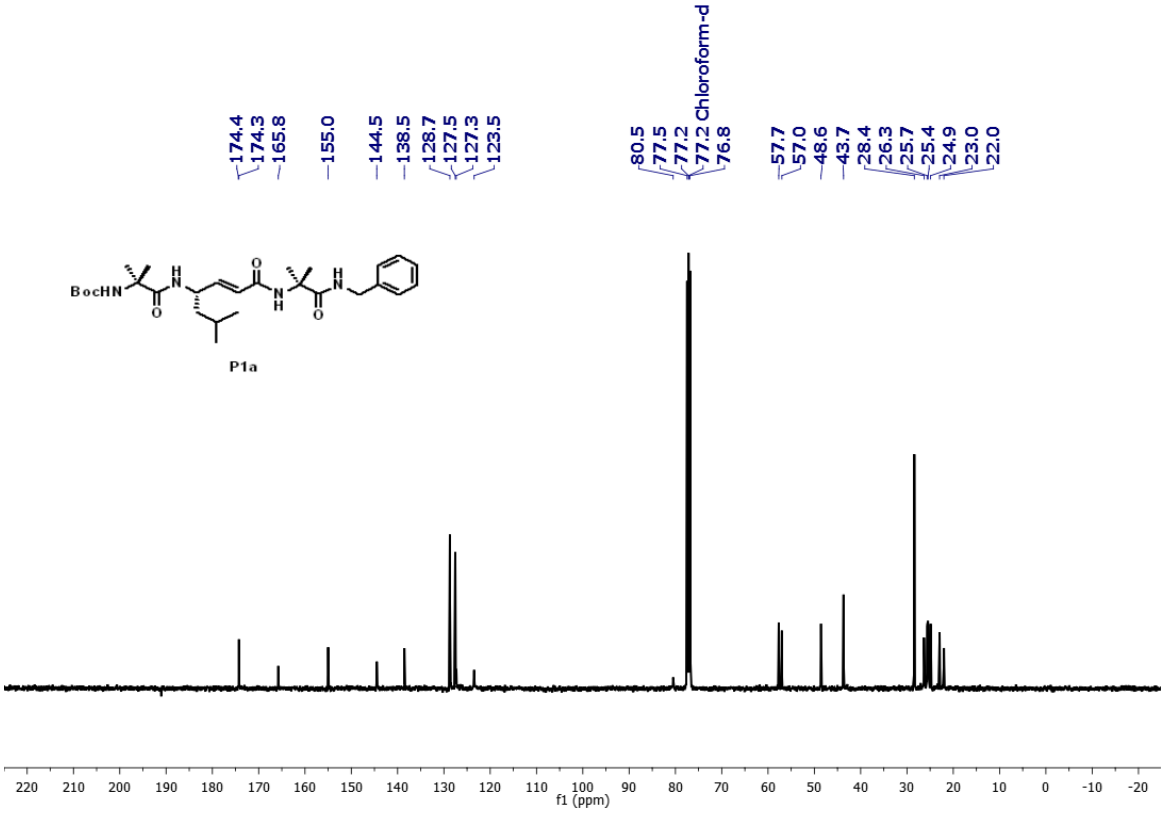
174.4
174.3
165.8
155.0
144.5
138.5
128.7
127.5
127.3
123.5
80.5
77.5
77.2 Chloroform-d
76.8
57.7
57.0
48.6
43.7
28.4
26.3
25.7
25.4
24.9
23.0
22.0
BocHN
P1a
f1 (ppm)

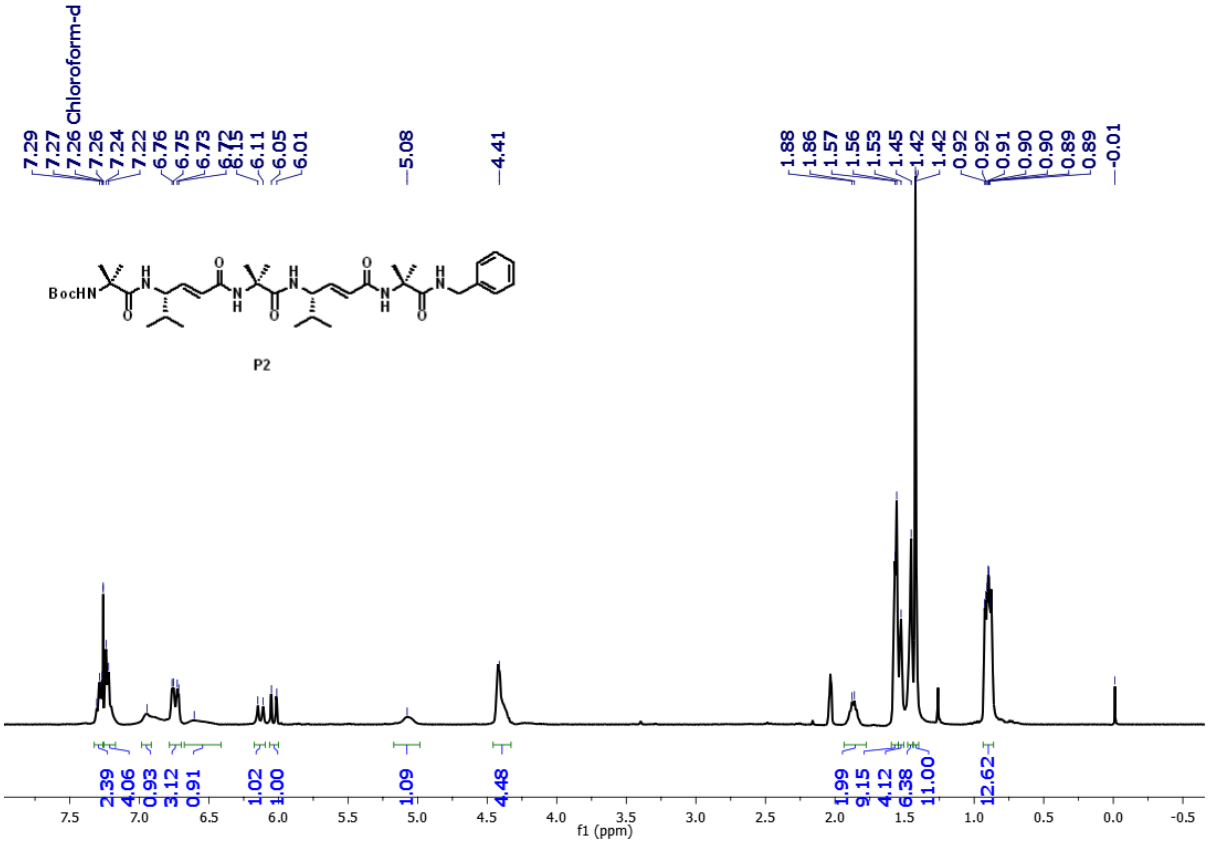
7.29
7.27
7.26 Chloroform-d
7.26
7.24
7.22
6.76
6.75
6.73
6.72
6.15
6.11
6.05
6.01
5.08
4.41
1.88
1.86
1.57
1.56
1.53
1.45
1.42
1.42
0.92
0.92
0.91
0.90
0.90
0.89
0.89
-0.01
BocHN
P2
2.39
4.06
0.93
3.12
0.91
1.02
1.00
1.09
4.48
1.99
9.15
4.12
6.38
11.00
12.62
f1 (ppm)

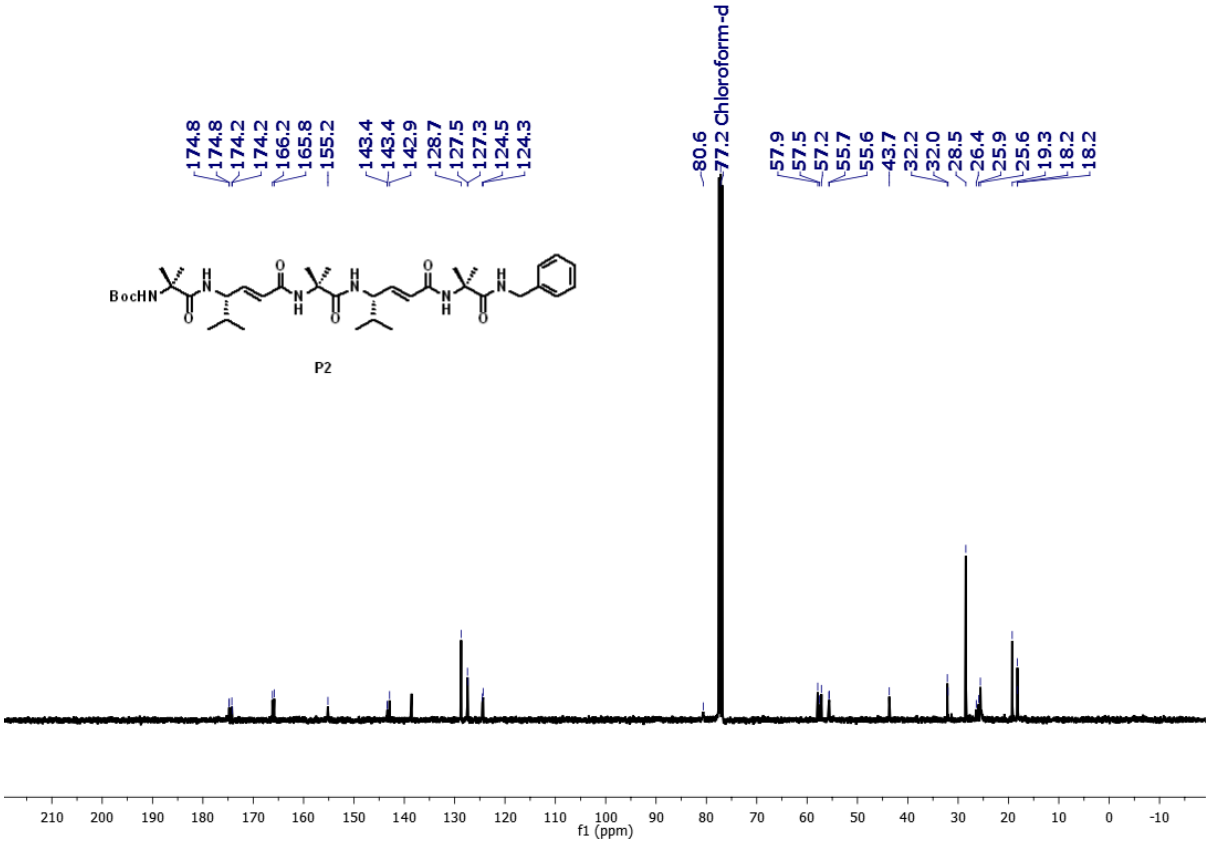
174.8
174.8
174.2
174.2
166.2
165.8
155.2
143.4
143.4
142.9
128.7
127.5
127.3
124.5
124.3
80.6
77.2 Chloroform-d
57.9
57.5
57.2
55.7
55.6
43.7
32.2
32.0
28.5
26.4
25.9
25.6
19.3
18.2
18.2
BocHN
P2
f1 (ppm)

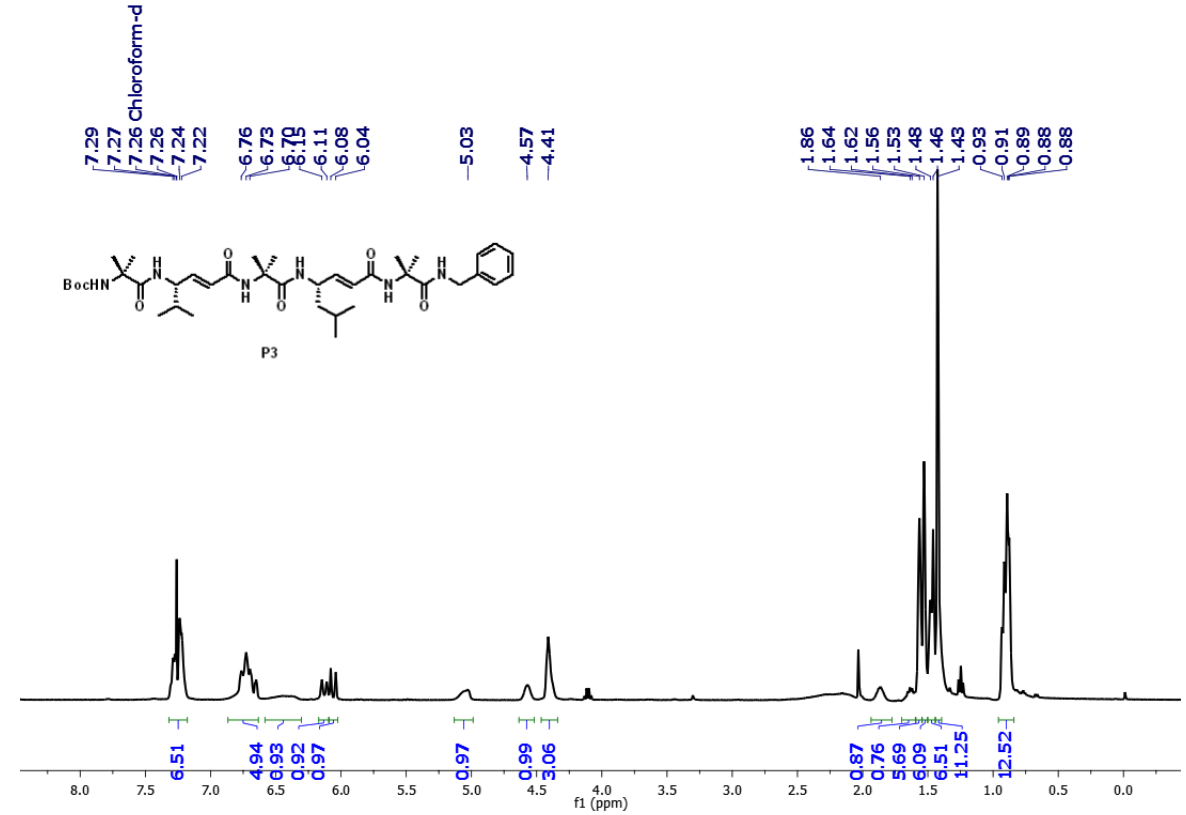
7.29
7.27
7.26 Chloroform-d
7.26
7.24
7.22
6.76
6.73
6.70
6.15
6.11
6.08
6.04
5.03
4.57
4.41
1.86
1.64
1.62
1.56
1.53
1.48
1.46
1.43
0.93
0.91
0.89
0.88
0.88
BocHN
P3
6.51
4.94
0.93
0.92
0.97
0.97
0.99
3.06
0.87
0.76
5.69
6.09
6.51
11.25
12.52
f1 (ppm)

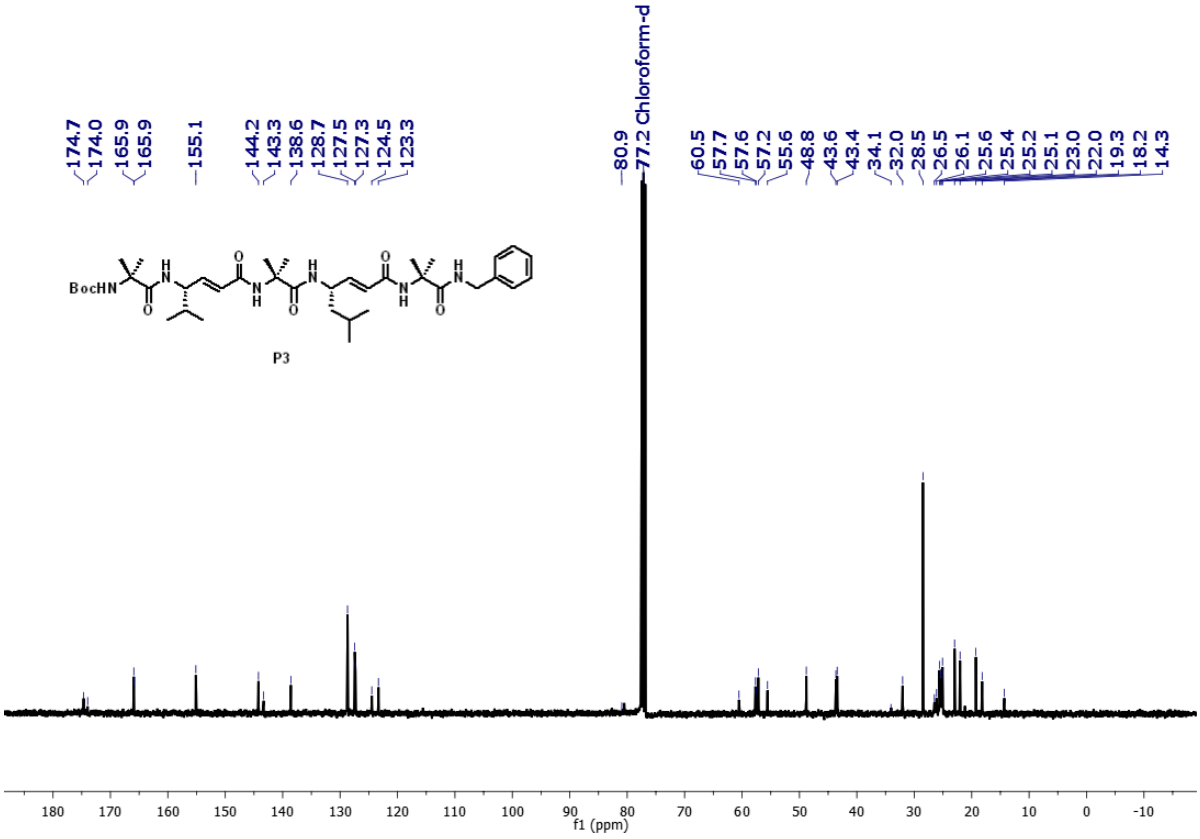
174.7
174.0
165.9
165.9
155.1
144.2
143.3
138.6
128.7
127.5
127.3
124.5
123.3
80.9
77.2 Chloroform-d
60.5
57.7
57.6
57.2
55.6
48.8
43.6
43.4
34.1
32.0
28.5
26.5
26.1
25.6
25.4
25.2
25.1
23.0
22.0
19.3
18.2
14.3
BocHN
P3
f1 (ppm)

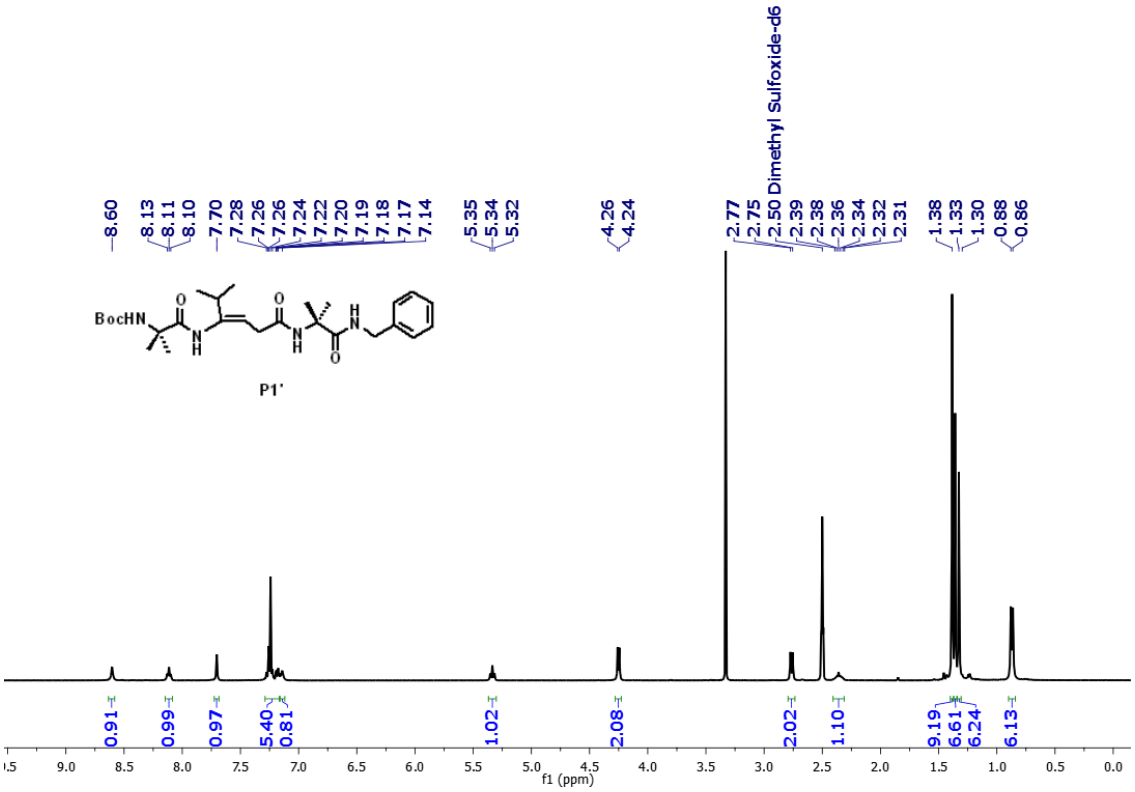
8.60
8.13
8.11
8.10
7.70
7.28
7.26
7.26
7.24
7.22
7.20
7.19
7.18
7.17
7.14
5.35
5.34
5.32
4.26
4.24
2.77
2.75
2.50 Dimethyl Sulfoxide-d6
2.39
2.38
2.36
2.34
2.32
2.31
1.38
1.33
1.30
0.88
0.86
BocHN
P1'
0.91
0.99
0.97
5.40
0.81
1.02
2.08
2.02
1.10
9.19
6.61
6.24
6.13
f1 (ppm)

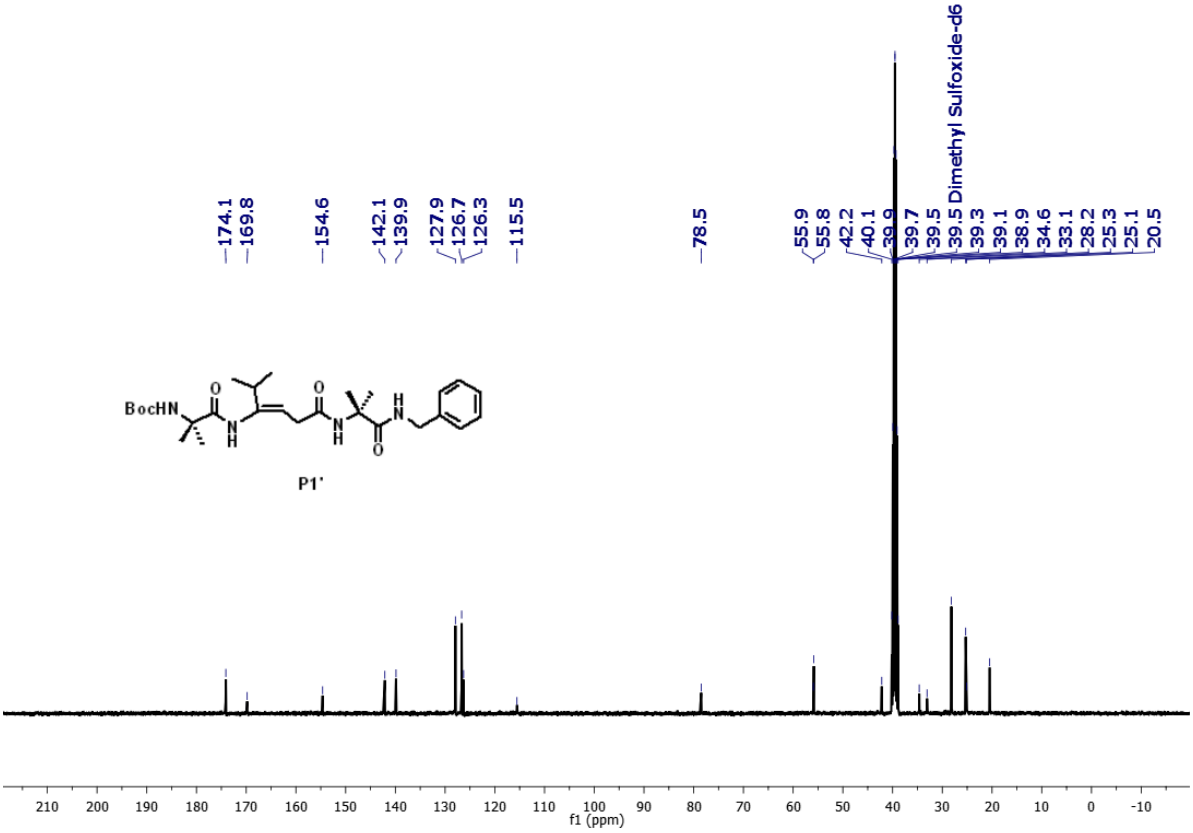
174.1
169.8
154.6
142.1
139.9
127.9
126.7
126.3
115.5
78.5
55.9
55.8
42.2
40.1
39.9
39.7
39.5
39.5 Dimethyl Sulfoxide-d6
39.3
39.1
38.9
34.6
33.1
28.2
25.3
25.1
20.5
BocHN
P1'
f1 (ppm)

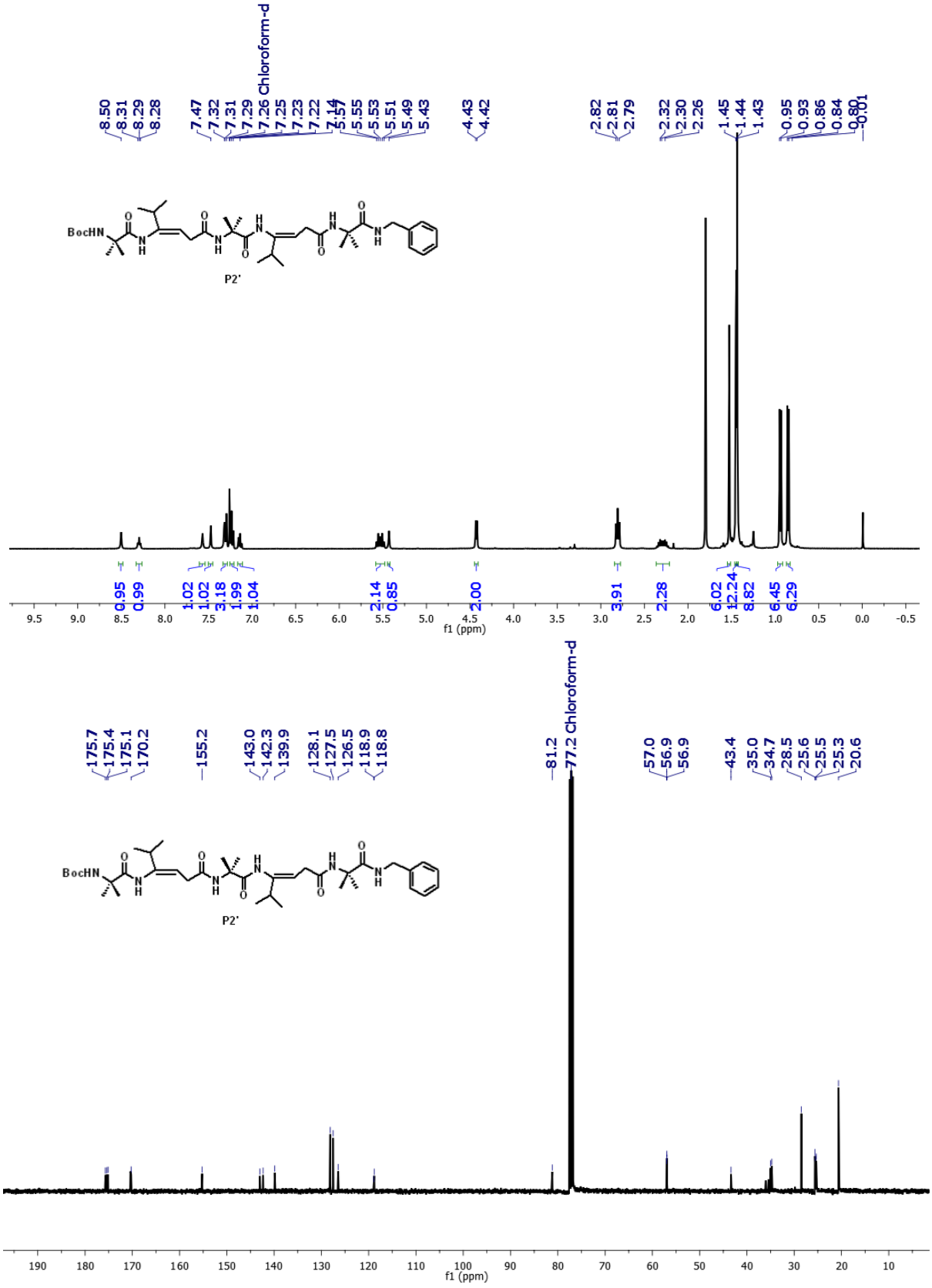
Chloroform-d
8.50
8.31
8.29
8.28
7.47
7.32
7.31
7.29
7.26
7.25
7.23
7.22
5.55
5.53
5.51
5.49
5.43
4.43
4.42
2.82
2.81
2.79
2.32
2.30
2.26
1.45
1.44
1.43
0.95
0.93
0.86
0.84
0.80
0.01
BocHN
P2'
0.95
0.99
1.02
1.02
3.18
1.99
1.04
2.14
0.85
2.00
3.91
2.28
6.02
12.24
8.82
6.45
6.29
f1 (ppm)
175.7
175.4
175.1
170.2
155.2
143.0
142.3
139.9
128.1
127.5
126.5
118.9
118.8
81.2
77.2
Chloroform-d
57.0
56.9
56.9
43.4
35.0
34.7
28.5
25.6
25.5
25.3
20.6
BocHN
P2'
f1 (ppm)

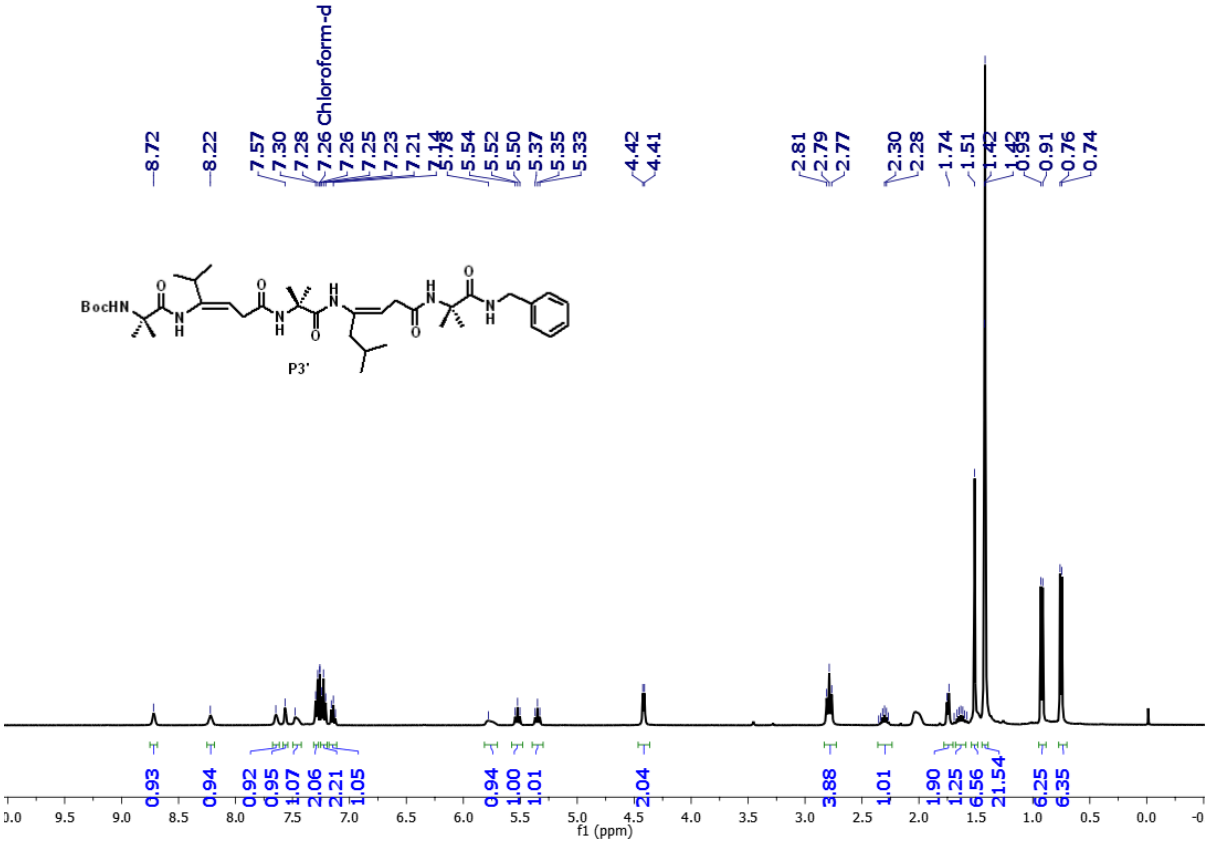
8.72
8.22
7.57
7.30
7.28
7.26 Chloroform-d
7.26
7.25
7.23
7.21
5.54
5.52
5.50
5.37
5.35
5.33
4.42
4.41
2.81
2.79
2.77
2.30
2.28
1.74
1.51
1.42
0.91
0.76
0.74
BocHN
P3'
0.93
0.94
0.92
0.95
1.07
2.06
2.21
1.05
0.94
1.00
1.01
2.04
3.88
1.01
1.90
1.25
6.56
21.54
6.25
6.35
f1 (ppm)

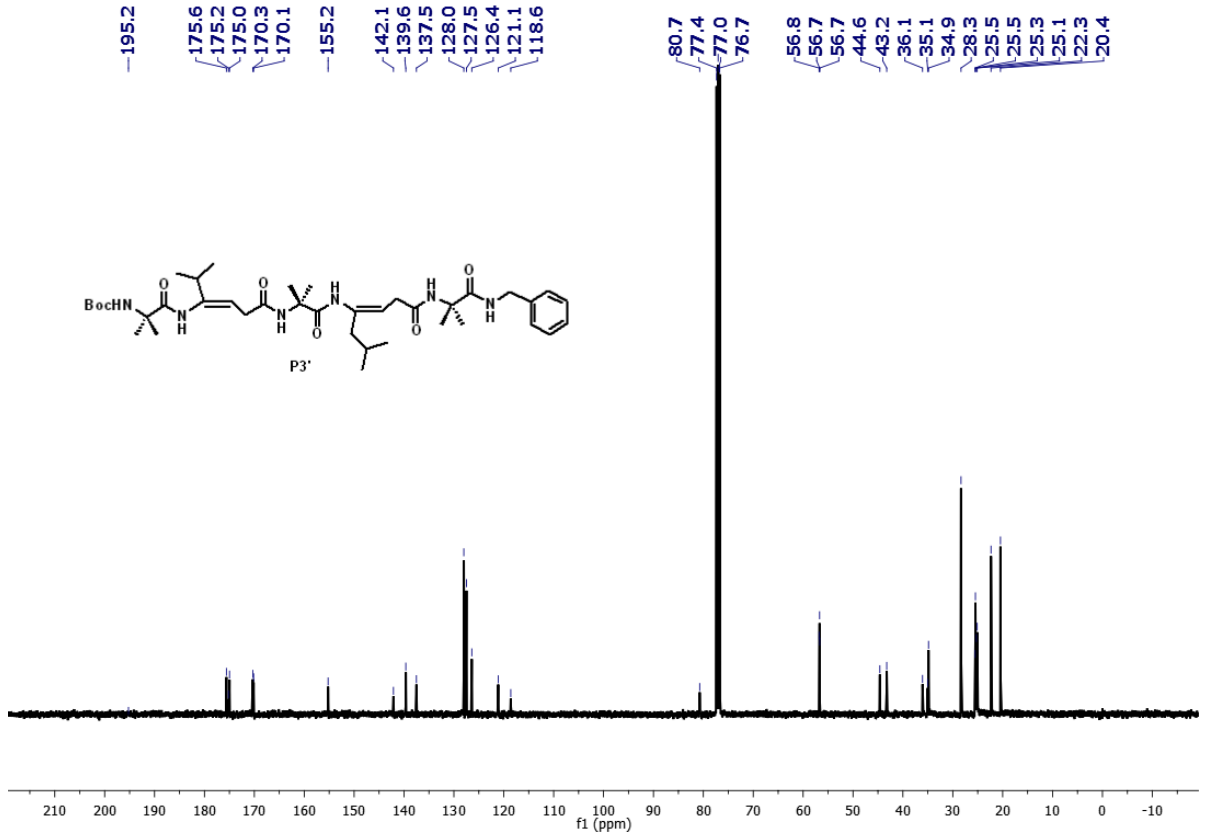
195.2
175.6
175.2
175.0
170.3
170.1
155.2
142.1
139.6
137.5
128.0
127.5
126.4
121.1
118.6
80.7
77.4
77.0
76.7
56.8
56.7
56.7
44.6
43.2
36.1
35.1
34.9
28.3
25.5
25.5
25.3
25.1
22.3
20.4
BocHN
P3'
f1 (ppm)

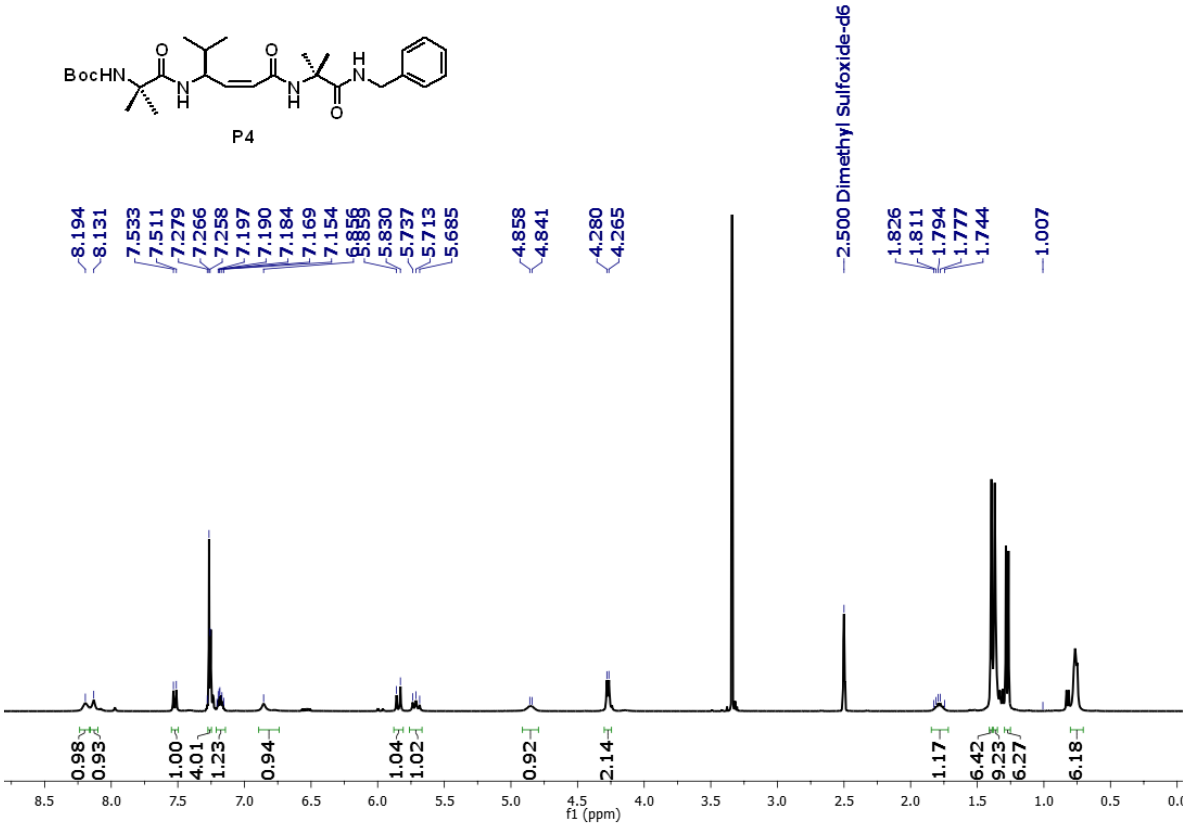
BocHN
P4
8.194
8.131
7.533
7.511
7.279
7.266
7.258
7.197
7.190
7.184
7.169
7.154
6.856
6.839
5.830
5.737
5.713
5.685
4.858
4.841
4.280
4.265
2.500 Dimethyl Sulfoxide-d6
1.826
1.811
1.794
1.777
1.744
1.007
0.98
0.93
1.00
4.01
1.23
0.94
1.04
1.02
0.92
2.14
1.17
6.42
9.23
6.27
6.18
f1 (ppm)

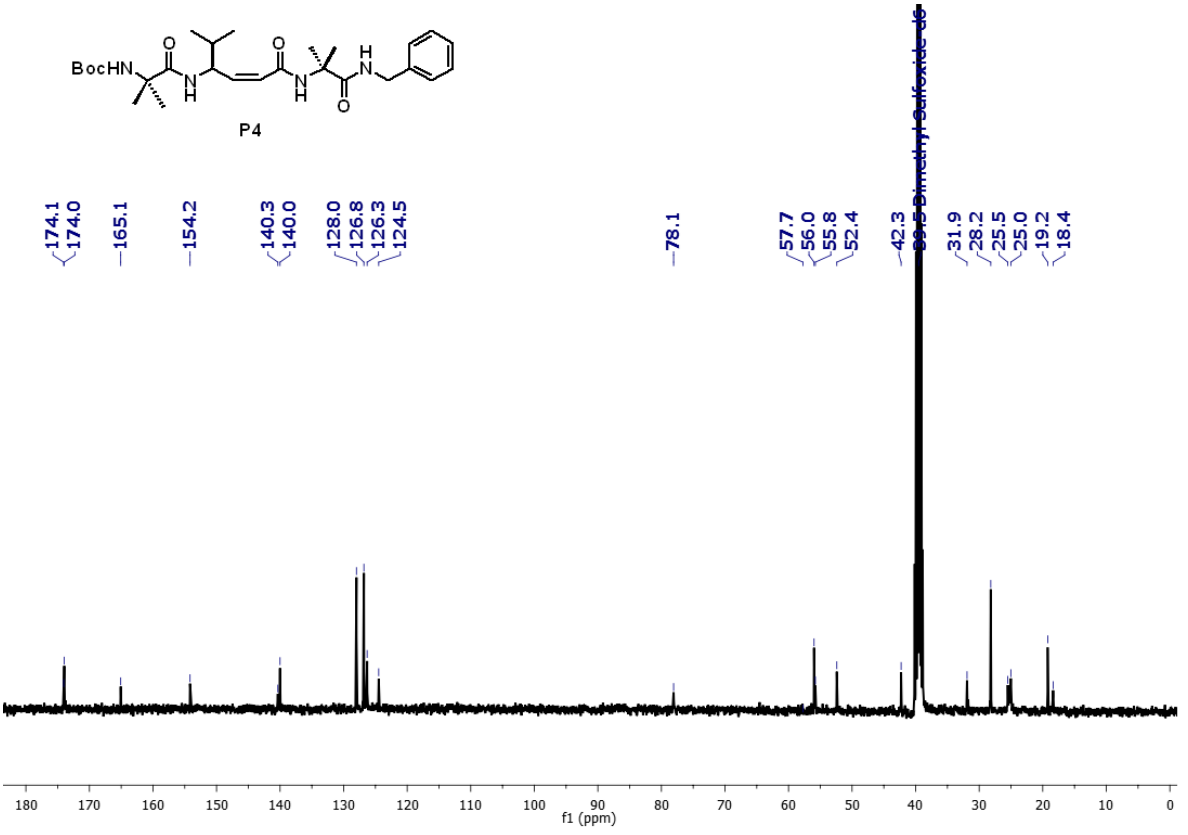
BocHN
P4
174.1
174.0
165.1
154.2
140.3
140.0
128.0
126.8
126.3
124.5
78.1
57.7
56.0
55.8
52.4
42.3
39.5 Dimethyl Sulfoxide-d6
31.9
28.2
25.5
25.0
19.2
18.4
f1 (ppm)

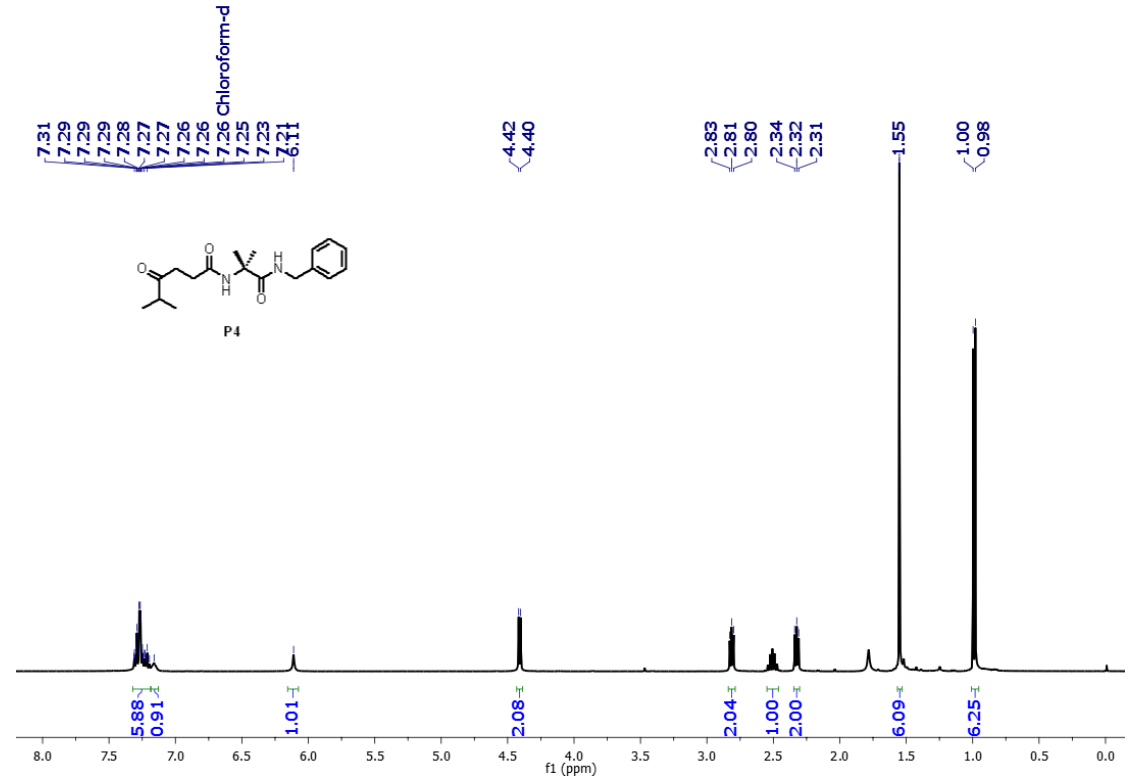
Chloroform-d
7.31
7.29
7.29
7.29
7.28
7.27
7.27
7.26
7.26
7.26
7.25
7.23
7.11
6.11
4.42
4.40
2.83
2.81
2.80
2.34
2.32
2.31
1.55
1.00
0.98
P4
5.88
0.91
1.01
2.08
2.04
1.00
2.00
6.09
6.25
f1 (ppm)

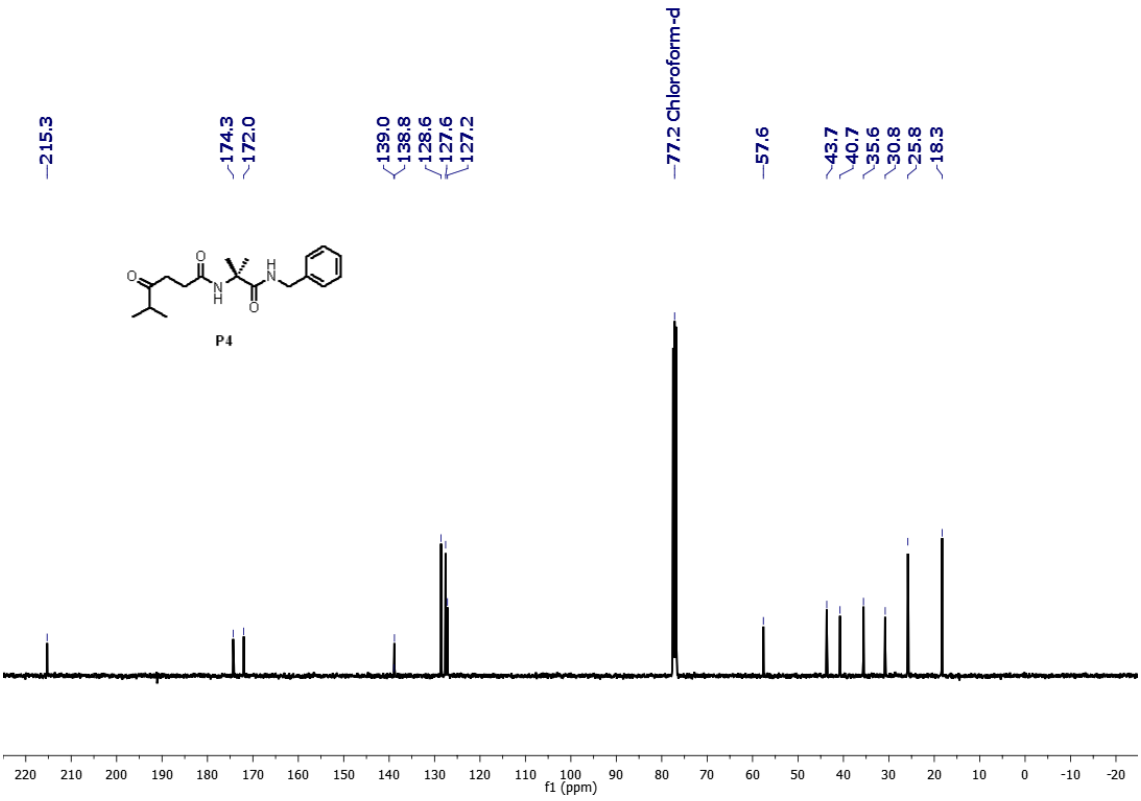
215.3
174.3
172.0
139.0
138.8
128.6
127.6
127.2
77.2 Chloroform-d
57.6
43.7
40.7
35.6
30.8
25.8
18.3
P4
f1 (ppm)

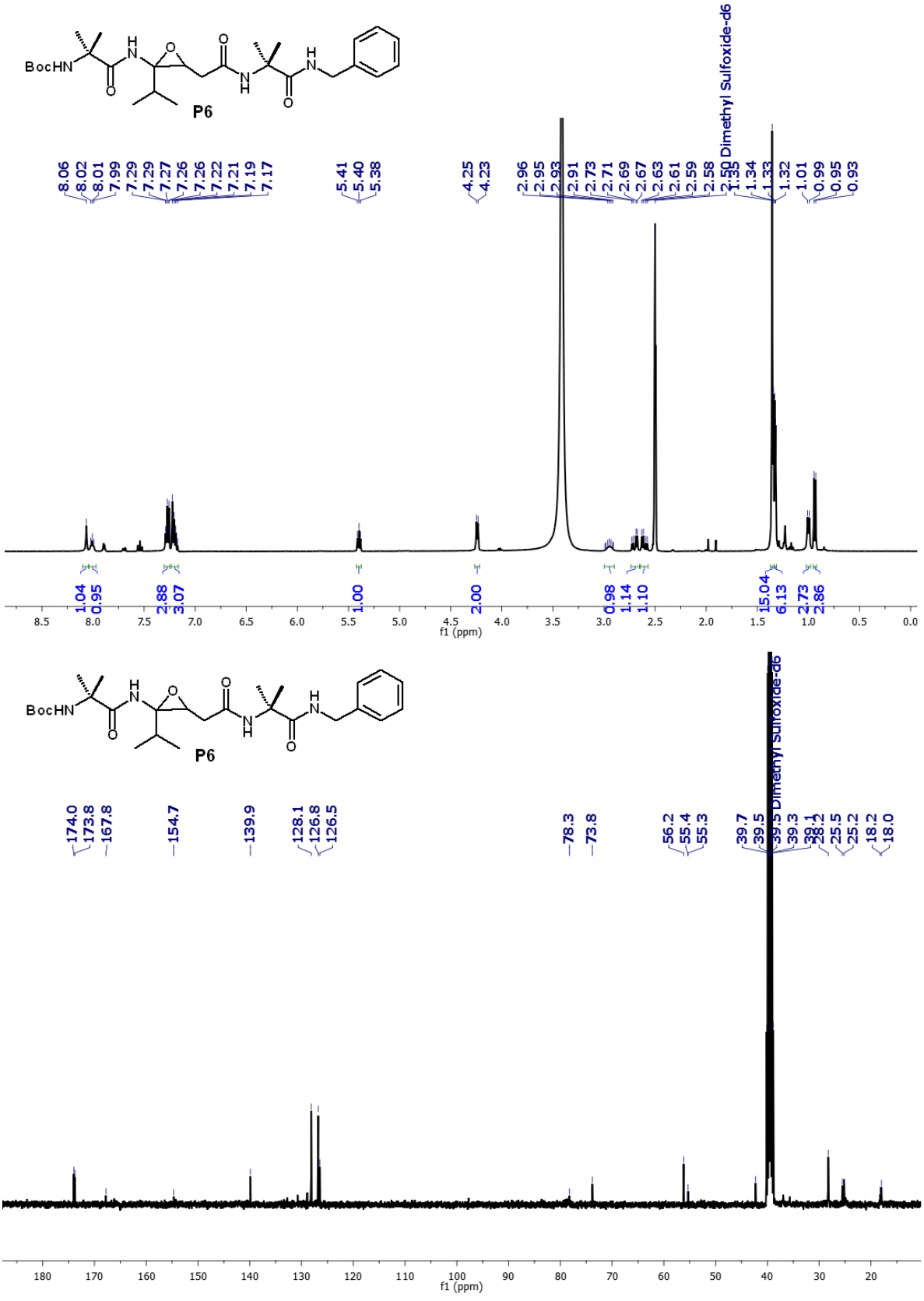
BocHN
P6
8.06
8.02
8.01
7.99
7.29
7.29
7.27
7.26
7.26
7.22
7.21
7.19
7.17
5.41
5.40
5.38
4.25
4.23
2.96
2.95
2.93
2.91
2.73
2.71
2.69
2.67
2.63
2.61
2.59
2.58
2.50 Dimethyl Sulfoxide-d6
1.35
1.34
1.33
1.32
1.01
0.99
0.95
0.93
1.04
0.95
2.88
3.07
1.00
2.00
0.98
1.14
1.10
15.04
6.13
2.73
2.86
f1 (ppm)
BocHN
P6
174.0
173.8
167.8
154.7
139.9
128.1
126.8
126.5
78.3
73.8
56.2
55.4
55.3
39.7
39.5
39.5 Dimethyl Sulfoxide-d6
39.3
28.1
28.1
25.5
25.2
18.2
18.0
f1 (ppm)

3. Mass spectrums of peptides

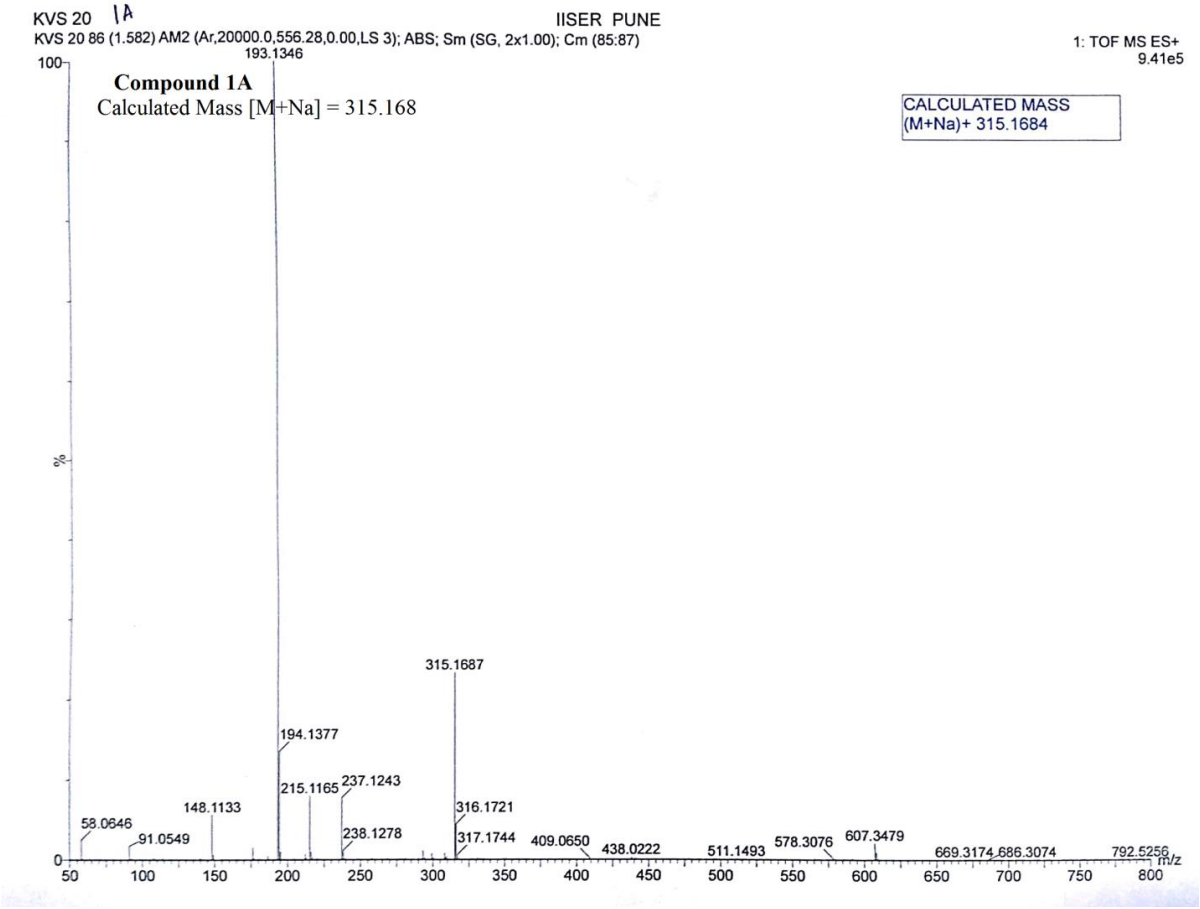

Spectrum Report

P1

Final - Shots 500 - IISER-96-1-2018; Run #175; Label B1

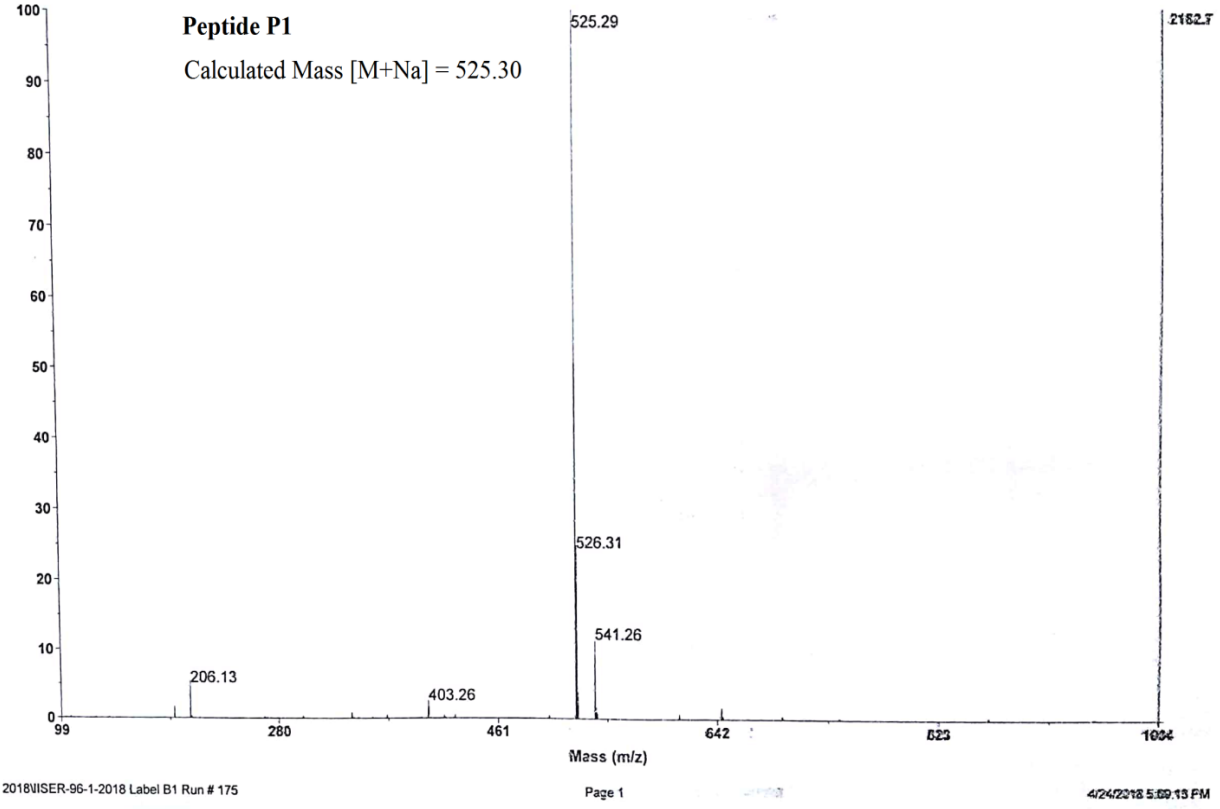

2018\IISER-96-1-2018 Label B1 Run # 175

Page 1

Spectrum Report

Final - Shots 500 - IISER-96-1-2018; Run #175; Label A1

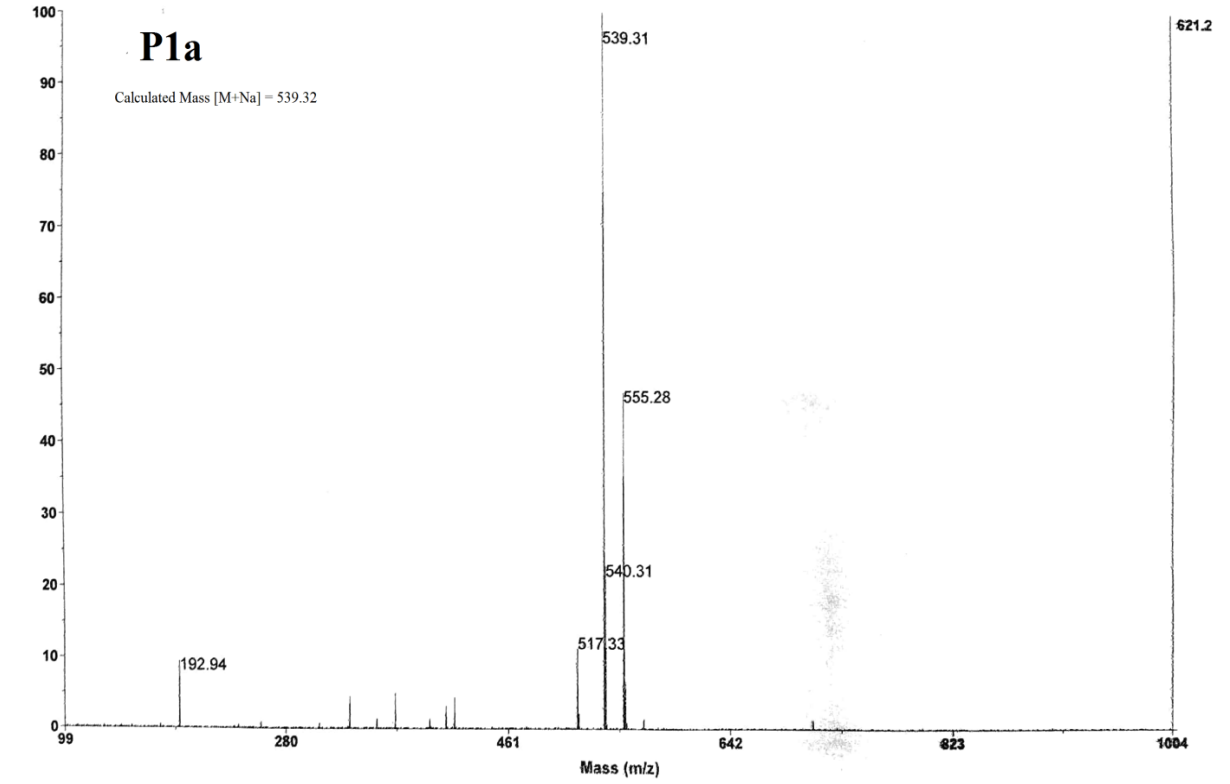

2018\IISER-96-1-2018 Label A1 Run # 175

Page 1

4/24/2018 5:08:55 PM

Spectrum Report

Final - Shots 500 - IISER-96-1-2018; Run #175; Label C1

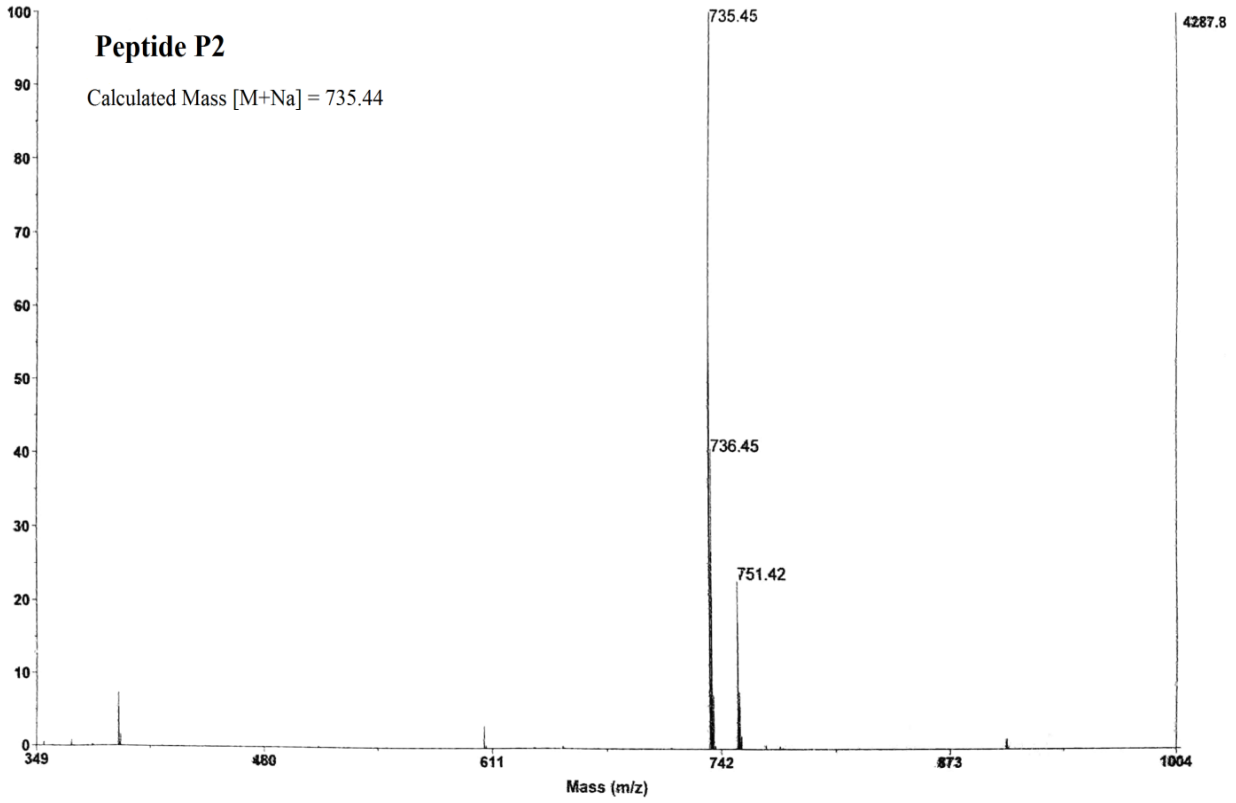

2018\IISER-96-1-2018 Label C1 Run # 175

Page 1

4/24/2018 5:16:35 PM

Spectrum Report

Final - Shots 500 - IISER-96-1-2018; Label D2

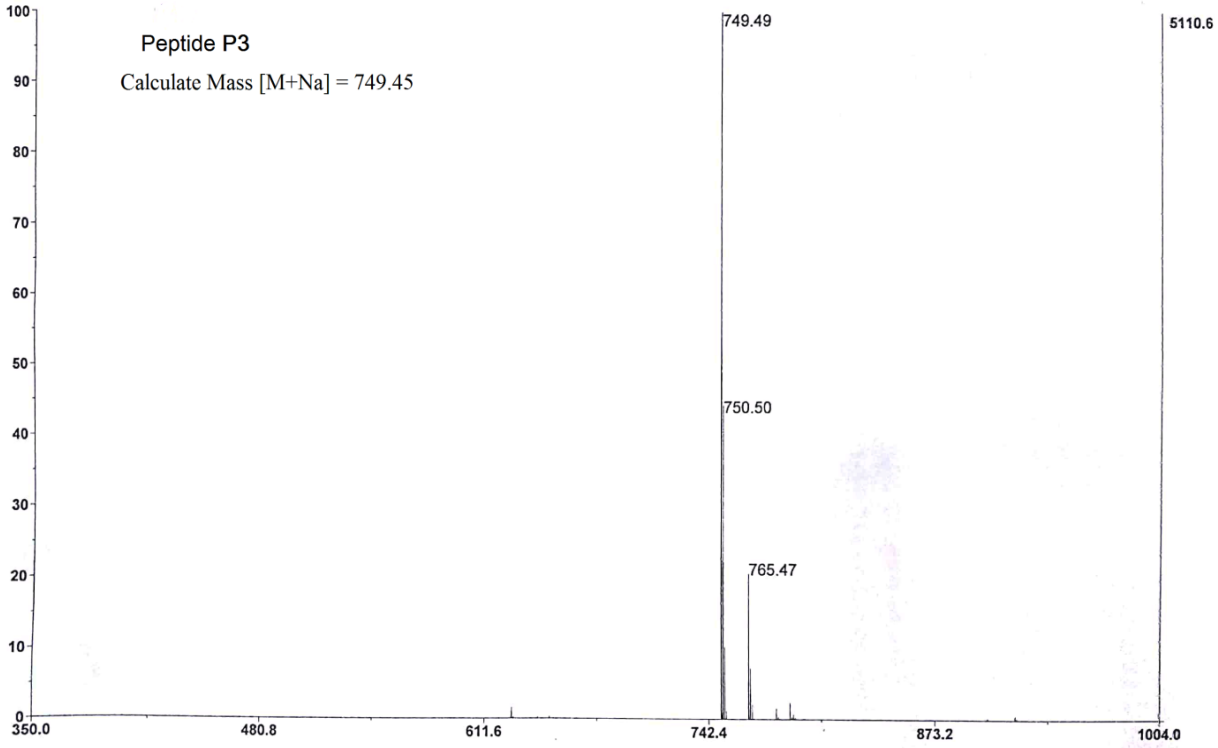

2018\IISER-96-1-2018 Label D2 Run # 175

Page 1

4/24/2018 5:19:27 PM

Spectrum Report

Final - Shots 500 - IISER-96-1-2018; Run #175; Label B2

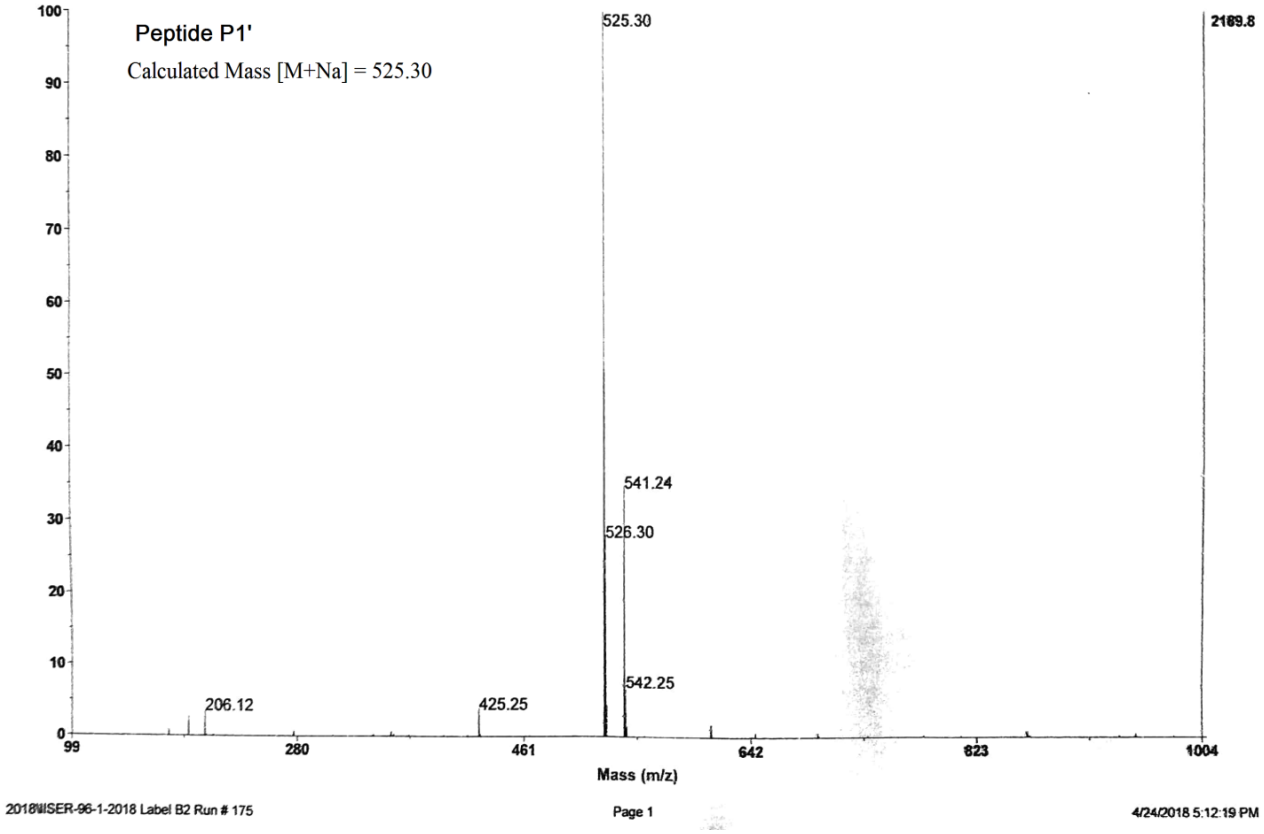

2018\IISER-96-1-2018 Label B2 Run # 175 Page 1 4/24/2018 5:12:19 PM

Spectrum Report

Final - Shots 500 - IISER-96-1-2018; Label C2

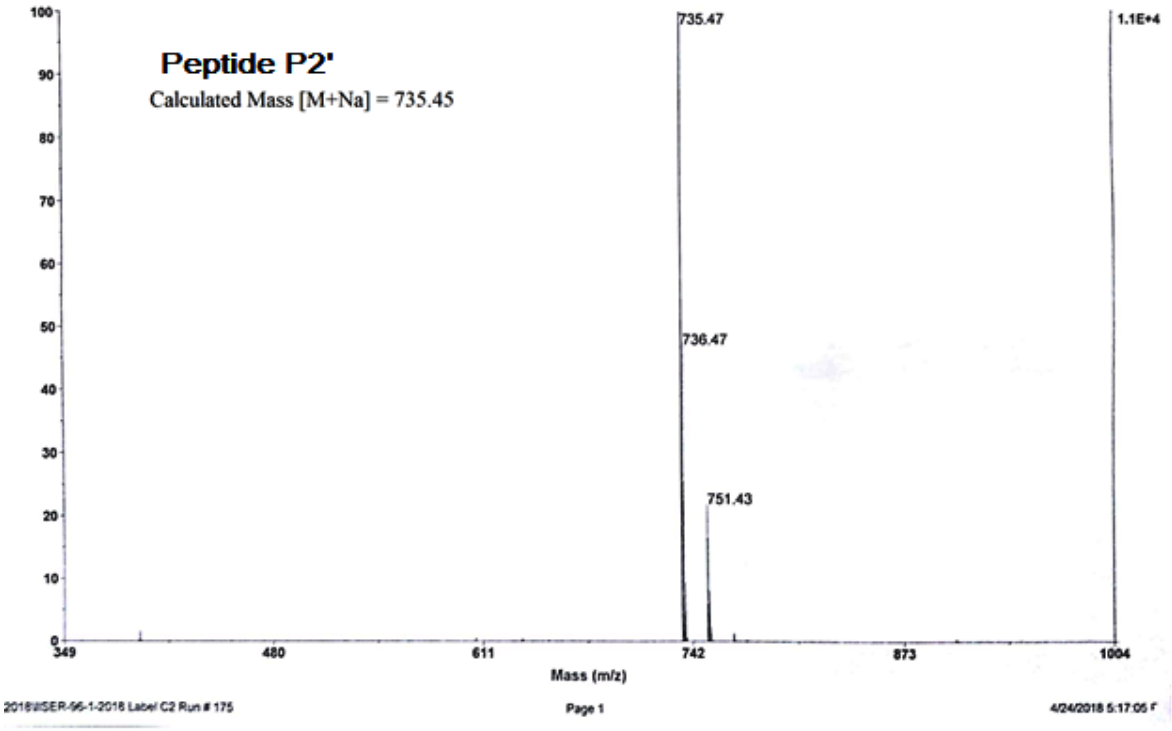

2018\IISER-96-1-2018 Label C2 Run # 175 Page 1 4/24/2018 5:17:05 F

Spectrum Report

Final - Shots 500 - IISER-96-1-2018; Label D1

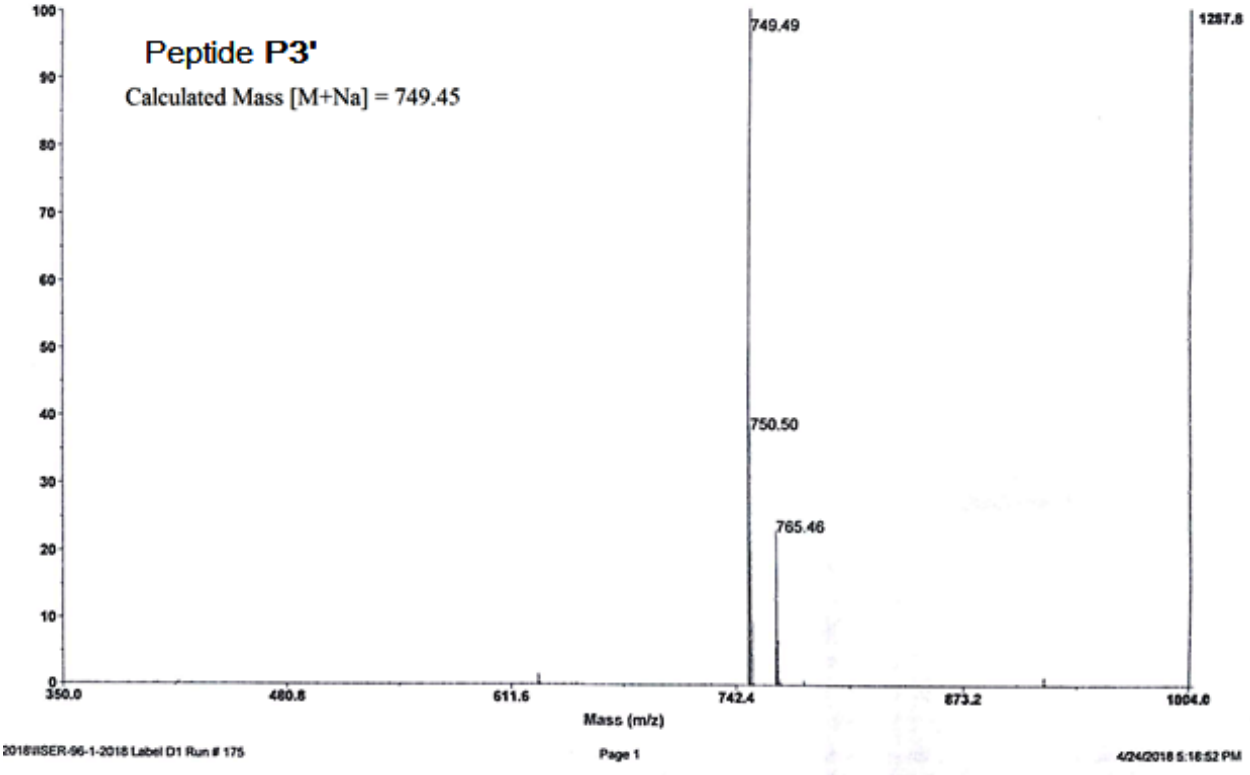

2018\IISER-96-1-2018 Label D1 Run # 175

Page 1

4/24/2018 5:16:52 PM

Spectrum Report

Final - Shots 500 - IISER-96-1-2018; Run #175; Label A1

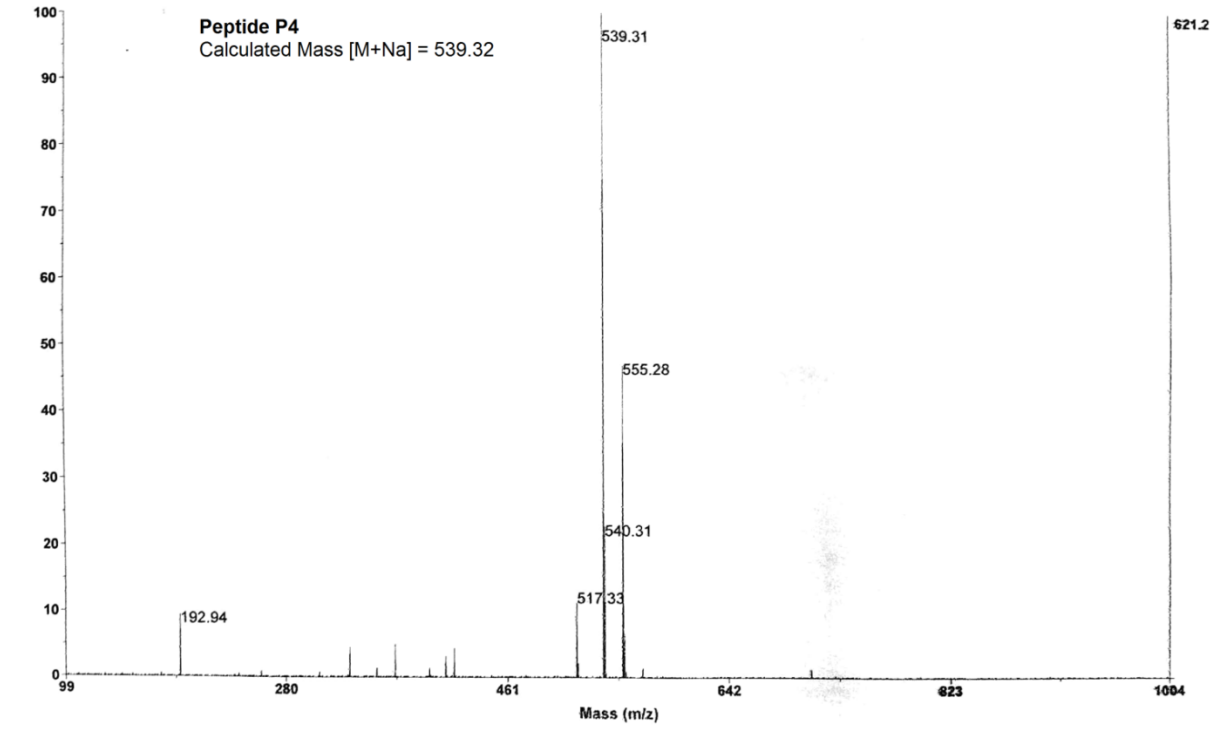

2018\IISER-96-1-2018 Label A1 Run # 175

Page 1

4/24/2018 5:08:55 PM

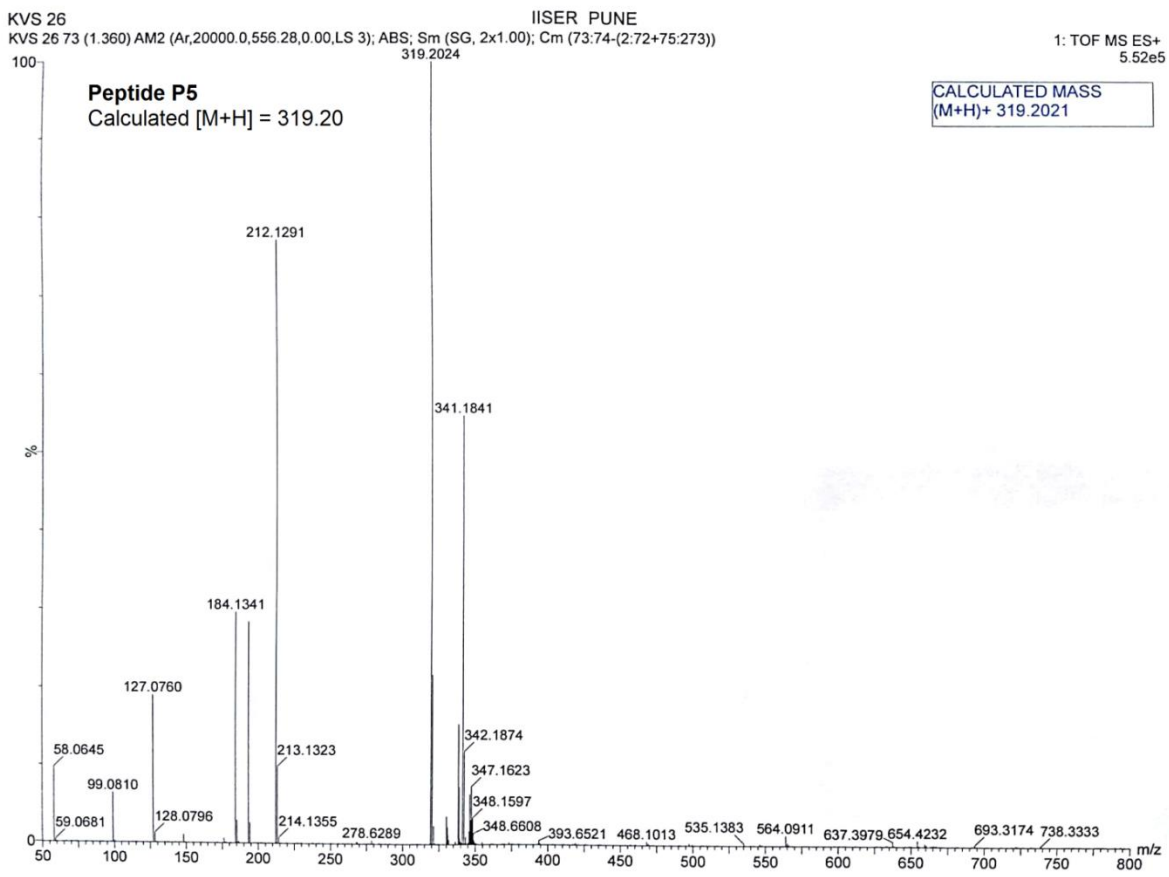
KVS 26
IISER PUNE
KVS 26 73 (1.360) AM2 (Ar,20000.0,556.28,0.00,LS 3); ABS; Sm (SG, 2x1.00); Cm (73:74-(2:72+75:273))
1: TOF MS ES+
5.52e5
Peptide P5
Calculated [M+H] = 319.20
CALCULATED MASS
(M+H)+ 319.2021
319.2024
212.1291
341.1841
184.1341
127.0760
58.0645
213.1323
342.1874
347.1623
99.0810
348.1597
59.0681
128.0796
214.1355
348.6608
278.6289
393.6521
468.1013
535.1383
564.0911
637.3979
654.4232
693.3174
738.3333
%
m/z

CHAPTER 3

Transformation of *N*-protected α,β-Unsaturated γ-Amino Amides into γ-Lactams through a Base Mediated Molecular Rearrangement

The original work of this chapter has been published in the "The Journal of Organic Chemistry" journal. Here, we adopted the text from Ref. Ganesh Kumar, Veeresh, K.; M.; Nalawade, S. A.; Nithun, R. V.; Gopi, H. N. *J. Org. Chem.* **2019**, *84*, 23, 15145 with permission from the American Chemical Society. A copy of permission letter attached at the end of the chapter.

1. Introduction

The γ-Lactam moiety is an ingredient in the core structures of various biologically active natural products and synthetic pharmaceutical drugs.[1, 2] The derivatives of γ-lactams have been finding applications in the medicinal chemistry to treatment cancer,[3] epilepsy,[4] Alzheimer's disease,[5] human immune-deficient virus-1 (HIV-1) infection[6] as well as fungal and bacterial infections.[1a,7] In addition, γ-lactam derivatives have shown excellent inhibitory activities against various enzymes[8] and protein-protein interactions.[9] Besides their biological activities, γ-lactam templates have been used to construct constrained peptidomimetics.[10] Medicinally active natural products containing γ-lactam in their core structure and their source are shown in Scheme **1**.

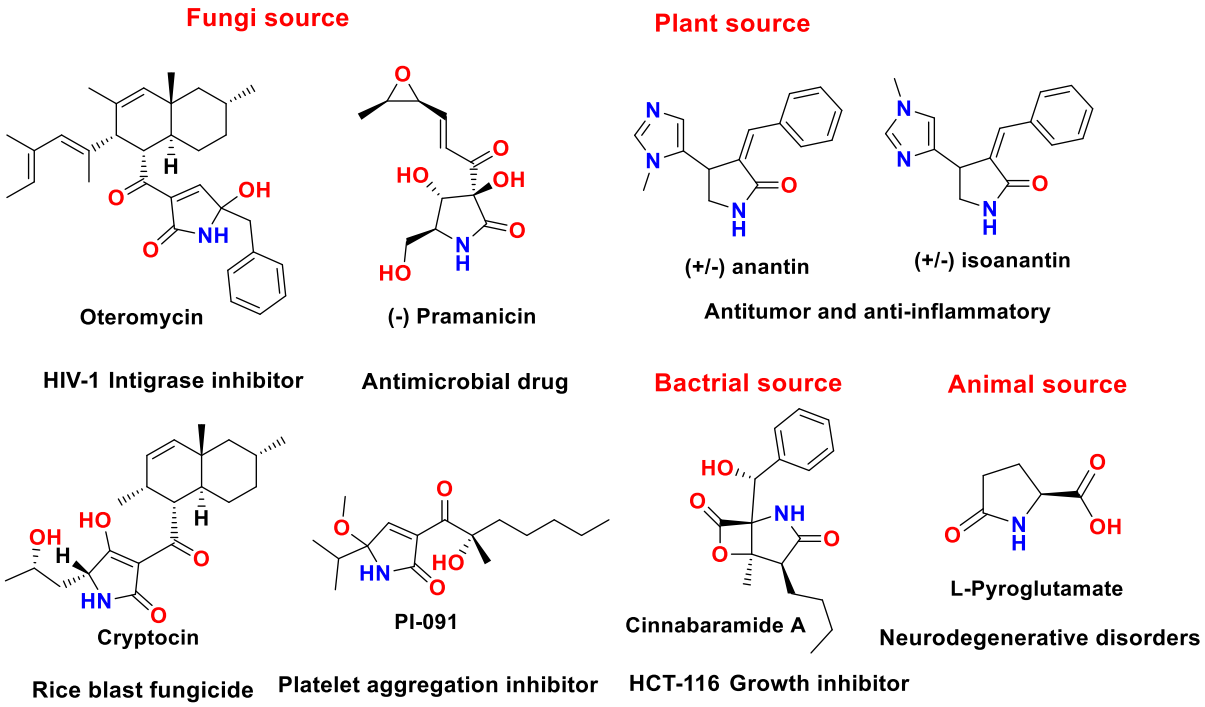

Scheme 1: Structures of γ-lactam containing natural products from different sources and their therapeutic applications.

The natural prevalence and broad spectrum of biological activities of γ-lactams have attracted considerable attention from the synthetic community to develop feasible synthetic strategies.[2] In addition to the intramolecular condensation of amine and carboxylic acid functional groups of γ-amino acids,[11] a variety of transition metal-catalyzed C-N bond formation reactions such as Pd-catalyzed oxidative intramolecular allylic alkylations[12] and gold(I) catalyzed intramolecular

cyclization of homopropargyl amides,[13] Ir (III) catalyzed C-H amidation.[14] C-C bond formation reactions such as Pd-catalyzed intramolecular reactions of *N*-allylpropiolamides,[15] Fe(X_2) catalyzed cyclization of enynamides,[16] and gold(I) catalyzed cyclization of *N*-alkenyl β-ketoamides[17] and ring-closing metathesis[18] have been reported. Besides these cyclization strategies, annulation reactions (3+2)[19] and (4+1)[20] were also used in the construct biologically active γ-lactam products. Our view of the strategies used are schematically represented in Scheme **2**.

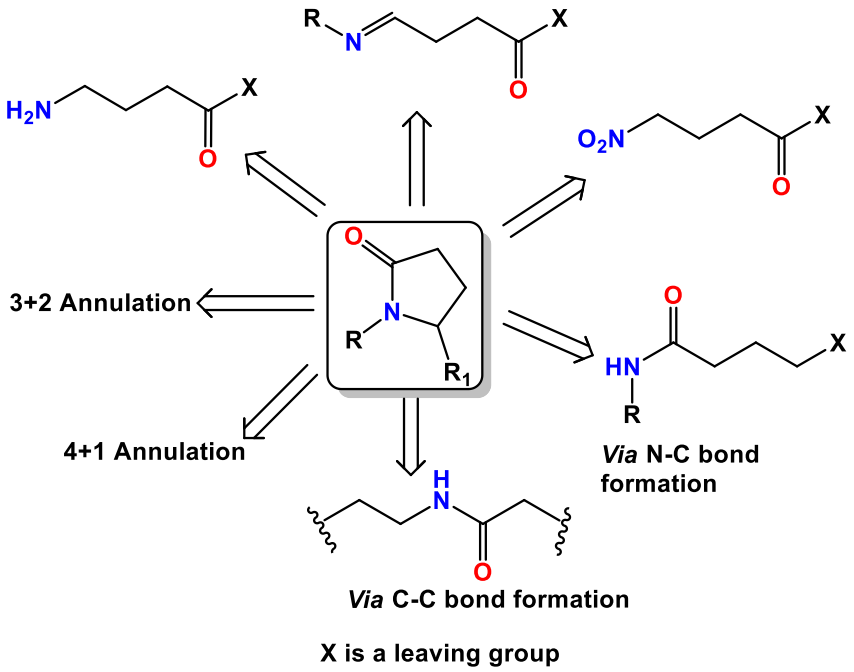

Scheme 2: Strategies used to synthesize the biologically active γ-lactam containing products.

2. Aim and rationale of the work

Recently, my senior Ganesh, M. from our group observed the base mediated single-step transformation of amides of *N*-protected α,β-unsaturated γ-amino acids into 5,5-disubstituted γ-lactams.[21] In continuation, we sought to further investigate the substrate scope and reaction mechanism of this interesting transformation and also improve the yields of the reaction.

3. Results and discussion

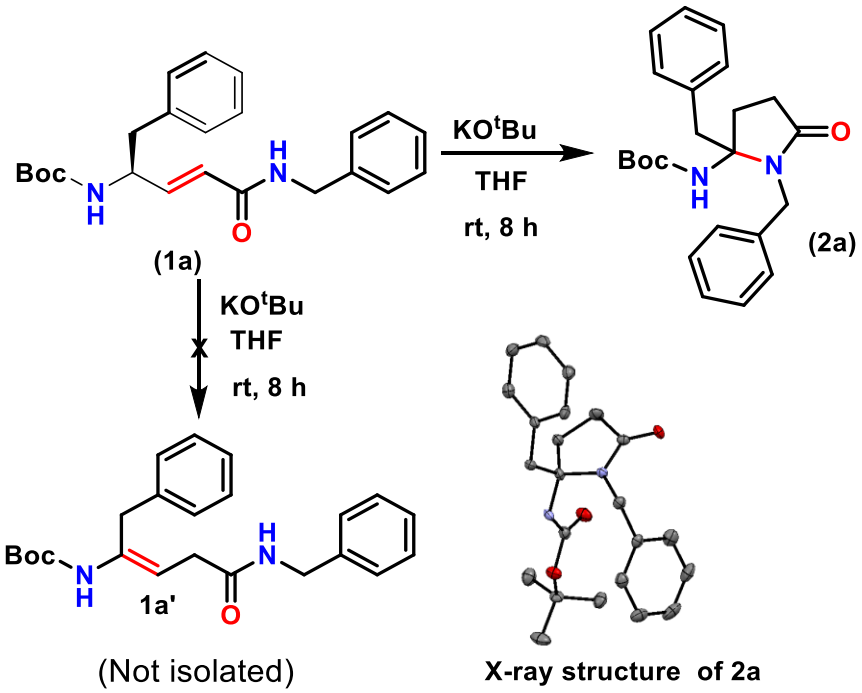

Scheme 3: Transformation of (*S, E*) *N*-Boc-α,β-unsaturated γPhe *N*-benzyl amide (**1a**) into 5,5-disubstituted γ-lactam (**2a**)

In order to improve yields of the transformation reaction of *N*-protected α,β-unsaturated γ-amino amides of into 5,5-disubstituted γ-lactams, we synthesized (*S,E*) *N*-Boc-α,β-unsaturated γ-phenylalanine benzyl amide **1a** as a model system and and examined the possibility of **1a** to **2a** conversion using various bases such as NaOH, LiOH, CsOH, DBU, and n-BuLi. Poor yields were observed with NaOH and CsOH. No γ-lactam formation was observed in the case of LiOH and DBU. We obtained γ-lactam (**2a**) in excellent yield (92%) with KO^{t}Bu in dry THF solvent at room temperature within 8 hr. The schematic representation of the reaction is shown in Scheme **3**. The formation of γ-lactam was confirmed by the ^{1}H and ^{13}C NMR as well as X-ray crystallography. The X-ray structure of γ-lactam **2a** is shown in Scheme **3**. The X-ray analysis of **2a** reveals the presence of two molecules in the asymmetric unit with opposite chirality suggesting the loss of stereochemistry during the process of cyclization.

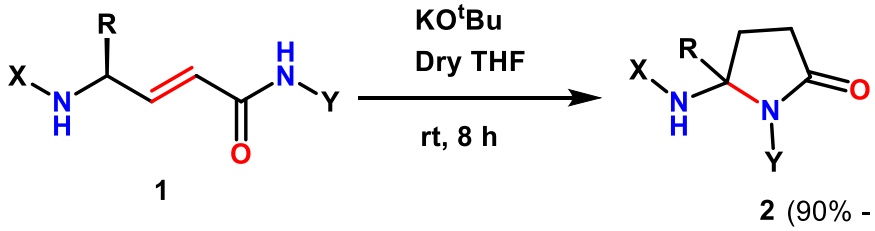

	X	R	Y	yield (%)
a:	Boc	$CH_2C_6H_5$	$CH_2C_6H_5$	92
b:	Boc	CH_3	$CH_2C_6H_5$	93
c:	Boc	$CH_2CH(CH_3)_2$	$CH_2C_6H_5$	90
d:	Boc	$CH(CH_3)_2$	$CH_2C_6H_5$	90
e:	Boc	$CH_2C_6H_5$	CH_2CH_2-Indole	91
f:	Boc	$CH(C_2H_5)(CH_3)$	$CH_2C_6H_5$	90
g:	Boc	$CH_2C_6H_5$	$CH(CH_3)C_6H_5$	90
h:	Boc	$CH_2C_6H_5$	$(CH_2)_3CH_3$	93
i:	Boc	CH_2-Indole	$CH_2CH(CH_3)_2$	95
j:	Boc	CH_2-Indole	$CH_2C_6H_5$	93
k:	Boc	$CH_2C_6H_5$	CH_3	94
l:	Boc	H	$CH_2C_6H_5$	91
m:	Cbz	$CH_2C_6H_5$	$CH(CH3)_2$	95
n:	Cbz	$CH_2CH(CH3)_2$	$CH_2C_6H_5$	90

Scheme 4: Facile transformation of (*S,E*) *N*-protected α,β-unsaturated γ-amino amides into *N*-alkyl 5,5-disubstituted γ-lactams mediated by KO^{t}Bu.

Excellent yields and high functionalization scope of the **1a** to **2a** transformation and high medicinal importance of γ-lactam containing products motivated us to check the feasibility of the reaction with different substrates. We have synthesized various other (*S,E*) *N*-Boc-α,β-unsaturated γ-amino acids through Wittig reaction[23] and coupled with different alkyl amines. All N-alkyl substituted amides of (*S,E*) *N*-Boc-α,β-unsaturated γ-amino acids (**1b-1l)** were isolated in good yields and subjected to KO^{t}Bu mediated molecular rearrangement to give γ-lactams. Similar to **1a**, all α,β-unsaturated γ-amino amides in Scheme **2** (**1b-1l**) were transformed into corresponding γ-lactams (**2b-2l**) in a single step at room temperature. Irrespective of the amino acid side-chains and *N*-alkyl substituents, all γ-lactams (**2b-2l**) were isolated in excellent yields (90-92%). Further, we examined the compatibility of this reaction with the Cbz-protecting group. In this context, we have synthesized **1m** and **1n** and subjected them to KO^{t}Bu mediated γ-lactam

synthesis (Scheme **4**). Both *N*-Cbz-α,β-unsaturated γ-amino amides **1m** and **1n** gave corresponding γ-lactams **2m** and **2n**, respectively in excellent yields, suggesting that both Boc- and Cbz- urethane protecting groups are compatible to this molecular rearrangement.

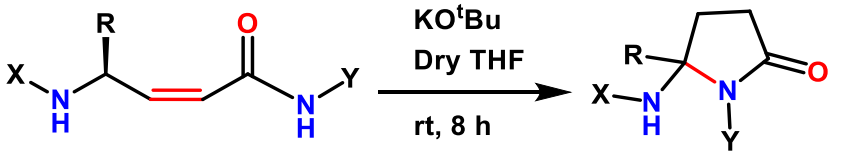

3 **2** **(90% - 94%)**

X	R	Y	3	2	yield (%)
Boc	$CH_2C_6H_5$	$(CH_2)_3CH_3$	3a	2h	90
Boc	$CH_2CH(CH_3)_2$	$CH_2C_6H_5$	3b	2c	94

Scheme 5: The facile transformation of (*S,Z*) *N*-Boc-α,β-unsaturated γ-amino amide into *N*-alkyl 5,5-disubstituted γ-lactams mediated by KO^{t}Bu.

In order to understand whether or not this transformation is specific to (*E*)-α,β-unsaturated γ-amino amides, we have synthesized (*Z*)-α,β-unsaturated γ-amino amides **3a** and **3b**, and subjected to the KO^{t}Bu mediated molecular transformation under identical conditions (Scheme **5**). The (*Z*)-α,β-unsaturated γ-amino acid residues were synthesized using Wittig-Horner reaction as reported earlier.[24] Both **3a** and **3b** gave corresponding γ-lactams **2h** and **2c**, respectively in excellent yields, suggesting that both (*E*) and (*Z*)-α,β-unsaturated γ-amino amides are compatible to the KO^{t}Bu mediated synthesis of γ-lactams. These results suggest that irrespective of the stereochemistry of the double bonds, both (*E*) and (*Z*)-α,β-unsaturated γ-amino amides gave the same γ-lactams. Notably, biosynthesis of various antibiotics involving double bond migration from α,β→ β,γ position also uses the *N*-urethane protected (*E*)-α,β-unsaturated γ-amino derivatives.[25]

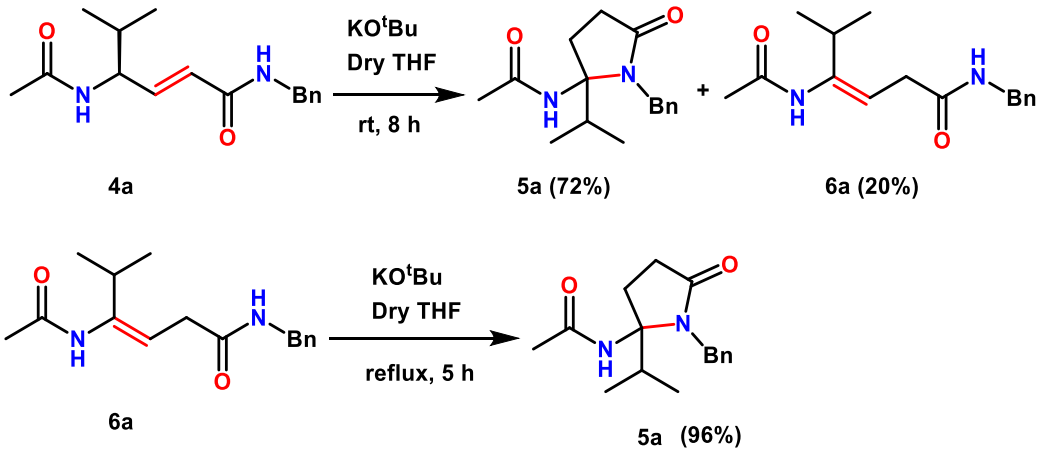

Scheme 6: Transformation of (*S,E*) *N*-acetyl-α,β-unsaturated γ-amino amides into γ-lactam and α,β→β,γ double bond migrated intermediate is also shown.

In order to understand the compatibility of this molecular transformation to *N*-acetyl protection, we synthesized (*S,E*) *N*-acetyl-α,β-unsaturated γ-amino amide **4a** and subjected to KO^{t}Bu mediated γ-lactam synthesis. In contrast to the urethane protected α,β-unsaturated γ-amino amides, **4a** gave a mixture of two products under identical conditions. Both products were separated through column chromatography. Along with the γ-lactam (**5a**), we have isolated α,β→β,γ double bond migrated product **6a**. The schematic representation of the reaction is shown in Scheme **6**. We hypothesize that **6a** is an intermediate in the transformation of **4a** to **5a**. To verify this, the isolated **6a** was subjected to KO^{t}Bu mediated rearrangement. Instructively, **6a** was completely transformed into **5a** upon refluxing in dry THF for about 4 h. These results suggested that *N*-urethane protecting groups are preferred over the N-acetyl groups for the smooth transformation of α,β-unsaturated γ-amino amides into γ-lactams.

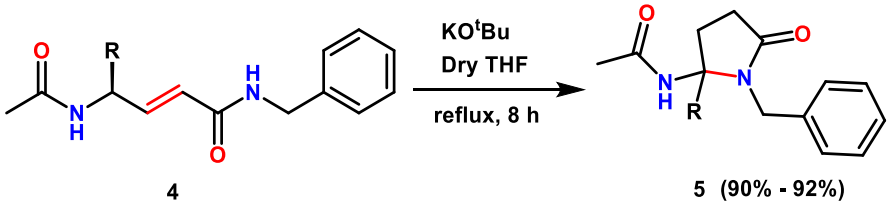

R	4	5	yield (%)
Isopropyl	4a	5a	92
Isobutyl	4b	5b	90
Benzyl	4c	5c	91

Scheme 7: KO^{t}Bu mediated synthesis of *N*-acetyl protected 5,5-disubstituted γ-lactams.

However, *N*-acetyl protected α,β-unsaturated γ-amino amides(**4a-c**) can be transformed into corresponding γ-lactams (**5a-c**) upon refluxing in dry THF in the presence of KO^{t}Bu as shown in Scheme **7.** All γ-lactams **5a-c** were isolated in good yields.

4. The γ-lactams as small molecule peptidomimetics

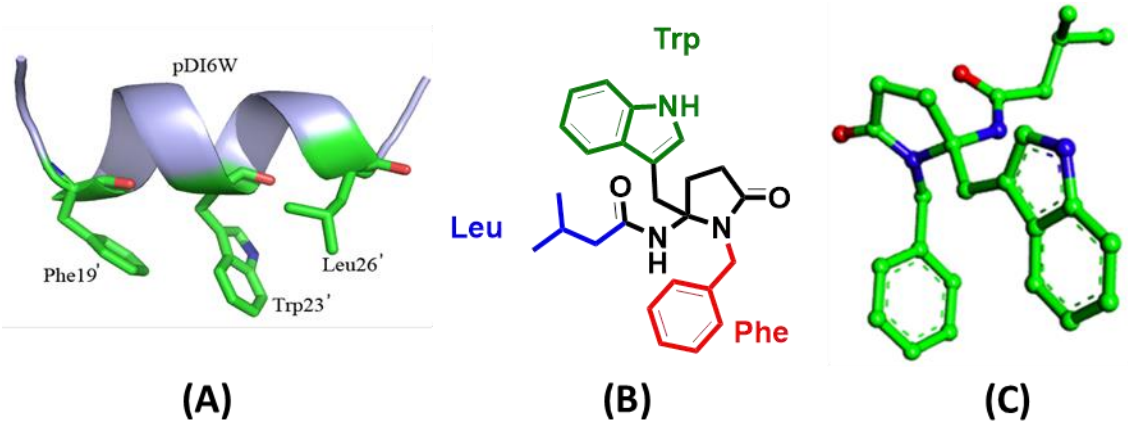

Figure 1: (A) Tumor suppressor protein p53, highlighting side-chains of Phe, Trp, and Leu amino acids, which are responsible for p53-MDM2 interaction (B) γ-lactams **4j,** highlighting the proteinogenic side-chains of Phe, Trp, and Leu amino acids as mimic of p53 (C) Crystal structure of **4j**.

The γ-lactams synthesized through this method are indigenously contained proteinogenic side-chains. Further, it is possible to design small-molecule peptidomimetics by designing the proteinogenic side chains on the γ-lactam ring. As an example, we have designed compound **4j**, which is organized with three different amino acid side-chain functionalities (Phe, Trp, and Leu) to mimics the tumor suppressor protein p53 as shown in Figure **1**. These three amino acid side chains are mainly responsible for cancer-causing p53-MDM2 protein-protein interaction.[26] The **4j** may serve as a P53-MDM2 protein-protein interaction inhibitor small molecule. For the synthesis of the **4j**, we selected γ-lactam **2j** and subjected for Boc group deprotection using 50% TFA in DCM (Scheme **8**). The free amine **3j** was isolated in excellent yield and free amine was further coupled to isovaleric acid using HBTU/HOBt. The *N*-acyl γ-lactam, **4j**, was isolated in excellent yield. These studies suggested that the free amine of γ-lactam can be exploited for further modifications. It is worth mentioning that these type of small templates constituted with proteinogenic side-chains can be explored to design potential small molecule peptidomimetics

with different amino acid side-chain substitutions. Out of all γ-lactams synthesized in the above Schemes **3**-**8**, we were able to confirm the identity of the compounds **2b**, **2e**, **2f**, **2h**, **2i**, **2j**, **2m**, **5c**, **3j** and **4j**, with the X-ray structures and the X-ray structures are shown in Figure **2**.

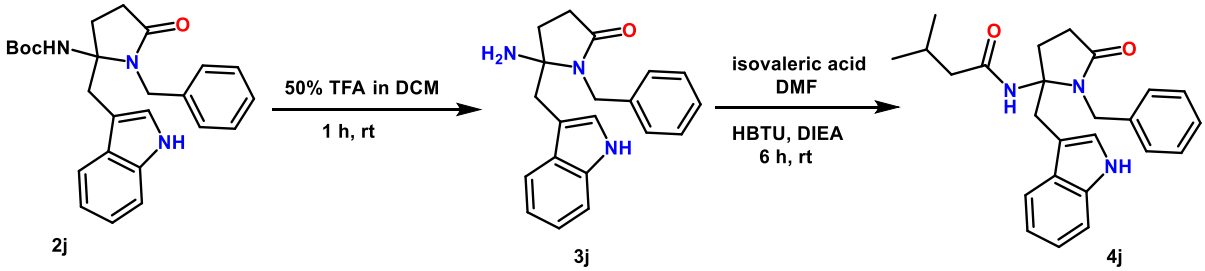

Scheme 8: Deprotection of *N*-Boc and *N*-acylation of the γ-lactam.

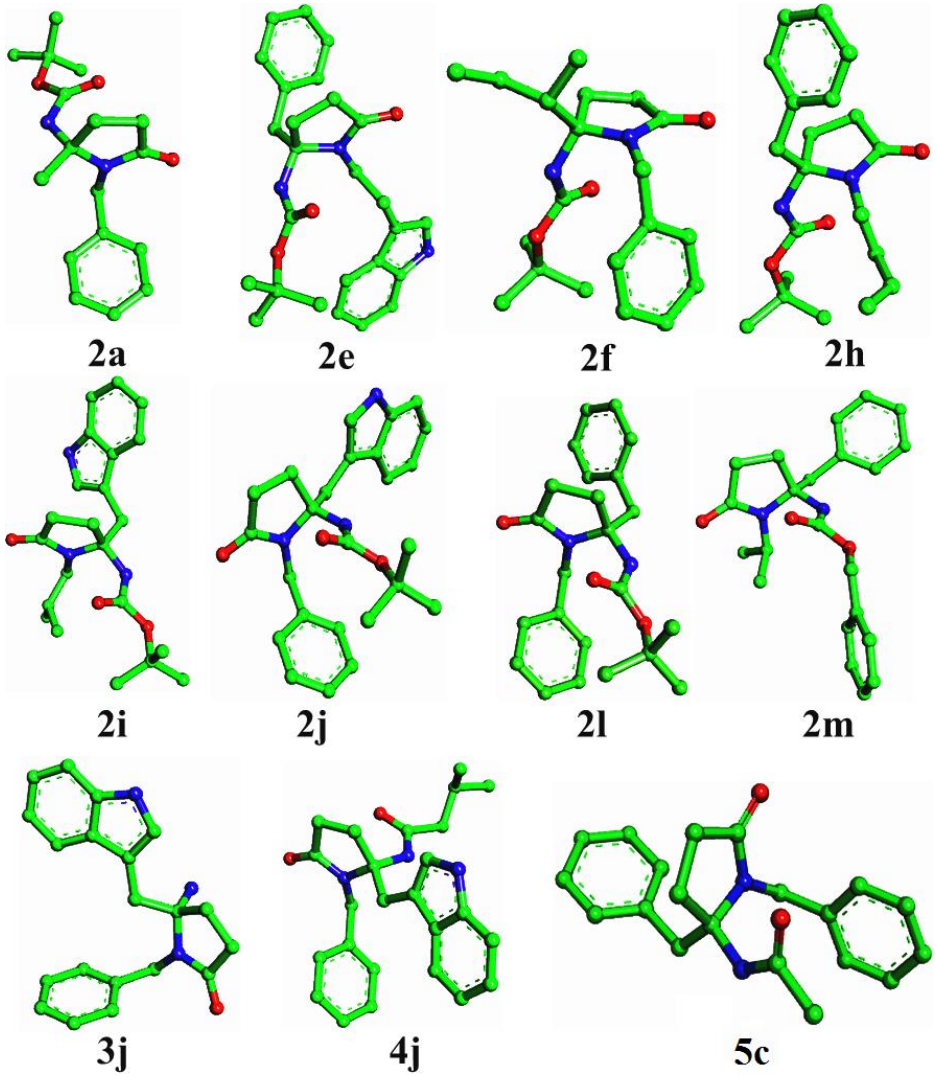

Figure 2: Single crystal structures of γ-lactams obtained in study

5. Plausible reaction mechanism

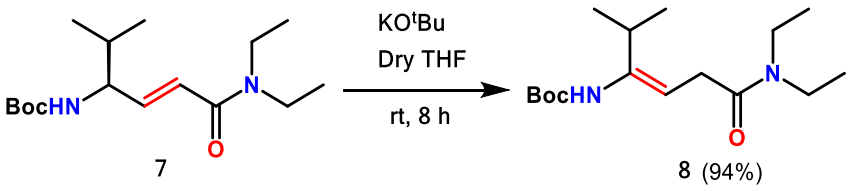

Scheme 9: Isolation of α,β→β,γ double bond migrated intermediate

Based on the evidence of α,β → β,γ double bond migration in the (*S,E*) *N*-acetyl α,β-unsaturated γ-amino amide **4a→6a**, we hypothesized that the base mediated transformation of *N*-protected α,β-unsaturated γ-amino amides into corresponding γ-lactams is probably involving a consecutive double bond migrations. Further to support our hypothesis we have also isolated α,β→β,γ double bond migrated intermediate **8,** by using the *N,N*-dialkyl amide **7** as reactant, lack of C-terminal amide proton in the *N,N*-dialkyl amide **7** stopes the reaction at intermediate stage. (Scheme **9**). The possible mechanism of the rearrangement of *N*-urethane protected (*S,E*)-α,β-unsaturated γ-amino amides into γ-lactams is shown in Scheme **10**. The abstraction of acidic γ-proton by a base leads to the α,β→β,γ double bond migrated product **C1′** which will be in equilibrium with **C1″** by enamine–imine-tautomerism. Finally, the unstable imide **C1″**undergoes 5-exo-trig cyclization reaction with deprotonated C-terminal amide leads to the formation of γ-lactam. Overall, the smooth transformation of *N*-urethane *E (or Z)*-α,β-unsaturated γ-amino amides into γ-lactams can be achieved at room temperature in a single pot with excellent yields.

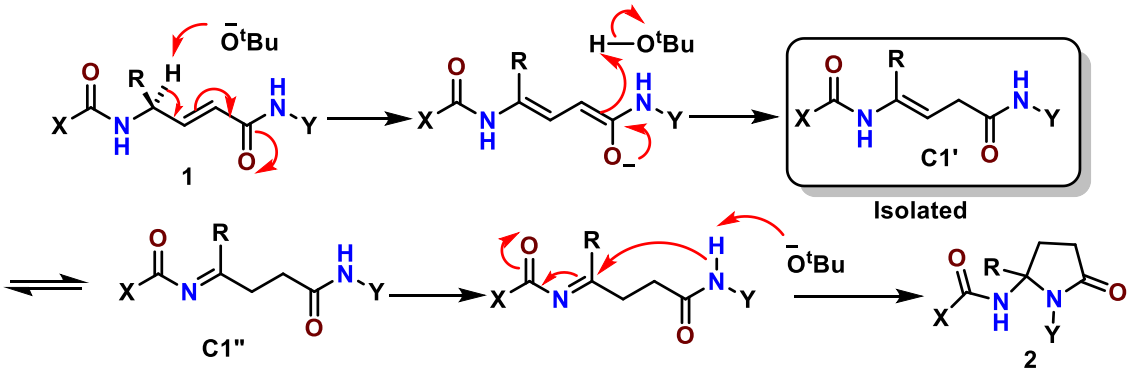

Scheme 10: Plausible mechanism of the base mediated transformation of the *N*-protected α,β-unsaturated γ-amino amides into 5,5-disubstituted γ-lactams.

6. Conclusion

In conclusion, we have demonstrated a base mediated novel molecular rearrangement that transforms *N*-alkyl amides of the *N*-protected α,β-unsaturated γ-amino acids into *N*-protected 5,5-disubstituted γ-lactams. Irrespective of the double bond stereochemistry either (*E*) or (*Z*)-both α,β-unsaturated γ-amino amides gave γ- lactams upon treatment with KO^tBu. In comparison with *N*-urethane and *N*-acetyl protections, *N*-urethane protected α,β-unsaturated γ-amino amides undergo a smooth transformation in the presence of KO^tBu to give remarkable γ-lactams in excellent yields. The temporary *N*-urethane protecting groups can be deprotected and the free amine can be acylated with different acylating derivatives. We believe that 5,5-disubstituted novel γ-lactams derived from this rearrangement in a single step may serve as a potential starting point to generate small molecule peptidomimetics. Overall, the *N*-protected α,β-unsaturated γ-amino amides can be explored to construct 5,5-disubstituted γ-lactam peptidomimetics through this new molecular rearrangement.

7. Experimental Section

General Method:

All reagents were used without further purification. Column chromatography was performed on neutral alumina (100 -200 mesh). ^{1}H NMR (400 MHz), ^{13}C NMR (100 MHz) were measured on a BrukerAvance 400 MHz spectrometer. Mass samples were analyzed by High resolution mass spectrometry using ESI TOF. The X-ray data were collected at 100K temperature on a Bruker APEX(II) DUO CCD diffractometer using Mo K_α radiation (λ = 0.71073 Å). (*E*)-*α, β*-Unsaturated *γ*-amino acids (Boc/Cbz-(*E*)d*γ*Xaa-COOH) and (*Z*)-*α,β*-unsaturated *γ*-amino acids (Boc-(*Z*)d*γ*Xaa-COOH) were prepared according to the previously reported procedures.[22, 23]

1. Synthesis of (*E*)-*α, β*-unsaturated *γ*-amino amides (1)

General procedure for the synthesis of (*E*)-*α, β*-unsaturated *γ*-amino amides (1): To the 3 mL DMF solution of Boc/Cbz-(*E*)d*γ*Xaa-COOH (3 mmol) diisopropylethylamine (3 mmol), benzylamine (3 mmol) were added. Then the mixture was treated with HBTU (3 mmol) at ice cold condition. The reaction mixture was stirred for about 12 h at room temperature. The reaction was monitored by TLC. After completion of the reaction, the reaction mixture was

diluted with EtOAc (150 mL) and washed with 0.5N HCl (3 × 50 mL), 10% Na_2CO_3 (1 × 50 mL) and brine solution (1 × 80 mL) respectively. The organic layer was dried over anhydrous Na_2SO_4 and concentrated under reduced pressure. The crude product was purified by column chromatography using petroleum ether /EtOAc (80/20) solvent system to get pure amides (**1a-n**).

(*S*, *E*)-*Tert*-butyl (5-(benzylamino)-5-oxo-1-phenylpent-3-en-2-yl)carbamate (**1a**): White solid, Yield= 1.083 g (95%); m. p 139-140 °C; $[\alpha]_D^{25}$ = 2.0 (*c* 0.1, MeOH); ^{1}H NMR (400 MHz, DMSO-d_6) δ 8.56 (t, *J* = 8 Hz, 1H), 7.33-7.17 (m, 10H), 7.12 (d, *J* = 12 Hz, 1H), 6.62 (dd, *J* = 16 Hz, *J* = 4 Hz, 1H), 5.97 (d, *J* = 16 Hz, 1H), 4.30 (m, 3H), 2.83-2.70 (m, 2H), 1.31 (s, 9H); ^{13}C{^{1}H} NMR (100 MHz, DMSO-d_6) δ 164.6, 155.0, 143.1, 139.5, 138.4, 129.2, 128.7, 128.3, 128.1, 127.3, 126.8, 126.2, 123.3, 77.8, 52.7, 42.1, 28.2; HRMS (ESI-TOF) *m/z*: $[M + H]^+$ calcd for $C_{23}H_{29}N_2O_3$, 381.2178; Found, 381.2172.

(*S*, *E*)-*Tert*-butyl (5-(benzylamino)-5-oxopent-3-en-2-yl)carbamate (**1b**): White solid, Yield = 0.813 g (89%); m. p 129-132 °C; $[\alpha]_D^{25}$ = -20.0 (*c* 0.1, MeOH); ^{1}H NMR (400 MHz, $CDCl_3$) δ 7.34-7.25 (m, 5H), 6.74 (dd, *J* = 15.4 Hz, *J* = 5.2 Hz, 1H), 6.10 (bs, 1H), 5.88 (d, 1H, *J* = 12 Hz), 4.63 (bs, 1H), 4.48 (d, 2H, *J* = 8 Hz), 4.34 (m, 1H), 1.43 (s, 9H), 1.24 (d, 3H, *J* = 8 Hz); ^{13}C{^{1}H} NMR (100 MHz, $CDCl_3$) δ 165.6, 155.1, 145.5, 138.2, 128.8, 128.0, 127.6, 122.6, 79.8, 47.2, 43.8, 28.5, 20.7; HRMS (ESI-TOF) *m/z*: $[M + H]^+$ Calcd for $C_{17}H_{25}N_2O_3$ 305.1865; Found 305.1863.

(*S*, *E*)-*Tert*-butyl (1-(benzylamino)-6-methyl-1-oxohept-2-en-4-yl)carbamate (**1c**): White solid, Yield = 0.935 g (90%); m. p 142-143 °C; $[\alpha]_D^{25}$ = -32.0 (*c* 0.1, MeOH); ^{1}H NMR (400 MHz, DMSO-d_6) δ 8.55 (t, *J* = 8 Hz, 1H), 7.33-7.23 (m, 5H), 7.00 (d, *J* = 8 Hz, 1H), 6.52 (dd, *J* = 12 Hz, *J* = 4 Hz, 1H), 5.97 (d, *J* = 16 Hz, 1H), 4.31 (m, 2H), 4.11 (m, 1H), 1.57 (m, 1H), 1.38 (s, 9H), 1.26 (m, 1H), 0.87 (d, *J* = 4 Hz, 6H); ^{13}C{^{1}H} NMR (100 MHz, DMSO-d_6) δ 164.7, 155.1, 143.9, 139.5, 128.7, 128.3, 127.7, 127.4, 126.8, 122.9, 77.7, 49.3, 42.9, 42.1, 28.3, 24.3, 22.7, 21.9; HRMS (ESI-TOF) *m/z*: $[M + Na]^+$ Calcd for $C_{20}H_{30}N_2O_3Na$ 369.2149; Found 369.2155.

(*S*, *E*)-*Tert*-butyl (6-(benzylamino)-2-methyl-6-oxohex-4-en-3-yl)carbamate (**1d**): White solid, Yield = 0.876 g (88%); m. p 153-155 °C; $[\alpha]_D^{25}$ = -18.0 (*c* 0.1, MeOH); ^{1}H NMR (400 MHz, DMSO-d_6) δ 8.54 (t, *J* = 8 Hz, 1H), 7.33-7.21 (m, 5H), 7.01 (d, *J* = 12 Hz, 1H), 6.55

(dd, *J* = 16 Hz, *J* = 4 Hz, 1H), 5.98 (d, *J* = 16 Hz, 1H), 4.31 (m, 2H), 3.85 (m, 1H), 1.72 (m, 1H), 1.38 (s, 9H), 0.83 (m, 6H); $^{13}C\{^{1}H\}$ NMR (100 MHz, DMSO-d_6) δ 164.7, 155.3, 142.0, 139.5, 128.3, 127.4, 126.8, 124.3, 77.7, 57.0, 40.1, 38.3, 31.9, 28.3, 19.1, 18.7; HRMS (ESI-TOF) *m/z*: $[M + Na]^+$ Calcd for $C_{19}H_{28}N_2O_3Na$ 355.1992; Found 355.1996.

(*S*, *E*)-*Tert*-butyl(5-((2-(1*H*-indol-3-yl)ethyl)amino)-5-oxo-1-phenylpent-3-en-2-yl)carbamate (**1e**): Brown color solid, Yield = 1.120 g (86%); m. p 164-166 °C; $[\alpha]_D^{25}$ = -8.0 (*c* 0.1, MeOH); ^{1}H NMR (400 MHz, DMSO-d_6) δ 10.81 (s, 1H), 8.16 (t, *J* = 8 Hz, 1H), 7.52 (d, *J* = 8 Hz, 1H), 7.34-6.95 (m, 12 H), 6.58 (dd, *J* = 16 Hz, J = 4 Hz, 1H), 5.90 (d, *J* = 16 Hz, 1H), 4.29 (m, 1H), 3.38 (m, 2H), 2.78 (m, 4H), 1.31 (s, 9H); $^{13}C\{^{1}H\}$ NMR (100 MHz, DMSO-d_6) δ 164.6, 154.9, 142.4, 138.4, 136.2, 129.2, 128.1, 127.2, 126.1, 123.6, 122.6, 120.9, 118.2, 111.8, 111.4, 77.7, 52.7, 28.2, 25.2; HRMS (ESI-TOF) *m/z*: $[M + H]^+$ Calcd for $C_{26}H_{32}N_3O_3$ 434.2444; Found 434.2441.

***Tert*-butyl ((*4S*, *5S*, *E*)-1-(benzylamino)-5-methyl-1-oxohept-2-en-4-yl)carbamate** (**1f**): White solid, Yield = 0.923 g (89%); m. p 158-159 °C; $[\alpha]_D^{25}$ = -16.0 (*c* 0.1, MeOH); ^{1}H NMR (400 MHz, DMSO-d_6) δ 8.55 (t, *J* = 8 Hz, 1H), 7.33-7.04 (m, 5H), 7.05 (d, *J* = 8 Hz, 1H), 6.53 (dd, *J* = 16 Hz, *J* = 8 Hz, 1H), 5.97 (d, *J* = 16 Hz, 1H), 4.32 (m, 2H), 3.93 (m, 1H), 1.49 (m, 1H), 1.38 (s, 9H), 1.08 (m, 1H), 0.82 (m, 6H); $^{13}C\{^{1}H\}$ NMR (100 MHz, DMSO-d_6) δ 164.6, 155.2, 141.7, 139.5, 128.3, 127.4, 126.8, 124.4, 77.7, 55.6, 42.2, 38.3, 28.3, 25.2, 15.4, 11.2; HRMS (ESI-TOF) *m/z*: $[M + Na]^+$ Calcd for $C_{20}H_{30}N_2O_3Na$ 369.2149; Found 369.2157.

***Tert*-butyl((*S*, *E*)-5-oxo-1-phenyl-5-(((*R*)-1-phenylethyl)amino)pent-3-en-2-yl)carbamate** (**1g**): White solid, Yield = 1.005 g (85%); m. p 186-188 °C; $[\alpha]_D^{25}$ = 44.0 (*c* 0.1, MeOH); ^{1}H NMR (400 MHz, $CDCl_3$) δ 7.34-7.52 (m, 10H), 6.78 (d, 1H, *J* = 16 Hz), 5.78 (d, 2H, *J* = 16 Hz), 5.20-5.11 (m, 1H), 4.55 (s, 2H), 2.91-2.83 (m, 2H), 1.49 (d, 3H, *J* = 8 Hz), 1.38 (s, 9H); $^{13}C\{^{1}H\}$ NMR (100 MHz, $CDCl_3$) δ 164.4, 155.2, 143.6, 143.1, 136.7, 129.6, 128.8, 128.6, 127.5, 126.9, 126.4, 123.7, 79.9, 52.5, 49.0, 41.2, 38.7, 28.4, 23.6, 21.8.; HRMS (ESI-TOF) *m/z*: $[M + H]^+$ Calcd for $C_{24}H_{31}N_2O_3$ 395.2335; Found 395.2334.

***Tert*-butyl (*S*, *E*)-(5-(butylamino)-5-oxo-1-phenylpent-3-en-2-yl)carbamate**(**1h**): Colorless viscous liquid, Yield = 0.902 g (87%); $[\alpha]_D^{25}$ = -2.0 (*c* 0.1, MeOH); ^{1}H NMR ($CDCl_3$, 400 MHz) δ 7.30-7.15 (m, 5H), 6.75 (dd, *J* = 16 Hz, *J* = 4 Hz, 1H), 5.77 (d, *J* = 16 Hz, 1H), 5.59

(bs, 1H), 4.58 (d, *J* = 12 Hz, 1H), 3.28 (q, *J* = 8 Hz, 2H), 2.87 (d, *J* = 8 Hz, 2H), 1.48 (quint, *J* = 8 Hz, 2H), 1.38-1.30 (m, 11H), 0.91 (t, *J* = 8 Hz, 3H); $^{13}C\{^{1}H\}$ NMR ($CDCl_3$, 100 MHz) δ 165.3, 155.2, 142.9, 136.8, 129.6, 128.6, 126.8, 123.9, 79.9, 52.6, 41.2, 39.4, 31.7, 28.4, 20.2, 13.9; HRMS (ESI-TOF) *m/z*: $[M + H]^+$ Calcd for $C_{20}H_{31}N_2O_3$ 347.2335; Found 347.2331.

***Tert*-butyl (*S, E*)-(1-(1*H*-indol-3-yl)-5-(isobutylamino)-5-oxopent-3-en-2-yl)carbamate** (**1i**): White solid, Yield = 1.00 g (87) %; m. p 150-153 °C; $[\alpha]_D^{25}$ = 8.0 (*c* 0.1, MeOH); ^{1}H NMR (400 MHz, DMSO-d_6) δ 10.84 (d, *J* = 0.8 Hz, 1H), 7.98 (t, *J* = 4 Hz, 1H), 7.54 (d, *J* = 8 Hz, 1H), 7.11-6.96 (m, 4H), 6.59 (dd, *J* = 16 Hz, *J* = 4 Hz, 1H), 5.92 (d, *J* = 16 Hz, 1H), 4.37 (quint, *J* = 8 Hz, 1H), 2.90 (m, 4H), 1.66 (m, 1H), 1.35 (s, 9H), 0.82 (d, *J* = 8 Hz, 6H); $^{13}C\{^{1}H\}$ NMR (100 MHz, DMSO-d_6) δ 164.7, 155.1, 142.7, 136.2, 127.3, 123.6, 123.4, 120.9, 118.4, 118.3, 111.4, 110.6, 77.8, 51.9, 46.1, 30.5, 28.3, 28.1, 20.2; HRMS (ESI-TOF) *m/z*: $[M + H]^+$ Calcd for $C_{22}H_{32}N_3O_3$ 386.2444; Found 386.2441.

***Tert*-butyl (*S, E*)-(5-(benzylamino)-1-(1*H*-indol-3-yl)-5-oxopent-3-en-2-yl)carbamate** (**1j**): White solid, Yield = 1.15 g (92%); m. p 180-181 °C; $[\alpha]_D^{25}$ = 18.0 (*c* 0.1, MeOH); ^{1}H NMR (400 MHz, DMSO-d_6) δ 10.84 (d, *J* = 1.2 Hz, 1H), 8.51 (t, *J* = 8 Hz, 1H), 7.55 (d, *J* = 8 Hz, 1H), 7.31 (m, 3H), 7.23 (m, 3H), 7.12 (m, 2H), 7.05 (t, *J* = 4 Hz, 1H), 6.98 (t, *J* = 4 Hz, 1H), 6.66 (dd, *J* = 4 Hz, *J* = 16 Hz, 1H), 5.96 (d, *J* = 16 Hz, 1H), 4.40-4.29 (m, 3H), 2.89 (d, *J* = 8 Hz, 2H), 1.35 (s, 9H); $^{13}C\{^{1}H\}$ NMR (100 MHz, DMSO-d_6) δ 164.7, 155.0, 143.3, 139.5, 136.1, 128.3, 127.3, 126.8, 123.4, 123.3, 120.8, 118.3, 118.2, 111.3, 110.6, 77.7, 51.9, 42.1, 30.3, 28.2; HRMS (ESI-TOF) *m/z*: $[M + H]^+$ Calcd for $C_{25}H_{30}N_3O_3$ 420.2287; Found 420.2281.

***Tert*-butyl (*S, E*)-(5-(methylamino)-5-oxo-1-phenylpent-3-en-2-yl)carbamate** (**1k**): Colorless solid; Yield = 0.793 g (87%); mp = 112-116 °C; $[\alpha]_D^{25}$ = -8.0 (*c* 0.1, MeOH); ^{1}H NMR (400 MHz, $CDCl_3$) δ 7.33-7.18 (m, 5H), 6.78 (bd, *J* = 16 Hz, 1H), 5.79 (d, *J* = 16 Hz, 1H), 5.60 (bs, 1H), 4.58 (bs, 1H), 2.90 (d, *J* = 6, 2H), 2.87 (d, *J* = 5 Hz, 3H), 1.40 (s, 9H); $^{13}C\{^{1}H\}$ NMR (100 MHz, $CDCl_3$) δ 166.2, 155.2, 143.0, 136.7, 129.7, 128.4, 126.8, 123.8, 79.5, 52.6, 41.0, 28.4, 26.4; HRMS (ESI-TOF) *m/z*: $[M + H]^+$ Calcd for $C_{17}H_{25}N_2O_3$ 305.1865; Found 305.1863.

***Tert*-butyl (*E*)-(4-(benzylamino)-4-oxobut-2-en-1-yl)carbamate** (**1l**): White solid, Yield = 0.783 g (90 %); m. p 140-143 °C; ^{1}H NMR (400 MHz, DMSO-d_6) δ 8.54 (t, *J* = 5.8 Hz, 1H), 7.42 – 7.19 (m, 5H), 7.12 (t, *J* = 5.7 Hz, 1H), 6.57 (dt, *J* = 15.4, 4.9 Hz, 1H), 5.99 (d, *J* =

15.5 Hz, 1H), 4.32 (d, *J* = 6.0 Hz, 1H), 3.68 (t, *J* = 4.6 Hz, 1H), 1.39 (s, 1H); $^{13}C\{^{1}H\}$ NMR (100 MHz, $CDCl_3$) δ 165.2, 155.8, 140.9, 138.2, 128.9, 128.0, 127.7, 123.8, 79.7, 43.8, 41.5, 28.5; HRMS (ESI-TOF) *m/z*: $[M + H]^+$ Calcd for $C_{16}H_{23}N_2O_3$ 291.1709; Found 291.1710.

Benzyl (*E*)-(5-(isopropylamino)-5-oxo-1-phenylpent-3-en-2-yl)carbamate(**1m**): White solid, Yield = 0.99 g (90 %); m. p 193-196 °C; $[\alpha]_D^{25}$ = -17.6 (*c* 0.1, MeOH); ^{1}H NMR (400 MHz, $CDCl_3$) δ 7.39 – 7.22 (m, 10H), 6.79 (dd, *J* = 16 Hz, *J* = 4 Hz, 1H), 5.74 (d, *J* = 16 Hz, 1H), 5.35 (d, *J* = 4 Hz, 1H), 5.07 (s, 1H), 4.87 (bs, 1H), 4.13 (m, 1H), 2.93 (m, 2H), 1.16 (d, *J* = 4 Hz, 1H); $^{13}C\{^{1}H\}$ NMR (100 MHz, $CDCl_3$) δ 164.1, 155.6, 142.3, 136.3, 129.4, 128.6, 128.5, 128.2, 126.9, 124.2, 66.8, 53.0, 41.5, 40.8, 22.7; HRMS (ESI-TOF) *m/z*: $[M + H]^+$ Calcd for $C_{22}H_{27}N_2O_3$ 367.2022; Found 367.2020.

Benzyl (*S, E*)-(1-(benzylamino)-6-methyl-1-oxohept-2-en-4-yl)carbamate (1n): White solid, Yield = 0.98 g (86 %); m. p 131-133 °C; $[\alpha]_D^{25}$ = -14.0 (*c* 0.1, MeOH); ^{1}H NMR (400 MHz, $CDCl_3$) δ 7.32-7.26 (m, 10H), 6.71(dd, *J* = 16 Hz, *J* = 4 Hz, 1H), 5.93 (bs, 1H), 5.86 (d, *J* = 16 Hz, 1H), 5.06 (s, 2H), 4.81 (bs, 1H), 4.46 (d, 4 Hz, 1H), 4.35 (t, *J* = 4 Hz, 1H), 1.67 (m, 1H), 1.39 (t, *J* = 6 Hz, 2H), 0.91 (d, *J* = 4 Hz, 6H); $^{13}C\{^{1}H\}$ NMR (100 MHz, $CDCl_3$) δ 165.2, 155.7, 144.3, 138.1, 136.3, 128.7, 128.5, 128.2, 127.9, 127.6, 127.6, 123.1, 66.9, 50.5, 43.8, 43.7, 24.7, 22.6, 22.2; HRMS (ESI-TOF) *m/z*: $[M + H]^+$ Calcd for $C_{23}H_{29}N_2O_3$ 381.2178; Found 381.2175.

2. Synthesis of 5, 5-disubstituted *N*-protected *γ*-lactams (2)

General procedure for the synthesis of *γ*-lactams (2): To the solution of N-protected *α,β*-unsaturated *γ*-amino amide (2 mmol, 1 equvi) in dry THF (10 mL), KO^{t}Bu (6 mmol, 3 equvi) was added under N_2 atmosphere and stirred for about 8 h at room temperature. The progress of the reaction was monitored by TLC. After completion of the reaction, water (30 mL) was added and the aqueous layer was extracted with EtOAc (30 mL × 3) and then the combined organic layer was washed with brine (30 mL × 2), dried over anhydrous Na_2SO_4 and concentrated under reduced pressure. The crude products were purified by column chromatography using petroleum ether/EtOAc (80/20) solvent system to get pure products in 90-95% yields.

***Tert*-butyl (1, 2-dibenzyl-5-oxopyrrolidin-2-yl)carbamate** (**2a**): Colorless solid, Yield = 0.699 (92%); m. p 193-196 °C; ^{1}H NMR (400 MHz, $CDCl_3$) δ 7.41 (d, *J* = 8 Hz, 2H,), 7.33-

7.24 (m, 6H), 7.09 (d, *J* = 4 Hz, 2H,), 4.92 (s, 1H), 4.61 (s, 2H), 3.06-2.95 (m, 2H), 2.51-2.48 (m, 1H), 2.33-2.27 (m, 2H), 1.92-1.86 (m, 1H), 1.32 (s, 9H); $^{13}C\{^{1}H\}$ NMR (100 MHz, $CDCl_3$) δ 175.5, 153.5, 138.4, 134.4, 130.3, 128.9, 128.7, 128.4, 127.6, 127.4, 77.8, 77.4, 44.5, 43.4, 30.0, 29.6, 28.3; HRMS (ESI-TOF) *m/z*: $[M + H]^+$ Calcd for $C_{23}H_{29}N_2O_3$ 381.2178; Found 381.2171.

***Tert*-butyl (1-benzyl-2-methyl-5-oxopyrrolidin-2-yl)carbamate** (**2b**): Colorless solid, Yield = 0.565 g (93%); m. p 129-130 °C; $[\alpha]_D^{25}$ = 0.0 (*c* 0.1, MeOH); ^{1}H NMR (400 MHz, $CDCl_3$) δ 7.29-7.20 (m, 5H), 4.89 (bs, 1H), 4.60 (d, 1H, *J* = 12 Hz), 4.27 (d, 1H, *J* = 12 Hz), 2.81 (bs, 1H), 2.55-2.40 (m, 2H), 2.08-2.01 (m, 1H), 1.37 (s, 9H), 1.33 (s, 3H); $^{13}C\{^{1}H\}$ NMR (100 MHz, $CDCl_3$) δ 175.8, 175.1, 143.4, 142.4, 134.4, 130.2, 128.8, 128.6, 127.8, 127.1, 78.6, 78.6, 77.2, 53.1, 45.8, 30.3, 30.2, 29.8, 28.4, 28.2, 20.0, 19.7. HRMS (ESI-TOF) *m/z*: $[M + Na]^+$ Calcd for $C_{17}H_{24}N_2O_3Na$ 327.1685; Found 327.1683.

***Tert*-butyl (1-benzyl-2-isobutyl-5-oxopyrrolidin-2-yl)carbamate** (**2c**): Pale yellow thick liquid, Yield = 0.623 (90%); $[\alpha]_D^{25}$ = 0.0 (*c* 0.1, MeOH); ^{1}H NMR (400 MHz, $CDCl_3$) δ 7.29-7.12 (m, 5H), 4.79 (bs, 1H), 4.33 (bs, 2H), 2.75 (m, 1H), 2.45-2.08 (m, 3H), 1.61 (m, 1H), 1.36 (m, 2H), 1.25 (s, 9H), 0.89-0.73 (m, 6H); $^{13}C\{^{1}H\}$ NMR (100 MHz, $CDCl_3$) δ 175.8, 156.6, 137.2, 136.4, 128.5, 127.3, 110.1, 79.8, 43.7, 29.1, 28.4, 26.8, 23.6, 21.3; HRMS (ESI-TOF) *m/z*: $[M + H]^+$ Calcd for $C_{20}H_{31}N_2O_3$ 347.2335; Found 347.2332.

***Tert*-butyl (1-benzyl-2-isopropyl-5-oxopyrrolidin-2-yl)carbamate** (**2d**): Colorless solid, Yield = 0.597 g (90%); m. p 136-137 °C; $[\alpha]_D^{25}$ = 0.0 (*c* 0.1, MeOH); ^{1}H NMR (400 MHz, $CDCl_3$) δ 7.34-7.20 (m, 5H), 4.85 (s, 1H), 4.43-4.23 (m, 2H), 2.87-2.84 (m,1H), 2.35-1.98 (m, 4H), 1.31 (s, 9H), 0.96 (d, 3H, *J* = 8 Hz), 0.61 (bs, 3H).; $^{13}C\{^{1}H\}$ NMR (100 MHz, $CDCl_3$) δ 176.2, 153.4, 138.2, 128.7, 128.5, 127.8, 127.2, 80.6, 79.7, 43.7, 42.7, 40.9, 35.6, 34.5, 30.0, 29.8, 28.3, 24.1, 18.3, 16.7, 15.8; HRMS (ESI-TOF) *m/z*: $[M + H]^+$ Calcd for $C_{19}H_{29}N_2O_3$ 333.2178; Found 333.2176.

***Tert*-butyl (1-(2-(1*H*-indol-3-yl)ethyl)-2-benzyl-5-oxopyrrolidin-2-yl)carbamate** (**2e**): Brown color solid, Yield = 0.789 g (91%); m. p 171-173 °C; $[\alpha]_D^{25}$ = 0.0 (*c* 0.1, MeOH); ^{1}H NMR (400 MHz, $CDCl_3$) δ 7.41 (d, *J* = 8 Hz, 2H), 7.33-7.24 (m, 8H), 7.08 (m, 2H), 4.92 (s, 1H), 4.61 (s, 2H), 3.01 (m, 2H), 2.48 (m, 1H), 2.31 (m, 2H), 1.90 (m, 1H), 1.32 (s, 9H); $^{13}C\{^{1}H\}$ NMR (100 MHz, $CDCl_3$) δ 175.5, 138.4, 134.4, 130.3, 128.9, 128.7, 128.4, 127.6, 127.4, 77.8,

44.4, 43.4, 30.0, 29.6, 28.3; HRMS (ESI-TOF) *m/z*: $[M + Na]^+$ Calcd for $C_{26}H_{31}N_3O_3Na$ 456.2263; Found 456.2263.

***Tert*-butyl (1-benzyl-2-((*S*)-sec-butyl)-5-oxopyrrolidin-2-yl)carbamate** (**2f**) (diastereomer mixture): Pale yellow solid, Yield = 0.623 g (90%); $[\alpha]_D^{25}$ = 0.0 (*c* 0.1, MeOH); ^{1}H NMR (400 MHz, $CDCl_3$) δ 7.38-7.16 (m, 10H), 4.85 (bs, 1H) (major), 4.73 (bs, 1H) (minor), 4.52-4.41 (m, 2H) (major), 4.16 (m, 2H) (minor), 2.36-2.17 (m, 4H) (major), 2.06 (m, 2H) (minor), 1.85 (m, 2H) (minor), 1.59 (m, 2H), 1.35 (bs, 9H) (major), 1.28 (bs, 9H) (minor), 1.10 (m, 2H) (minor), 0.93 (m, 6H) (major), 0.65 (bs, 2H) (minor), 0.46 (bs, 2H) (minor); HRMS (ESI-TOF) *m/z*: $[M + H]^+$ Calcd for $C_{20}H_{31}N_2O_3$ 347.2335; Found 347.2335.

***Tert*-butyl (2-benzyl-5-oxo-1-((*S*)-1-phenylethyl)pyrrolidin-2-yl)carbamate** (**2g**): Pale yellow solid, Yield = 0.71 g (90%); $[\alpha]_D^{25}$ = -3.0 (*c* 0.1, MeOH); ^{1}H NMR (400 MHz, $CDCl_3$) δ 7.62-6.98 (m, 10H), 5.11 (s, 1H, Boc-N*H*, major), 4.93 (Boc-N*H*, minor) 4.64 (q, *J* = 8 Hz, 1H), 3.04-2.59 (m, 3H), 2.37-2.19 (m, 4H), 1.88 (d, *J* = 8 Hz, CH_3, minor), 1.84 (d, *J* = 8 Hz, 3H, CH_3major), 1.46 (s, 9H, Boc minor), 1.26 (s, 9H, Boc major); $^{13}C\{^1H\}$ NMR (100 MHz, $CDCl_3$) δ 175.8 (major), 175.1 (minor), 143.4 (major), 142,4 (minor), 134.4, 130.3 (major), 130.2 (minor), 128.9 (minor), 128.8 (major), 128.6, 128.3, 127.8, 127.4, 127.2, 126.3 (major), 126.2 (minor), 78.5 (minor), 78.4 (major), 53.0, 45.8, 30.3 (major), 30.2 (minor), 29.8, 28.4 (major), 28.2 (minor), 20.0 (minor), 19.7 (major); HRMS (ESI-TOF) *m/z*: $[M]^+$ Calcd for $C_{24}H_{30}N_2O_3$ 394.2256; Found 394.2250.

***Tert*-butyl (2-benzyl-1-butyl-5-oxopyrrolidin-2-yl)carbamate** (**2h**): Pale yellow solid, Yield = 0.646 g (93%); m. p 120-121 $^\circ$C; $[\alpha]_D^{25}$ = 0.0 (*c* 0.1, MeOH); ^{1}H NMR (400 MHz, $CDCl_3$) δ 7.33-7.22 (m, 3H), 7.15-7.09 (m, 2H), 5.15 (bs, 1H), 3.50-3.38 (m, 1H), 3.16-3.06 (m, 1H), 3.04 (d, *J* = 14 Hz, 1H), 2.42-2.28 (m, 2H), 2.25-2.13 (m, 1H), 1.79-1.66 (m, 1H), 1.65-1.50 (m, 2H), 1.42 (s, 9H), 1.39-1.31 (m, 2H), 0.92 (t, *J* = 8 Hz, 3H); $^{13}C\{^1H\}$ NMR (100 MHz, $CDCl_3$) δ 174.9, 153.5, 134.2, 130.3, 128.8, 127.6, 80.2, 77.3, 44.1, 40.3, 30.9, 29.8, 29.5, 28.9, 28.4, 20.9, 14.0; HRMS (ESI-TOF) *m/z*: $[M + Na]^+$ Calcd for $C_{20}H_{30}N_2O_3Na$ 369.2149; Found 369.2157.

***Tert*-butyl (2-((1*H*-indol-3-yl)methyl)-1-isobutyl-5-oxopyrrolidin-2-yl)carbamate** (**2i**): Brown colour solid, Yield = 0.732 g (95%); m. p 167-168 $^\circ$C; $[\alpha]_D^{25}$ = 0.0 (*c* 0.1, MeOH);

^{1}H NMR (400 MHz, $CDCl_3$) δ 8.91 (bs, 1H), 7.58 (d, J = 8 Hz, 1H), 7.38 (d, J = 8 Hz, 1H), 7.22 – 7.13 (m, 2H), 6.91 (s, 1H), 5.19 (s, 1H), 3.37 – 3.03 (m, 4H), 2.46 (m, 2H), 2.26-2.05 (m, 2H), 1.44 (m, 10), 0.98 (t, 6H); ^{13}C{^{1}H} NMR (100 MHz, $CDCl_3$) δ 176.0, 135.8, 128.1, 123.1, 122.4, 119.9, 117.9, 111.5, 108.0, 77.9, 77.3, 77.3, 77.0, 76.7, 47.4, 29.8, 28.6, 28.3, 21.0, 20.8; HRMS (ESI-TOF) *m/z*: $[M]^+$ Calcd for $C_{22}H_{31}N_3O_3$ 385.2365; Found 385.2361.

***Tert*-butyl(2-((1*H*-indol-3-yl)methyl)-1-benzyl-5-oxopyrrolidin-2-yl)carbamate** (**2j**): White colour solid, Yield = 0.780 g (93%); m. p 210-216 °C; $[\alpha]_D^{25}$ = 0.0 (*c* 0.1, MeOH); ^{1}H NMR (400 MHz, DMSO-d_6) δ 10.94 (s, 1H), 7.58 (d, J = 8 Hz, 1H), 7.44-7.37 (m, 3H), 7.35-7.25 (m, 3H), 7.24-7.18 (m, 1H), 7.06 (t, J = 7 Hz, 1H), 6.99 (t, J = 7 Hz, 1H), 6.89 (bs, 1H), 4.53-4.40 (m, 2H), 3.17 (d, J = 8 Hz, 1H), 3.06 (d, J = 12 Hz, 1H), 2.33-2.23 (m, 2H), 2.14-2.09 (m, 1H), 1.72-1.56 (m, 1H), 1.27 (s, 9H); ^{13}C{^{1}H} NMR (100 MHz, DMSO- d_6) δ 174.4, 153.7, 138.8, 135.6, 128.2, 128.0, 126.6, 124.2, 120.9, 118.7, 118.00, 111.4, 107.2, 77.7, 48.6, 42.4, 39.5, 30.7, 29.4, 28.1; HRMS (ESI-TOF) *m/z*: $[M + H]^+$ Calcd for $C_{25}H_{30}N_3O_3$ 420.2287; Found 420.2284.

***Tert*-butyl (2-benzyl-1-methyl-5-oxopyrrolidin-2-yl)carbamate** (**2k**): Pale yellow liquid; Yield = 0.572 g (94%); $[\alpha]_D^{25}$ = 0.0 (*c* 0.1, MeOH); ^{1}H NMR (400 MHz, $CDCl_3$) δ 7.36-7.30 (m, 3H), 7.15-7.13 (m, 2H), 5.01 (s, 1H), 3.05 (d, J = 12, 1H), 2.95-2.89 (m, 1H), 2.87 (s, 3H), 2.43-2.30 (m, 2H), 2.28-2.20 (m, 1H), 1.66-1.57 (m, 1H), 1.45 (s, 9H); ^{13}C{^{1}H} NMR (100 MHz, $CDCl_3$) δ 175.3, 133.8, 130.3, 128.8, 127.6, 77.0, 43.2, 29.6, 29.0, 28.3, 24.0; HRMS (ESI-TOF) *m/z*: $[M + Na]^+$ Calcd for $C_{17}H_{24}N_2O_3Na$ 327.1685; Found 327.1687.

***Tert*-butyl (1-benzyl-5-oxopyrrolidin-2-yl)carbamate** (**2l**): Colorless viscous liquid, Yield = 0.528 g (91%); $[\alpha]_D^{25}$ = 0.0 (*c* 0.1, MeOH); ^{1}H NMR (400 MHz, $CDCl_3$) δ 7.36 - 7.23 (m, 5H), 5.33 (s, 1H), 4.76 (d, J = 9.3 Hz, 1H), 4.64 (d, J = 14.6 Hz, 1H), 4.21 (d, J = 14.9 Hz, 1H), 2.69 – 2.48 (m, 1H), 2.46 – 2.33 (m, 2H), 1.83 - 1.73 (s, 1H), 1.43 (s, 9H); ^{13}C{^{1}H} NMR (100 MHz, $CDCl_3$) δ 173.8, 170.6, 136.9, 128.6, 128.4, 127.5, 80.3, 65.6, 44.1, 29.2, 28.2, 26.6. HRMS (ESI-TOF) *m/z*: $[M + H]^+$ Calcd for $C_{16}H_{22}N_2O_3Na$ 313.1528; Found 313.1526.

Benzyl (2-benzyl-1-isopropyl-5-oxopyrrolidin-2-yl)carbamate(**2m**): White crystalline solid, Yield = 0.696 g (95%); m. p 189-193 °C; $[\alpha]_D^{25}$ = 0.0 (*c* 0.1, MeOH); ^{1}H NMR (400 MHz, $CDCl_3$) δ 7.40-7.30 (m, 8H), 7.25-7.20 (m, 2H), 5.28 (bs, 1H), 5.14 (d, J = 12 Hz, 1H), 4.95 (d, J

= 12 Hz, 1H), 3.56 (m, 1H), 3.15 (d, *J* = 12 Hz, 1H), 2.88 (d, *J* = 12 Hz, 2H), 2.60 (bs, 1H), 2.36-2.28 (m, *J* = 12 Hz, 1H), 2.28-2.20 (bs, 1H), 2.19-2.07 (m, 1H), 1.66-1.59 (bs, 1H), 1.49 (d, *J* = 8 Hz, 3H), 1.32 (d, *J* = 8 Hz, 3H); $^{13}C\{^{1}H\}$ NMR (100 MHz, $CDCl_3$) δ 174.9, 134.5, 130.1, 129.1, 128.7, 128.6, 128.5, 127.8, 77.9, 44.8, 30.3, 29.7, 20.9, 19.5; HRMS (ESI-TOF) *m/z*: $[M + H]^+$ Calcd for $C_{22}H_{27}N_2O_3$ 367.2022; Found 367.2021.

Benzyl (1-benzyl-2-isobutyl-5-oxopyrrolidin-2-yl)carbamate (**2n**): Colorless viscous liquid, Yield = 0.684 g (90%); $[\alpha]_D^{25}$ = 0.0 (*c* 0.1, MeOH); ^{1}H NMR (400 MHz, $CDCl_3$) δ 7.36-7.22 (m, 10H), 6.07 (s, 1H), 4.43 (d, *J* = 4 Hz, 2H), 2.83 (t, *J* = 6 Hz, 2H), 2.48(t, *J* = 6 Hz, 2H), 2.34 (d, *J* = 4 Hz, 2H), 2.16 (m, 1H), 0.98 (d, *J* = 8 Hz, 2H), 0.93 (d, *J* = 8 Hz, 6H); $^{13}C\{^{1}H\}$ NMR (100 MHz, $CDCl_3$) δ 171.9, 138.3, 128.7, 128.5, 128.3, 127.7, 127.4, 127.1, 77.5, 51.8, 43.6, 38.3, 29.9, 24.7, 24.4, 24.1, 23.9, 22.6; HRMS (ESI-TOF) *m/z*: $[M + H]^+$ Calcd for $C_{23}H_{29}N_2O_3$ 381.2178; Found 381.2172.

3. **General procedure for the synthesis of *N*-alkyl amides (*S,Z*)-*N*-Boc-*α, β*-unsaturated *γ*-amino acids (3)**: Similar to *N*-alkyl amides of **(***S, E***)** *N*-Boc-*α*, *β*-unsaturated *γ*-amino acids (**1**) reported above, amides **(***S,Z*)-*N*-Boc-*α*, *β*-unsaturated *γ*-amino acids (**3**) were synthesized using Boc-(*S,Z*)d*γ*Xaa-COOH.

***Tert*-butyl (*S, Z*)-(5-(butylamino)-5-oxo-1-phenylpent-3-en-2-yl)carbamate** (**3a**):Colorless viscous liquid, Yield = 0.88 g (85%); $[\alpha]_D^{25}$ = -10.0 (*c* 0.1, MeOH); ^{1}H NMR (400 MHz, $CDCl_3$) δ 7.56 (s, 1H), 7.36 – 7.14 (m, 5H), 5.80 (d, *J* = 11.7 Hz, 1H), 5.68 (t, *J* = 10.4 Hz, 1H), 5.00 - 4.76 (m, 2H), 3.42 – 3.22 (m, 2H), 2.93 (dd, *J* = 13.9, 5.5 Hz, 1H), 2.81 (dd, *J* = 13.9, 7.7 Hz, 1H), 1.66 – 1.44 (m, 1H), 1.42 – 1.35 (m, 2H), 0.93 (t, *J* = 7.3 Hz, 1H); $^{13}C\{^{1}H\}$ NMR (100 MHz, $CDCl_3$) δ 166.1, 156.0, 138.6, 136.9, 129.5, 128.7, 126.9, 125.5, 80.1, 60.5, 50.5, 40.8, 39.3, 31.5, 28.4, 21.15, 20.3, 14.3, 13.9; HRMS (ESI-TOF) *m/z*: $[M + H]^+$ Calcd for $C_{20}H_{31}N_2O_3$ 347.2335; Found 347.2337.

***Tert*-butyl (*S, Z*)-(1-(benzylamino)-6-methyl-1-oxohept-2-en-4-yl)carbamate** (**3b**):White solid, Yield = 0.933 g (90%); m. p 142-143 $^{\circ}$C; $[\alpha]_D^{25}$ = -32.0 (*c* 0.1, MeOH); ^{1}H NMR (400 MHz, $CDCl_3$) δ 8.88 (s, 1H), 7.50 – 7.15 (m, 6H), 5.87 (d, *J* = 11.8 Hz, 1H), 5.44 (t, *J* = 11.0 Hz, 1H), 4.67 (d, *J* = 6.2 Hz, 1H), 4.57 (dd, *J* = 14.6, 5.8 Hz, 1H), 4.46 (dd, *J* = 14.5, 5.5 Hz, 2H), 1.65 – 1.51 (m, 1H), 1.39 (s, 10H), 1.34 – 1.22 (m, 3H), 0.80 (dd, *J* = 16.3, 6.5 Hz, 7H); $^{13}C\{^{1}H\}$

NMR (100 MHz, $CDCl_3$) δ 166.2, 156.1, 138.5, 137.5, 128.4, 128.1, 127.1, 126.0, 80.2, 47.8, 43.5, 43.4, 28.3, 24.5, 22.6, 22.1; HRMS (ESI-TOF) *m/z*: $[M + H]^+$ Calcd for $C_{20}H_{31}N_2O_3$ 347.2335; Found 347.2334.

4. Synthesis of compounds 2h and 2c from 3a and 3b: Compounds **3a** and **3b** were treated with KO^tBu as following the synthetic procedure of compounds **2**, in which **3a** produces **2h** with 90% yield and **3b** produces **2c** with 91% yield, respectively.

5. Synthesis of compounds 4a-c

General procedure for synthesis of 4a-c: The BocHN-(*E*)dγXaa-CONHBn (**1a**,**1c** or **1h,** 3 mmol, 1.0 equvi) were deprotected with 1:1 mixture TFA:DCM (5 mL), after completion of the reaction (monitored by TLC, 1h) the solvent was evaporated under reduced pressure to get TFA.H_2N-(*E*)dγXaa-CONHBn. To the TFA salt, pyridine (4 mL) and acetic anhydride (0.612 mL, 6 mmol, 2.0 equvi) were added. Reaction mixture was stirred for about 4 h and the progress of the reaction was monitored TLC. After completion of the reaction, the solvent was evaporated under reduced pressure to get crude products. The pure compounds of **4(a-c)** were obtained after column purification using petroleum ether/EtOAc (80/20) solvent system and subjected for further rearrangement studies.

(S, *E*)-4-Acetamido-*N*-benzyl-5-methylhex-2-enamide (**4a**): White solid, Yield = 0.756 g (92 %); m. p 180-185 $^\circ$C; $[\alpha]_D^{25}$ = -16.0 (*c* 0.1, MeOH); ^{1}H NMR (400 MHz, DMSO-d_6) δ 8.53 (t, *J* = 5.9 Hz, 1H), 7.89 (d, *J* = 8.8 Hz, 1H), 7.36 – 7.21 (m, 5H), 6.56 (dd, *J* = 15.4, 6.4 Hz, 1H), 5.99 (dd, *J* = 15.4, 1.4 Hz, 1H), 4.33 (dd, *J* = 5.9, 3.1 Hz, 1H), 4.26 -4.18 (m, 1H), 1.87 (s, 3H), 1.81-1.70(m, 1H), 0.85 (dd, *J* = 6.8, 3.0 Hz, 1H); ^{13}C{^{1}H} NMR (100 MHz, DMSO-d_6) δ 169.1, 165.0, 142.1, 139.9, 128.8, 127.8, 127.3, 124.8, 55.3, 39.8, 39.6, 39.4, 32.1, 23.1, 19.4, 19.0; HRMS (ESI-TOF) *m/z*: $[M + H]^+$ Calcd for $C_{16}H_{23}N_2O_2$ 275.1760; Found 275.176.

(S, *E*)-4-Acetamido-*N*-benzyl-6-methylhept-2-enamide (**4b**): White solid, Yield = 0.804 g (93 %); m. p 190-195°C; $[\alpha]_D^{25}$ = -13.0 (*c* 0.1, MeOH); ^{1}H NMR (400 MHz, $CDCl_3$) δ 7.34 – 7.22 (m, 5H), 6.66 (dd, *J* = 15.2, 6.8 Hz, 1H), 6.23 (s, 1H), 5.95 (d, *J* = 15.3 Hz, 1H), 5.75 (s, 1H), 4.63 (p, *J* = 7.7 Hz, 1H), 4.45 (s, 2H), 1.94 (s, 3H), 1.64 (m, 1H), 1.41 (t, *J* = 7.3 Hz, 2H), 0.91 (d, *J* = 6.6 Hz, 6H); ^{13}C{^{1}H} NMR (100 MHz, $CDCl_3$) δ 169.7, 165.6, 143.9, 138.2,

128.8, 128.0, 127.65, 123.8, 48.7, 43.8, 24.8, 23.4, 22.7, 22.5; HRMS (ESI-TOF) *m/z*: $[M + H]^+$ Calcd for $C_{17}H_{25}N_2O_2$ is 289.1916; Found 289.1910.

(S, *E*)-4-Acetamido-*N*-benzyl-5-phenylpent-2-enamide (**4c**): White solid, Yield = 0.87 g (90 %); m. p 150-155°C; $[\alpha]_D^{25}$ = -14.0 (*c* 0.1, MeOH); ^{1}H NMR (400 MHz, DMSO-d_6) δ 8.52 (t, *J* = 6.0 Hz, 1H), 8.08 (d, *J* = 8.4 Hz, 1H), 7.35 – 7.16 (m, 10H), 6.62 (dd, *J* = 15.4, 5.5 Hz, 1H), 5.97 (dd, *J* = 15.4, 1.6 Hz, 1H), 4.66 – 4.56 (m, 1H), 4.32 (d, *J* = 6.1 Hz, 2H), 2.84 (dd, *J* = 13.6, 6.2 Hz, 1H), 2.73 (dd, *J* = 13.6, 8.6 Hz, 1H), 1.78 (s, 3H); ^{13}C{^{1}H} NMR (100 MHz, DMSO-d_6) δ 170.8, 165.7, 143.6, 139.6, 138.6, 129.9, 129.2, 129.1, 128.1, 127.8, 127. 2, 124.1, 52.0, 43.0, 40.3, 39.5, 23.0; HRMS (ESI-TOF) *m/z*: $[M + H]^+$ Calcd for $C_{20}H_{23}N_2O_2$ 323.1760; Found 323.1764.

6. Synthesis of 5,5-disubstituted *N*-Ac-*γ*-lactams (5a-5c)

General procedure for the synthesis of 5, 5-disubstituted *N*-Ac-γ-lactams5 (5a-c): To the solution of *N*-Ac-*α,β*-unsaturated *γ*-amino amide (**4)** (2 mmol, 1.0 equvi) in dry THF, KO^{t}Bu (6 mmol, 3.0 equvi) was added under N_2 atmosphere and refluxed for about 8 h. Progress of the reaction was monitored by TLC. After completion of the reaction, water (30 mL) was added and the aqueous layer was extracted with EtOAc (30 mL × 3) and then the combined organic layer was washed with brine (30 mL × 2), dried over anhydrous Na_2SO_4 and concentrated under reduced pressure. The crude productswere purified by column chromatography using petroleum ether/EtOAc (80/20) solvent system to get pure products in 90-92% yields.

***N*-(1-Benzyl-2-isopropyl-5-oxopyrrolidin-2-yl)acetamide** (**5a**): Viscous oil, Yield = 0.504 g (92 %); $[\alpha]_D^{25}$ = 0.0 (*c* 0.1, MeOH); ^{1}H NMR (400 MHz, DMSO-d_6) δ 7.87 (s, 1H), 7.40 – 7.11 (m, 6H), 4.27 (d, *J* = 15.1 Hz, 1H), 4.08 (d, *J* = 15.1 Hz, 1H), 2.64 – 2.52 (m, 1H), 2.22 – 2.08 (m, 2H), 2.02 – 1.88 (m, 2H), 0.89 (d, *J* = 6.6 Hz, 3H), 0.49 (d, *J* = 6.7 Hz, 3H); ^{13}C{^{1}H} NMR (100 MHz, DMSO-d_6) δ 175.6, 170.1, 138.9, 128.9, 128.3, 127.1, 79.9, 42.2, 32.9, 30.0, 23.6, 23.3, 16.9, 15.6; HRMS (ESI-TOF) *m/z*: $[M + H]^+$ Calcd for $C_{16}H_{23}N_2O_2$ 275.1760; Found 275.176.

***N*-(1-Benzyl-2-isobutyl-5-oxopyrrolidin-2-yl)acetamide** (**5b**): Viscous oil, Yield = 0.519 g (90 %); $[\alpha]_D^{25}$ = 0.0 (*c* 0.1, MeOH); ^{1}H NMR (400 MHz, $CDCl_3$) δ 7.30 – 7.14 (m, 5H),

5.42 (s, 1H), 4.80 (d, *J* = 15.3 Hz, 1H), 4.02 (d, *J* = 15.3 Hz, 1H), 2.99 – 2.86 (m, 1H), 2.45 – 2.30 (m, 1H), 2.21 - 2.12 (m, 1H), 1.78 (dd, *J* = 13.8, 6.3 Hz, 1H), 1.74 - 1.64 (m, 1H), 1.56 (dd, *J* = 13.8, 5.3 Hz, 1H), 1.37 (s, 3H), 0.95 (d, *J* = 6.5 Hz, 3H), 0.88 (d, *J* = 6.6 Hz, 3H).$^{13}C\{^{1}H\}$ NMR (100 MHz, $CDCl_3$) δ 176.1, 169.4, 138.2, 128.7, 128.3, 127.3, 77.2, 60.5, 47.5, 42.9, 30.0, 29.1, 24.5, 24.2, 23.9, 23.6, 21.2, 14.3; HRMS (ESI-TOF) *m/z*: $[M + H]^+$ Calcd for $C_{17}H_{25}N_2O_2$ 289.1916; Found 289.1910.

***N*-(1,2-Dibenzyl-5-oxopyrrolidin-2-yl)acetamide** (**5c**): Viscous oil, Yield = 0.586 g (91 %); $[\alpha]_D^{25}$ = 0.0 (*c* 0.1, MeOH); ^1H NMR (400 MHz, $CDCl_3$) δ 7.39 – 7.23 (m, 8H), 7.13 (dd, *J* = 7.5, 1.8 Hz, 2H), 5.75 (s, 1H), 4.98 (d, *J* = 15.4 Hz, 1H), 4.34 (d, *J* = 15.3 Hz, 1H), 3.16 (q, *J* = 14.0 Hz, 2H), 2.71 – 2.50 (m, 1H), 2.39 – 2.21 (m, 2H), 1.85 (m, 1H), 1.50 (s, 3H); $^{13}C\{^{1}H\}$ NMR (100 MHz, $CDCl_3$) δ 175.8, 169.5, 138.1, 134.3, 130.0, 128.8, 128.7, 128.2, 127.5, 127.5, 114.0, 77.8, 77.0, 43.2, 33.8, 31.9, 29.7, 29.5, 29.3, 29.1, 28.9, 23.58, 22.7, 14.1; HRMS (ESI-TOF) *m/z*: $[M + H]^+$ Calcd for $C_{20}H_{23}N_2O_2$ 323.1760; Found 323.1764.

7. Procedure for the synthesis of compounds 5a and 6a: To the solution of *α,β*-unsaturated *γ*-amino amide (**4a,** 2 mmol, 1.0 equvi) in dry THF, KO^tBu (6 mmol, 3.0 equvi) was added under N_2 atmosphere and stirred the reaction at rt for about 8 h. The progress of the reaction was monitored by TLC. After completion of the reaction, water (30 mL) was added and the aqueous layer was extracted with EtOAc (30 mL × 3) and then the combined organic layer was washed with brine (30 mL × 2), dried over anhydrous Na_2SO_4 and concentrated under reduced pressure. The crude product was purified by column chromatography using petroleum ether/EtOAc (80/20) to get pure **5a** and **6a**.

4-Acetamido-*N*-benzyl-5-methylhex-3-enamide (**6a**): White solid, Yield = 0.11 g (20 %); m. p 170-175°C; ^1H NMR (400 MHz, $CDCl_3$) δ 7.36 – 7.19 (m, 5H), 6.99 (s, 1H), 5.39 (t, *J* = 7.7 Hz, 1H), 4.77 (s, 1H), 4.41 (d, *J* = 5.9 Hz, 2H), 2.92 (d, *J* = 7.7 Hz, 2H), 2.57 - 2.47 (m, 1H), 2.08 (s, 3H), 1.03 (d, *J* = 6.9 Hz, 6H); $^{13}C\{^{1}H\}$ NMR (100 MHz, $CDCl_3$) δ 171.6, 169.8, 142.6, 138.6, 128.7, 127.6, 127.3, 115.2, 77.2, 43.8, 36.3, 33.8, 23.9, 20.7; HRMS (ESI-TOF) *m/z*: $[M + H]^+$ Calcd for $C_{16}H_{23}N_2O_2$ 275.1760; Found 275.176.

8. Synthesis of compound 3j: Compound **2j** (1.2 g, 3 mmol) in 3 mL of DCM was cooled to 0 °C in ice bath followed by addition of neat 5 mL of TFA. The reaction was monitored by TLC.

After completion of the reaction (~ 30 min), the solvent was evaporated under reduced pressure. The crude was precipitated using cold diethyl ether to get pure compound **3j**. Brown color solid, Yield = 0.89 g (93%); m. p 215-216 °C; ^{1}H NMR (400 MHz, $CDCl_3$) δ 8.81 (s, 1H), 7.59 (d, *J* = 8 Hz, 1H), 7.39-7.28 (m, 5H), 7.27-7.21 (m, 1H), 7.19-7.09 (m, 2H), 6.81 (s, 1H), 4.88 (d, *J* = 15.4 Hz, 1H), 4.29 (d, *J* = 15.4 Hz, 1H), 3.10 (d, *J* = 14.6 Hz, 1H), 2.96 (d, *J* = 14.6 Hz, 1H), 2.43-2.32 (m, 1H), 2.30-21 (m, 1H), 1.83-1.74 (m, 1H), 1.72-61 (m, 1H); ^{13}C{^{1}H} NMR (100 MHz, $CDCl_3$) δ 174.8, 139.2, 136.0, 128.8, 128.7, 128.1, 127.8, 127.3, 127.2, 123.6, 122.2, 119.8, 118.3, 111.6, 109.5, 79.0, 42.7, 38.7, 34.6, 29.9; HRMS (ESI-TOF) *m/z*: $[M + H]^+$ Calcd for $C_{20}H_{22}N_3O$ 320.1765; Found 320.1763.

9. Synthesis of compound 4j: To the compound **3j** (0.64 g, 2 mmol, 1.0 equvi) in dry DMF (3 mL), isovaleric acid (0.2 g, 2 mmol, 1.0 equvi), HBTU (0.76 g, 2 mmol, 1.0 equvi) and DIEA (1.0 mL, 6 mmol, 3.0 equvi) were added. The reaction was stirred for 6 h at room temperature. After completion of the reaction, the reaction mixture was diluted with EtOAc (150 mL) and washed with 0.5 N HCl (3 × 50 mL), 10% Na_2CO_3 (1 × 50 mL) and brine solution (1 × 80 mL), respectively. The organic layer was dried over anhydrous Na_2SO_4 and concentrated under reduced pressure. The crude product was purified by column chromatography using DCM/MeOH (95/5) solvent system to get pure products **4j.** White solid, Yield = 0.65 g (81%); m. p 143-145 °C; ^{1}H NMR (400 MHz, $CDCl_3$) δ 8.77 (bs, 1H), 7.55 (d, *J* = 8 Hz, 1H), 7.40-7.15 (m, 8H), 6.85 (s, 1H), 5.89 (s, 1H), 4.78 (d, *J* = 16 Hz, 1H), 4.46 (d, *J* = 16 Hz, 1H), 3.43 (d, *J* = 16 Hz, 1H), 3.03 (d, *J* = 16 Hz, 1H), 2.77-2.64 (m, 1H), 2.13-2.00 (m, 1H), 1.84-1.72 (m, 1H), 1.59-1.52 (m, 2H), 0.76 (t, *J* = 6.4 Hz, 6H); ^{13}C{^{1}H} NMR (100 MHz, $CDCl_3$) δ 176.7, 172.3, 138.3, 136.0, 128.8, 128.3, 128.1, 127.6, 123.2, 122.4, 120.0, 117.8, 111.8, 107.8, 78.4, 46.1, 43.2, 34.1, 30.0, 29.8, 25.8, 22.8, 22.5, 22.3, 14.2; HRMS (ESI-TOF) *m/z*: $[M + Na]^+$ Calcd for $C_{25}H_{29}N_3O_2Na$ 426.2157; Found 426.2155.

10. Synthetic procedure for *tert*-butyl (*S,E*)-(6-(diethylamino)-2-methyl-6-oxohex-4-en-3-yl)carbamate (7): compound **7** was synthesized by following the similar procedure, reported for compound **1**. The crude product was purified by column chromatography using petroleum ether/EtOAc (80/20). White solid, Yield = 0.823 g (92%); m. p 140-142 °C; $[\alpha]_D^{25}$ = -10.0 (*c* 0.1, MeOH); ^{1}H NMR (400 MHz, $CDCl_3$) δ 6.73 (dd, *J* = 14.9, 6.6 Hz, 1H), 6.29 (dd, *J* = 15.0, 1.3 Hz, 1H), 4.59 (d, *J* = 9.1 Hz, 1H), 4.19 – 4.03 (m, 1H), 3.50 – 3.28 (m, 4H), 1.91 – 1.74 (m, 1H),

1.43 (s, 9H), 1.18 (t, *J* = 7.2 Hz, 3H), 1.13 (t, *J* = 7.1 Hz, 3H), 0.92 (t, *J* = 6.1 Hz, 6H); $^{13}C\{^{1}H\}$ NMR (100 MHz, $CDCl_3$) δ 165.5, 155.5, 143.7, 121.6, 79.6, 77.2, 57.5, 42.3, 41.0, 32.4, 28.5, 19.0, 18.4, 15.0, 13.3; HRMS (ESI-TOF) *m/z*: $[M + Na]^+$ Calcd for C16H30N2O3Na 321.2154; Found 321.2151.

11. Synthetic procedure for *tert*-butyl (*E*)-(6-(diethylamino)-2-methyl-6-oxohex-3-en-3-yl)carbamate (8): compound **8** was synthesized by following the similar procedure, reported for compound **2**. The crude product was purified by column chromatography using petroleum ether/EtOAc (80/20). White solid, Yield = 0.561 g (94%); m. p 160-163 °C; $[\alpha]_D^{25}$ = 0.0 (*c* 0.1, MeOH); ^1H NMR (400 MHz, $CDCl_3$) δ 6.73 (s, 1H), 5.19 (t, *J* = 6.5 Hz, 1H), 3.45 – 3.18 (m, 4H), 3.04 (d, *J* = 7.0 Hz, 2H), 1.44 (s, 9H), 1.17 (t, *J* = 7.2 Hz, 3H), 1.13 – 1.07 (m, 4H), 1.04 (d, *J* = 6.9 Hz, 6H); $^{13}C\{^{1}H\}$ NMR (100 MHz, $CDCl_3$) δ 171.3, 153.7, 143.8, 106.8, 79.7, 77.2, 42.5, 40.4, 32.0, 28.4, 21.0, 14.5, 13.1; HRMS (ESI-TOF) *m/z*: $[M + Na]^+$ Calcd for C16H30N2O3Na 321.2154; Found 321.2152.

8. References

1. a) Wilson, M. C.; Nam, S.-J.; Gulder, T. A. M.; Kauffman, C. A.; Jensen, P. R.; Fenical, W.; Moore, B. S. *J. Am. Chem. Soc.* **2011**, *133*, 1971−1977. b) Okazaki, Y.; Ishizuka, A.; Ishihara, A.; Nishioka, T.; Iwamura, H. *J. Org. Chem.* **2007**, *72*, 3830−3839. c) Feling, R. H.; Buchanan, G. O.; Mincer, T. J.; Kauffman, C. A.; Jensen, P. R.; Fenical, W. *Angew. Chem., Int. Ed.* **2003**, *42*, 355−357. d) Ai, Y.; Hu, Y.; Kang, F.; Lai, Y.; Jia, Y.; Huang, Z.; Peng, S.; Ji, H.; Tian, J.; Zhang, Y. *J. Med. Chem.* **2015**, *58*, 4506-4520.
2. For reviews: a) Caruano, J.; Muccioli, G. G.; Robiette, R. *Org. Biomol. Chem.* **2016**, *14*, 10134–10156. b) Ye, L.-W.; Shu, C.; Gagosz, F. *Org. Biomol. Chem.* **2014**, *12*, 1833−1845. c) Natural Lactones and Lactams: Synthesis, Occurrence and Biological Activity; Janecki, T., Ed. Wiley-VCH: Weinheim, Germany, **2013.** d) Kammerer, C.; Prestat, G.; Madec, D.; Poli, G. *Acc. Chem. Res*. **2014**, *47*, 3439−3447.
3. a) Fenical, W.; Jensen, P. R.; Palladino, M. A.; Lam, K. S.; Lloyd, G. K.; Potts, B. C. *Bioorg. Med. Chem.* **2009**, *17*, 2175−2180. b) Choi, E.; Lee, C.; Cho, M.; Seo, J. J.; Yang, J. S.; Oh, S. J.; Lee, K.; Park, S. K.; Kim, H. M.; Kwon, H. J.; Han, G. *J. Med. Chem.* **2012**, *55*, 10766−10770; c) Agatsuma, T.; Akama, T.; Nara, S.; Matsumiya, S.;

Nakai, R.; Ogawa, H.; Otaki, S.; Ikeda, S.; Saitoh, Y.; Kanda, Y. *Org. Lett.* **2002**, *4*, 4387–4390.

4. Kwan, P.; Trinka, E.; Van Paesschen, W.; Rektor, I.; Johnson, M. E.; Lu, S. *Epilepsia* **2014**, *55*, 38–46.
5. a) Yang, Z. Q.; Shu, Y.; Ma, L.; Wittmann, M.; Ray, W. J.; Seager, M. A.; Koeplinger, K. A.; Thompson, C. D.; Hartman, G. D.; Bilodeau, M. T.; Kuduk, S. D. *ACS Med. Chem. Lett.* **2014**, *5*, 604−608. b) Feng. Z.; Li. X; Zheng. G.; Huang. L. *Bioorg. Med. Chem. Lett*. **2009**, *19*, 2112–2115.
6. Kazmierski, W. M.; Andrews, W.; Furfine, E.; Spaltenstein, A.; Wright, L. *Bioorg. Med. Chem. Lett*. **2004**, *14*, 5689−5692.
7. Manam, R. R.; Teisan, S.; White, D. J.; Nicholson, B.; Grodberg, J.; Neuteboom, S. T. C.; Lam, K. S.; Mosca, D. A.; Lloyd, G. K.; Potts, B. C. M. *J. Nat. Prod*. **2005**, *68*, 240−243.
8. a) Duan, J. J. W.; Chen, L.; Wasserman, Z. R.; Lu, Z.; Liu, R. –Q.; Covington, M. B.; Qian, M.; Hardman, K. D.; Magolda, R. L.; Newton, R. C.; Christ, D. D.; Wexler, R. R.; Decicco, C. P. *J. Med. Chem*. **2002**, *45*, 4954–4957. b) Qiao, L.; Wang, S.; George, C.; Lewin, N. E.; Blumberg, P. M.; Kozikowski, A. P. *J. Am. Chem. Soc*. **1998**, *120*, 6629–6630. c) Yoon, C. H.; Nagle, A.; Chen, C.; Gandhi, D.; Jung, K. W. *Org. Lett*. **2003**, *5*, 2259–2262.
9. Zhuang, C.; Miao, Z.; Zhu, L.; Dong, G.; Guo, Z.; Wang, S.; Zhang, Y.; Wu, Y.; Yao, J.; Sheng, C.; Zhang, W. *J. Med. Chem*. **2012**, *55*, 9630–9642.
10. Geranurimi, A.; Lubell, W. D. *Org. Lett.* **2018**, *20*, 6126-6129.
11. a) Martelli, G.; Orena, M.; Rinaldi, S. *Curr. Org. Chem*. **2014**, *18*, 1373–1481; b) Lettan, R. B.; Woodward, C. C.; Scheidt, K. A. *Angew. Chem. Int. Ed.* **2008**, *47*, 2294-2297.
12. Trend, R. M.; Ramtohul, Y. K.; Ferreira, E. M.; Stoltz, B. M. *Angew. Chem. Int. Ed*. **2003**, *42*, 2892-2895.
13. Shu, C.; Liu, M.-Q.; Wang, S.-S.; Li, L.; Ye, L.-W. *J. Org. Chem.***2013**, *78*, 3292-3299.
14. Hong, S. Y.; Park, Y.; Hwang, Y.; Kim, Y. B.; Baik, M.-H.; Chang, S. *Science* **2018**, *359*, 1016-1021.
15. Welbes, L. L.; Lyons, T. W.; Cychosz, K. A.; Sanford, M. S. *J. Am. Chem. Soc*. **2007**, *129*, 5836-5837.

16. Yeh, M.-C. P.; Shiue, Y.-S.; Lin, H. –H.; Yu, T.-Y.; Hu, T.-C.; Hong, J.-J. *Org. Lett.* **2016**, *18*, 2407−2410.
17. Zhou, C.-Y.; Che, C.-M. *J. Am. Chem. Soc*. **2007**, *129*, 5828-5829.
18. Lee, C.; Choi, E.; Cho, M.; Lee, B.; Oh, S. J.; Park, S.-K.; Lee, K.; Kim, H. M.; Han, G. *Bioorg. Med. Chem. Lett*. **2012**, *22*, 4189-4192.
19. a) Pinza, M.; Farina, C.; Cerri, A.; Pfeiffer, U.; Riccaboni, M. T.; Banfi, S.; Biagetti, R.; Pozzi, O.; Magnani, M.; Dorigotti, L.; *J. Med. Chem.* **1993**, ***36***, 4214-4220. b) Xi, N.; Arvedson, S.; Eisenberg, S.; Han, N.; Handley, M.; Huang, L.; Huang, Q.; Kiselyov, A.; Liu, Q.; Lu, Y.; Nunez, G.; Osslund, T.; Powers, D.; Tasker, A. S.; Wang, L.; Xiang, T.; Xu, S.; Zhang, J.; Zhu, J.; Kendall, R.; Dominguez, C. *Bioorg. Med. Chem. Lett.* **2004**, *14*, 2905 —2909.
20. a) Fishwick, C. W. G.; Foster, R. J.; Carr, R. E. *Tetrahedron Lett.* **1996**, ***37***, 3915 —3918. b) S. Gao, S.; Tu, Y. Q.; Hu, X.; Wang, S.; Hua, R.; Jiang, Y.; Zhao, Y. Fan, X. Zhang, S. *Org. Lett.* **2006**, *8*, 2373.
21. Ganesh Kumar, M. *Exploring Stereochemical Constraints and Chemical Reactivity of Vinylogous Amino acids in the Design of Foldamers*. PhD Thesis, IISER Pune, India, **2016.**
22. Veeresh, K, Gopi, H. N. *Org. Lett.***2019**, *21*, 4500−4504.
23. Mali, S. M.; Bandyopadhyay, A.; Jadhav, S. V.; Ganesh Kumar, M.; Gopi, H. N. *Org. Biomol. Chem*. **2011,** 9, 6566.
24. a) Ando, K.; Oishi, T.; Hirama, M.; Ohno, H.; Ibuka, T. *J. Org. Chem.* **2000**, 65, 4745. b) Ganesh Kumar, M.; Thombare, V. J.; Katariya, M. M.; Veeresh, K.; Raja, K. M. P.; Gopi, H. N. *Angew. Chem. Int. Ed*. **2016**, *55*, 7847-7851.
25. a) Zocher, G.; Vilstrup, J.; Heine, D.; Hallab, A.; Goralski, E.; Hertweck, C.; Stahl, M.; Schäberle, T. F.; Stehle, T. *Chem. Sci.* **2015**, *6*, 6525-6536. b) Sucipto, H.; Wenzel, S. C.; Müller, R. *ChemBioChem* **2013**, *14*, 1581-1589. c) Helfrich, E. J. N.; Piel, J. *Nat. Prod. Rep*. **2016**, *33*, 231-316.
26. a) Shangary, S.; Wang Annu. S. *Rev. Pharmacol. Toxicol.* **2009**, *49*, 223–41. b) Zhao, Y.; Aguilar, A.; Bernard, D.; Wang, S. *J. Med. Chem.* **2015**, *58*, 1038-1052.

9. Appendix

1. Crystallographic Information:

Compound 2a: Crystals of **2a** were grown by slow evaporation from a solution of EtOAc. A single crystal (0.2 × 0.1 × 0.08 mm) was mounted on loop with a small amount of the paraffin oil. The X-ray data were collected at 100K temperature on a Bruker APEX(II) DUO CCD diffractometer using Mo K_α radiation (λ = 0.71073 Å), ω-scans (2θ = 57.04), for a total of 12065 independent reflections. Space group P12(1)1, a = 6.639 (3), b = 8.413 (3), c = 36.816 (16), β = 90.173 (10), V = 2065.3 (16) $Å^3$, Monoclinic, Z = 4 for chemical formula C23 H28 N2 O3, with two molecules in asymmetric unit; ρ calcd = 1.229 gcm^{-3}, μ = 0.081 mm^{-1}, F (000) = 816, R_{int}= 0.0529. The structure was obtained by intrinsic methods using SHELXS-97.The final R value was 0.0620 (wR2 = 0.1167) 8305 observed reflections ($F_0 \geq 4\sigma$ ($|F_0|$)) and 511 variables, S = 0.973.

Compound 2b: Crystals of **2b** were grown by slow evaporation from a solution of EtOAc. A single crystal (0.15 × 0.1 × 0.05 mm) was mounted on loop with a small amount of the paraffin oil. The X-ray data were collected at 100K temperature on a Bruker APEX(II) DUO CCD diffractometer using Mo K_α radiation (λ = 0.71073 Å), ω-scans (2θ = 66.65), for a total of 20711 independent reflections. Space group C 2, a = 14.9637(5), b = 11.3042(4), c = 21.2771(9), β = 110.4360(10), V = 3372.6 (2) $Å^3$, Monoclinic, Z = 8 for chemical formula C17 H24 N2 O3, with two molecule in asymmetric unit; ρcalcd = 1.199 gcm^{-3}, μ = 0.665 mm^{-1}, F (000) = 1312, R_{int}= 0.0243. The structure was obtained by intrinsic methods using SHELXS-97.The final R value was 0.055 (wR2 = 0.2125) 5783 observed reflections ($F_0 \geq 4\sigma$ ($|F_0|$)) and 405 variables, S = 2.070.

Compound 2e: Crystals of **2e** were grown by slow evaporation from a solution of EtOAc. A single crystal (0.1 × 0.05 × 0.03 mm) was mounted on loop with a small amount of the paraffin oil. The X-ray data were collected at 100K temperature on a Bruker APEX(II) DUO CCD diffractometer using Mo K_α radiation (λ = 0.71073 Å), ω-scans (2θ = 66.39), for a total of 9955 independent reflections. Space group P1, a = 6.8272 (3), b = 8.0949 (3), c = 42.0284 (15), β = 89.977 (2), V = 2322.72(16) $Å^3$, triclinic, Z = 4 for chemical formula C26 H31 N3 O3, with four

molecule in asymmetric unit; ρcalcd = 1.240 gcm^{-3}, μ = 0.652 mm^{-1}, F (000) = 1012, R_{int}= 0.0950. The structure was obtained by intrinsic methods using SHELXS-97.The final R value was 0.0664 (wR2 = 0.1056) 14782 observed reflections ($F_0 \geq 4\sigma$ (|F_0|)) and 1165 variables, S = 1.263.

Compound 2f: Crystals of **2f** were grown by slow evaporation from a solution of aqueous methanol. A single crystal (0.15 × 0.1 × 0.05 mm) was mounted on loop with a small amount of the paraffin oil. The X-ray data were collected at 100K temperature on a Bruker APEX(II) DUO CCD diffractometer using Mo K_α radiation (λ = 0.71073 Å), ω-scans (2θ = 50.48), for a total of 15144 independent reflections. Space group P21, a = 6.696(2), b = 13.783(4), c = 10.694(4), β = 102.690(8), V = 962.8(5) Å^3, monoclinic, Z = 2 for chemical formula C20 H30 N2 O3, with one molecule in asymmetric unit; ρcalcd = 1.195 gcm^{-3}, μ = 0.080 mm^{-1}, F (000) = 376, R_{int}= 0.0551. The structure was obtained by intrinsic methods using SHELXS-97.The final R value was 0.0599 (wR2 = 0.1470) 4750 observed reflections ($F_0 \geq 4\sigma$ (|F_0|)) and 231 variables, S = 1.026.

Compound 2h: Crystals of **2h**were grown by slow evaporation from a solution of EtOAc. A single crystal (0.1 × 0.07 × 0.05 mm) was mounted on loop with a small amount of the paraffin oil. The X-ray data were collected at 100K temperature on a Bruker APEX(II) DUO CCD diffractometer using Mo K_α radiation (λ = 0.71073 Å), ω-scans (2θ = 57.358), for a total of 34755 independent reflections. Space group C 2/c, a = 28.90(4), b = 10.508(13), c = 13.397(17), β = 106.42(3), V = 3902(9) Å^3, monoclinic, Z = 8 for chemical formula C20 H29 N2 O3, with one molecule in asymmetric unit; ρcalcd = 1.176 gcm^{-3}, μ = 0.079 mm^{-1}, F (000) = 1480, R_{int}= 0.0719. The structure was obtained by intrinsic methods using SHELXS-97.The final R value was 0.1511 (wR2 = 0.3044) 4863 observed reflections ($F_0 \geq 4\sigma$ (|F_0|)) and 230 variables, S = 1.308. Author comment on check CIF: The investigated single crystal was a small-sized,brittle and poorly diffracting. Numerous datasets were collected on singlecrystals from different batches, whereof the one of the highest quality is reported herein.

Compound 2i: Crystals of **2i**were grown by slow evaporation from a solution of EtOAc. A single crystal (0.15 × 0.1 × 0.05 mm) was mounted on loop with a small amount of the paraffin oil. The X-ray data were collected at 100K temperature on a Bruker APEX(II) DUO CCD diffractometer using Mo K_α radiation (λ = 0.71073 Å), ω-scans (2θ = 50.48), for a total of 52510

independent reflections. Space group P -1, a = 6.8063(18), b = 13.002(4), c = 13.629(4), β = 92.523(7), V = 1106.6(5) Å^3, triclinic, Z = 2 for chemical formula C22 H30 N3 O3, with one molecule in asymmetric unit; ρcalcd = 1.154 gcm^{-3}, μ = 0.077 mm^{-1}, F (000) = 484, R_{int}= 0.2621. The structure was obtained by intrinsic methods using SHELXS-97.The final R value was 0.0841 (wR2 = 0.1747) 5554 observed reflections ($F_0 \geq 4\sigma$ (|F_0|)) and 257 variables, S = 1.017. Author comment on check CIF: The investigated single crystal was a small-sized, brittle and poorly diffracting. Numerous datasets were collected on single crystals from different batches, whereof the one of the highest quality is reported herein.

Compound 2j: Crystals of **2j**were grown by slow evaporation from a solution of aqueous methanol. A single crystal (0.15 × 0.1 × 0.05 mm) was mounted on loop with a small amount of the paraffin oil. The X-ray data were collected at 100K temperature on a Bruker APEX(II) DUO CCD diffractometer using Cu K_α radiation (λ = 1.54178 Å), ω-scans (2θ = 66.765), for a total of 34755 independent reflections. Space group P 21/n, a = 6.7044(10), b = 28.659(4), c = 11.4082(18), β = 91.966(9), V = 2190.7(6) Å^3, monoclinic, Z = 4 for chemical formula C25 H29 N3 O3, with one molecule in asymmetric unit; ρ calcd = 1.272 gcm^{-3}, μ = 0.675 mm^{-1}, F (000) = 816, R_{int}= 0.0721. The structure was obtained by intrinsic methods using SHELXS-97.The final R value was 0.0712 (wR2 = 0.1771) 3756 observed reflections ($F_0 \geq 4\sigma$ (|F_0|)) and 283 variables, S = 1.090.

Compound 2m: Crystals of **2m** were grown by slow evaporation from a solution of EtOAc. A single crystal (0.12 × 0.1 × 0.06 mm) was mounted on loop with a small amount of the paraffin oil. The X-ray data were collected at 100K temperature on a Bruker APEX(II) DUO CCD diffractometer using Mo K_α radiation (λ = 0.71073 Å), ω-scans (2θ = 50.48), for a total of 47013 independent reflections. Space group P 21/c, a = 12.367(5), b = 16.811(7), c = 19.201(8), β = 90.00, V = 3992(3) Å^3, monoclinic, Z = 8 for chemical formula C22 H26 N2 O3, with two molecule in asymmetric unit; ρ calcd = 1.219 gcm^{-3}, μ = 0.081 mm^{-1}, F (000) = 1706, R_{int}= 0.077. The structure was obtained by intrinsic methods using SHELXS-97.The final R value was 0.0407 (wR2 = 0.1008) 6229 observed reflections ($F_0 \geq 4\sigma$ (|F_0|)) and 491 variables, S = 0.665.

Compound 5c: Crystals of **5c** were grown by slow evaporation from a solution of EtOAc. A single crystal (0.13 × 0.1 × 0.05 mm) was mounted on loop with a small amount of the paraffin oil. The X-ray data were collected at 100K temperature on a Bruker APEX(II) DUO CCD

diffractometer using Mo K_α radiation (λ = 0.71073 Å), ω-scans (2θ = 57.172), for a total of 11092independent reflections. Space group P-1, a=6.6014(15), b = 9.469(2), c= 35.287(8) α = 93.454(5) β=93.826(5) γ=98.649(5), V = 2170.3(8) $Å^3$, monoclinic, Z = 2 for chemical formula C_{20} H_{22} N_2 O_2, C H Cl_3, with two molecule in asymmetric unit; ρ calcd = 1.352 gcm^{-3}, μ = 0.442 mm^{-1}, F (000) = 918.0, The structure was obtained by intrinsic methods using SHELXS-97.The final R value was 0.0913, wR2 =0.3006 (11029) observed reflections ($F_0 \geq 4\sigma$ ($|F_0|$)) and 507 variables, S = 0.781.

Compound 3j: Crystals of **3j**were grown by slow evaporation from a solution of EtOAc. A single crystal (0.2 × 0.1 × 0.08 mm) was mounted on loop with a small amount of the paraffin oil. The X-ray data were collected at 100K temperature on a Bruker APEX(II) DUO CCD diffractometer using Mo K_α radiation (λ = 0.71073 Å), ω-scans (2θ = 50.48), for a total of 15583 independent reflections. Space group P -1, a = 6.5787(11), b = 9.2449(14), c = 14.324(2), β = 77.982(4), V = 822.4(2) $Å^3$, triclinic, Z = 4 for chemical formula C20 H21 N3 O, with one molecule in asymmetric unit; ρ calcd = 1.290 gcm^{-3}, μ = 0.081 mm^{-1}, F (000) = 364, R_{int}= 0.0273. The structure was obtained by intrinsic methods using SHELXS-97.The final R value was 0.0523 (wR2 = 0.1857) 4106 observed reflections ($F_0 \geq 4\sigma$ ($|F_0|$)) and 217 variables, S = 1.563. Author comment on check CIF: It is possible that shorter D-H..H-D distances are an artifact of refinement.

Compound 4j: Crystals of **4j** were grown by slow evaporation from a solution of EtOAc. A single crystal (0.18 × 0.1 × 0.06 mm) was mounted on loop with a small amount of the paraffin oil. The X-ray data were collected at 100K temperature on a Bruker APEX(II) DUO CCD diffractometer using Mo K_α radiation (λ = 0.71073 Å), ω-scans (2θ = 50.48), for a total of 34755 independent reflections. Space group Cc, a = 6.9007(11), b = 25.211(4), c = 13.042(2), β = 101.886(4), V = 2220.2(6) $Å^3$, monoclinic, Z = 4 for chemical formula C25 H29 N3 O2, with one molecule in asymmetric unit; ρ calcd = 1.207 gcm^{-3}, μ = 0.077 mm^{-1}, F (000) = 968, R_{int}= 0.0412. The structure was obtained by intrinsic methods using SHELXS-97.The final R value was 0.0361 (wR2 = 0.0975) 11452 observed reflections ($F_0 \geq 4\sigma$ ($|F_0|$)) and 635 variables, S = 0.761.

2. ^{1}H and ^{13}C NMR of all compounds

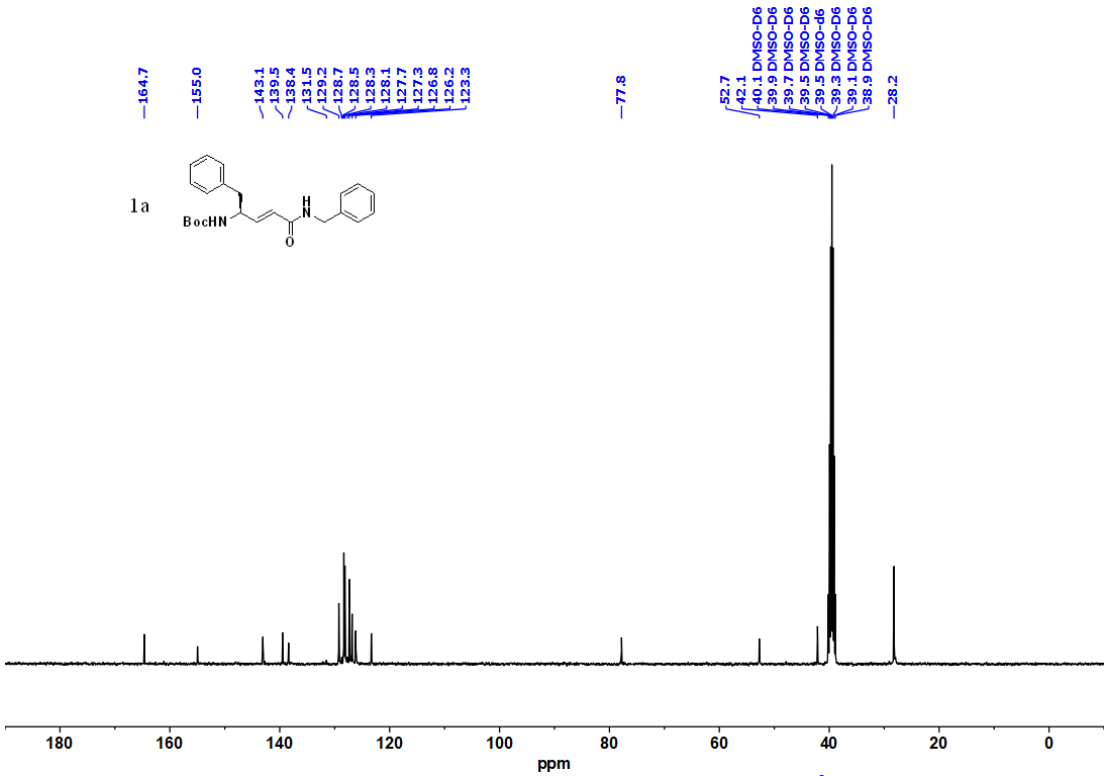

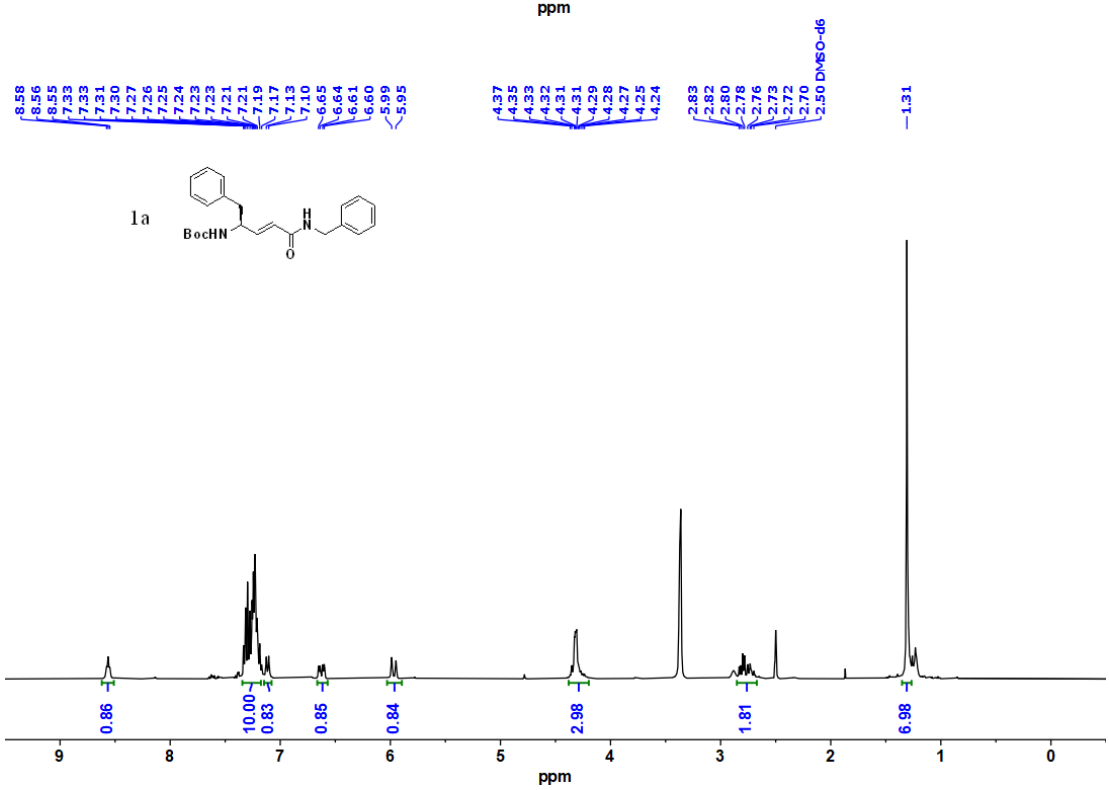

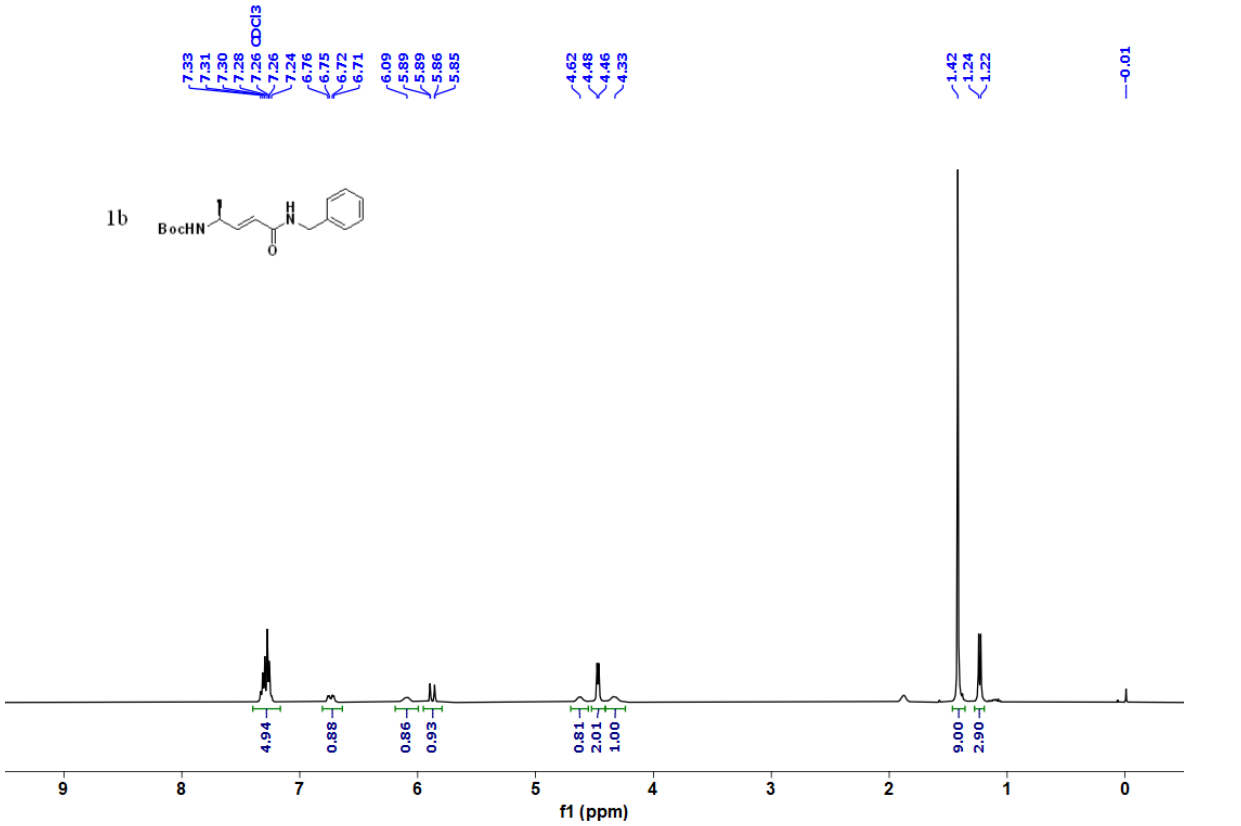
7.33
7.31
7.30
7.28
7.26 CDCl3
7.26
7.24
6.76
6.75
6.72
6.71
6.09
5.89
5.89
5.86
5.85
4.62
4.48
4.46
4.33
1.42
1.24
1.22
0.01
1b
BocHN
4.94
0.88
0.86
0.93
0.81
2.01
1.00
9.00
2.90
f1 (ppm)

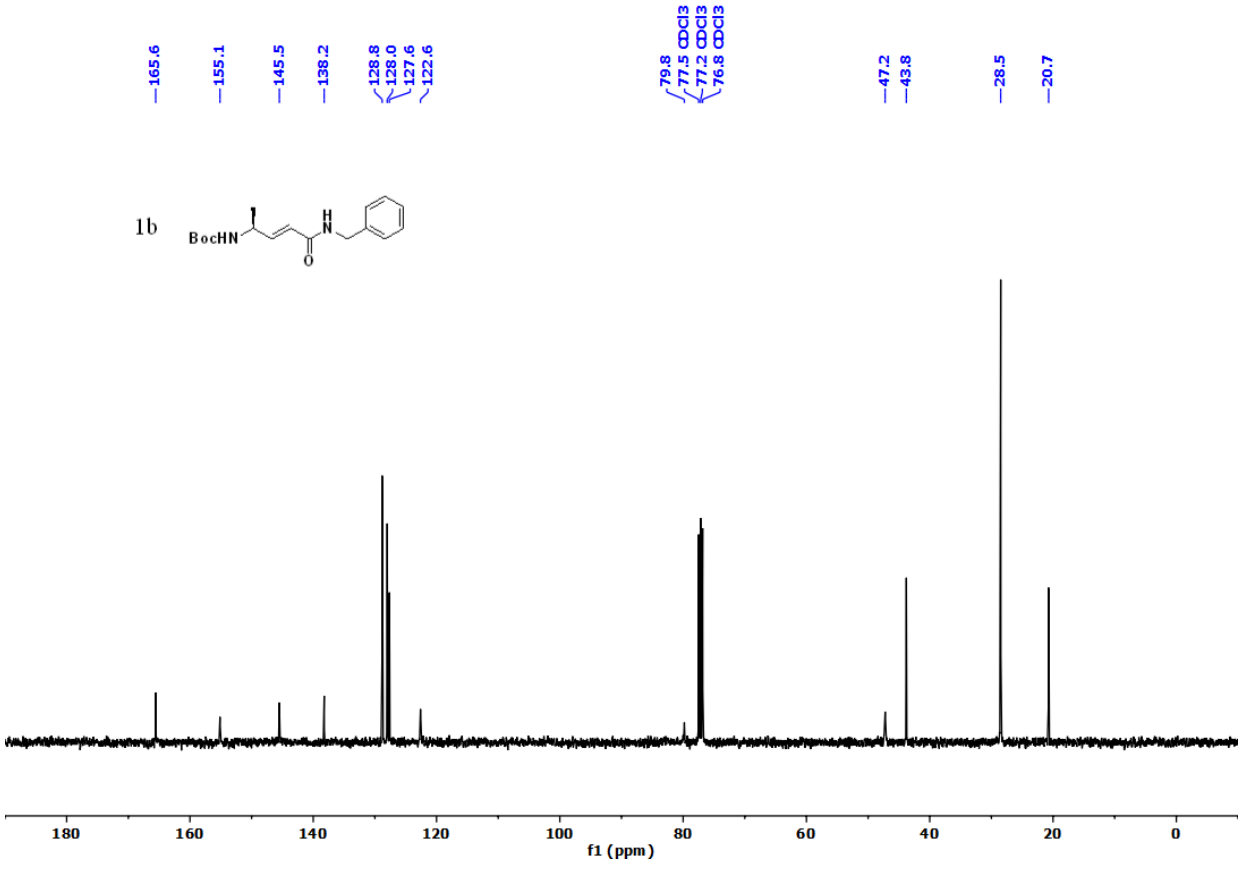
165.6
155.1
145.5
138.2
128.8
128.0
127.6
122.6
79.8
77.5 CDCl3
77.2 CDCl3
76.8 CDCl3
47.2
43.8
28.5
20.7
1b
BocHN
f1 (ppm)

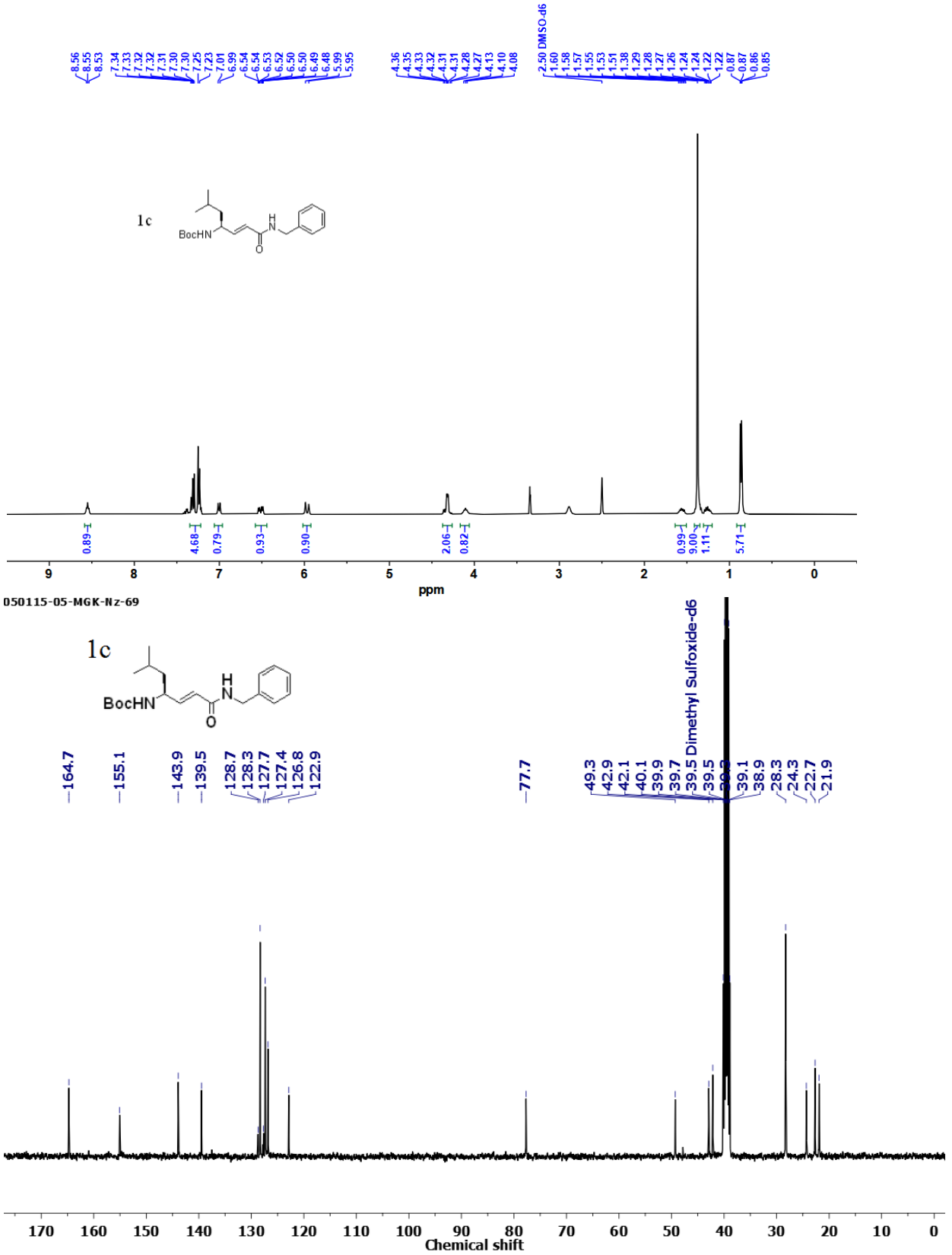
1c
BocHN
ppm
050115-05-MGK-Nz-69
1c
BocHN
Dimethyl Sulfoxide-d6
Chemical shift

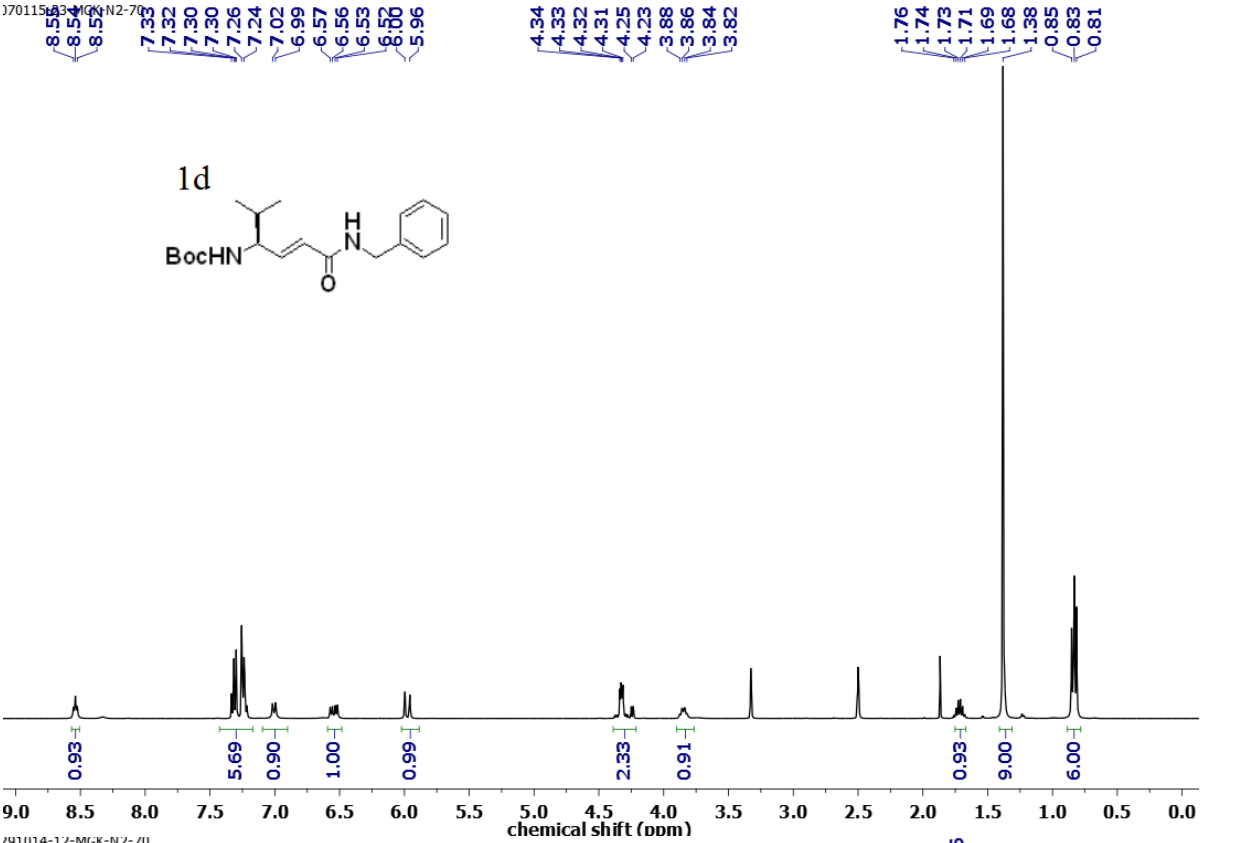
1d
BocHN
H
N
O
8.55
8.54
8.52
7.33
7.32
7.30
7.26
7.24
7.02
6.99
6.57
6.56
6.53
6.52
6.00
5.96
4.34
4.33
4.32
4.31
4.25
4.23
3.88
3.86
3.84
3.82
1.76
1.74
1.73
1.71
1.69
1.68
1.38
0.85
0.83
0.81
0.93
5.69
0.90
1.00
0.99
2.33
0.91
0.93
9.00
6.00
chemical shift (ppm)

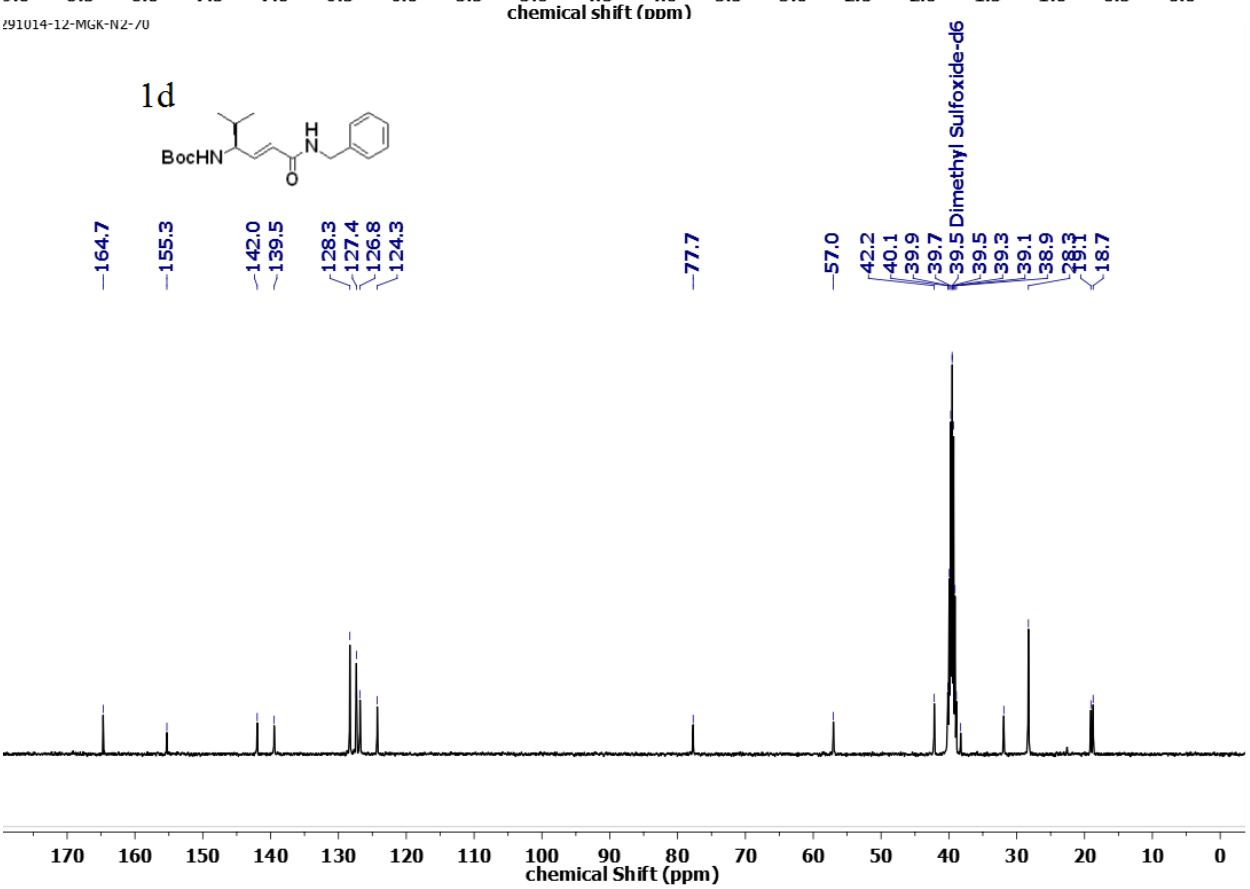
1d
BocHN
H
N
O
Dimethyl Sulfoxide-d6
164.7
155.3
142.0
139.5
128.3
127.4
126.8
124.3
77.7
57.0
42.2
40.1
39.9
39.7
39.5
39.5
39.3
39.1
38.9
28.3
19.1
18.7
chemical Shift (ppm)

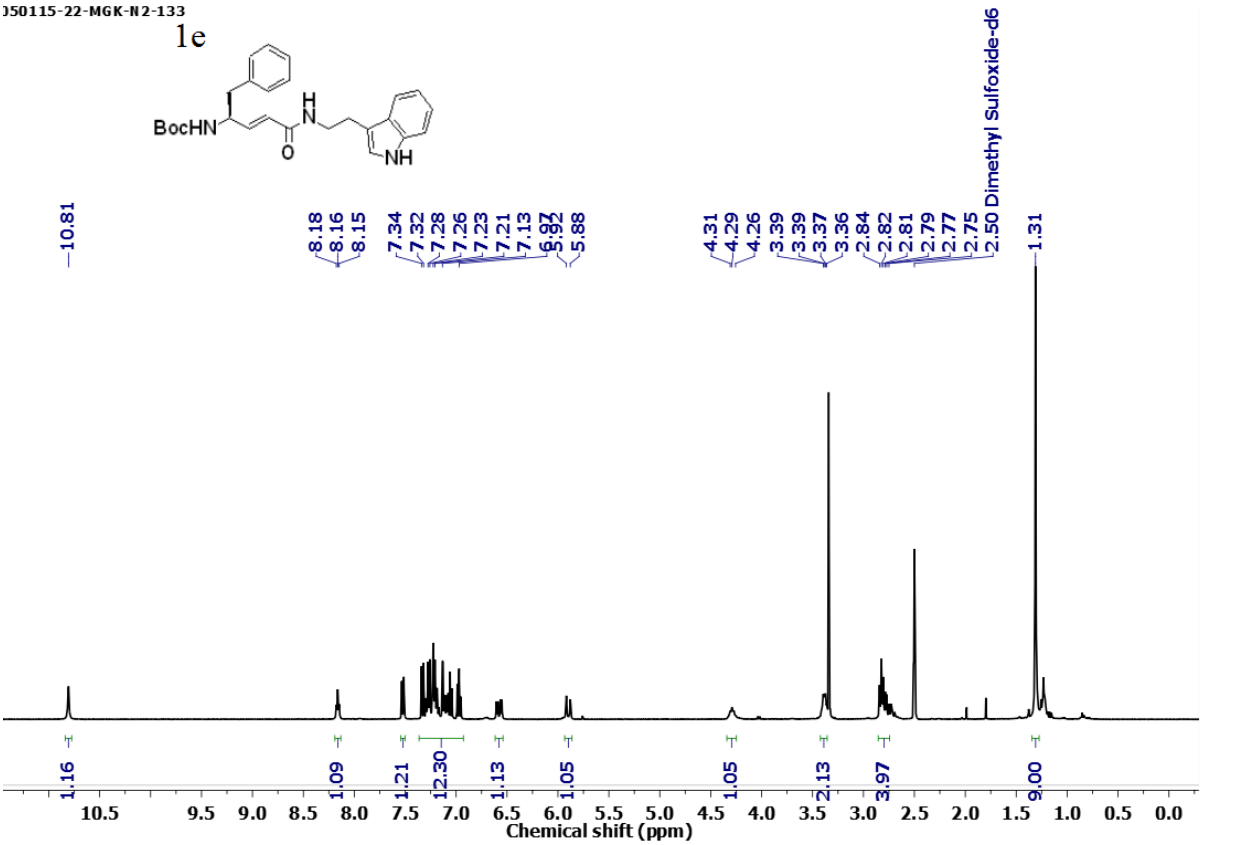
J50115-22-MGK-N2-133
1e
BocHN
H
N
O
NH
10.81
8.18
8.16
8.15
7.34
7.32
7.28
7.26
7.23
7.21
7.13
6.97
6.92
5.88
4.31
4.29
4.26
3.39
3.37
3.36
2.84
2.82
2.81
2.79
2.77
2.75
2.50 Dimethyl Sulfoxide-d6
1.31
1.16
1.09
1.21
12.30
1.13
1.05
1.05
2.13
3.97
9.00
Chemical shift (ppm)

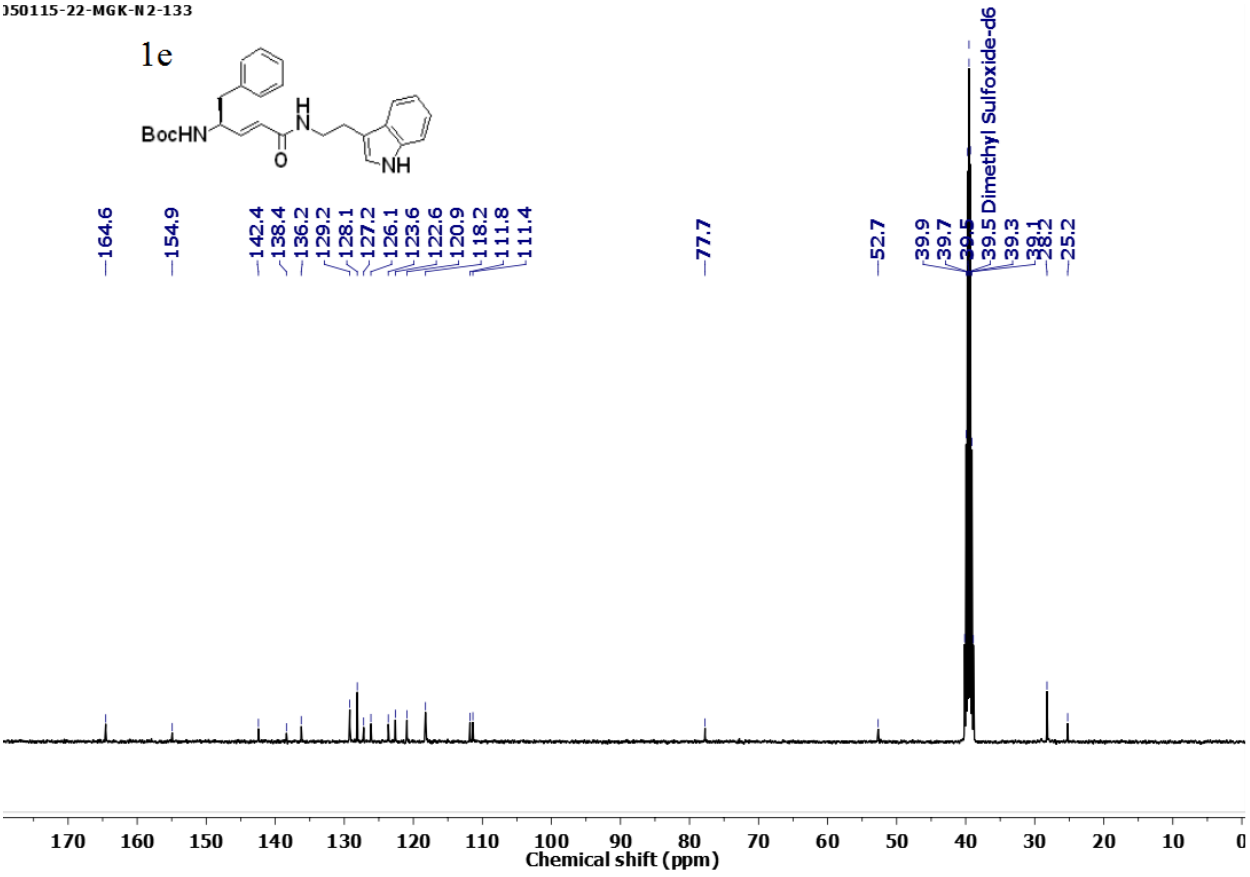
J50115-22-MGK-N2-133
1e
BocHN
H
N
O
NH
164.6
154.9
142.4
138.4
136.2
129.2
128.1
127.2
126.1
123.6
122.6
120.9
118.2
111.8
111.4
77.7
52.7
39.9
39.7
39.5 Dimethyl Sulfoxide-d6
39.3
28.2
25.2
Chemical shift (ppm)

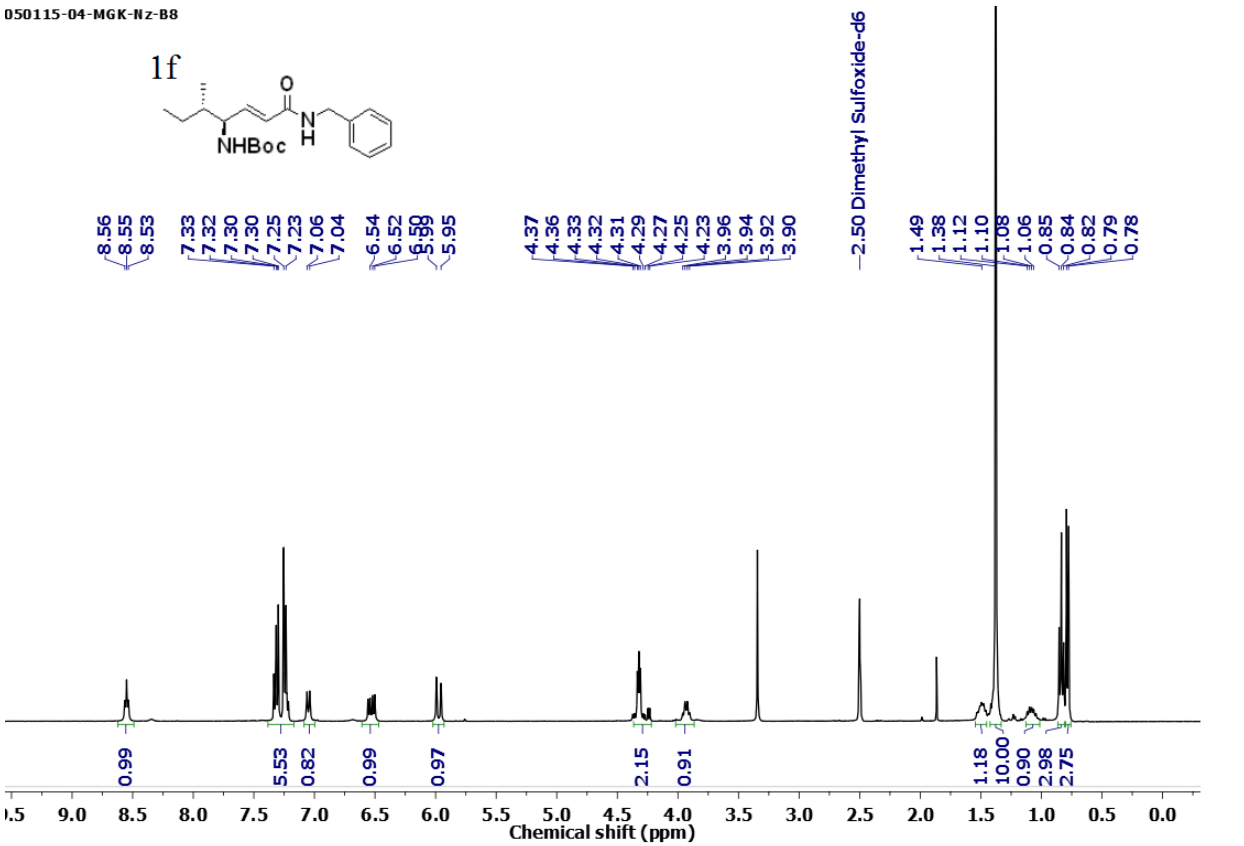
050115-04-MGK-Nz-B8
1f
NHBoc
2.50 Dimethyl Sulfoxide-d6
Chemical shift (ppm)

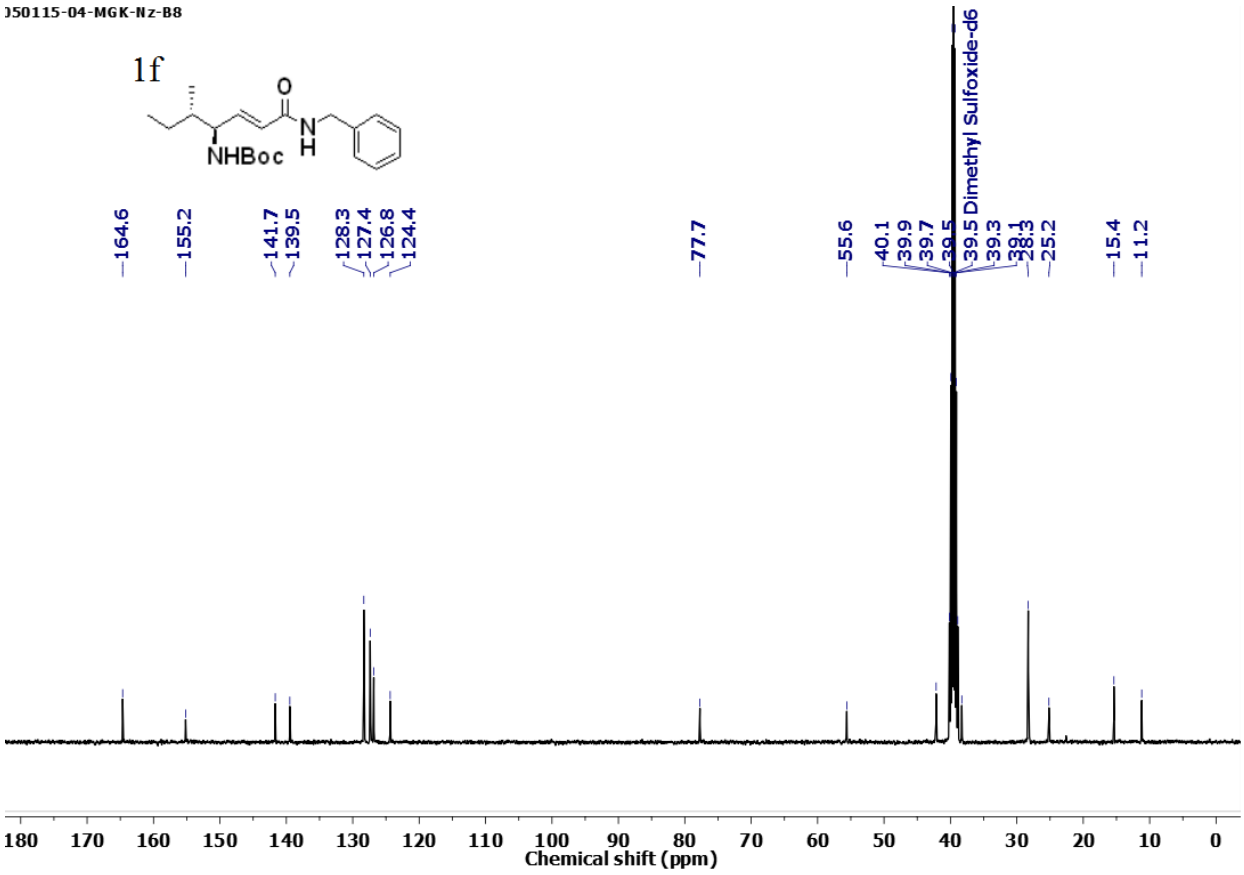
050115-04-MGK-Nz-B8
1f
NHBoc
39.5 Dimethyl Sulfoxide-d6
Chemical shift (ppm)

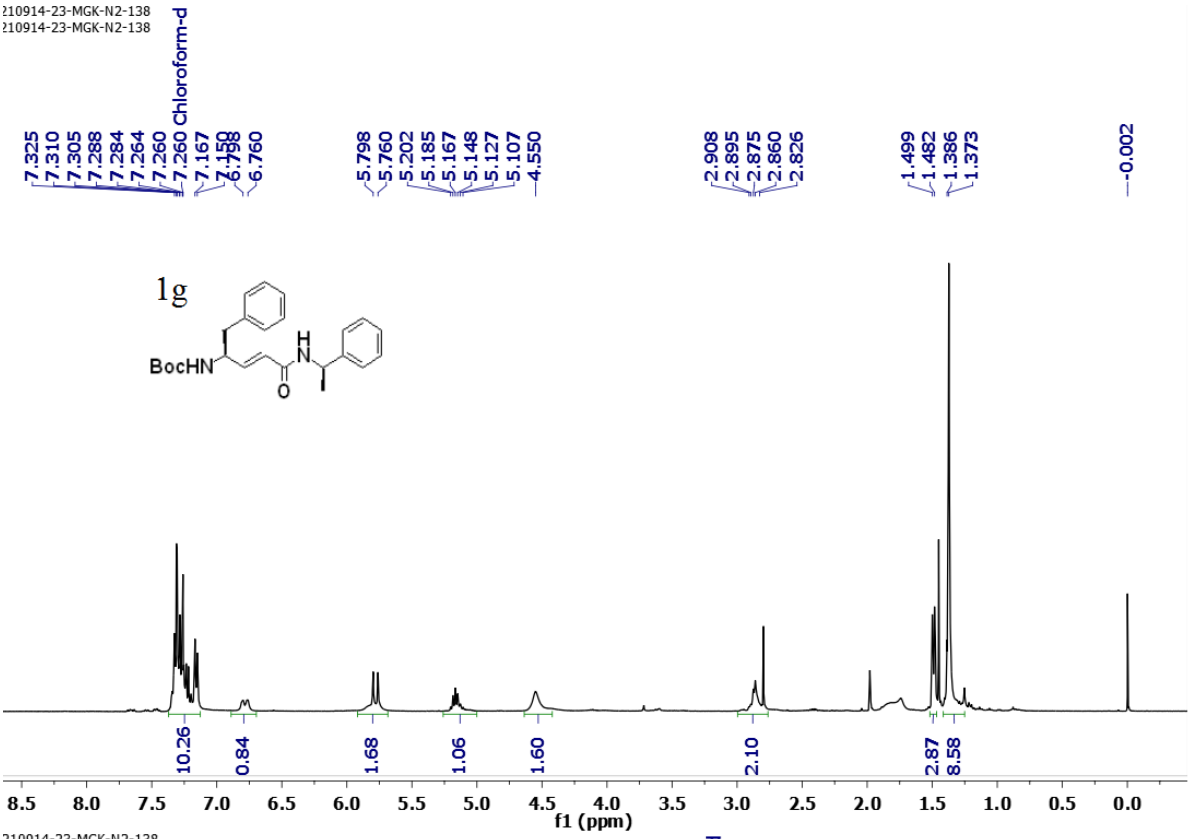
210914-23-MGK-N2-138
210914-23-MGK-N2-138
7.325
7.310
7.305
7.288
7.284
7.264
7.260
7.260 Chloroform-d
7.167
6.798
6.760
5.798
5.760
5.202
5.185
5.167
5.148
5.127
5.107
4.550
2.908
2.895
2.875
2.860
2.826
1.499
1.482
1.386
1.373
-0.002
1g
BocHN
H
N
O
10.26
0.84
1.68
1.06
1.60
2.10
2.87
8.58
8.5 8.0 7.5 7.0 6.5 6.0 5.5 5.0 4.5 4.0 3.5 3.0 2.5 2.0 1.5 1.0 0.5 0.0
f1 (ppm)

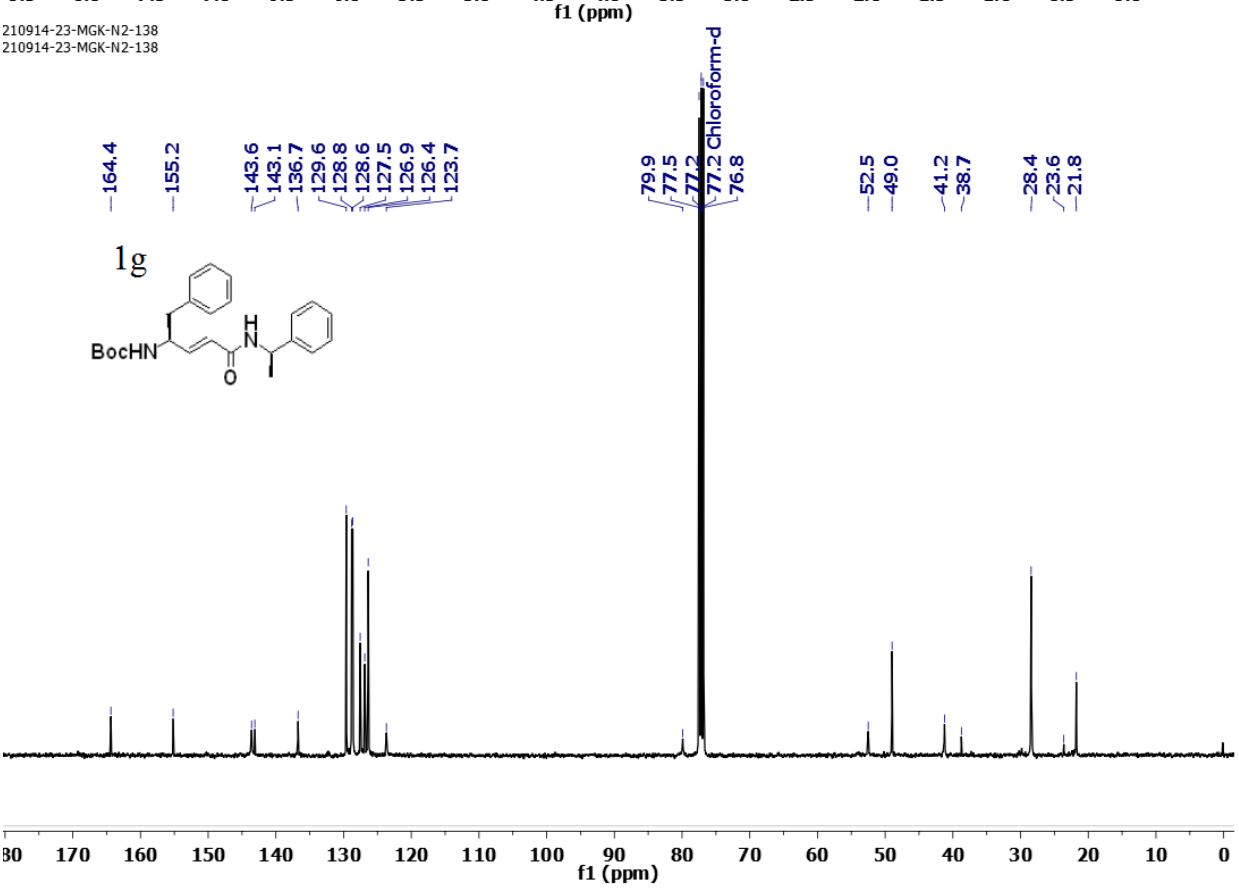
210914-23-MGK-N2-138
210914-23-MGK-N2-138
164.4
155.2
143.6
143.1
136.7
129.6
128.8
128.6
127.5
126.9
126.4
123.7
79.9
77.5
77.2
77.2 Chloroform-d
76.8
52.5
49.0
41.2
38.7
28.4
23.6
21.8
1g
BocHN
H
N
O
180 170 160 150 140 130 120 110 100 90 80 70 60 50 40 30 20 10 0
f1 (ppm)

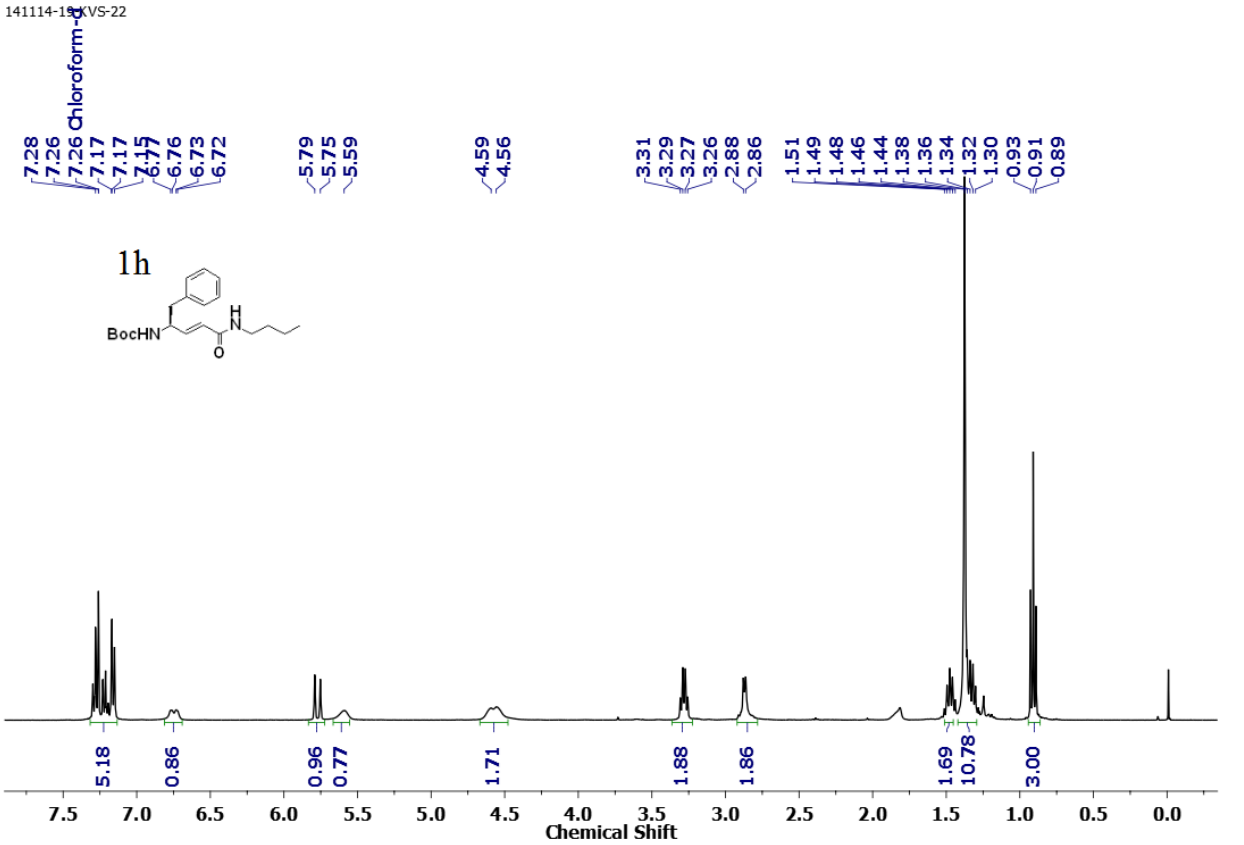
141114-19-KVS-22
Chloroform-d
7.28
7.26
7.26
7.17
7.17
7.15
6.77
6.76
6.73
6.72
5.79
5.75
5.59
4.59
4.56
3.31
3.29
3.27
3.26
2.88
2.86
1.51
1.49
1.48
1.46
1.44
1.38
1.36
1.34
1.32
1.30
0.93
0.91
0.89
1h
BocHN
H
N
O
5.18
0.86
0.96
0.77
1.71
1.88
1.86
1.69
10.78
3.00
7.5
7.0
6.5
6.0
5.5
5.0
4.5
4.0
3.5
3.0
2.5
2.0
1.5
1.0
0.5
0.0
Chemical Shift

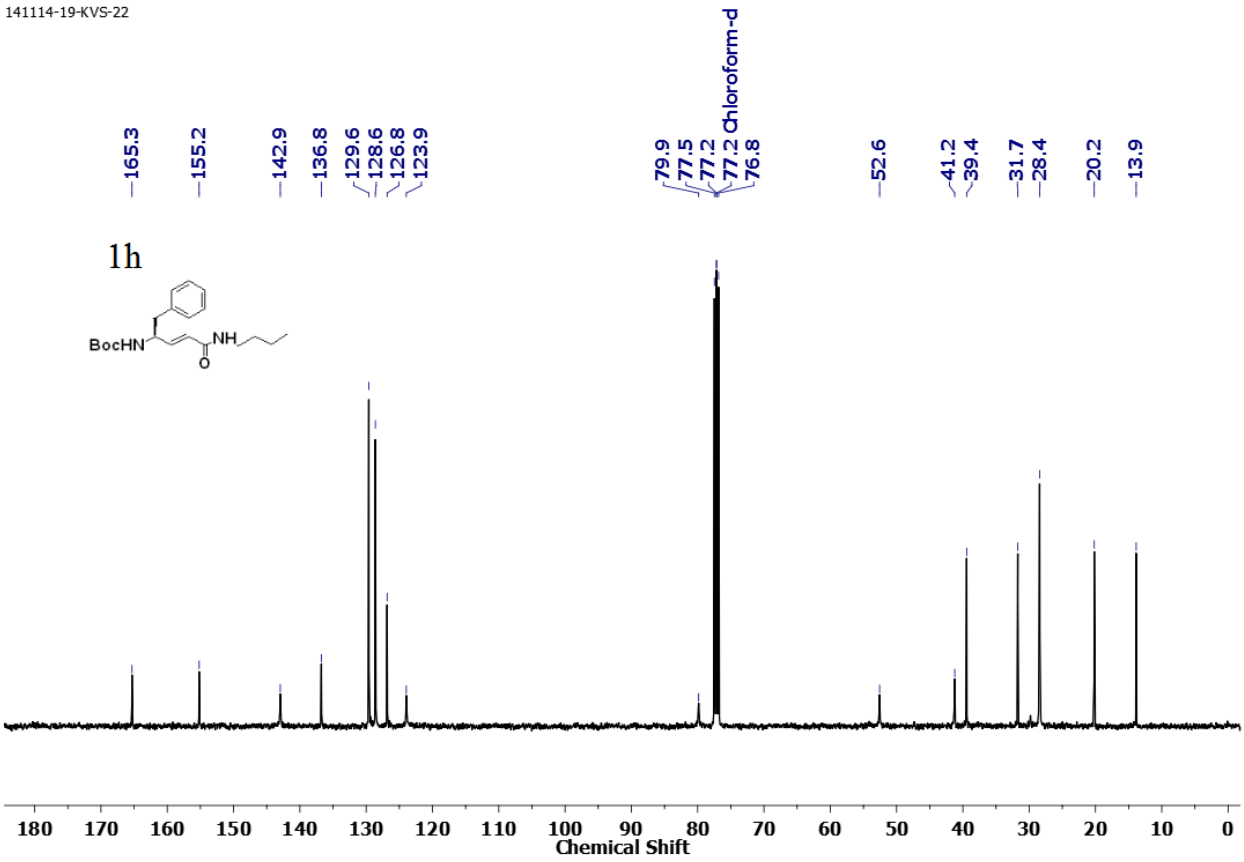
141114-19-KVS-22
165.3
155.2
142.9
136.8
129.6
128.6
126.8
123.9
79.9
77.5
77.2
77.2
Chloroform-d
76.8
52.6
41.2
39.4
31.7
28.4
20.2
13.9
1h
BocHN
NH
O
180
170
160
150
140
130
120
110
100
90
80
70
60
50
40
30
20
10
0
Chemical Shift

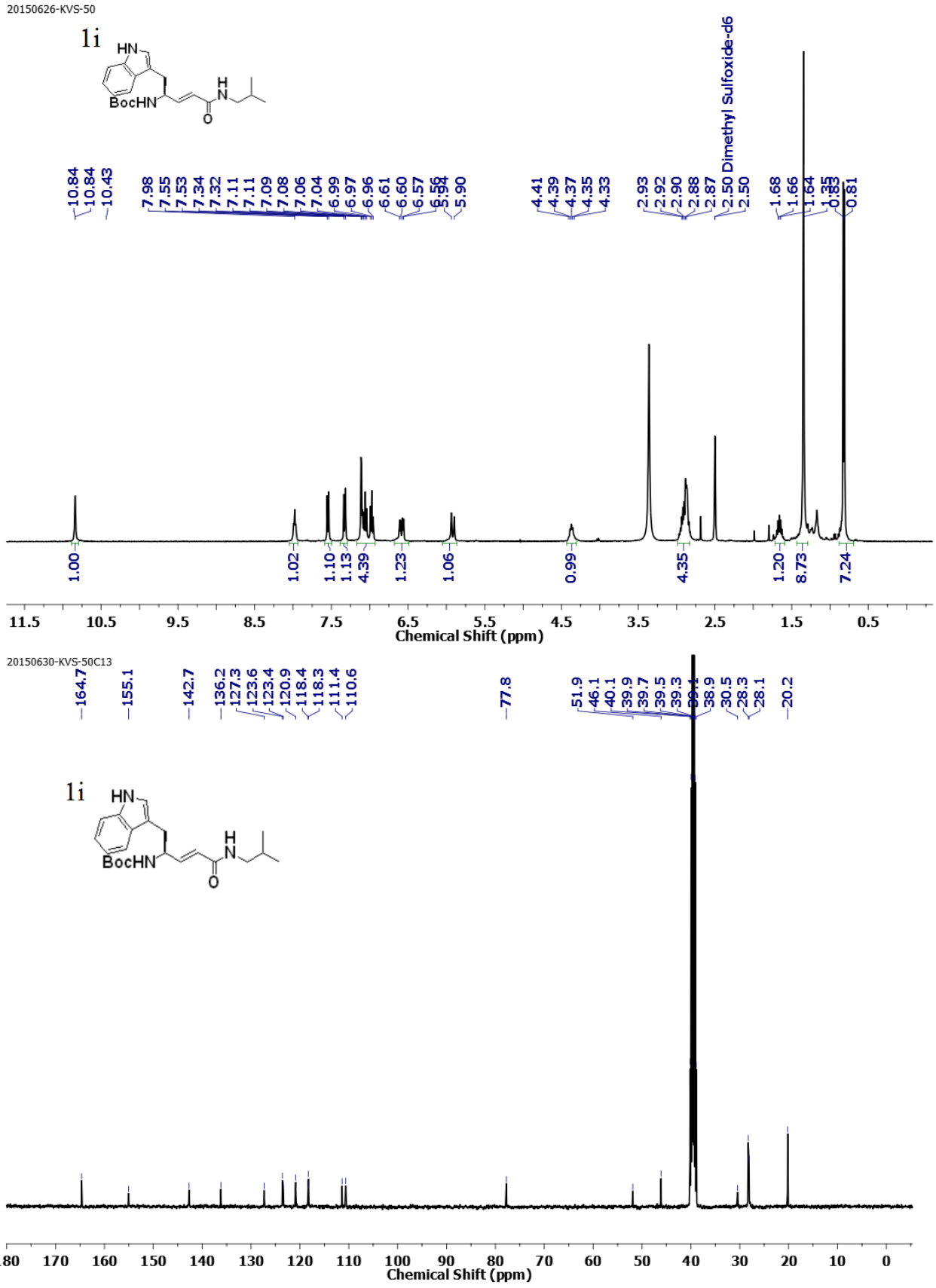
20150626-KVS-50
1i
HN
BocHN
H
N
O
Dimethyl Sulfoxide-d6
10.84
10.84
10.43
7.98
7.55
7.53
7.34
7.32
7.11
7.11
7.09
7.08
7.06
7.04
6.99
6.97
6.96
6.61
6.60
6.57
5.90
4.41
4.39
4.37
4.35
4.33
2.93
2.92
2.90
2.88
2.87
2.50
2.50
1.68
1.66
1.64
0.83
0.81
1.00
1.02
1.10
1.13
4.39
1.23
1.06
0.99
4.35
1.20
8.73
7.24
11.5
10.5
9.5
8.5
7.5
6.5
5.5
4.5
3.5
2.5
1.5
0.5
Chemical Shift (ppm)
20150630-KVS-50C13
164.7
155.1
142.7
136.2
127.3
123.6
123.4
120.9
118.4
118.3
111.4
110.6
77.8
51.9
46.1
40.1
39.9
39.7
39.5
39.3
38.9
30.5
28.3
28.1
20.2
1i
HN
BocHN
H
N
O
180
170
160
150
140
130
120
110
100
90
80
70
60
50
40
30
20
10
0
Chemical Shift (ppm)

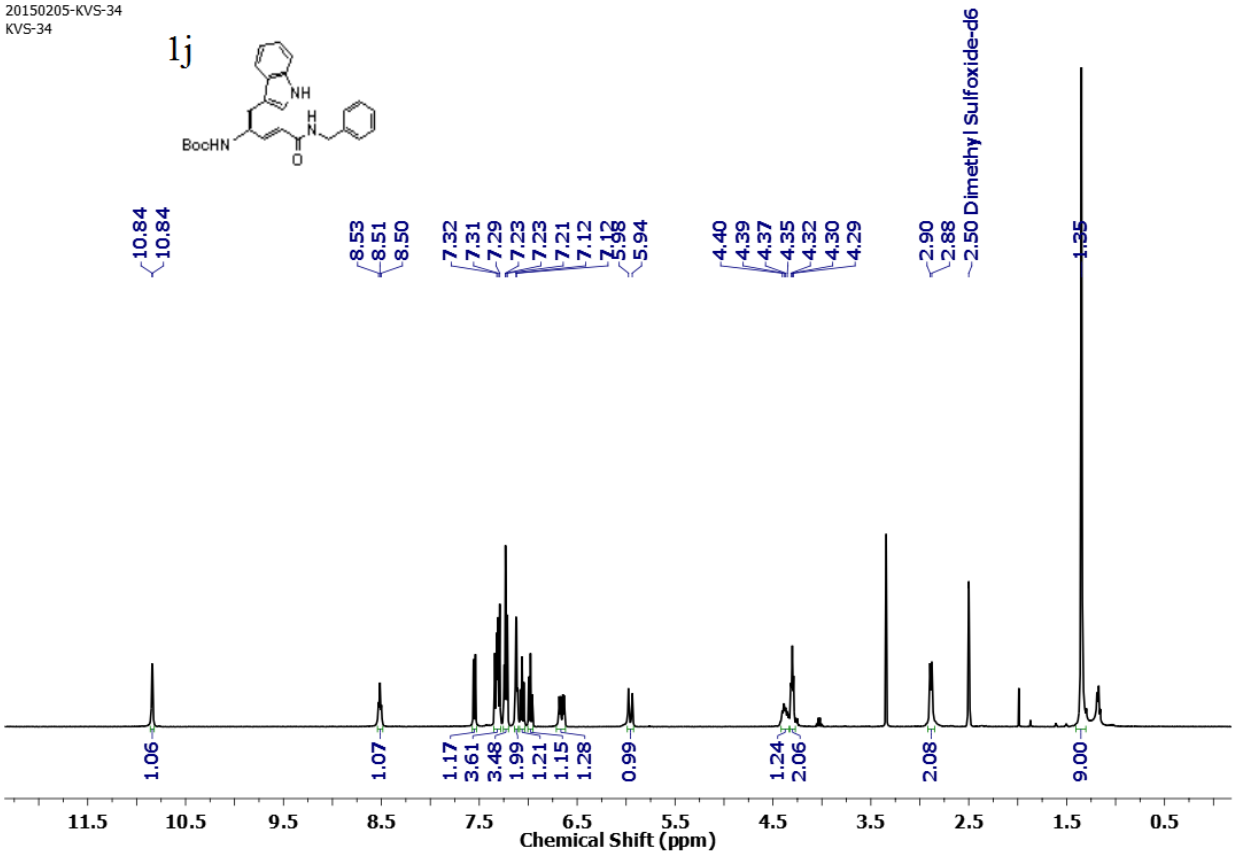
20150205-KVS-34
KVS-34
1j
BocHN
NH
Dimethyl Sulfoxide-d6
10.84
8.53
8.51
8.50
7.32
7.31
7.29
7.23
7.23
7.21
7.12
5.98
5.94
4.40
4.39
4.37
4.35
4.32
4.30
4.29
2.90
2.88
2.50
1.35
1.06
1.07
1.17
3.61
3.48
1.99
1.21
1.15
1.28
0.99
1.24
2.06
2.08
9.00
Chemical Shift (ppm)

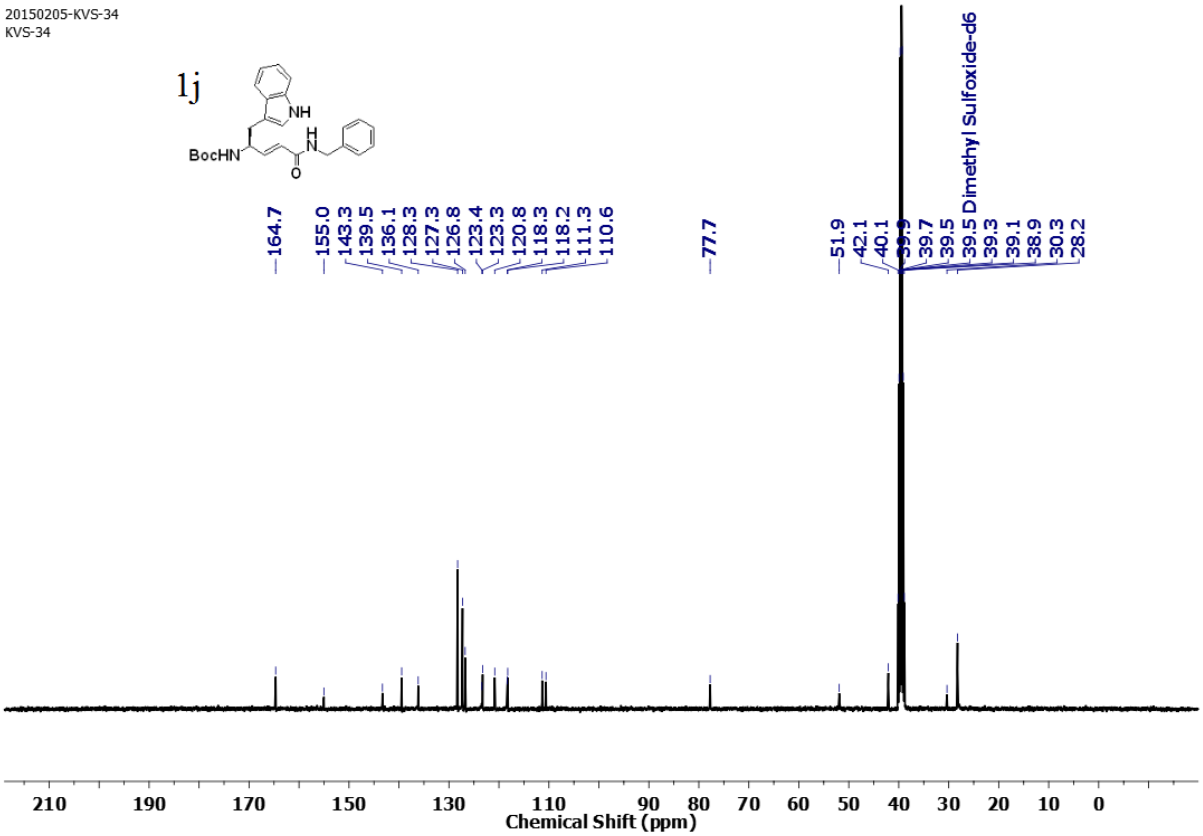
20150205-KVS-34
KVS-34
1j
BocHN
NH
Dimethyl Sulfoxide-d6
164.7
155.0
143.3
139.5
136.1
128.3
127.3
126.8
123.4
123.3
120.8
118.3
118.2
111.3
110.6
77.7
51.9
42.1
40.1
39.9
39.7
39.5
39.5
39.3
39.1
38.9
30.3
28.2
Chemical Shift (ppm)

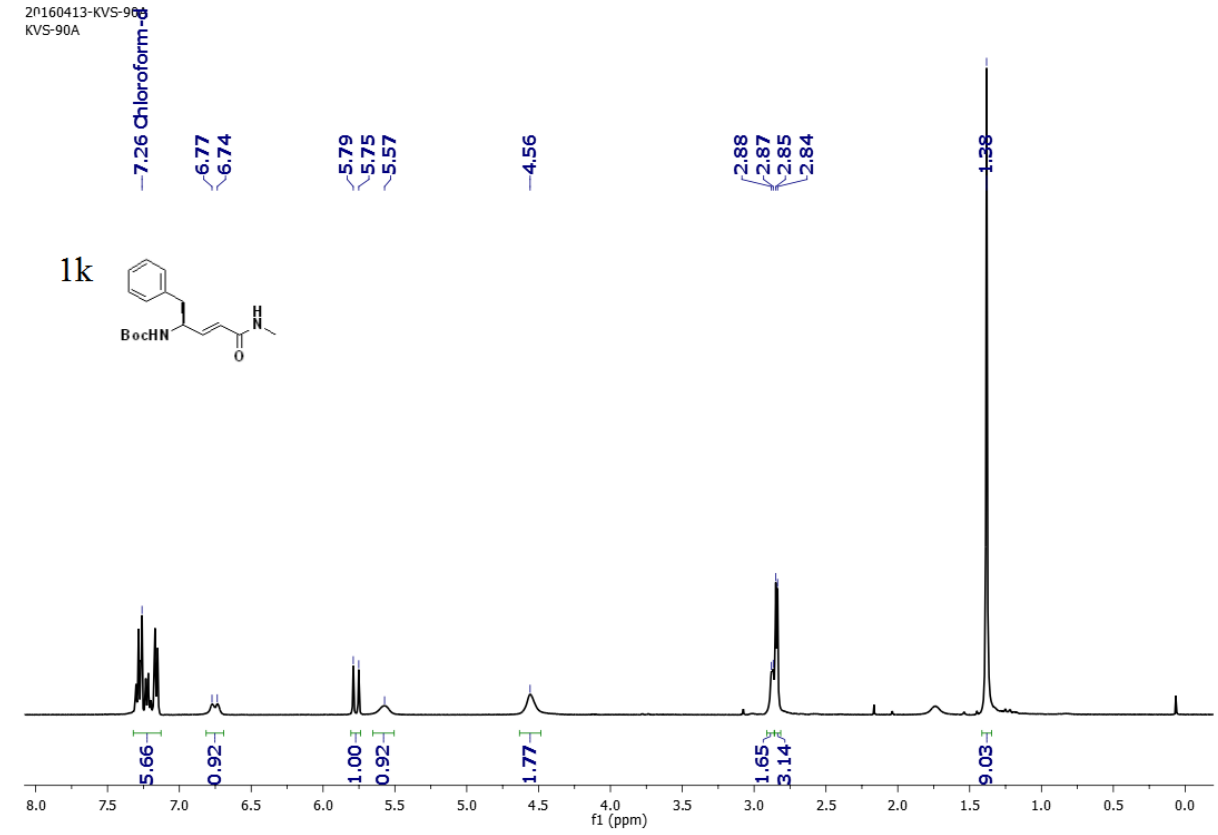
20160413-KVS-90A
KVS-90A
7.26 Chloroform-d
6.77
6.74
5.79
5.75
5.57
4.56
2.88
2.87
2.85
2.84
1.38
1k
BocHN
5.66
0.92
1.00
0.92
1.77
1.65
3.14
9.03
f1 (ppm)

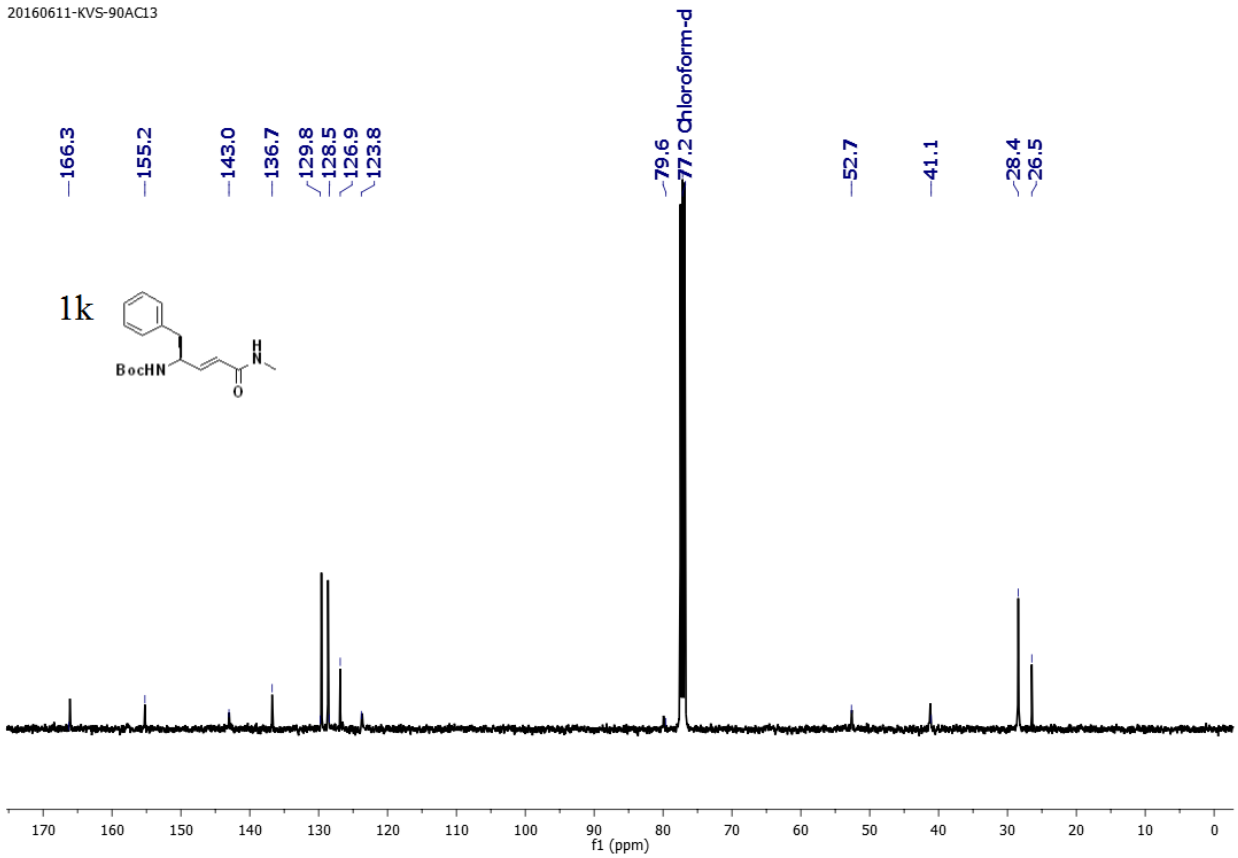
20160611-KVS-90AC13
166.3
155.2
143.0
136.7
129.8
128.5
126.9
123.8
79.6
77.2 Chloroform-d
52.7
41.1
28.4
26.5
1k
BocHN
f1 (ppm)

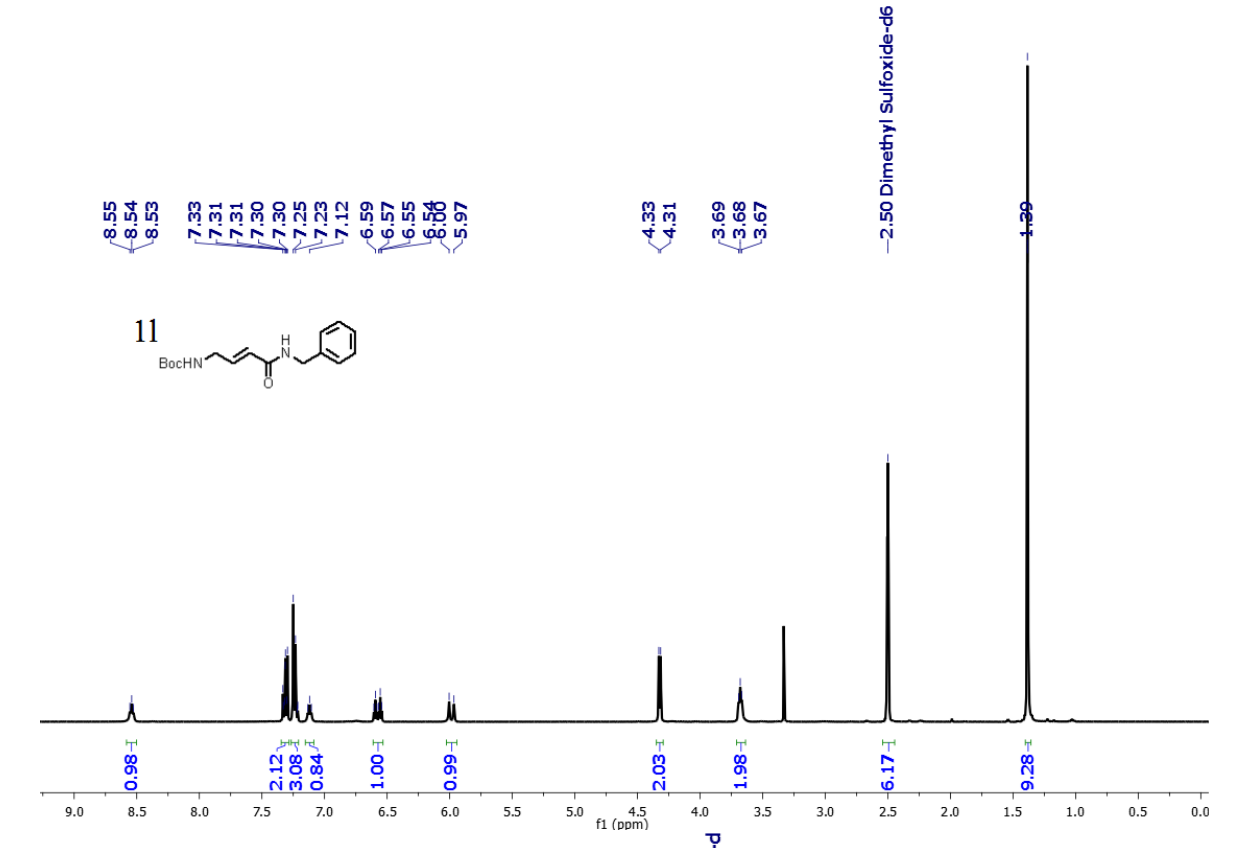
8.55
8.54
8.53
7.33
7.31
7.31
7.30
7.30
7.25
7.23
7.12
6.59
6.57
6.55
6.54
6.00
5.97
4.33
4.31
3.69
3.68
3.67
2.50 Dimethyl Sulfoxide-d6
1.39
11
BocHN
0.98
2.12
3.08
0.84
1.00
0.99
2.03
1.98
6.17
9.28
f1 (ppm)

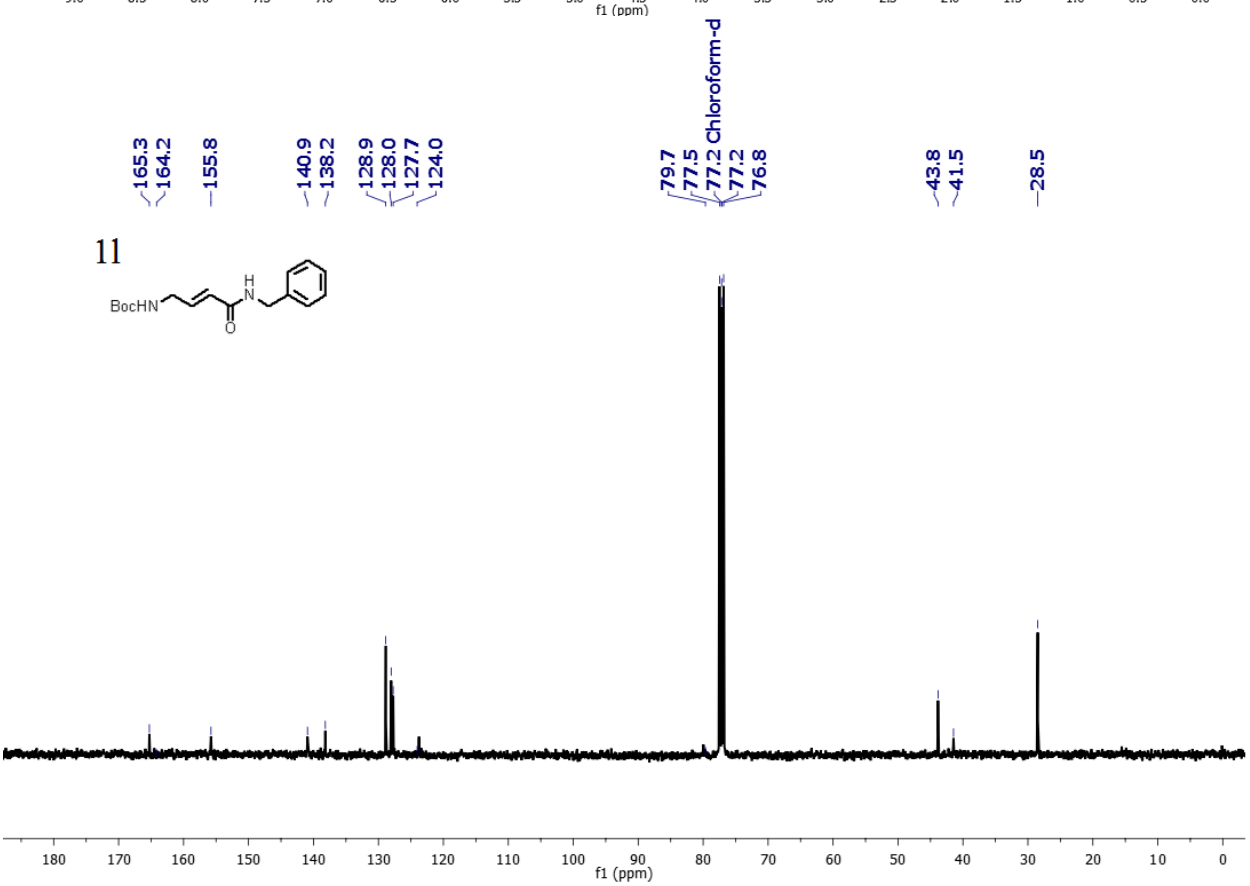
165.3
164.2
155.8
140.9
138.2
128.9
128.0
127.7
124.0
79.7
77.5
77.2 Chloroform-d
77.2
76.8
43.8
41.5
28.5
11
BocHN
f1 (ppm)

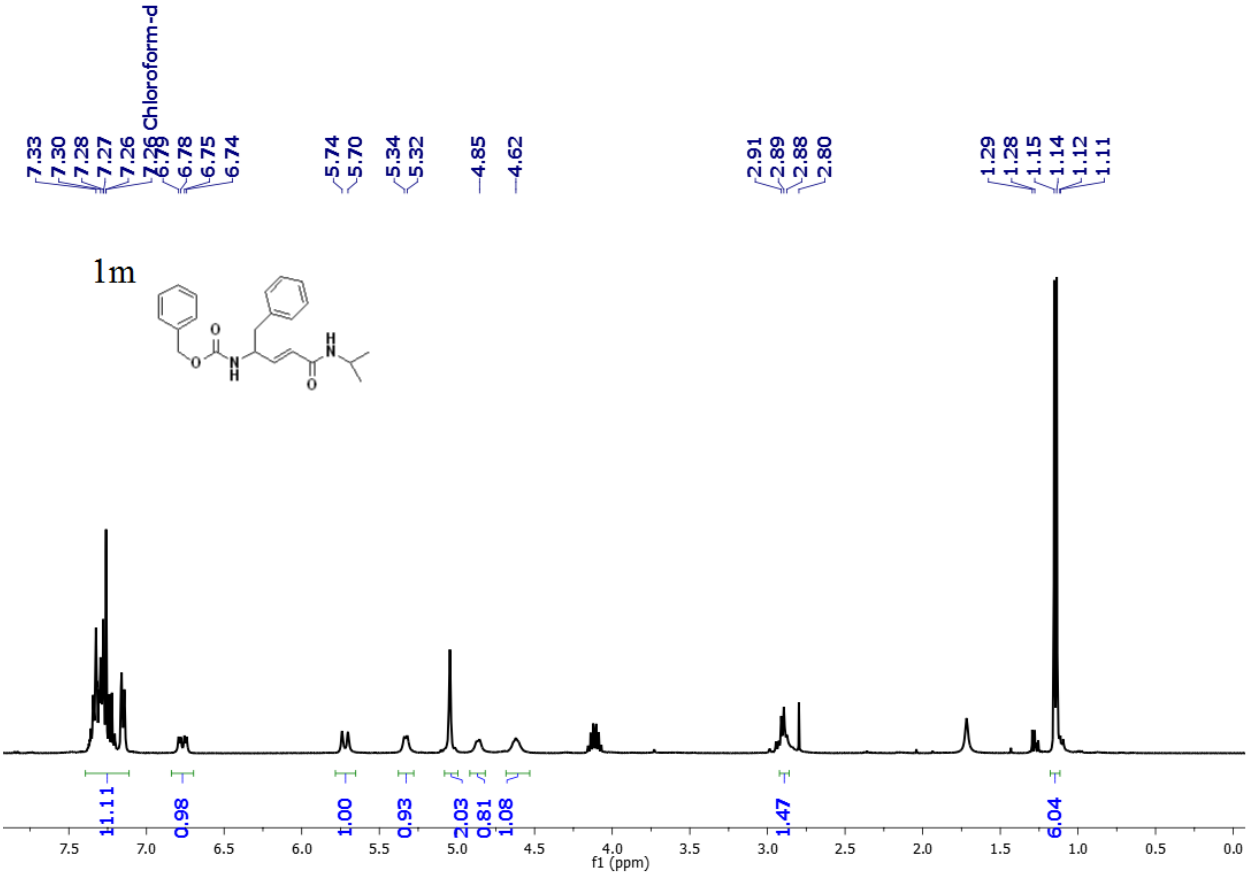
Chloroform-d
7.33
7.30
7.28
7.27
7.26
6.79
6.78
6.75
6.74
5.74
5.70
5.34
5.32
4.85
4.62
2.91
2.89
2.88
2.80
1.29
1.28
1.15
1.14
1.12
1.11
1m
11.11
0.98
1.00
0.93
2.03
0.81
1.08
1.47
6.04
f1 (ppm)

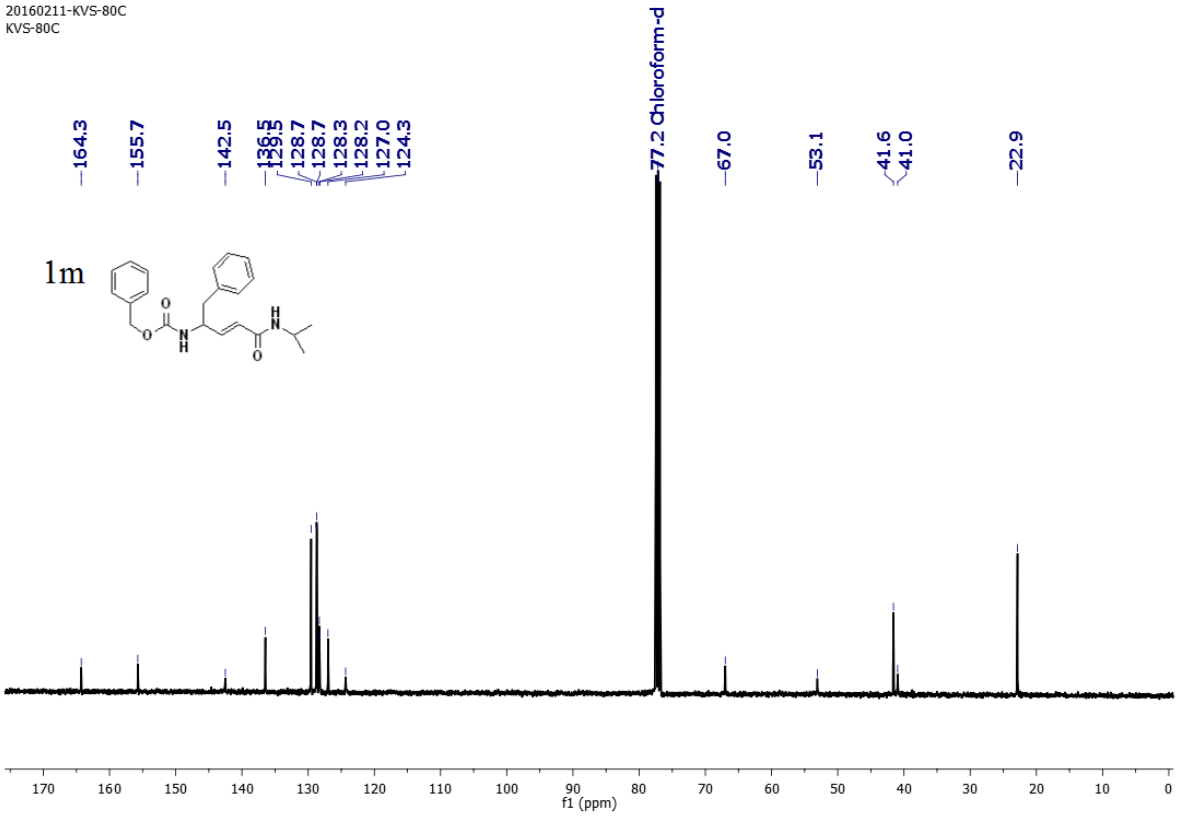
20160211-KVS-80C
KVS-80C
164.3
155.7
142.5
136.5
129.5
128.7
128.7
128.3
128.2
127.0
124.3
77.2 Chloroform-d
67.0
53.1
41.6
41.0
22.9
1m
f1 (ppm)

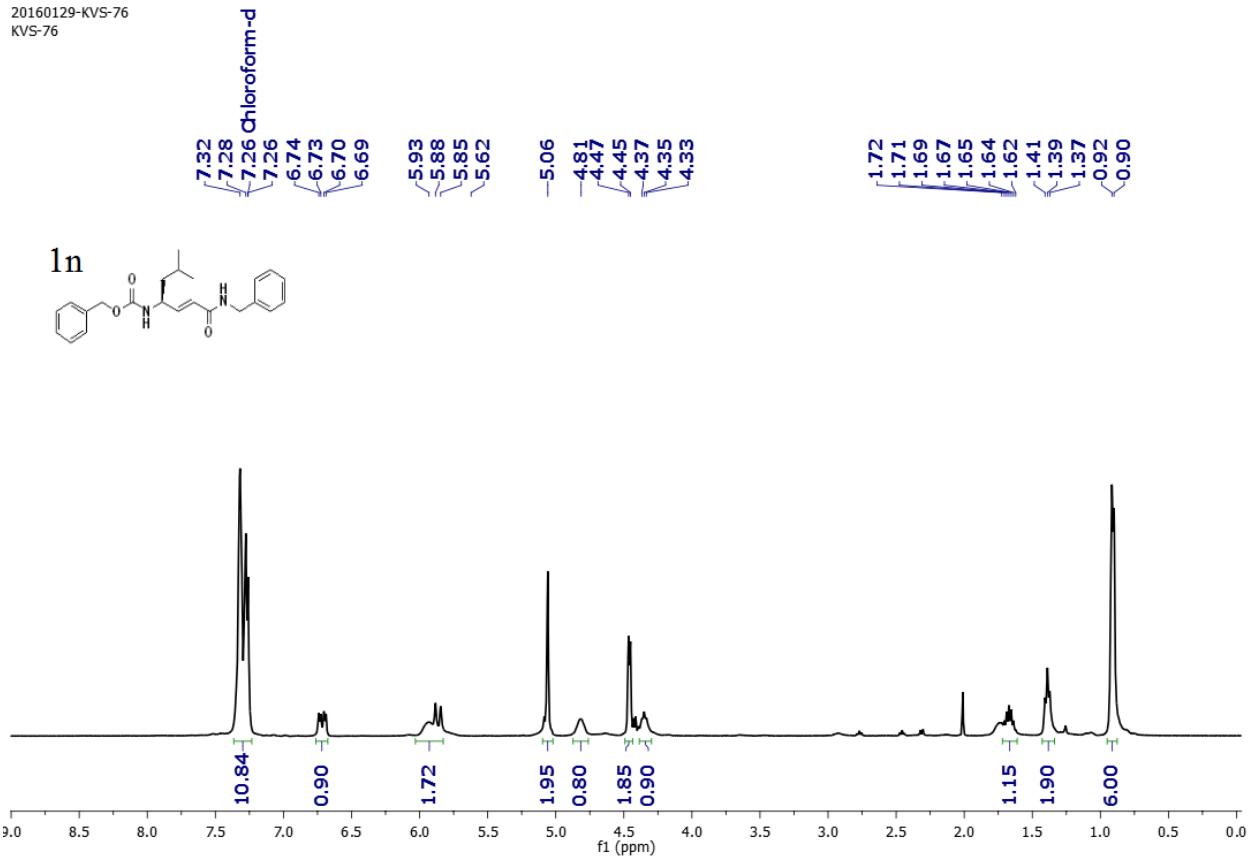
20160129-KVS-76
KVS-76
7.32
7.28
7.26 Chloroform-d
7.26
6.74
6.73
6.70
6.69
5.93
5.88
5.85
5.62
5.06
4.81
4.47
4.45
4.37
4.35
4.33
1.72
1.71
1.69
1.67
1.65
1.64
1.62
1.41
1.39
1.37
0.92
0.90
1n
10.84
0.90
1.72
1.95
0.80
1.85
0.90
1.15
1.90
6.00
f1 (ppm)

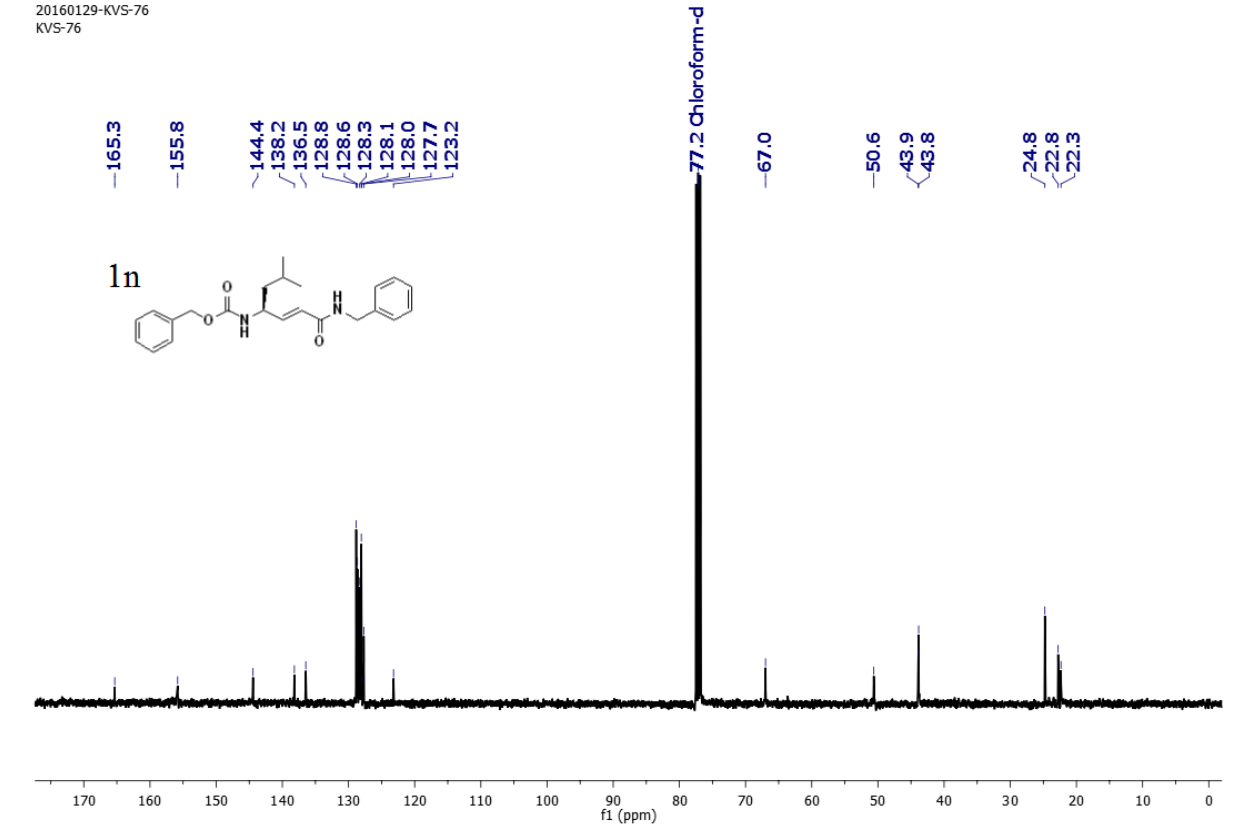
20160129-KVS-76
KVS-76
165.3
155.8
144.4
138.2
136.5
128.8
128.6
128.3
128.1
128.0
127.7
123.2
77.2 Chloroform-d
67.0
50.6
43.9
43.8
24.8
22.8
22.3
1n
f1 (ppm)

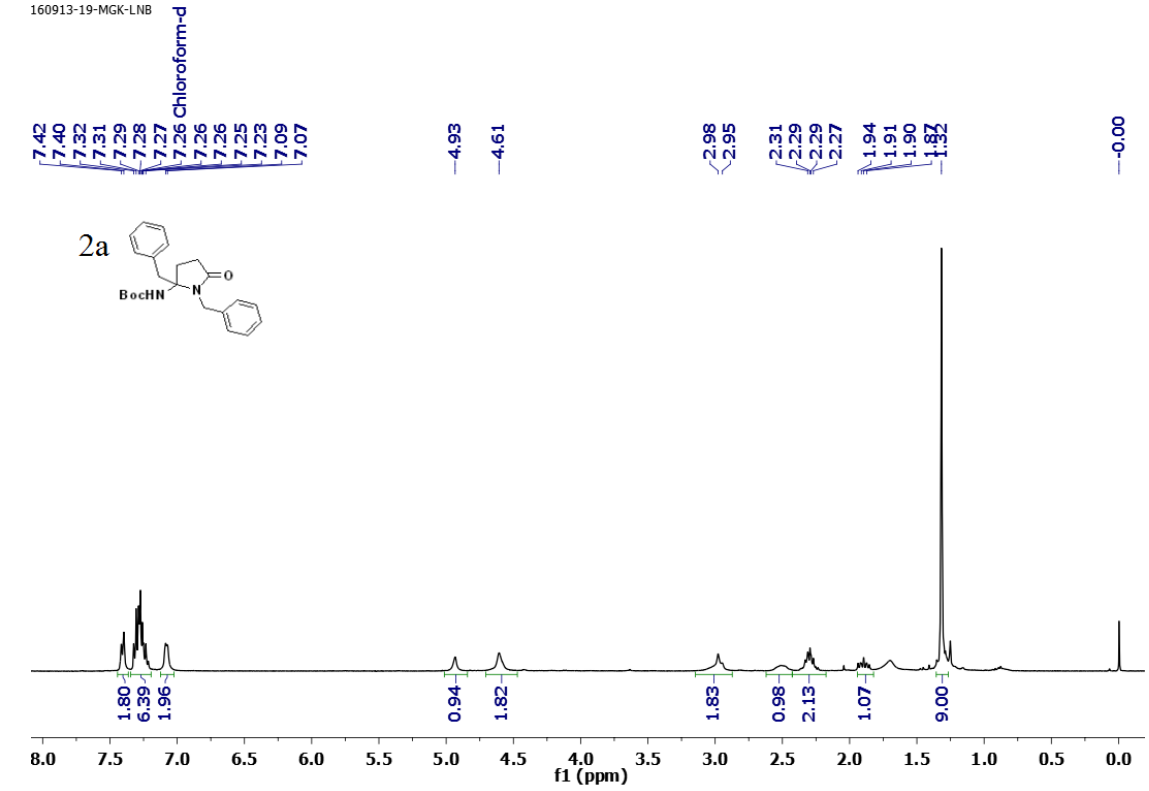
160913-19-MGK-LNB
Chloroform-d
7.42
7.40
7.32
7.31
7.29
7.28
7.27
7.26
7.26
7.26
7.25
7.23
7.09
7.07
4.93
4.61
2.98
2.95
2.31
2.29
2.29
2.27
1.94
1.91
1.90
1.87
1.82
0.00
2a
BocHN
O
N
1.80
6.39
1.96
0.94
1.82
1.83
0.98
2.13
1.07
9.00
8.0
7.5
7.0
6.5
6.0
5.5
5.0
4.5
4.0
3.5
3.0
2.5
2.0
1.5
1.0
0.5
0.0
f1 (ppm)

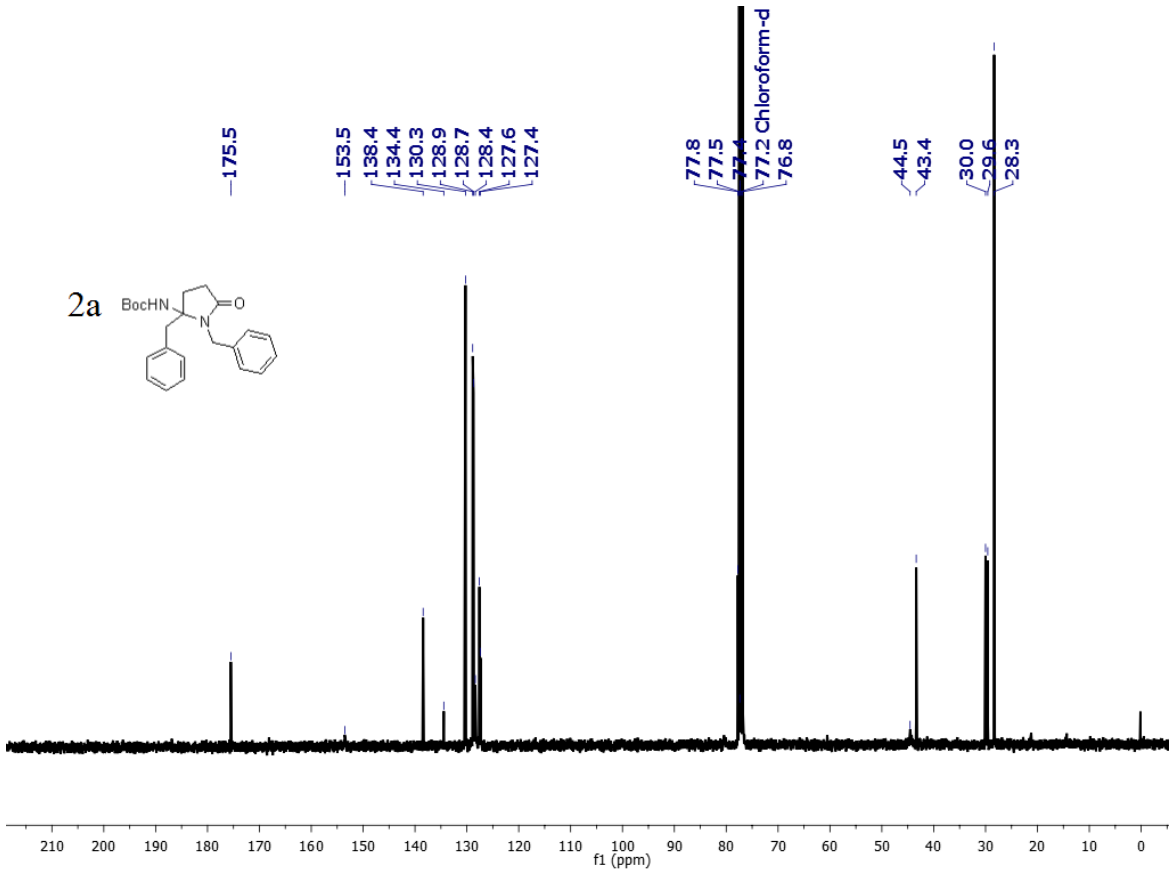
175.5
153.5
138.4
134.4
130.3
128.9
128.7
128.4
127.6
127.4
77.8
77.5
77.1
77.2 Chloroform-d
76.8
44.5
43.4
30.0
29.6
28.3
2a
BocHN
O
N
210
200
190
180
170
160
150
140
130
120
110
100
90
80
70
60
50
40
30
20
10
0
f1 (ppm)

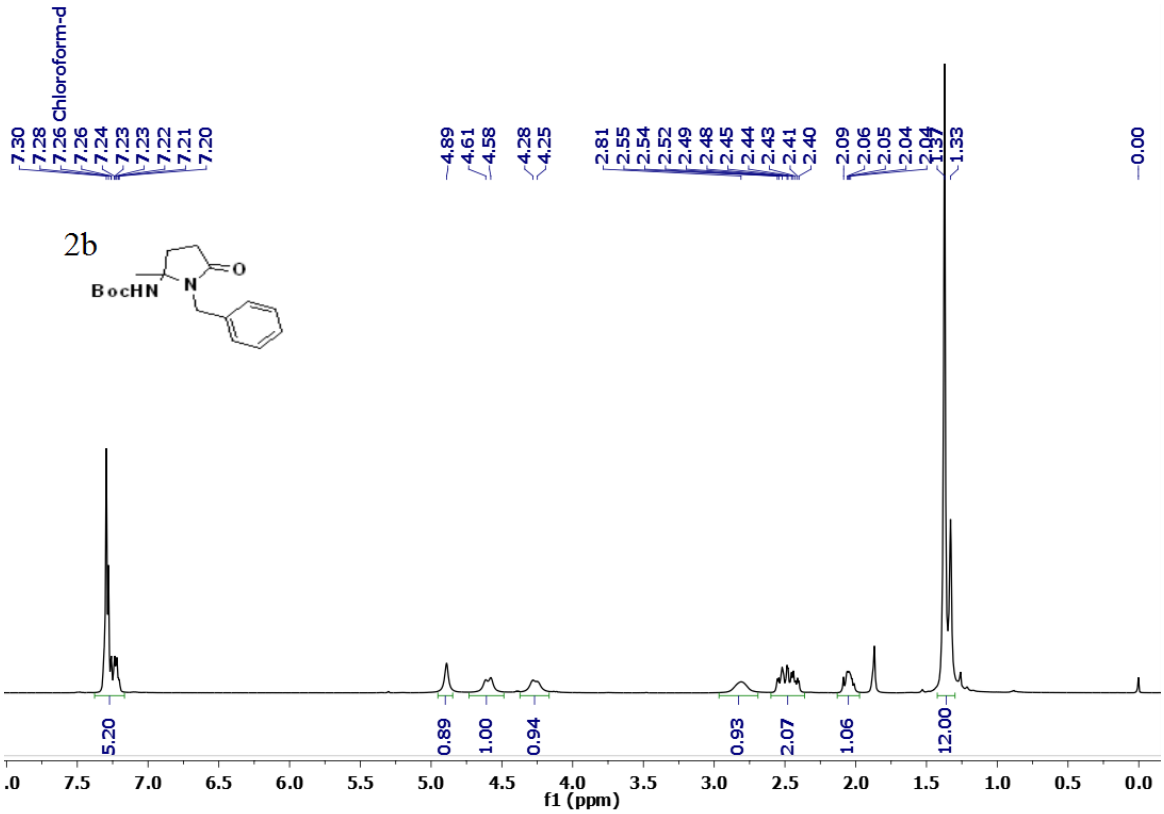
7.30
7.28
7.26 Chloroform-d
7.26
7.24
7.23
7.23
7.22
7.21
7.20
4.89
4.61
4.58
4.28
4.25
2.81
2.55
2.54
2.52
2.49
2.48
2.45
2.44
2.43
2.41
2.40
2.09
2.06
2.05
2.04
1.37
1.33
0.00
2b
BocHN
O
N
5.20
0.89
1.00
0.94
0.93
2.07
1.06
12.00
f1 (ppm)

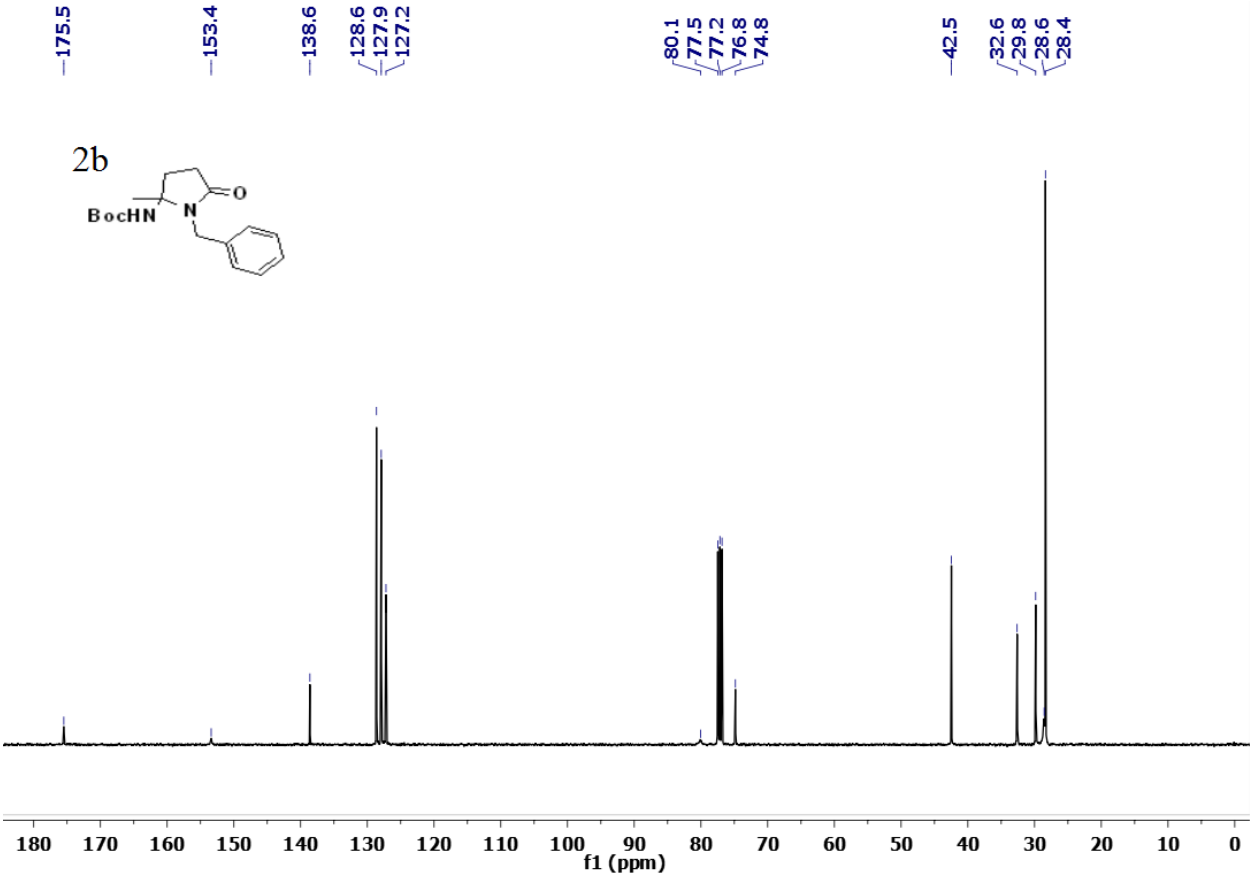
175.5
153.4
138.6
128.6
127.9
127.2
80.1
77.5
77.2
76.8
74.8
42.5
32.6
29.8
28.6
28.4
2b
BocHN
O
N
f1 (ppm)

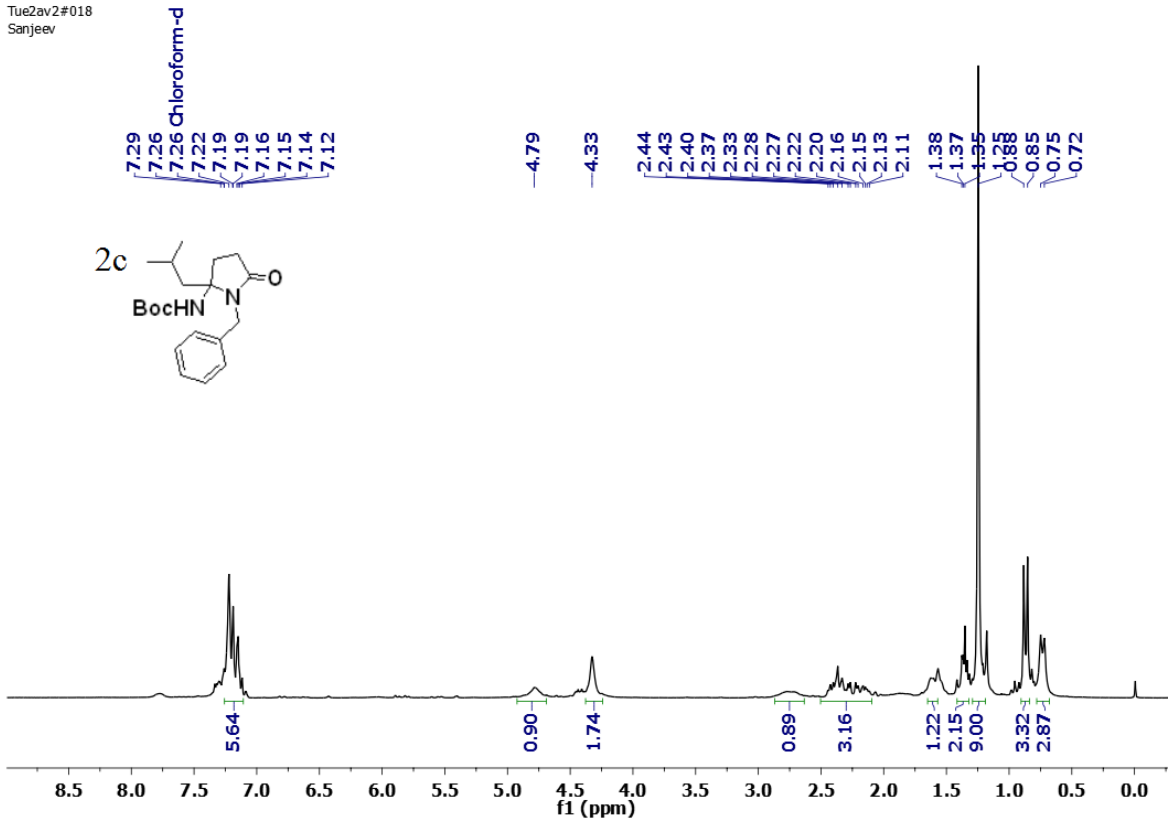
Tue2av2#018
Sanjeev
Chloroform-d
7.29
7.26
7.26
7.22
7.19
7.19
7.16
7.15
7.14
7.12
4.79
4.33
2.44
2.43
2.40
2.37
2.33
2.28
2.27
2.22
2.20
2.16
2.15
2.13
2.11
1.38
1.37
1.35
1.25
0.88
0.85
0.75
0.72
2c
BocHN
O
N
5.64
0.90
1.74
0.89
3.16
1.22
2.15
9.00
3.32
2.87
8.5
8.0
7.5
7.0
6.5
6.0
5.5
5.0
4.5
4.0
3.5
3.0
2.5
2.0
1.5
1.0
0.5
0.0
f1 (ppm)

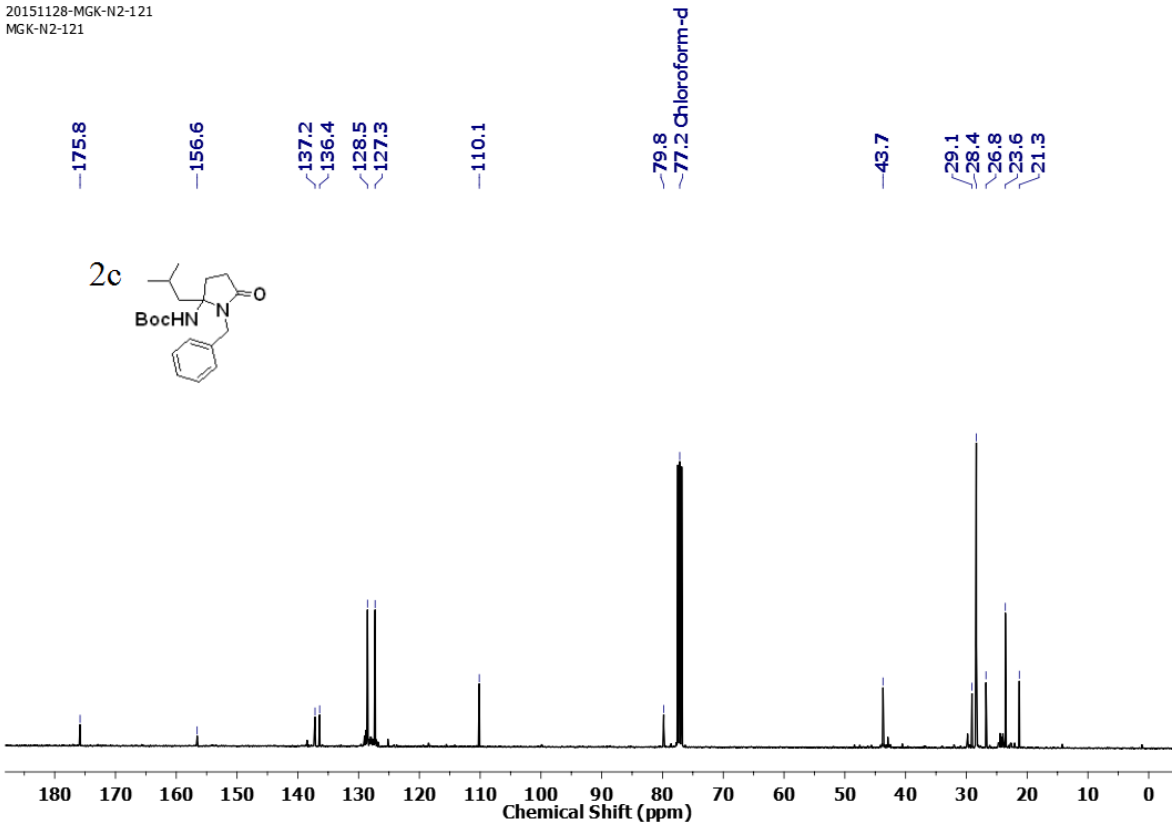
20151128-MGK-N2-121
MGK-N2-121
175.8
156.6
137.2
136.4
128.5
127.3
110.1
79.8
Chloroform-d
77.2
43.7
29.1
28.4
26.8
23.6
21.3
2c
BocHN
O
N
180
170
160
150
140
130
120
110
100
90
80
70
60
50
40
30
20
10
0
Chemical Shift (ppm)

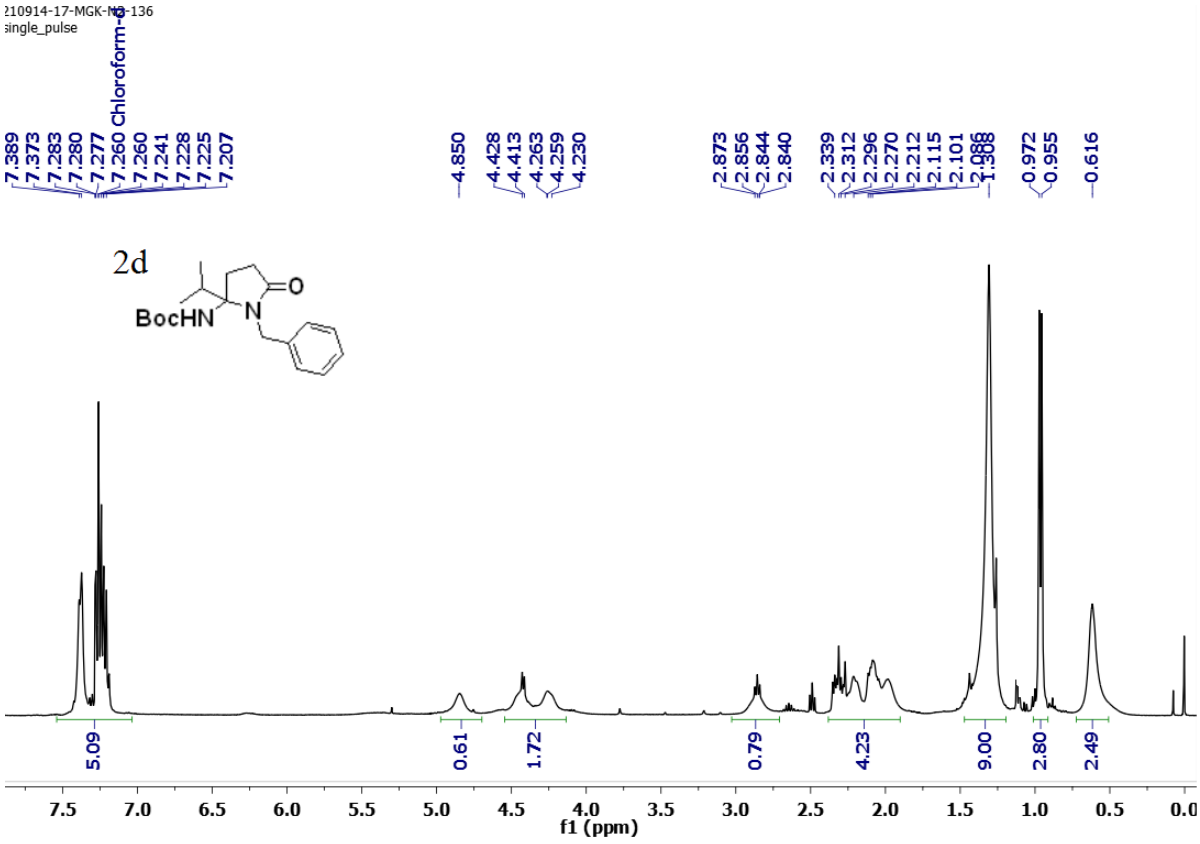
210914-17-MGK-N2-136
single_pulse
Chloroform-d
7.389
7.373
7.283
7.280
7.277
7.260
7.260
7.241
7.228
7.225
7.207
4.850
4.428
4.413
4.263
4.259
4.230
2.873
2.856
2.844
2.840
2.339
2.312
2.296
2.270
2.212
2.115
2.101
2.086
1.388
0.972
0.955
0.616
2d
BocHN
O
N
5.09
0.61
1.72
0.79
4.23
9.00
2.80
2.49
7.5
7.0
6.5
6.0
5.5
5.0
4.5
4.0
3.5
3.0
2.5
2.0
1.5
1.0
0.5
0.0
f1 (ppm)

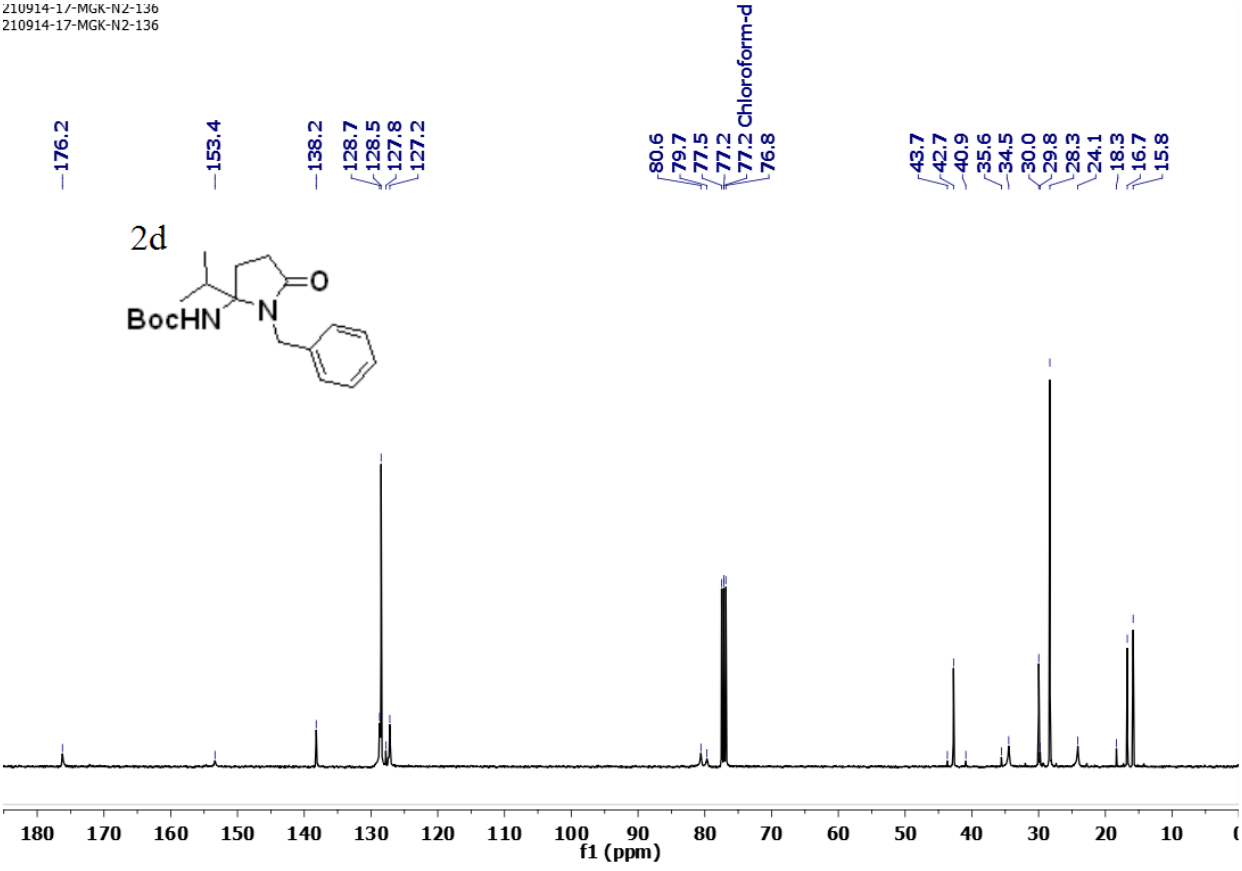
210914-17-MGK-N2-136
210914-17-MGK-N2-136
Chloroform-d
176.2
153.4
138.2
128.7
128.5
127.8
127.2
80.6
79.7
77.5
77.2
77.2
76.8
43.7
42.7
40.9
35.6
34.5
30.0
29.8
28.3
24.1
18.3
16.7
15.8
2d
BocHN
O
N
180
170
160
150
140
130
120
110
100
90
80
70
60
50
40
30
20
10
f1 (ppm)

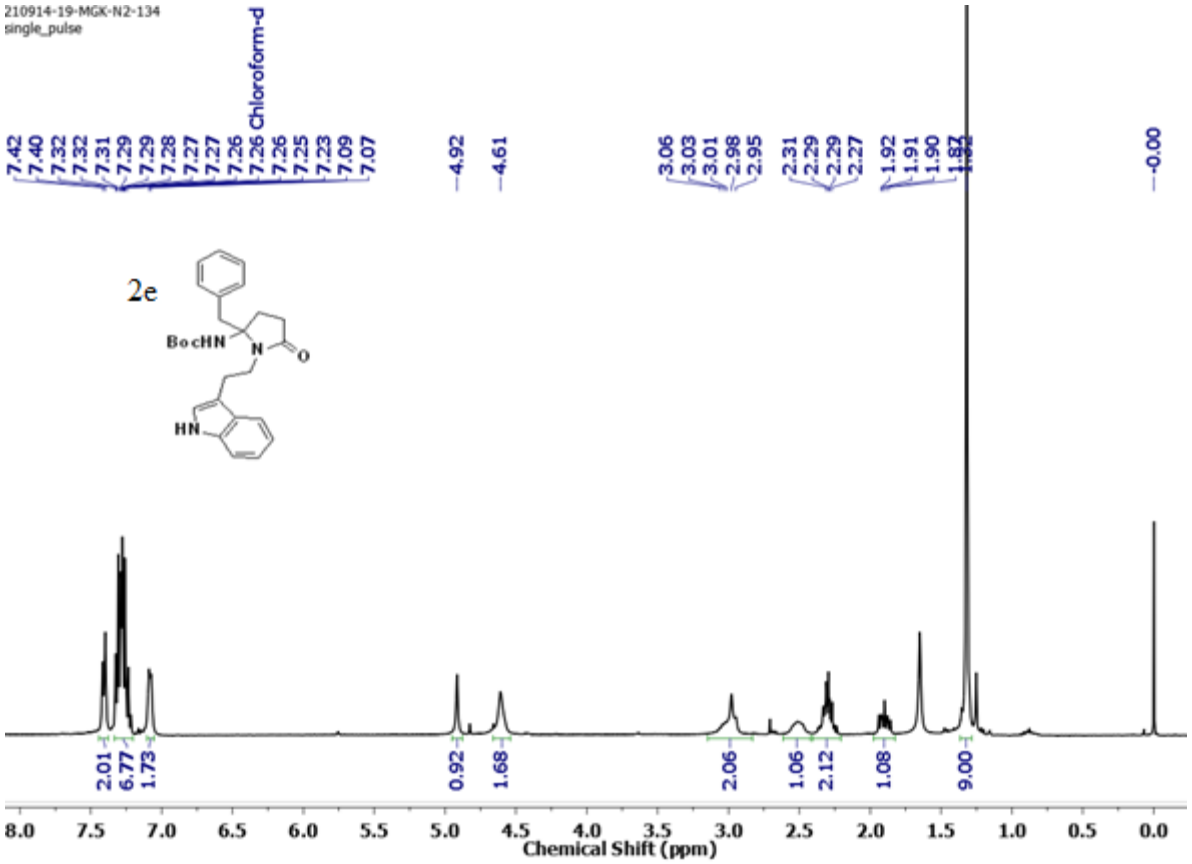
210914-19-MGK-N2-134
single_pulse
Chloroform-d
2e
BocHN
HN
Chemical Shift (ppm)

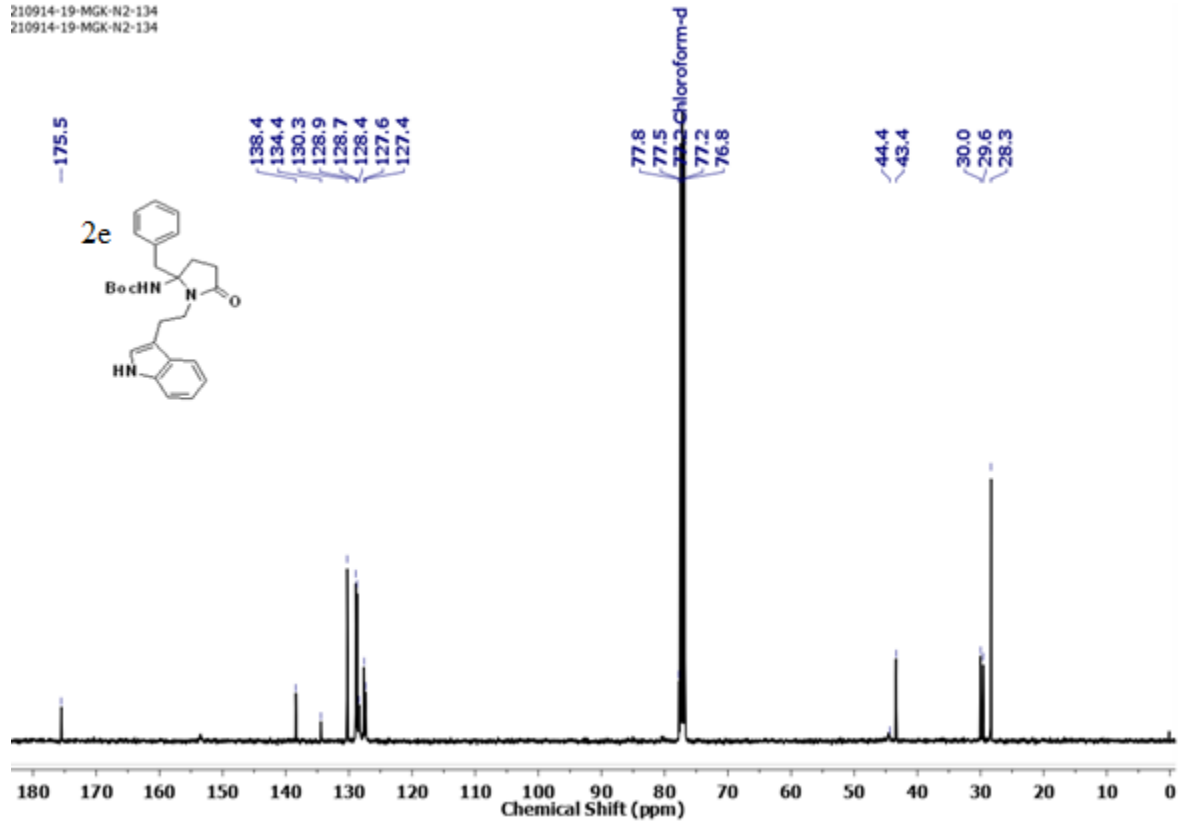
210914-19-MGK-N2-134
210914-19-MGK-N2-134
Chloroform-d
2e
BocHN
HN
Chemical Shift (ppm)

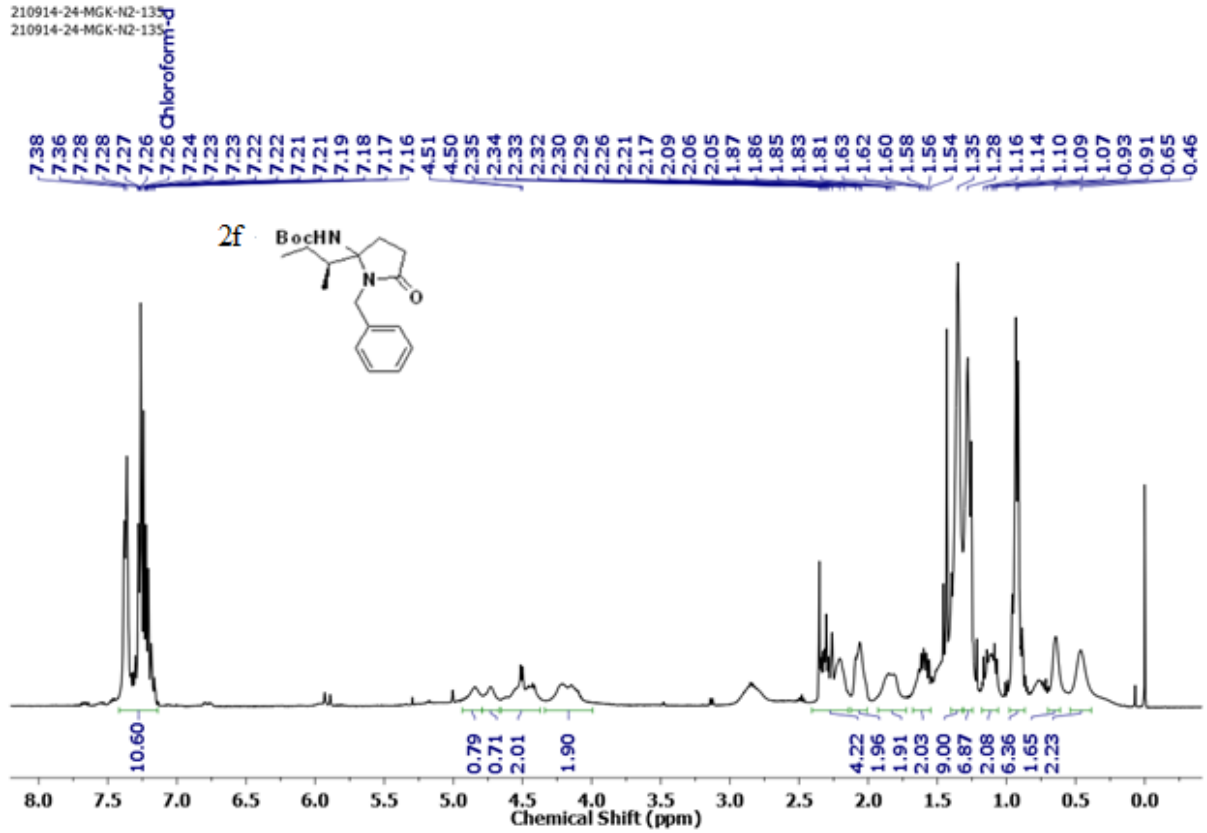
210914-24-MGK-N2-135
210914-24-MGK-N2-135-d
Chloroform-d
2f
BocHN
N
O
Chemical Shift (ppm)

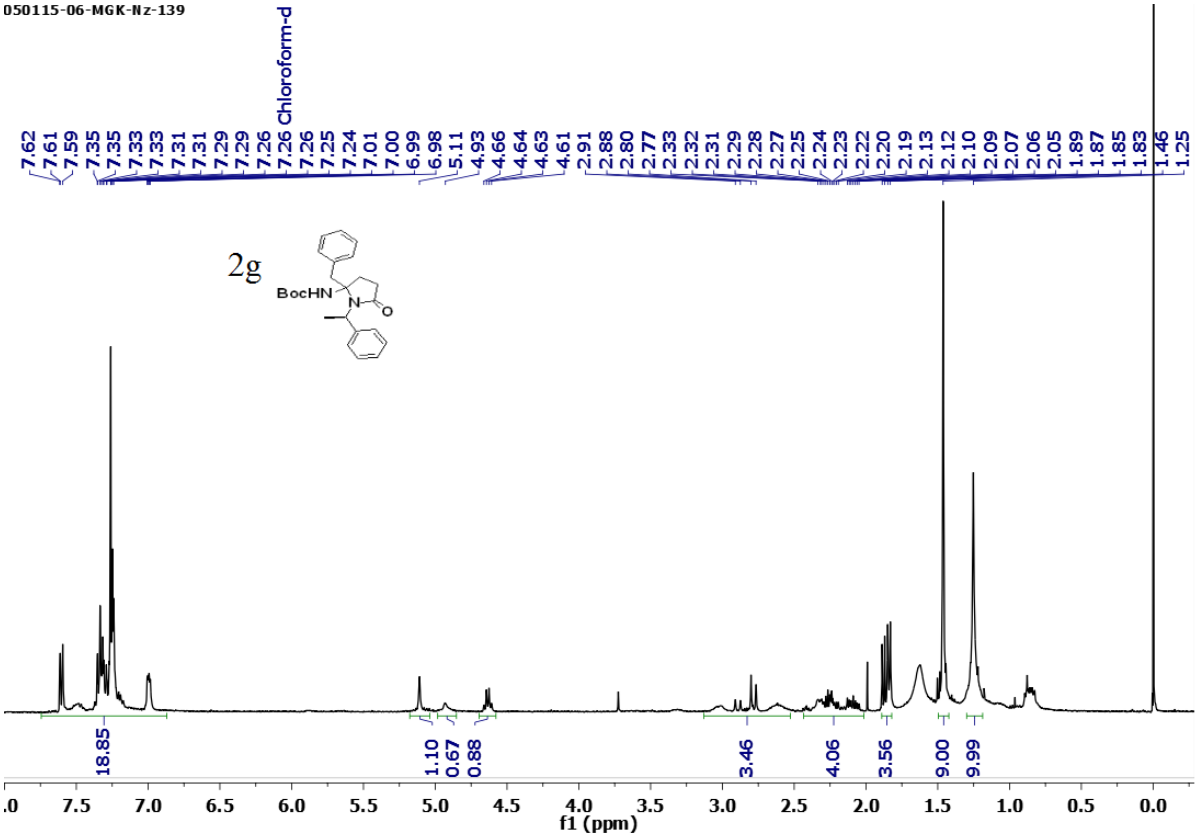
050115-06-MGK-Nz-139
Chloroform-d
2g
BocHN
N
O
f1 (ppm)

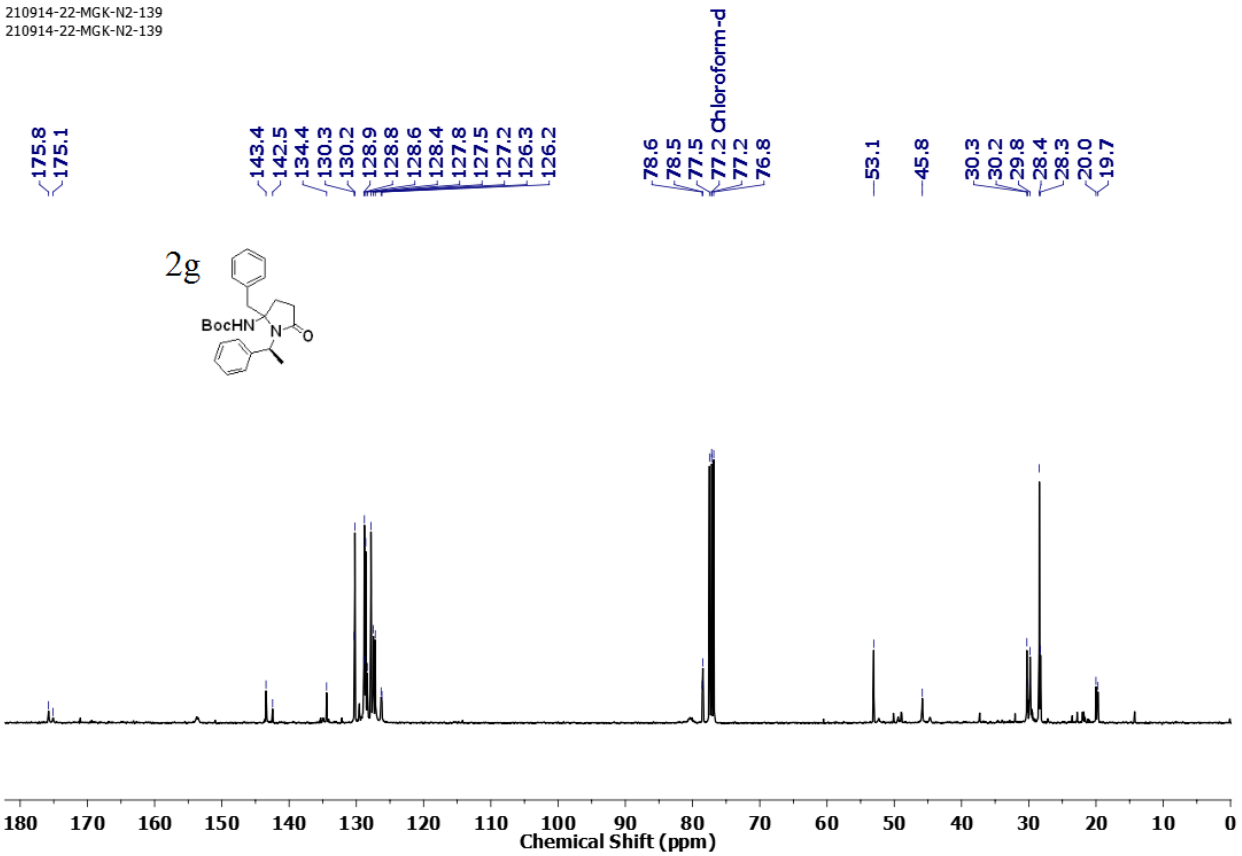
210914-22-MGK-N2-139
210914-22-MGK-N2-139
175.8
175.1
143.4
142.5
134.4
130.3
130.2
128.9
128.8
128.6
128.4
127.8
127.5
127.2
126.3
126.2
78.6
78.5
77.5
77.2 Chloroform-d
77.2
76.8
53.1
45.8
30.3
30.2
29.8
28.4
28.3
20.0
19.7
2g
BocHN
O
180 170 160 150 140 130 120 110 100 90 80 70 60 50 40 30 20 10 0
Chemical Shift (ppm)

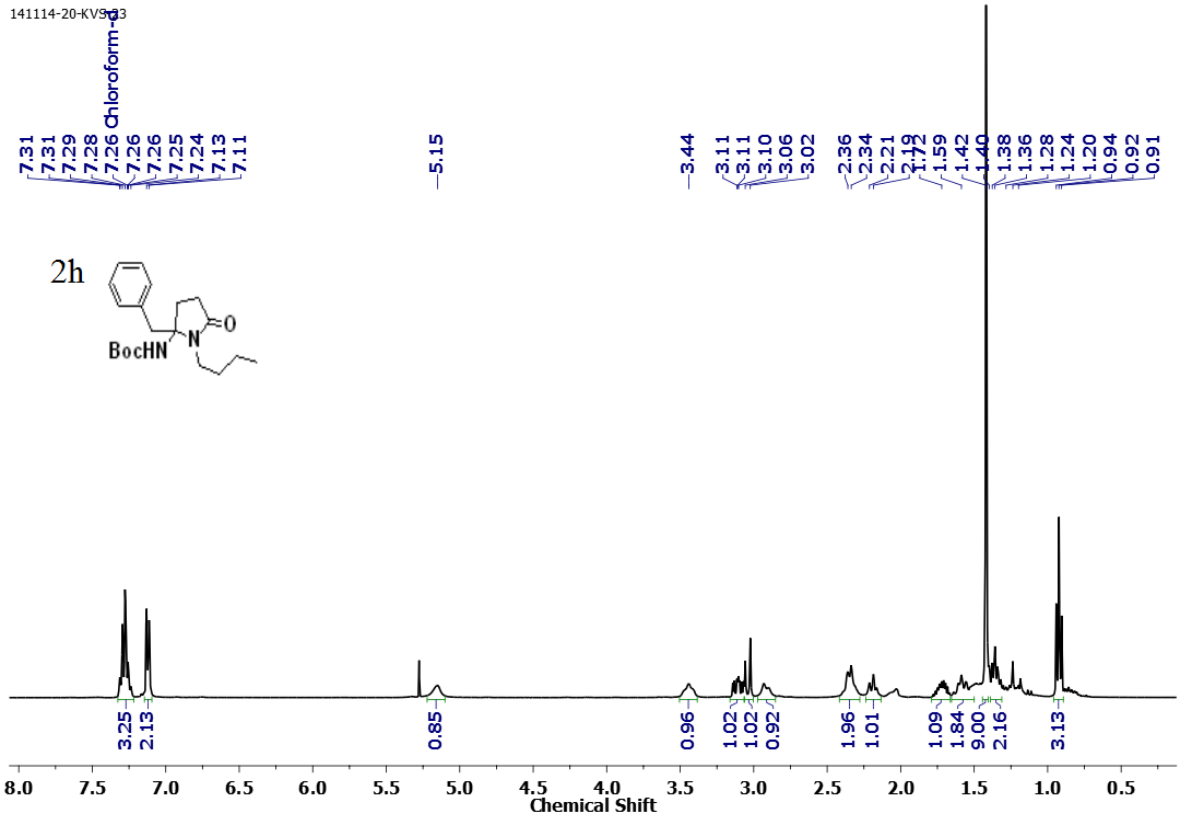
141114-20-KVS-03
7.31
7.31
7.29
7.28
7.26 Chloroform-d
7.26
7.26
7.25
7.24
7.13
7.11
5.15
3.44
3.11
3.11
3.10
3.06
3.02
2.36
2.34
2.21
1.59
1.42
1.40
1.38
1.36
1.28
1.24
1.20
0.94
0.92
0.91
2h
BocHN
O
3.25
2.13
0.85
0.96
1.02
1.02
0.92
1.96
1.01
1.09
1.84
9.00
2.16
3.13
8.0 7.5 7.0 6.5 6.0 5.5 5.0 4.5 4.0 3.5 3.0 2.5 2.0 1.5 1.0 0.5
Chemical Shift

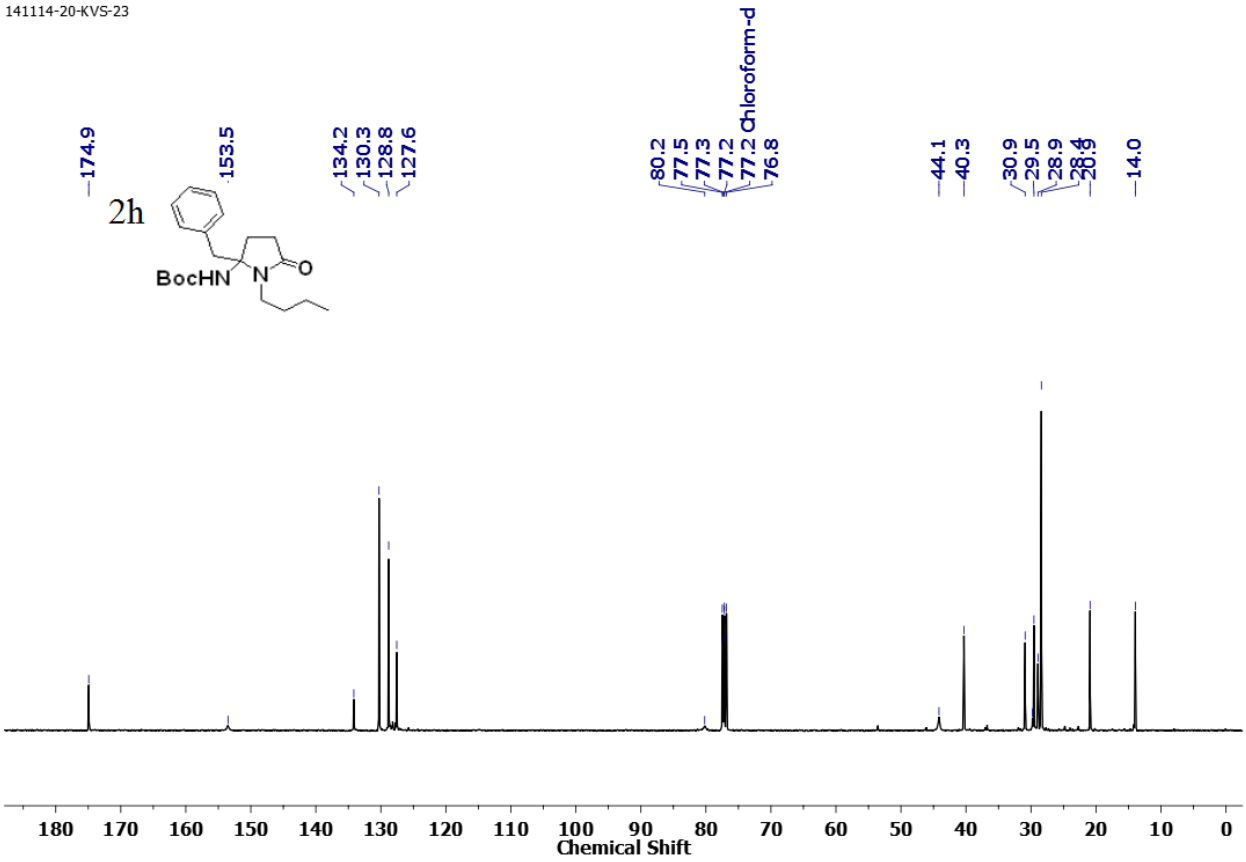
141114-20-KVS-23
174.9
153.5
134.2
130.3
128.8
127.6
80.2
77.5
77.3
77.2
Chloroform-d
77.2
76.8
44.1
40.3
30.9
29.5
28.9
28.4
20.9
14.0
2h
BocHN
N
O
180 170 160 150 140 130 120 110 100 90 80 70 60 50 40 30 20 10 0
Chemical Shift

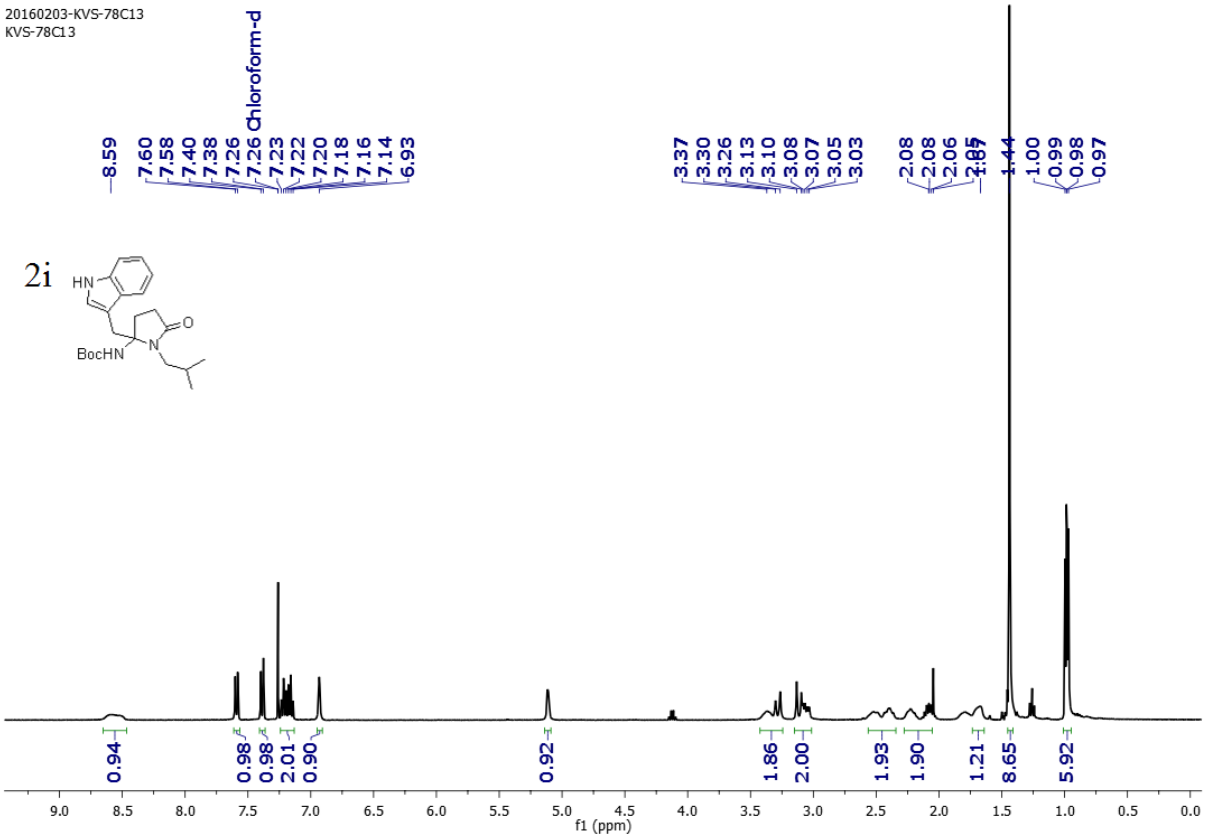
20160203-KVS-78C13
KVS-78C13
Chloroform-d
8.59
7.60
7.58
7.40
7.38
7.26
7.26
7.23
7.22
7.20
7.18
7.16
7.14
6.93
3.37
3.30
3.26
3.13
3.10
3.08
3.07
3.05
3.03
2.08
2.08
2.06
1.44
1.00
0.99
0.98
0.97
2i
HN
O
BocHN
N
0.94
0.98
0.98
2.01
0.90
0.92
1.86
2.00
1.93
1.90
1.21
8.65
5.92
9.0
8.5
8.0
7.5
7.0
6.5
6.0
5.5
5.0
4.5
4.0
3.5
3.0
2.5
2.0
1.5
1.0
0.5
0.0
f1 (ppm)

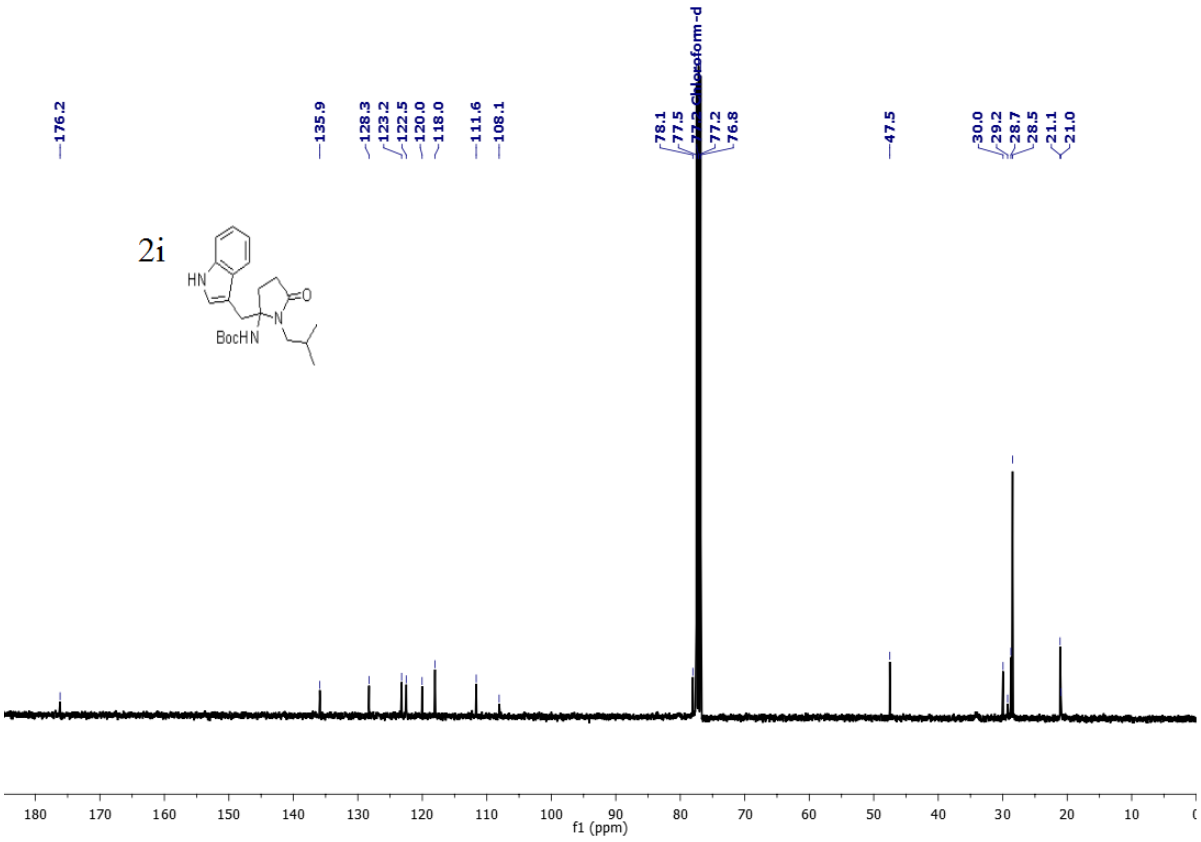
176.2
135.9
128.3
123.2
122.5
120.0
118.0
111.6
108.1
78.1
77.5
77.2
76.8
47.5
30.0
29.2
28.7
28.5
21.1
21.0
Chloroform-d
2i
HN
O
N
BocHN
180 170 160 150 140 130 120 110 100 90 80 70 60 50 40 30 20 10
f1 (ppm)

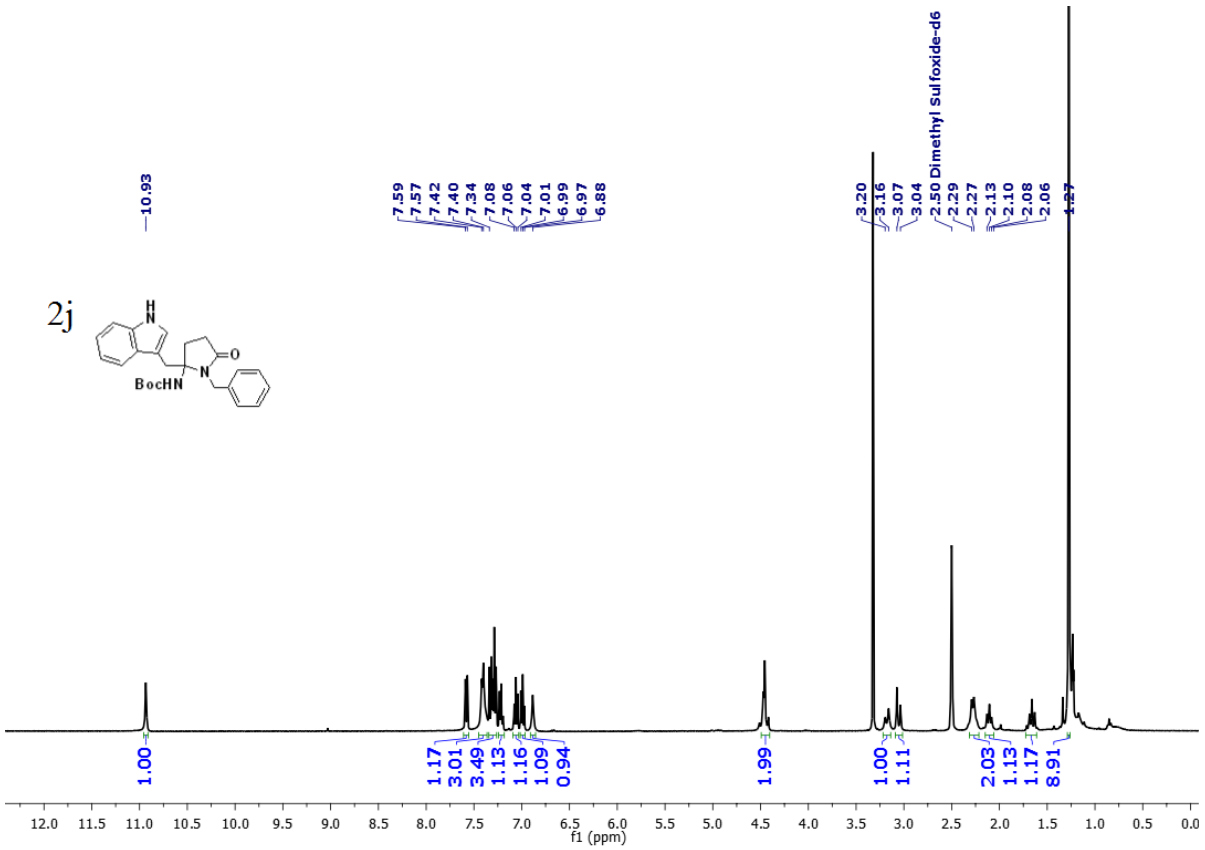
10.93
7.59
7.57
7.42
7.40
7.34
7.08
7.06
7.04
7.01
6.99
6.97
6.88
3.20
3.16
3.07
3.04
2.50 Dimethyl Sulfoxide-d6
2.29
2.27
2.13
2.10
2.08
2.06
1.27
2j
H
N
O
N
BocHN
1.00
1.17
3.01
3.49
1.13
1.16
1.09
0.94
1.99
1.00
1.11
2.03
1.13
1.17
8.91
12.0 11.5 11.0 10.5 10.0 9.5 9.0 8.5 8.0 7.5 7.0 6.5 6.0 5.5 5.0 4.5 4.0 3.5 3.0 2.5 2.0 1.5 1.0 0.5 0.0
f1 (ppm)

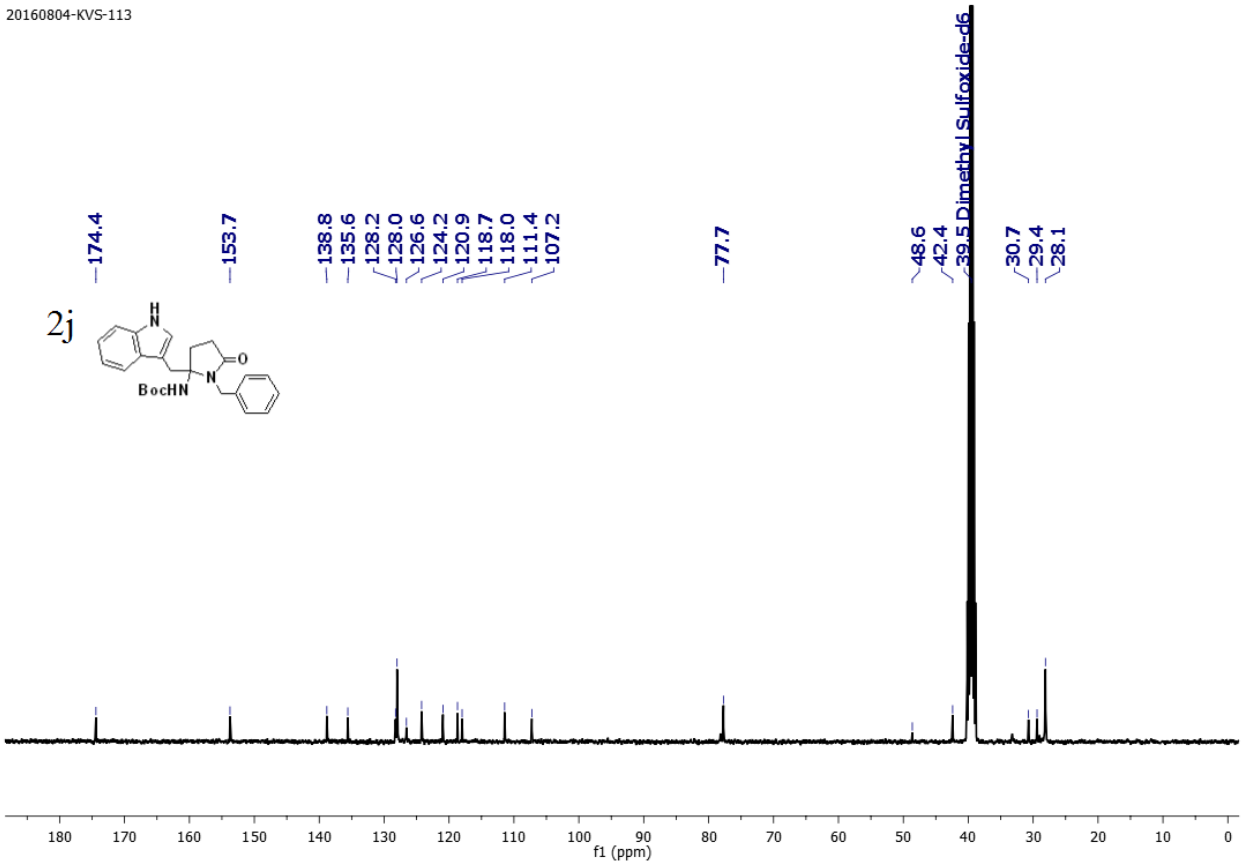
20160804-KVS-113
174.4
153.7
138.8
135.6
128.2
128.0
126.6
124.2
120.9
118.7
118.0
111.4
107.2
77.7
48.6
42.4
39.5 Dimethyl Sulfoxide-d6
30.7
29.4
28.1
2j
BocHN
f1 (ppm)

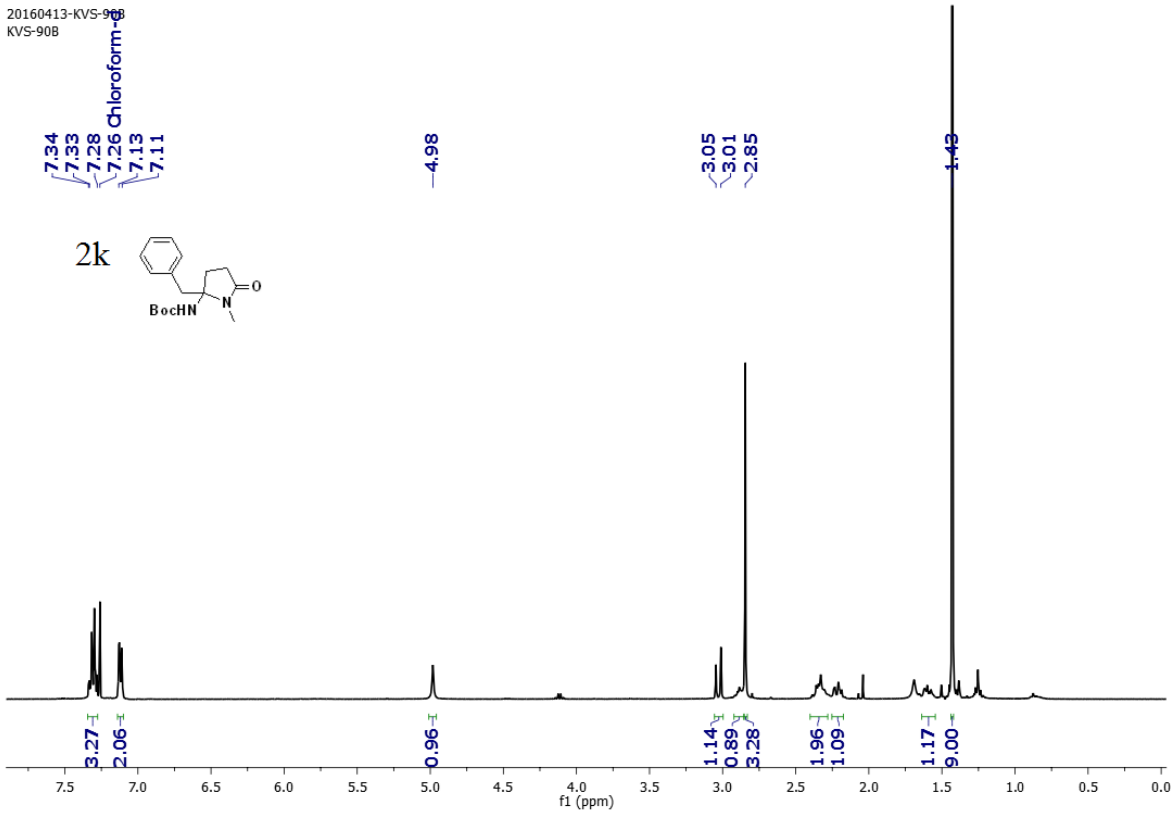
20160413-KVS-90B
KVS-90B
7.34
7.33
7.28
7.26 Chloroform-d
7.13
7.11
4.98
3.05
3.01
2.85
1.43
2k
BocHN
3.27
2.06
0.96
1.14
0.89
3.28
1.96
1.09
1.17
9.00
f1 (ppm)

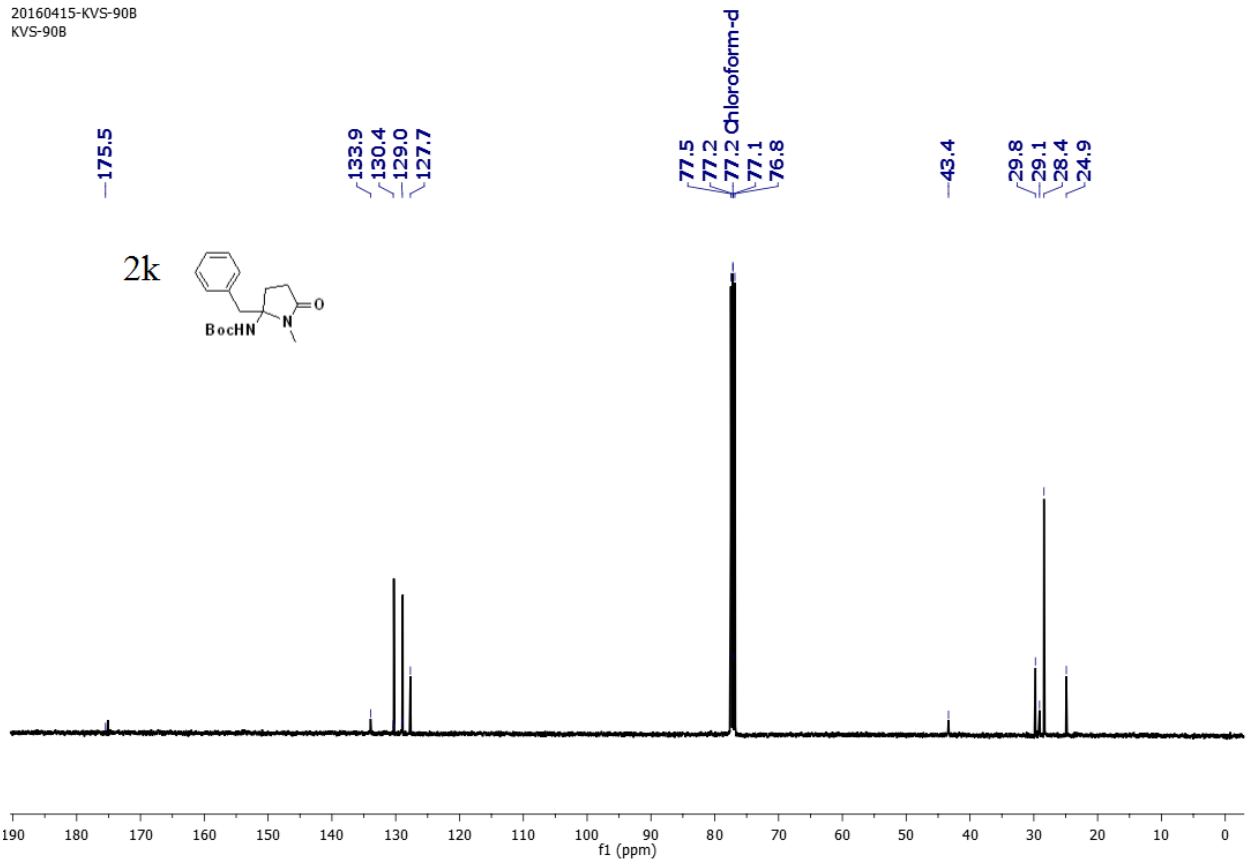
20160415-KVS-90B
KVS-90B
175.5
133.9
130.4
129.0
127.7
77.5
77.2
77.2 Chloroform-d
77.1
76.8
43.4
29.8
29.1
28.4
24.9
2k
BocHN
f1 (ppm)

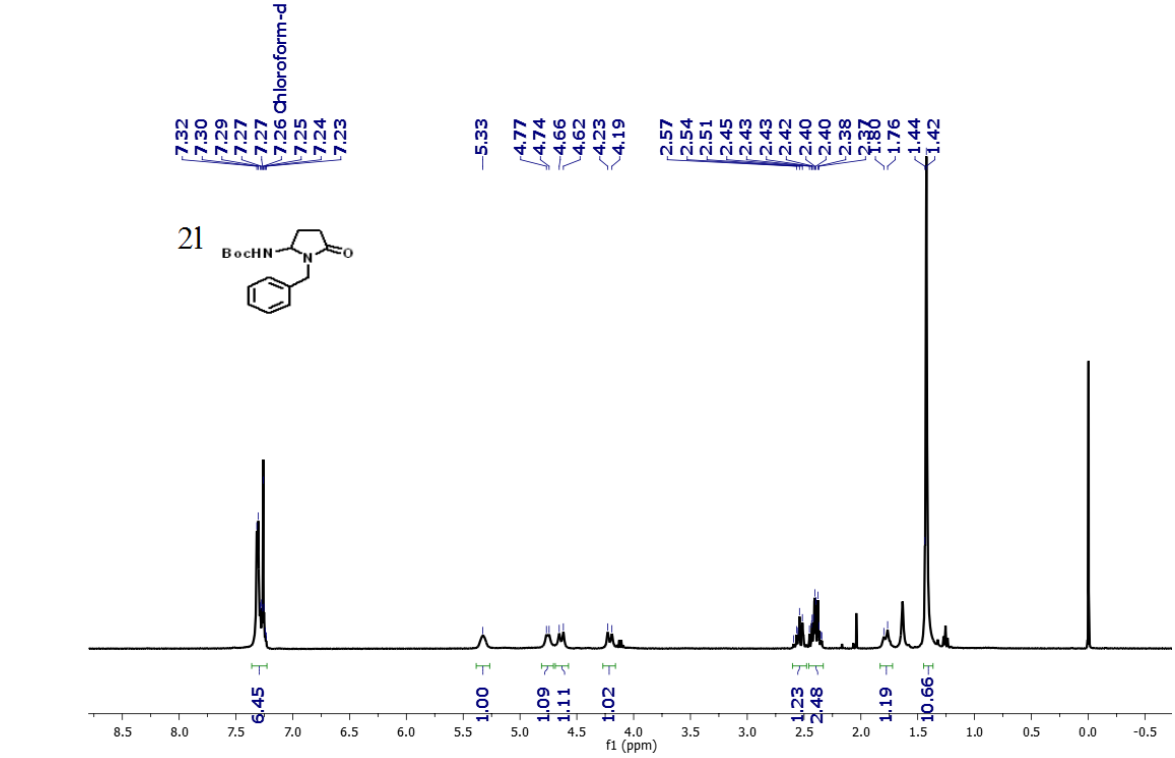
7.32
7.30
7.29
7.27
7.27
7.26 Chloroform-d
7.25
7.24
7.23
5.33
4.77
4.74
4.66
4.62
4.23
4.19
2.57
2.54
2.51
2.45
2.43
2.43
2.42
2.40
2.40
2.38
1.76
1.44
1.42
21
BocHN
6.45
1.00
1.09
1.11
1.02
1.23
2.48
1.19
10.66
f1 (ppm)

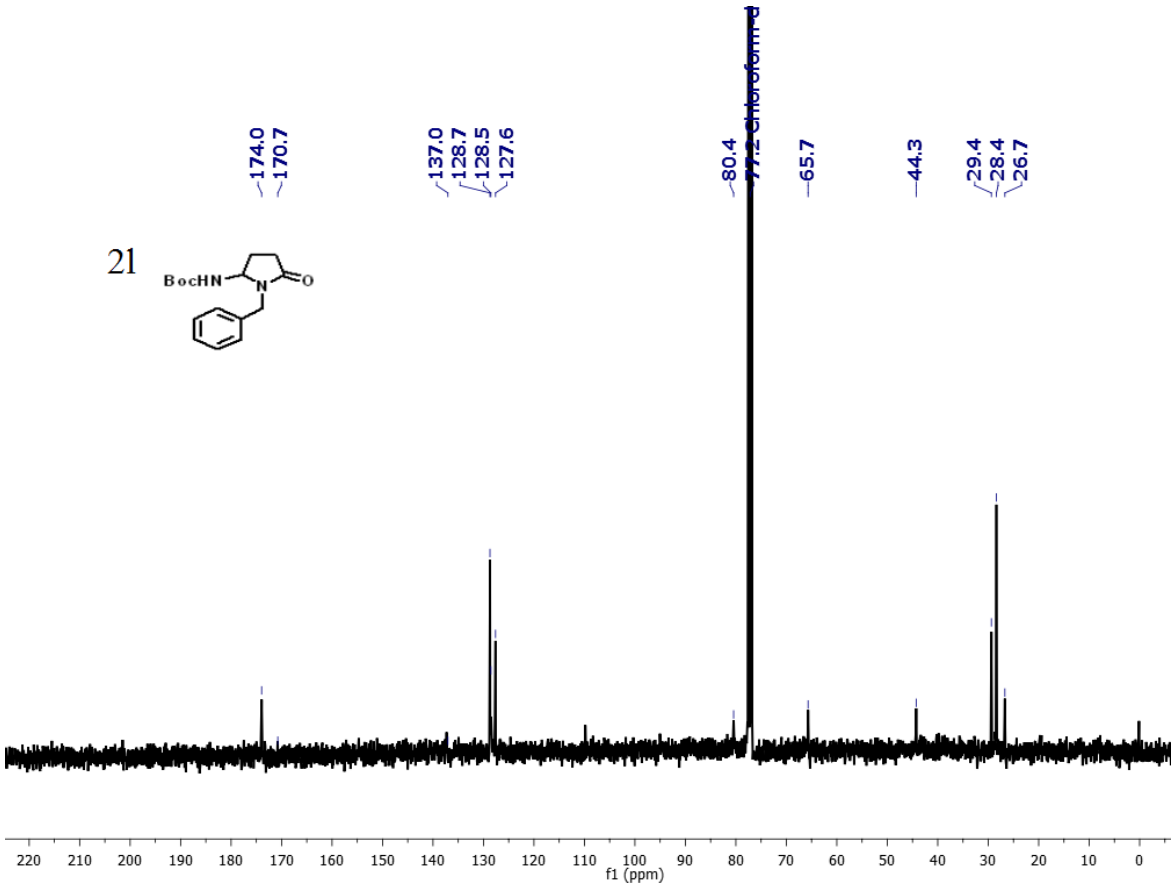
21
BocHN
174.0
170.7
137.0
128.7
128.5
127.6
80.4
77.2 Chloroform-d
65.7
44.3
29.4
28.4
26.7
f1 (ppm)

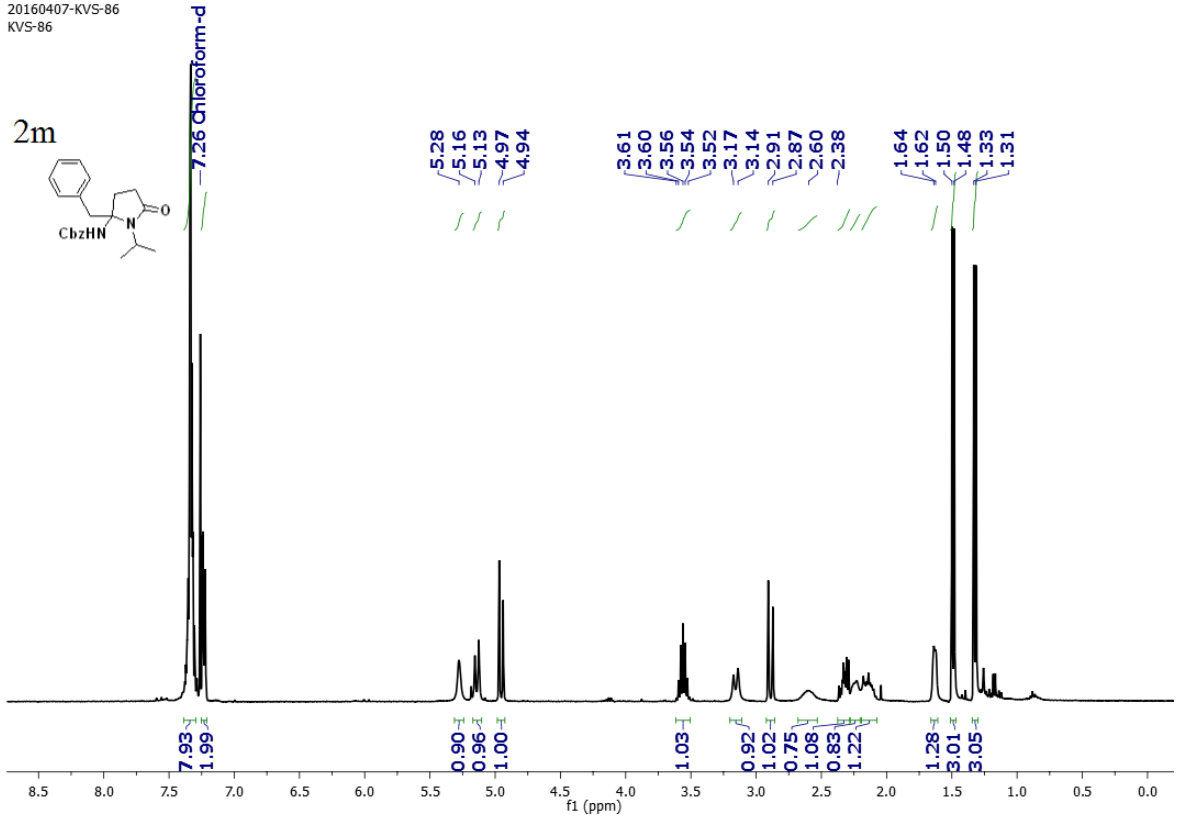
20160407-KVS-86
KVS-86
2m
CbzHN
7.26 Chloroform-d
5.28
5.16
5.13
4.97
4.94
3.61
3.60
3.56
3.54
3.52
3.17
3.14
2.91
2.87
2.60
2.38
1.64
1.62
1.50
1.48
1.33
1.31
7.93
1.99
0.90
0.96
1.00
1.03
0.92
1.02
0.75
1.08
0.83
1.22
1.28
3.01
3.05
f1 (ppm)

20160411-KVS-86C
KVS-86C

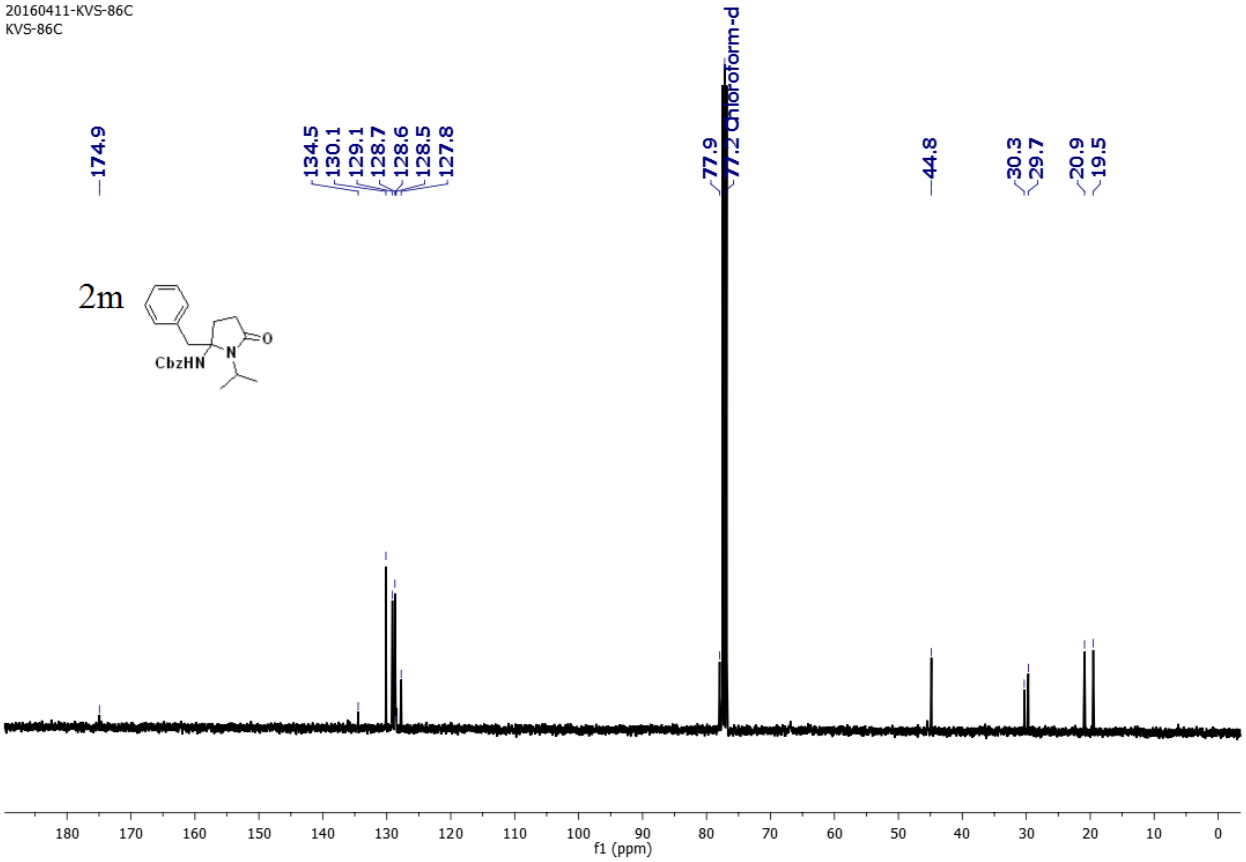

2m

20160121-KVS-76B
KVS-76B

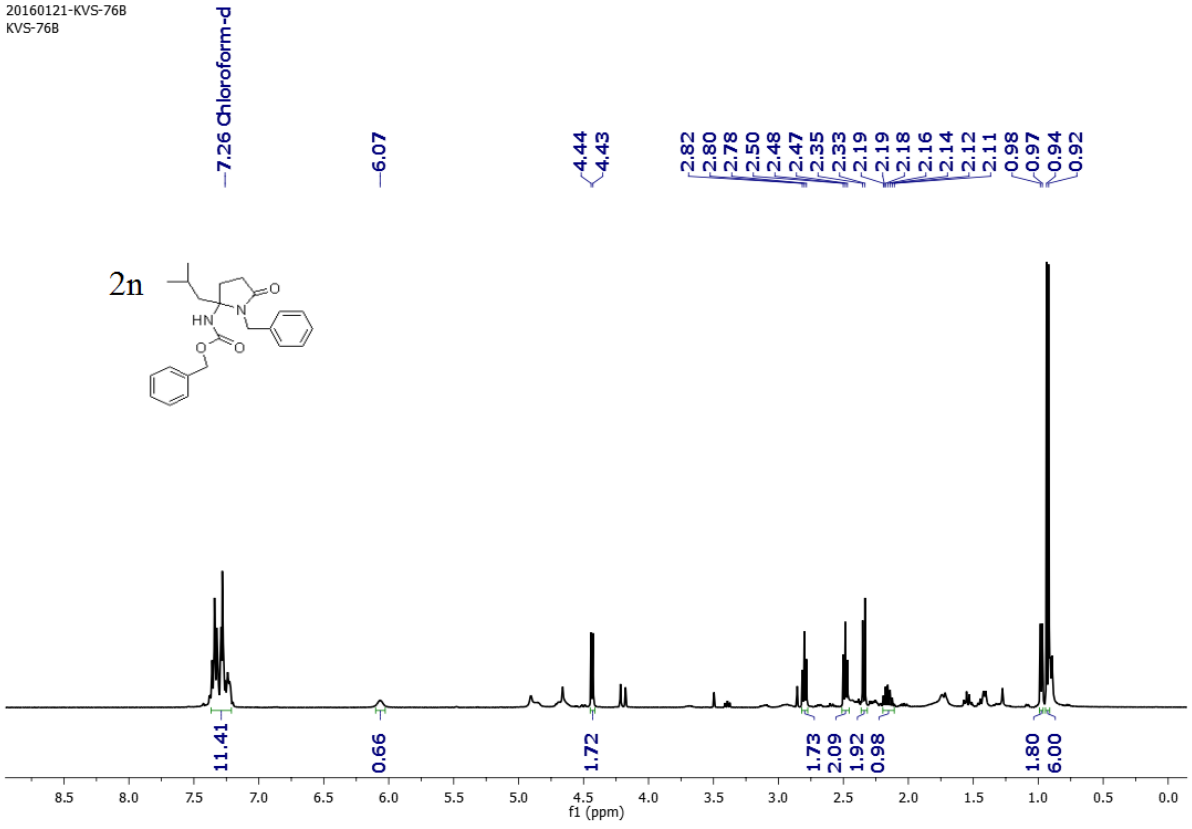

2n

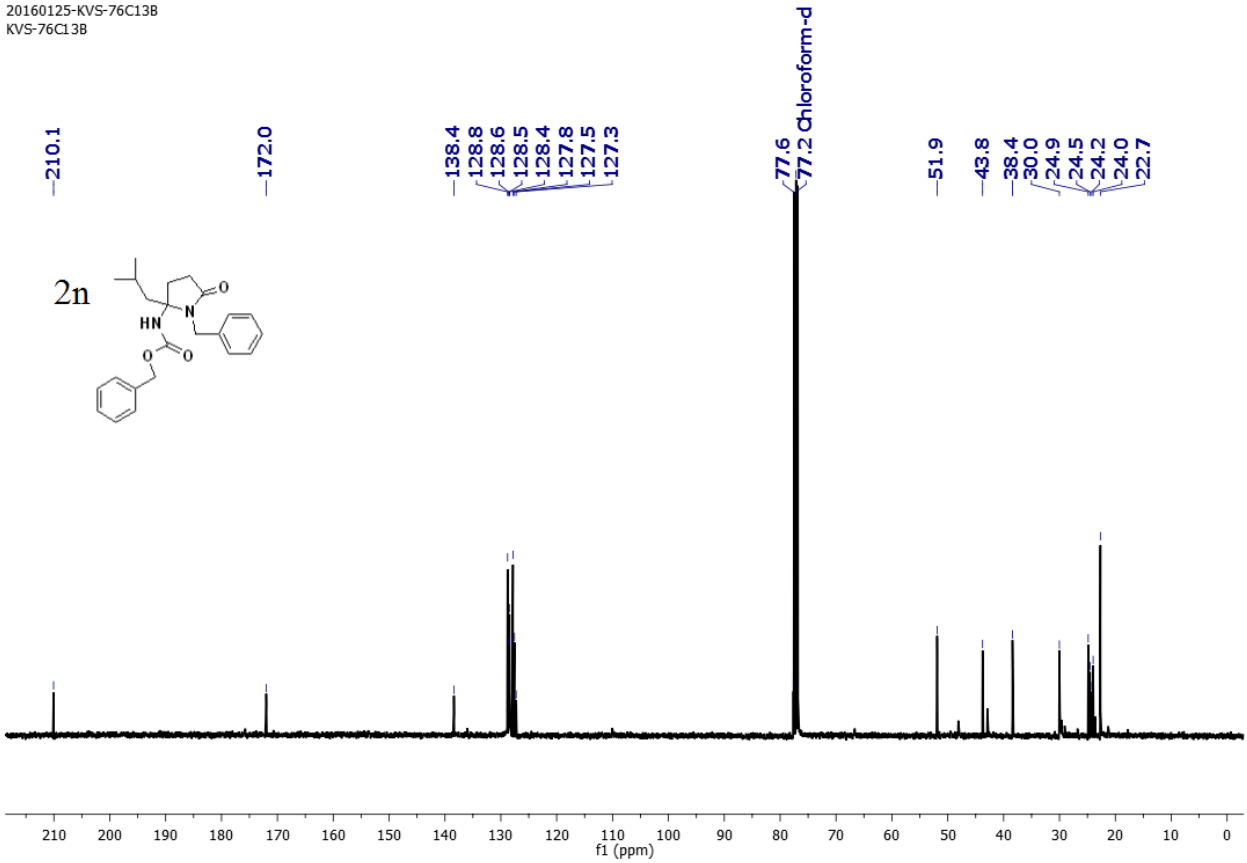
20160125-KVS-76C13B
KVS-76C13B
210.1
172.0
138.4
128.8
128.6
128.5
128.4
127.8
127.5
127.3
77.6
77.2 Chloroform-d
51.9
43.8
38.4
30.0
24.9
24.5
24.2
24.0
22.7
2n
f1 (ppm)

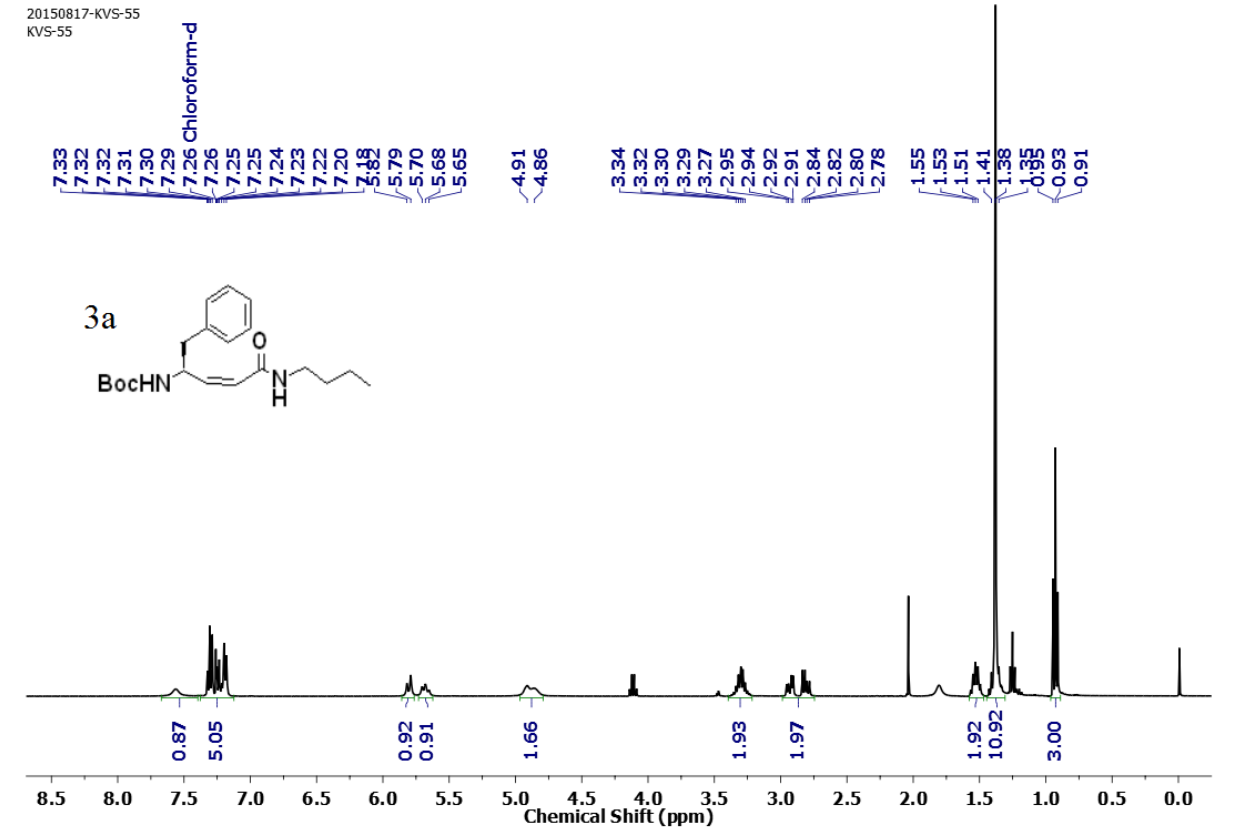
20150817-KVS-55
KVS-55
Chloroform-d
7.33
7.32
7.32
7.31
7.30
7.29
7.26
7.26
7.25
7.25
7.24
7.23
7.22
7.20
5.79
5.70
5.68
5.65
4.91
4.86
3.34
3.32
3.30
3.29
3.27
2.95
2.94
2.92
2.91
2.84
2.82
2.80
2.78
1.55
1.53
1.51
1.41
1.38
0.93
0.91
3a
BocHN
0.87
5.05
0.92
0.91
1.66
1.93
1.97
1.92
10.92
3.00
Chemical Shift (ppm)

20150818-KVS-55C
KVS-55C

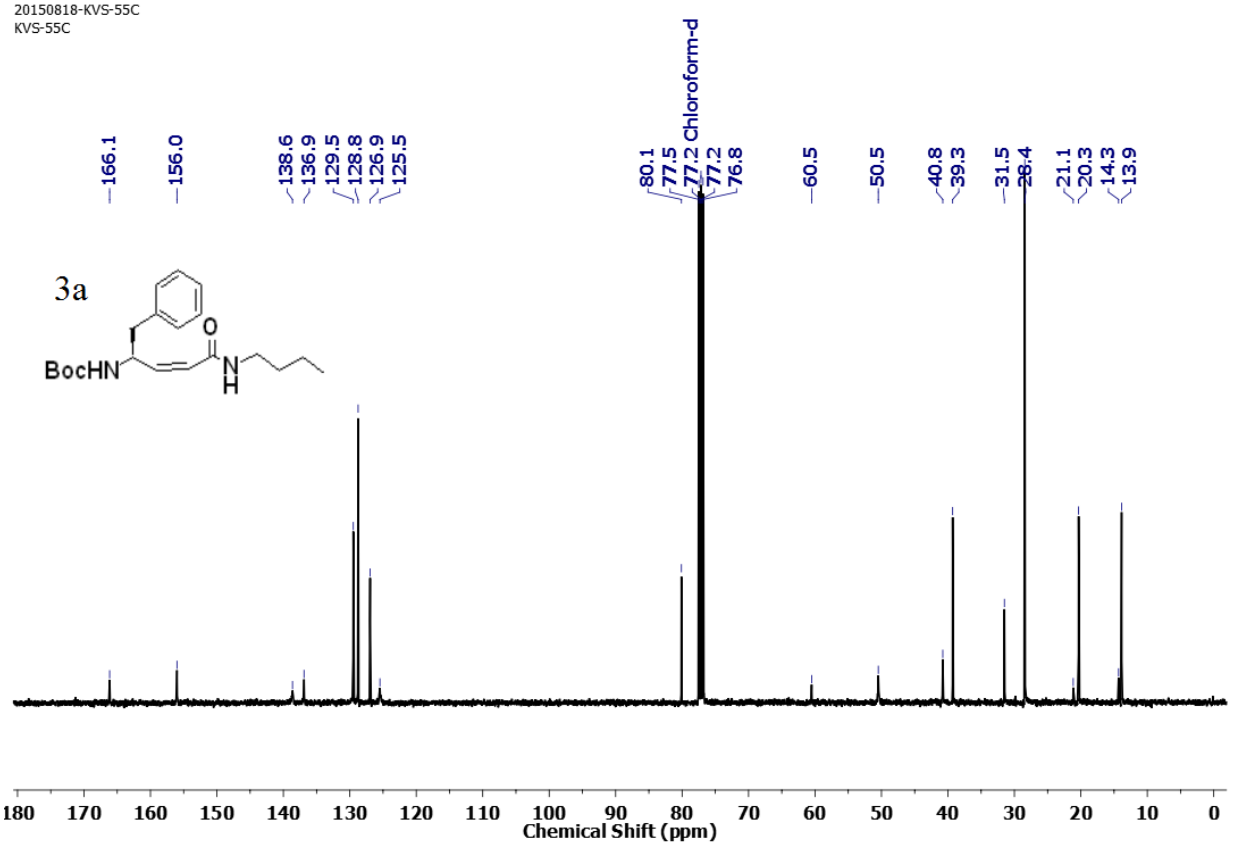

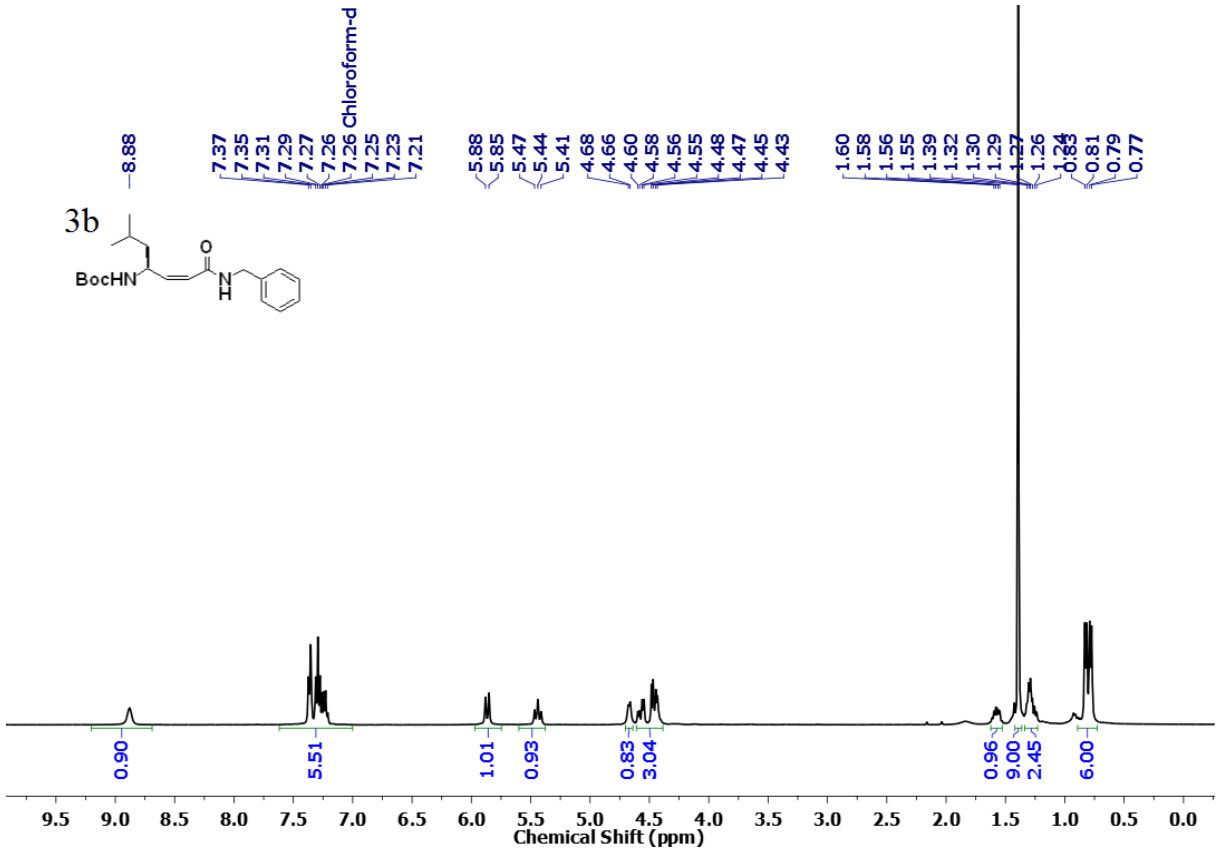

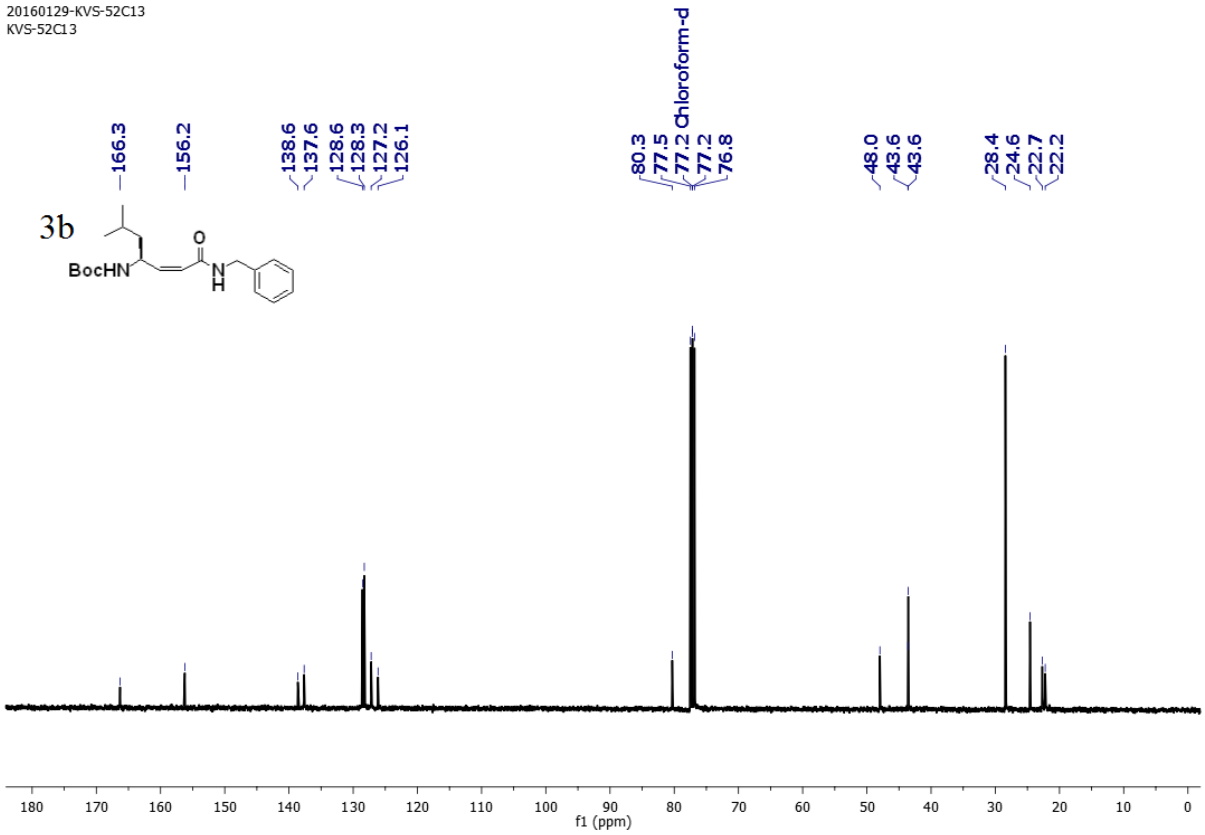
20160129-KVS-52C13
KVS-52C13
166.3
156.2
138.6
137.6
128.6
128.3
127.2
126.1
80.3
77.5
77.2 Chloroform-d
77.2
76.8
48.0
43.6
43.6
28.4
24.6
22.7
22.2
3b
BocHN
O
N
H
f1 (ppm)

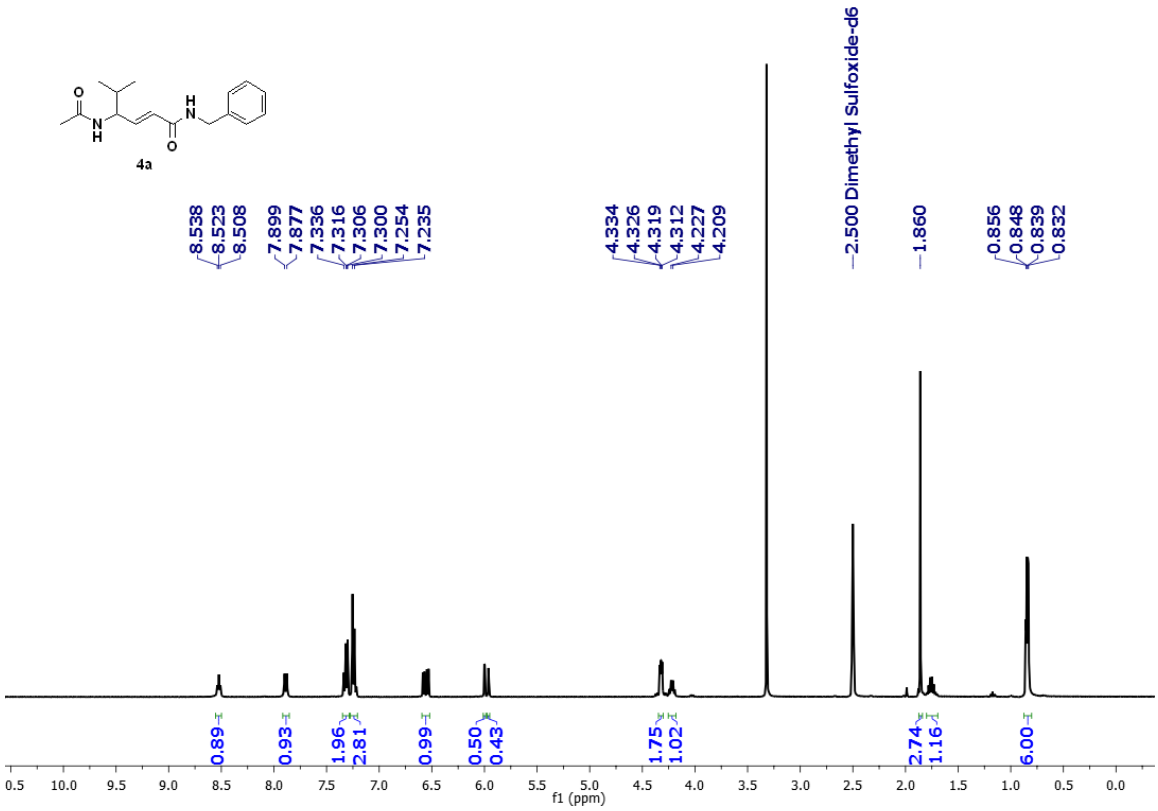
4a
8.538
8.523
8.508
7.899
7.877
7.336
7.316
7.306
7.300
7.254
7.235
4.334
4.326
4.319
4.312
4.227
4.209
2.500 Dimethyl Sulfoxide-d6
1.860
0.856
0.848
0.839
0.832
0.89
0.93
1.96
2.81
0.99
0.50
0.43
1.75
1.02
2.74
1.16
6.00
f1 (ppm)

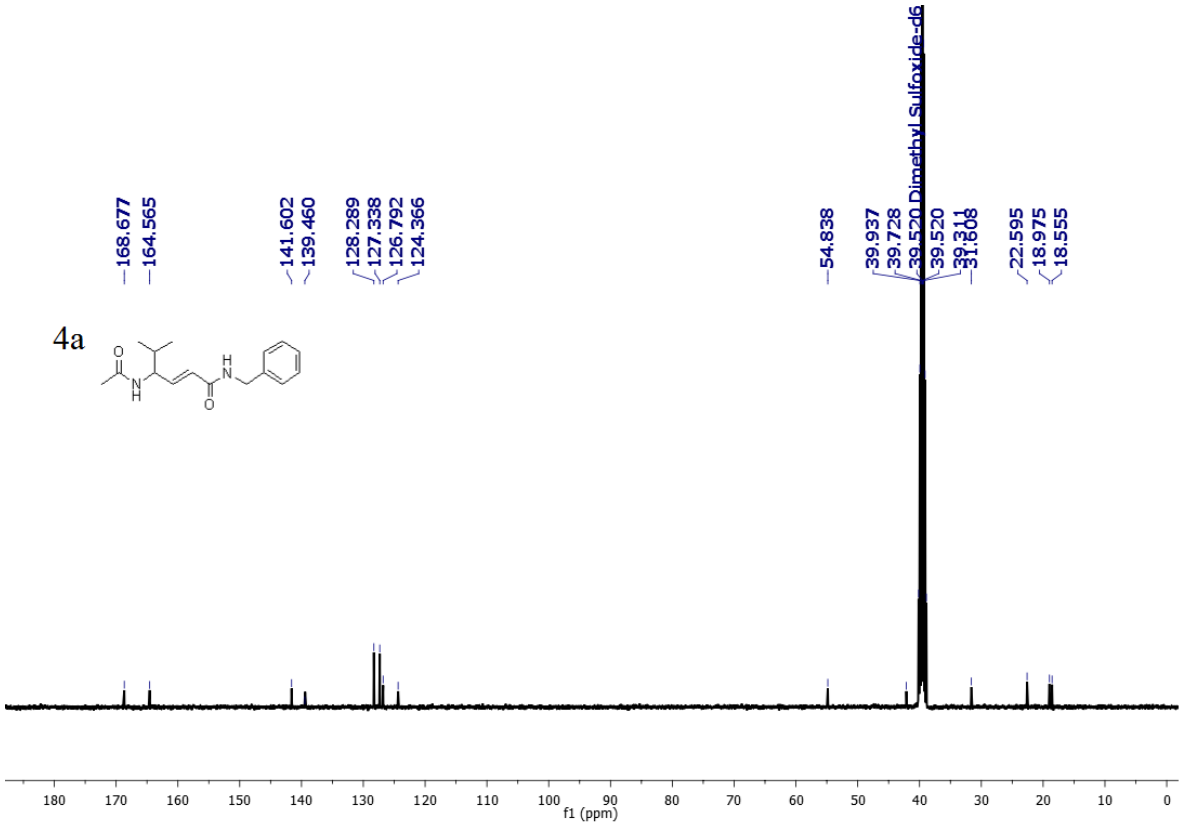
168.677
164.565
141.602
139.460
128.289
127.338
126.792
124.366
54.838
39.937
39.728
39.520 Dimethyl Sulfoxide-d6
39.520
39.311
31.808
22.595
18.975
18.555
4a
f1 (ppm)

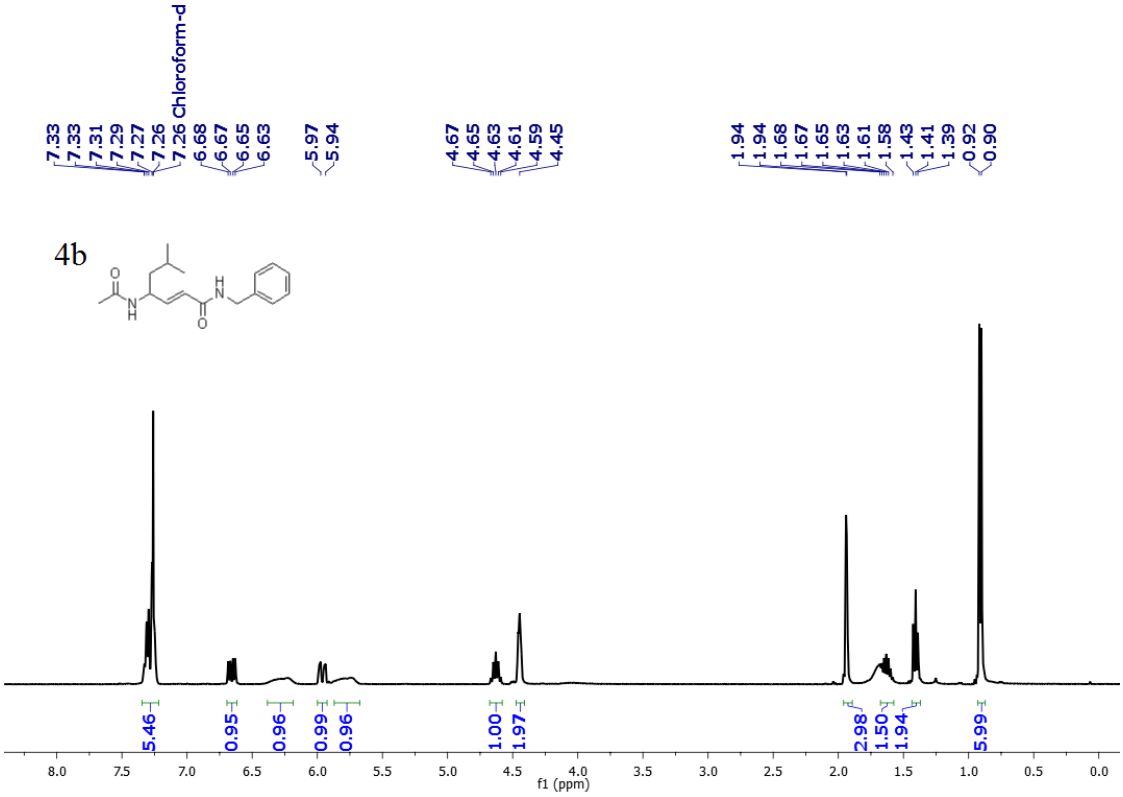
7.33
7.33
7.31
7.29
7.27
7.26
7.26 Chloroform-d
6.68
6.67
6.65
6.63
5.97
5.94
4.67
4.65
4.63
4.61
4.59
4.45
1.94
1.94
1.68
1.67
1.65
1.63
1.61
1.58
1.43
1.41
1.39
0.92
0.90
4b
5.46
0.95
0.96
0.99
0.96
1.00
1.97
2.98
1.50
1.94
5.99
f1 (ppm)

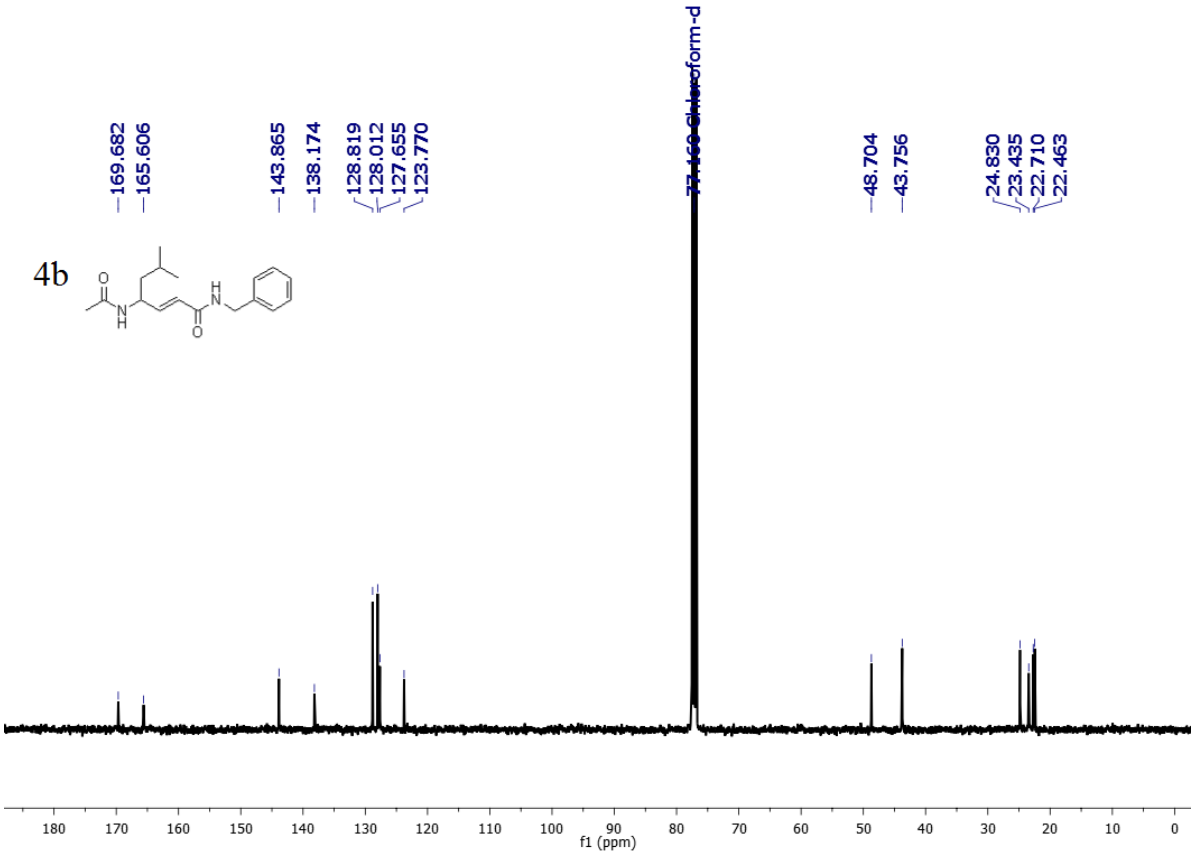
169.682
165.606
143.865
138.174
128.819
128.012
127.655
123.770
77.160 Chloroform-d
48.704
43.756
24.830
23.435
22.710
22.463
4b
f1 (ppm)

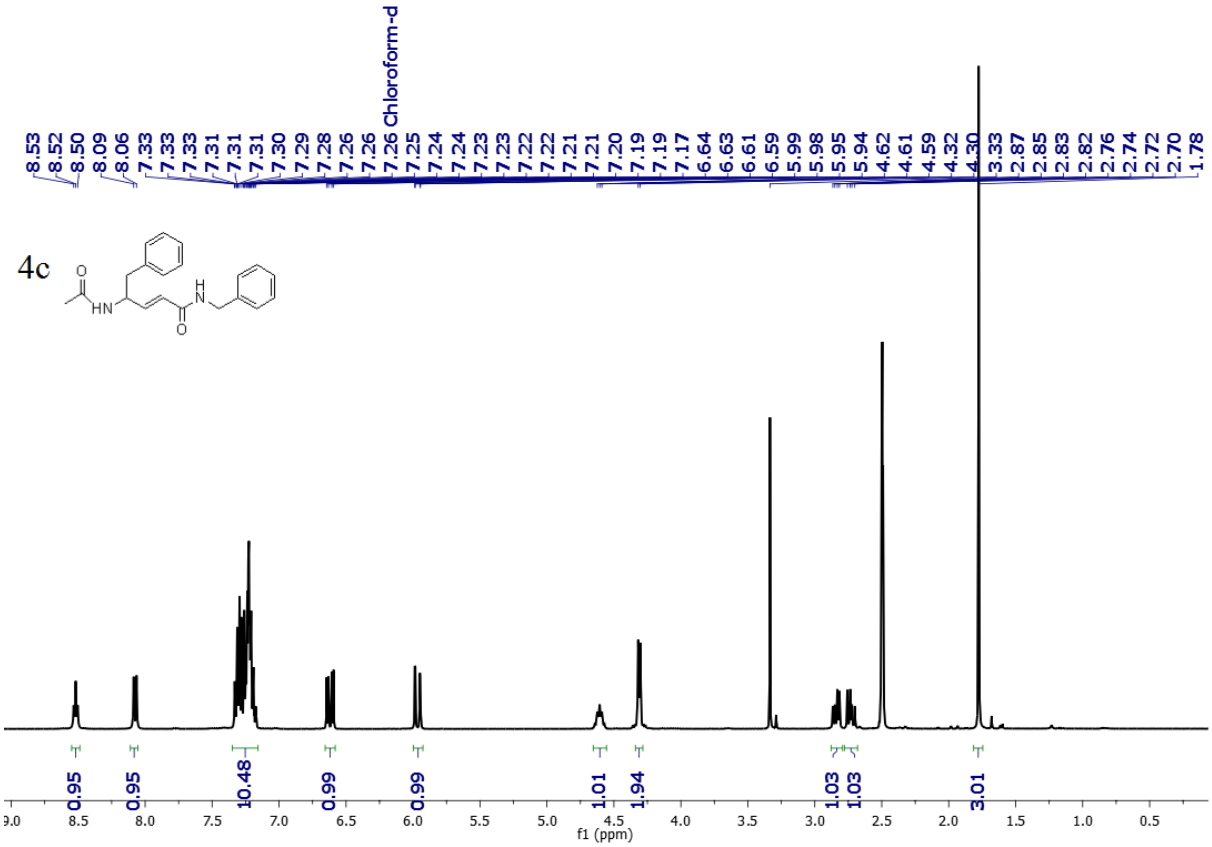
Chloroform-d
8.53
8.52
8.50
8.09
8.06
7.33
7.33
7.33
7.31
7.31
7.31
7.30
7.29
7.28
7.26
7.26
7.26
7.25
7.24
7.24
7.23
7.23
7.22
7.22
7.21
7.21
7.20
7.19
7.19
7.17
6.64
6.63
6.61
6.59
5.99
5.98
5.95
5.94
4.62
4.61
4.59
4.32
4.30
3.33
2.87
2.85
2.83
2.82
2.76
2.74
2.72
2.70
1.78
4c
0.95
0.95
10.48
0.99
0.99
1.01
1.94
1.03
1.03
3.01
f1 (ppm)

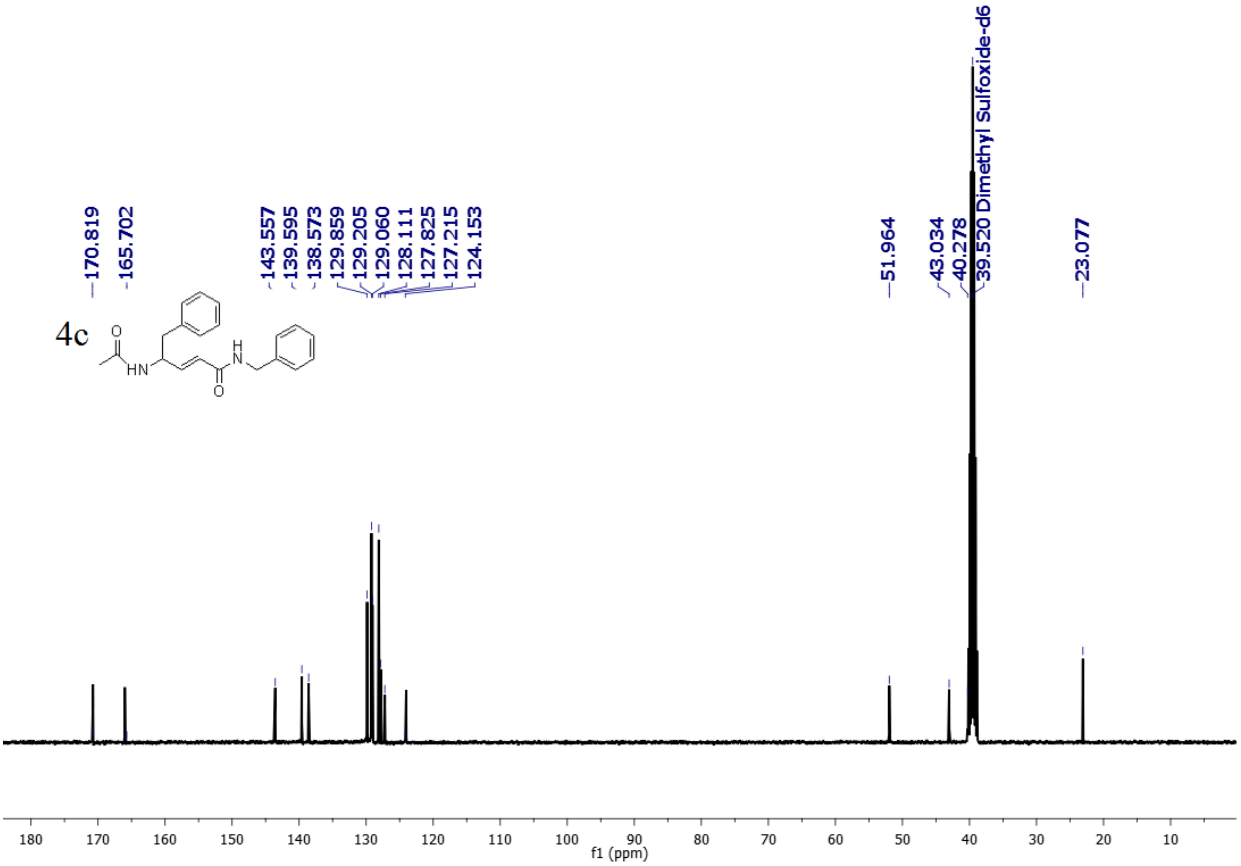
170.819
165.702
143.557
139.595
138.573
129.859
129.205
129.060
128.111
127.825
127.215
124.153
51.964
43.034
40.278
39.520 Dimethyl Sulfoxide-d6
23.077
4c
f1 (ppm)

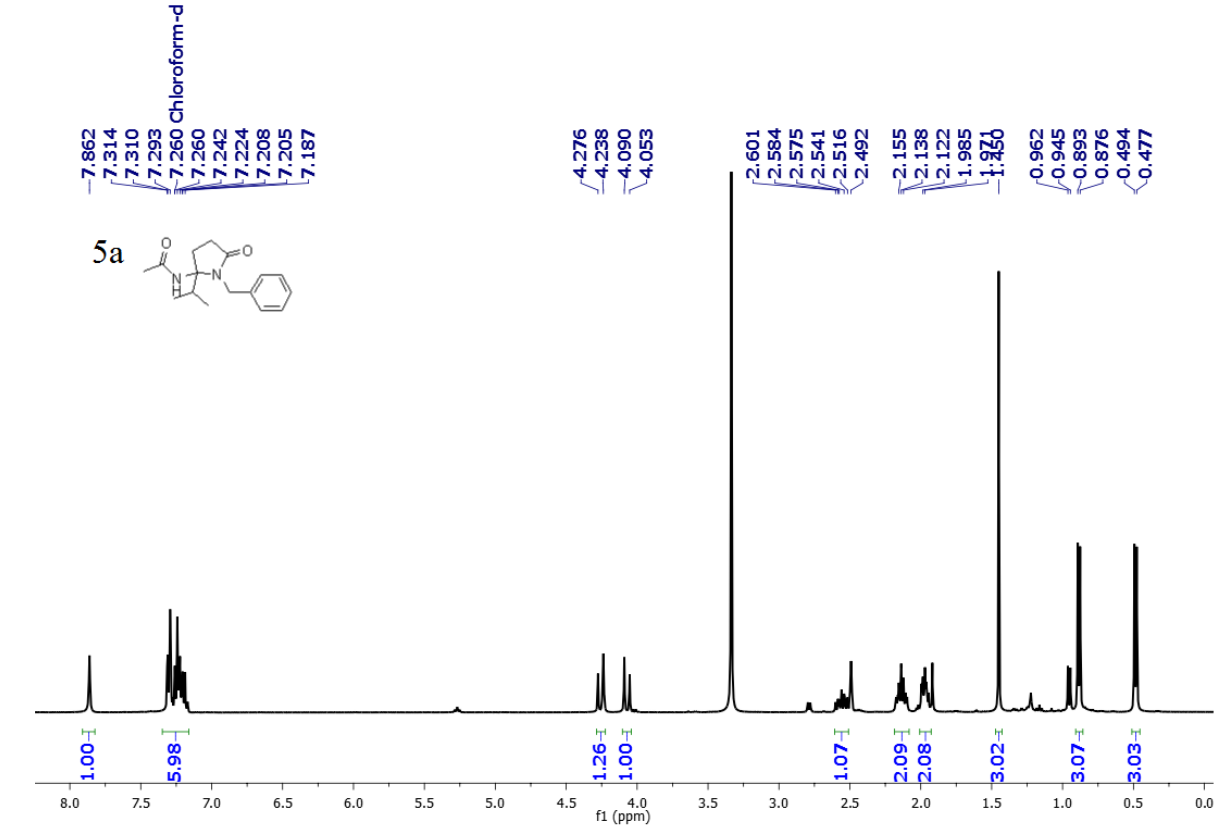
7.862
7.314
7.310
7.293
7.260 Chloroform-d
7.260
7.242
7.224
7.208
7.205
7.187
4.276
4.238
4.090
4.053
2.601
2.584
2.575
2.541
2.516
2.492
2.155
2.138
2.122
1.985
1.971
1.450
0.962
0.945
0.893
0.876
0.494
0.477
5a
1.00
5.98
1.26
1.00
1.07
2.09
2.08
3.02
3.07
3.03
f1 (ppm)

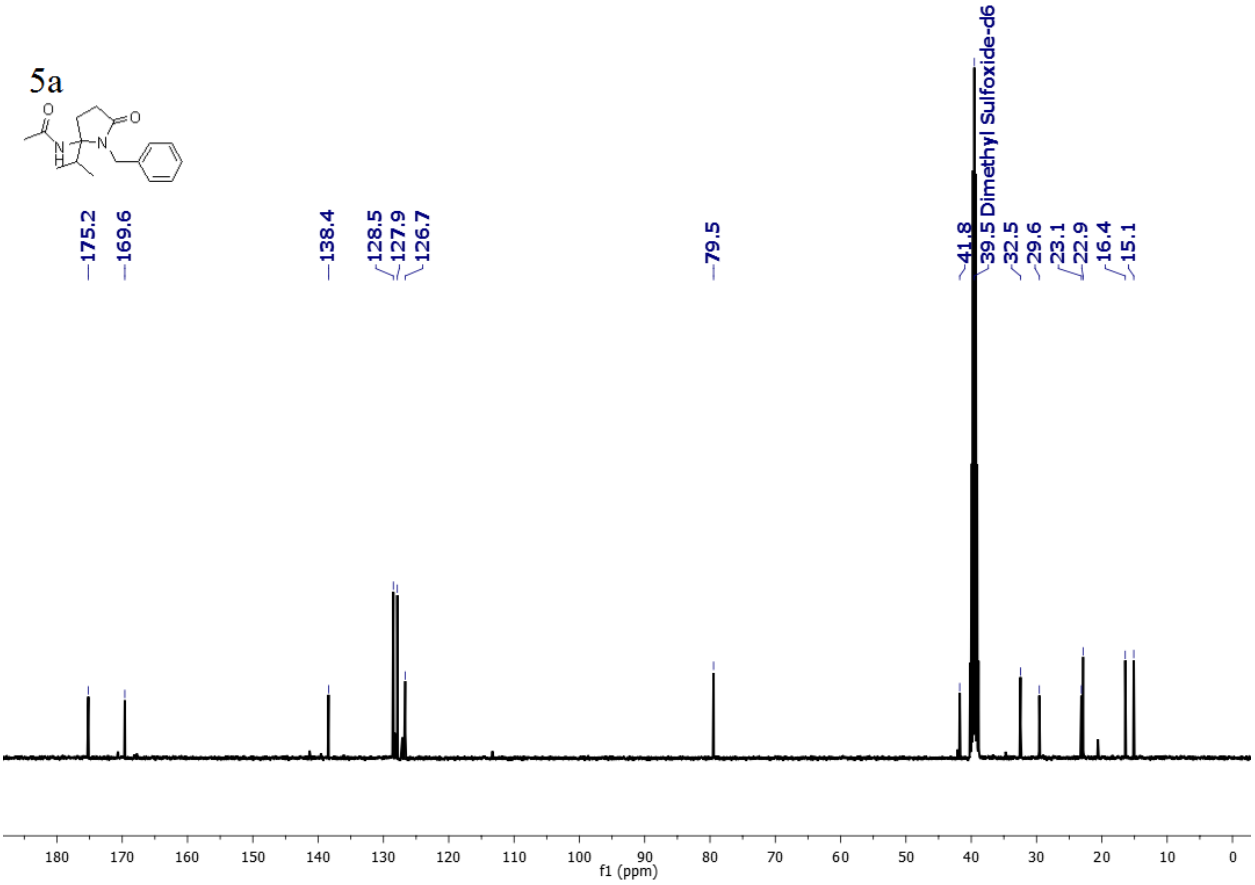
5a
175.2
169.6
138.4
128.5
127.9
126.7
79.5
41.8
39.5 Dimethyl Sulfoxide-d6
32.5
29.6
23.1
22.9
16.4
15.1
f1 (ppm)

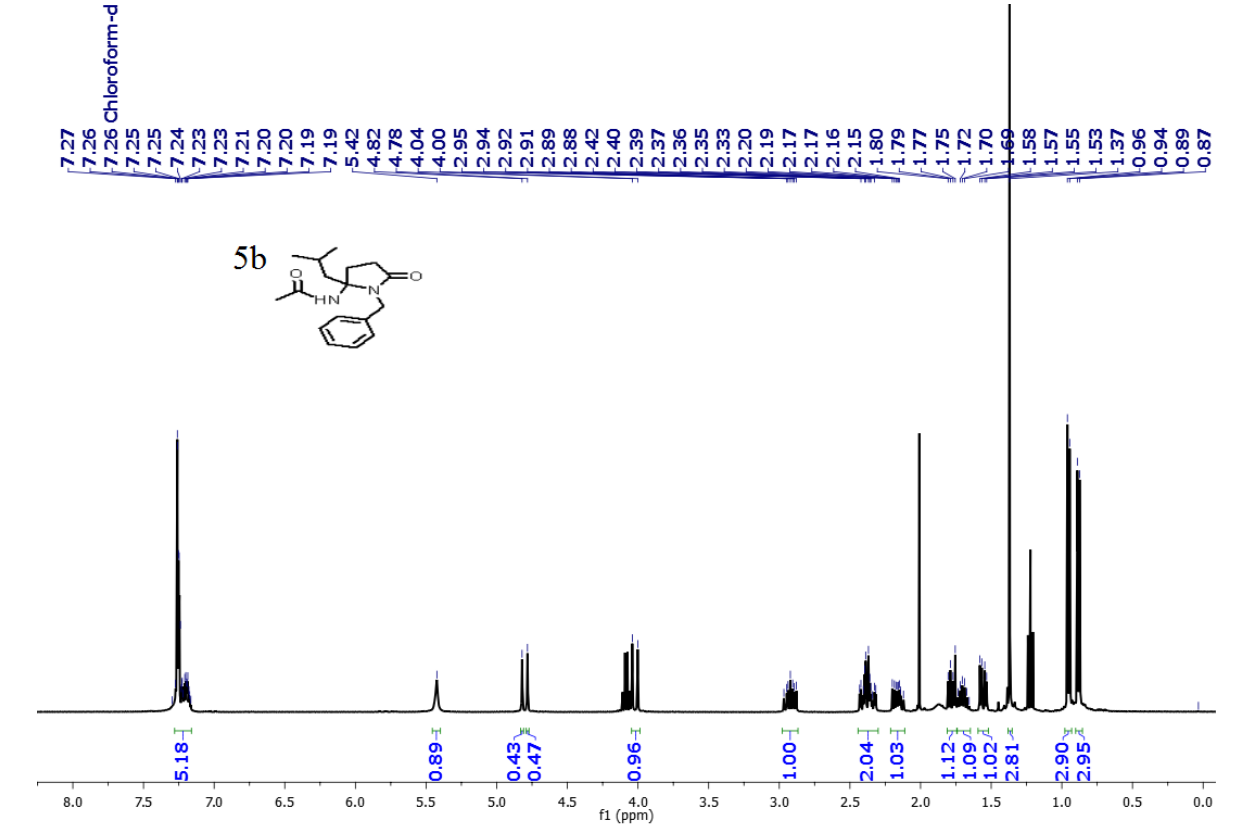
7.27
7.26 Chloroform-d
7.26
7.25
7.25
7.24
7.23
7.23
7.21
7.20
7.20
7.19
7.19
5.42
4.82
4.78
4.04
4.00
2.95
2.94
2.92
2.91
2.89
2.88
2.42
2.40
2.39
2.37
2.36
2.35
2.33
2.20
2.19
2.17
2.17
2.16
2.15
1.80
1.79
1.77
1.75
1.72
1.70
1.69
1.58
1.57
1.55
1.53
1.37
0.96
0.94
0.89
0.87
5b
5.18
0.89
0.43
0.47
0.96
1.00
2.04
1.03
1.12
1.09
1.02
2.81
2.90
2.95
f1 (ppm)

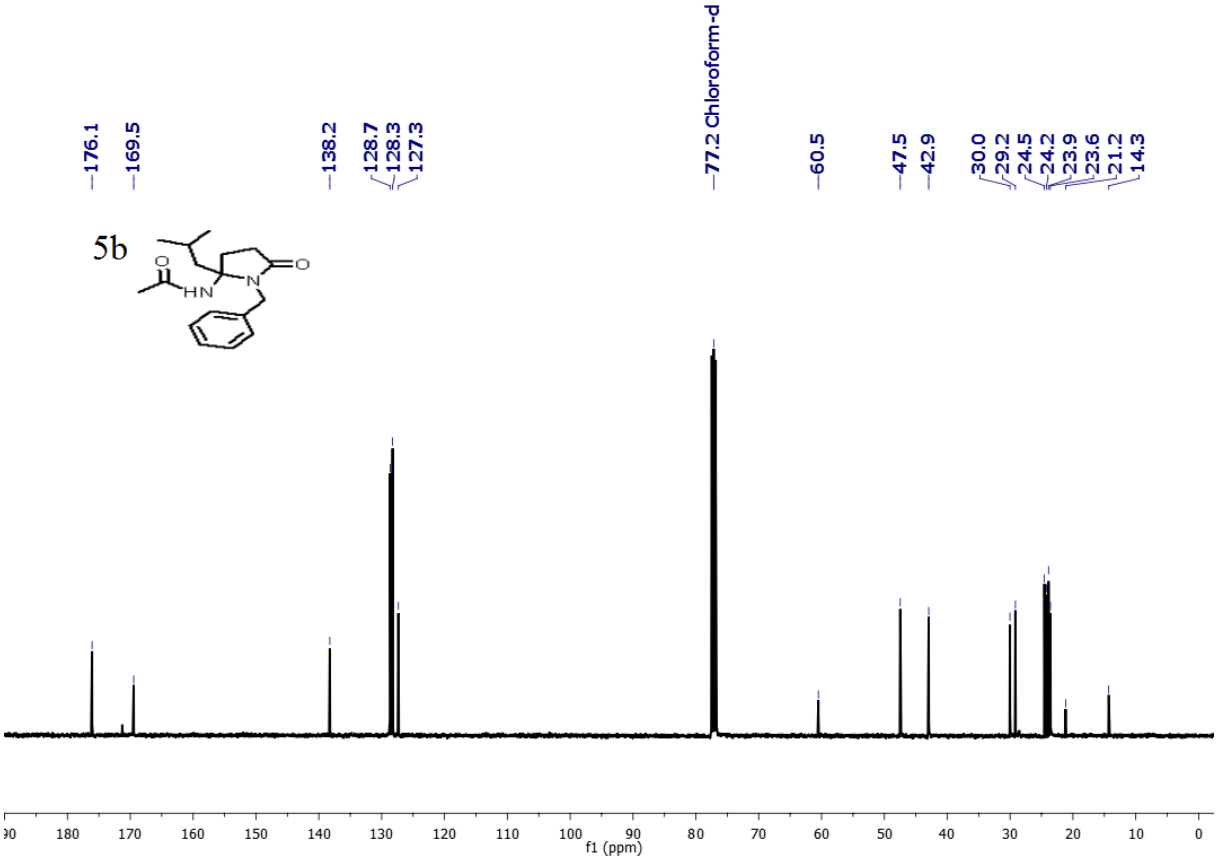
176.1
169.5
138.2
128.7
128.3
127.3
77.2 Chloroform-d
60.5
47.5
42.9
30.0
29.2
24.5
24.2
23.9
23.6
21.2
14.3
5b
f1 (ppm)

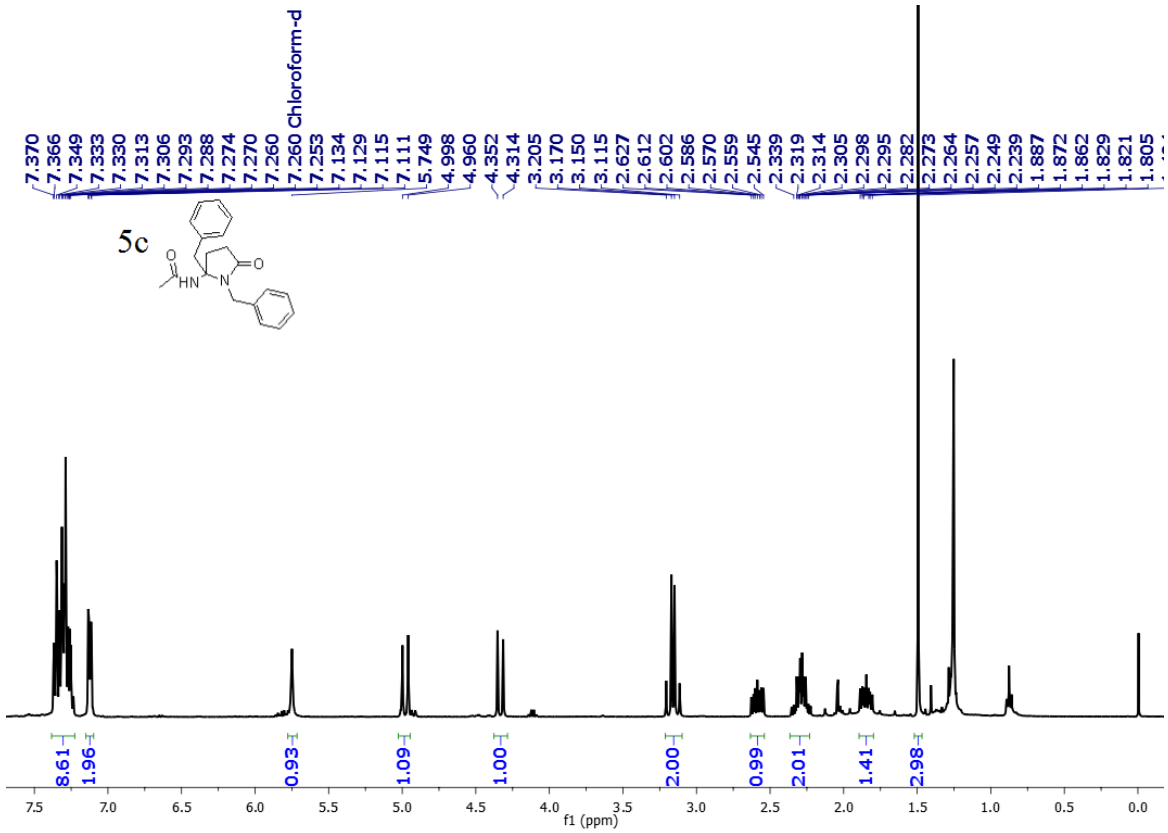
7.260 Chloroform-d
5c
8.61
1.96
0.93
1.09
1.00
2.00
0.99
2.01
1.41
2.98
f1 (ppm)

5c

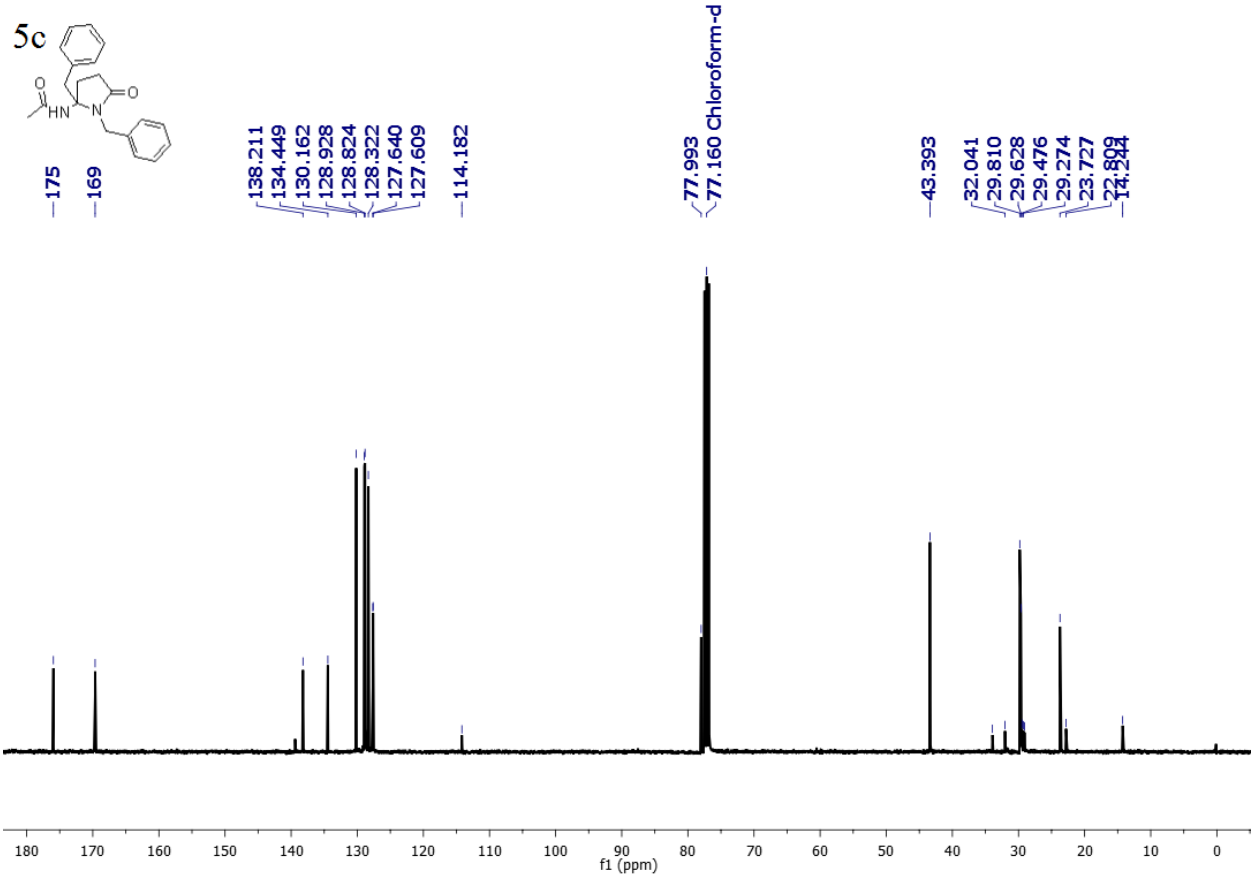
175
169
138.211
134.449
130.162
128.928
128.824
128.322
127.640
127.609
114.182
77.993
77.160 Chloroform-d
43.393
32.041
29.810
29.628
29.476
29.274
23.727
22.809
14.244
f1 (ppm)

3j

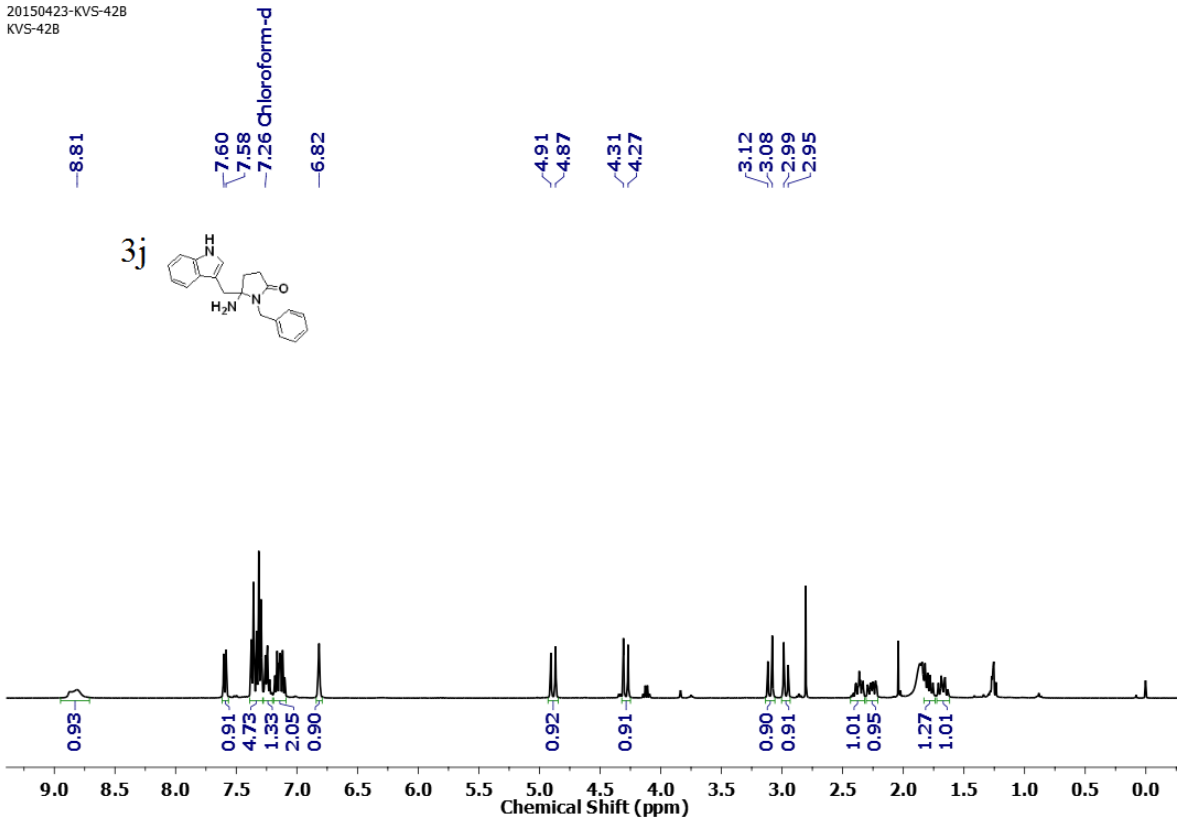
20150423-KVS-42B
KVS-42B
8.81
7.60
7.58
7.26 Chloroform-d
6.82
4.91
4.87
4.31
4.27
3.12
3.08
2.99
2.95
0.93
0.91
4.73
1.33
2.05
0.90
0.92
0.91
0.90
0.91
1.01
0.95
1.27
1.01
Chemical Shift (ppm)

20150421-KVS-42
KVS-42

174.8
139.2
136.0
128.8
128.7
128.1
127.8
127.3
127.2
123.6
122.2
119.8
118.3
111.6
109.5
79.0
77.5
77.2 Chloroform-d
77.2
76.8
42.7
38.7
34.6
34.3
29.9

3j

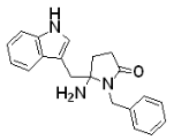

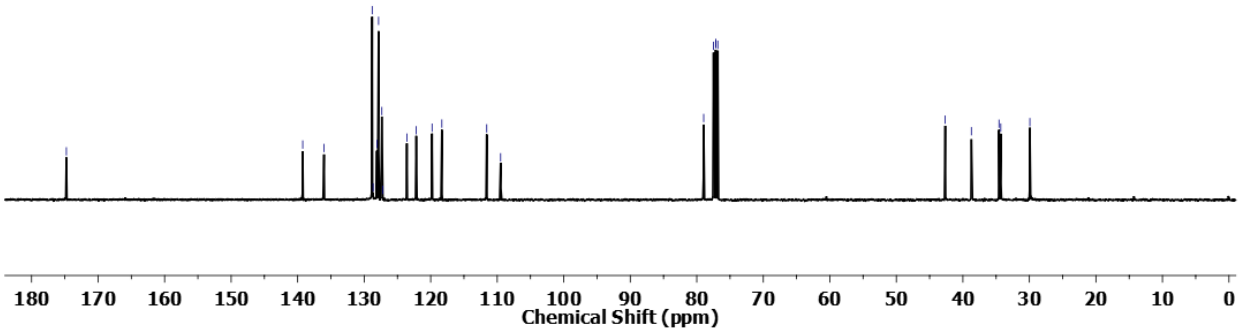

20150516-KVS-45
KVS-45

8.77
7.56
7.54
7.26 Chloroform-d
6.86
5.89
4.80
4.76
4.48
4.44
3.46
3.42
3.05
3.01
2.35
2.33
2.31
2.09
2.05
1.78
1.57
1.57
1.56
1.55
0.78
0.77
0.75

4j

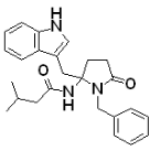

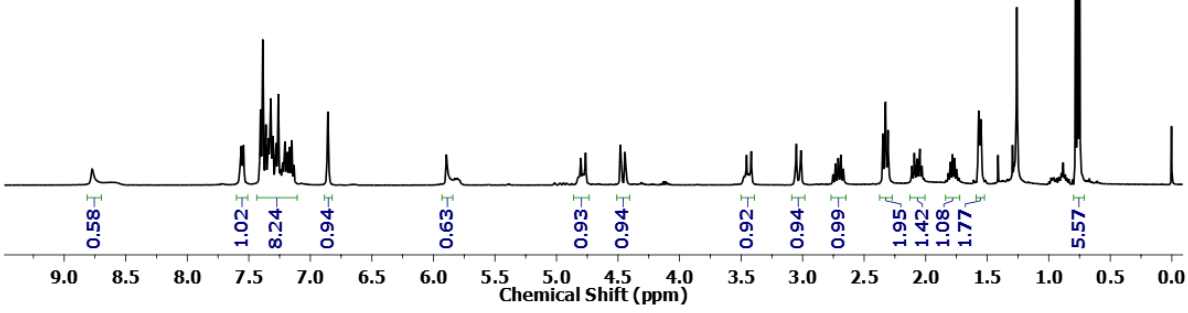

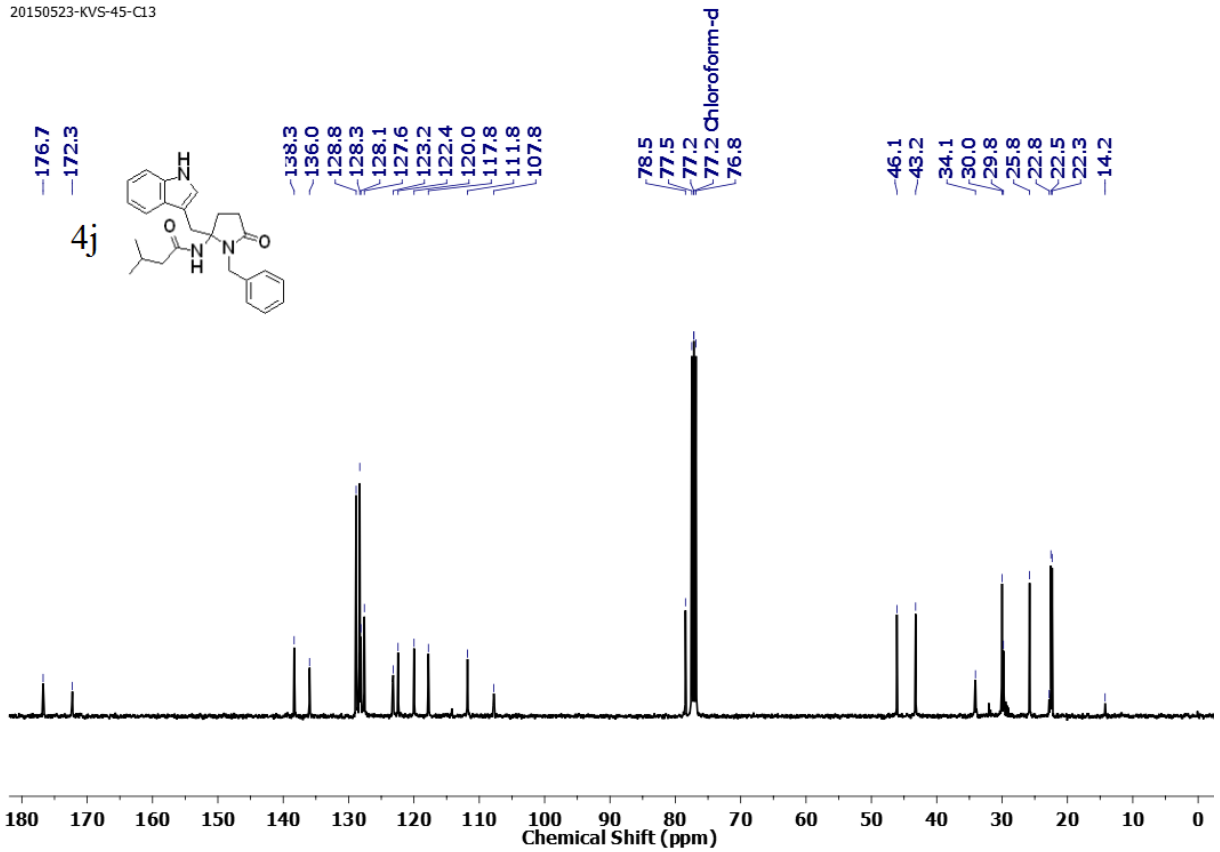
20150523-KVS-45-C13
176.7
172.3
138.3
136.0
128.8
128.3
128.1
127.6
123.2
122.4
120.0
117.8
111.8
107.8
78.5
77.5
77.2
77.2 Chloroform-d
76.8
46.1
43.2
34.1
30.0
29.8
25.8
22.8
22.5
22.3
14.2
4j
Chemical Shift (ppm)

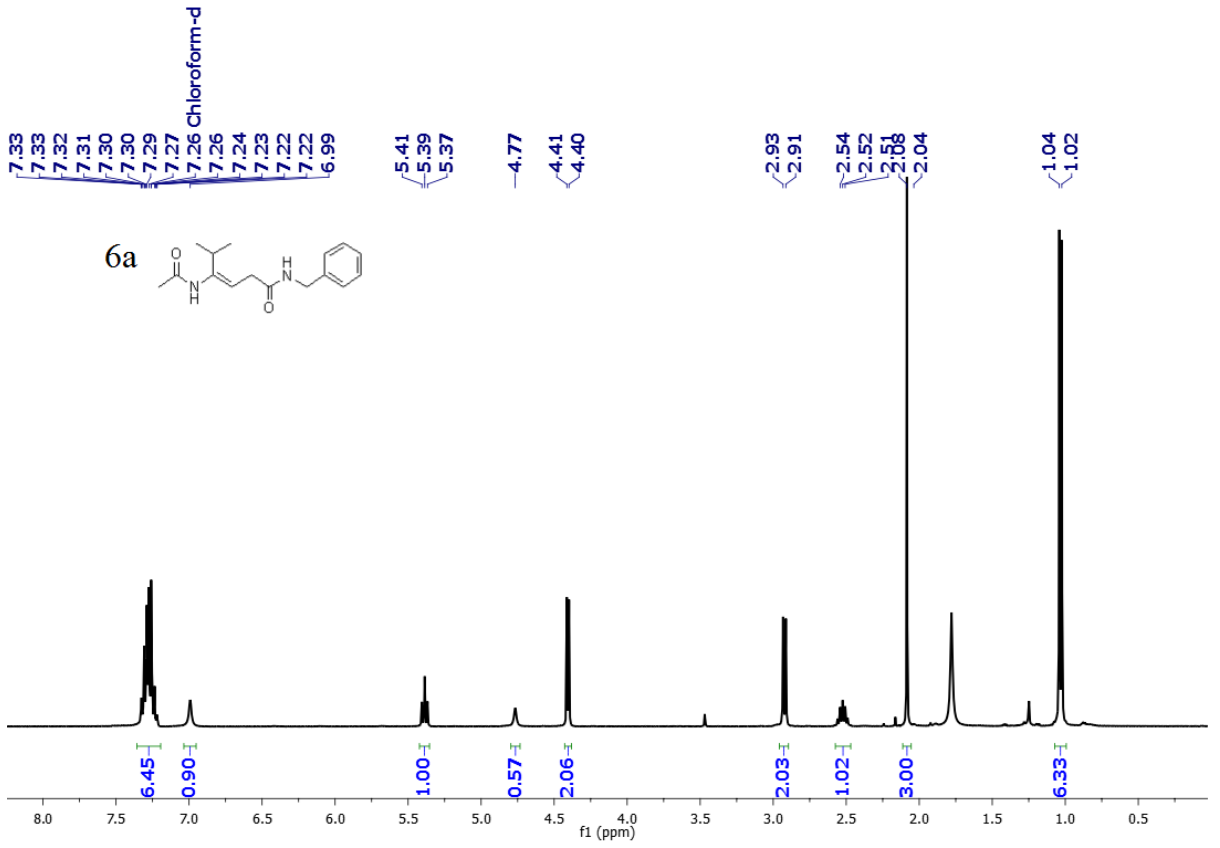
7.33
7.33
7.32
7.31
7.30
7.30
7.29
7.27
7.26 Chloroform-d
7.26
7.24
7.23
7.22
7.22
6.99
5.41
5.39
5.37
4.77
4.41
4.40
2.93
2.91
2.54
2.52
2.51
2.08
2.04
1.04
1.02
6a
6.45
0.90
1.00
0.57
2.06
2.03
1.02
3.00
6.33
f1 (ppm)

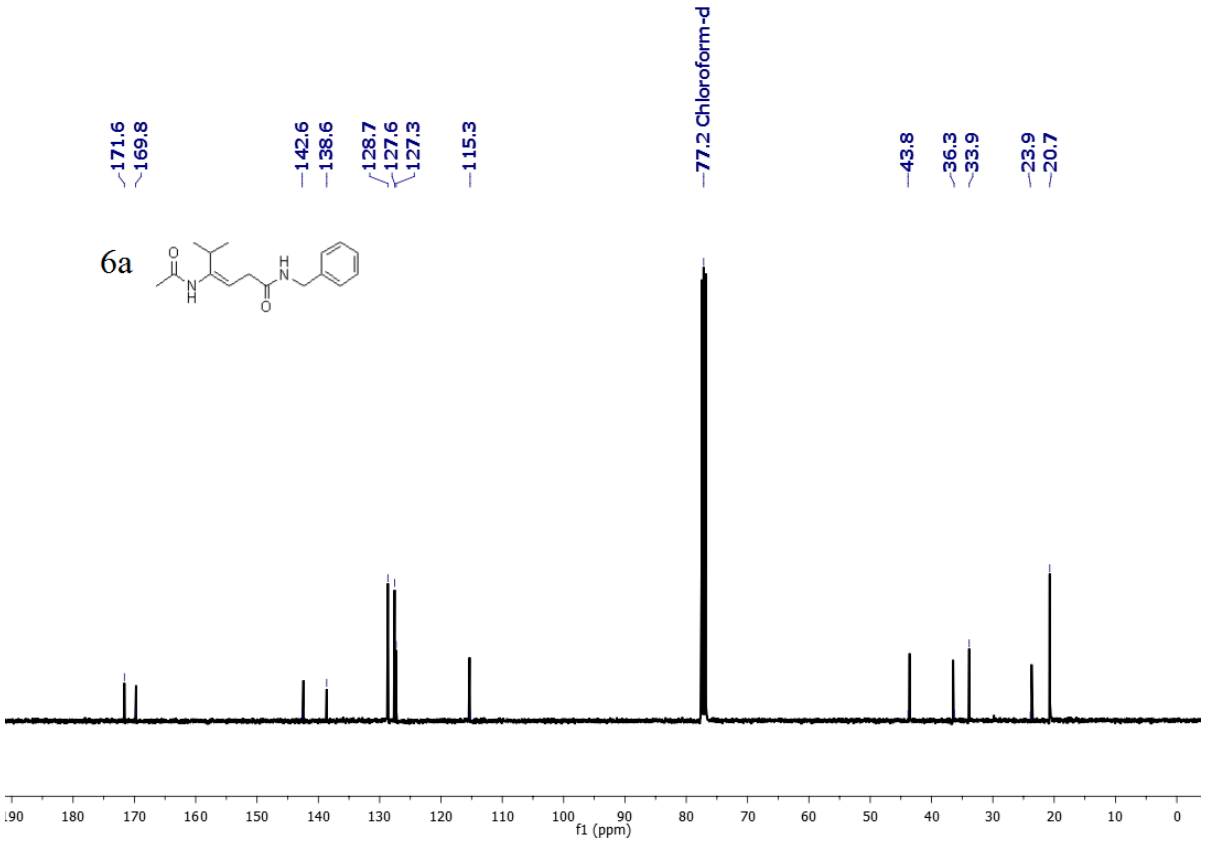
171.6
169.8
142.6
138.6
128.7
127.6
127.3
115.3
77.2 Chloroform-d
43.8
36.3
33.9
23.9
20.7
6a
f1 (ppm)

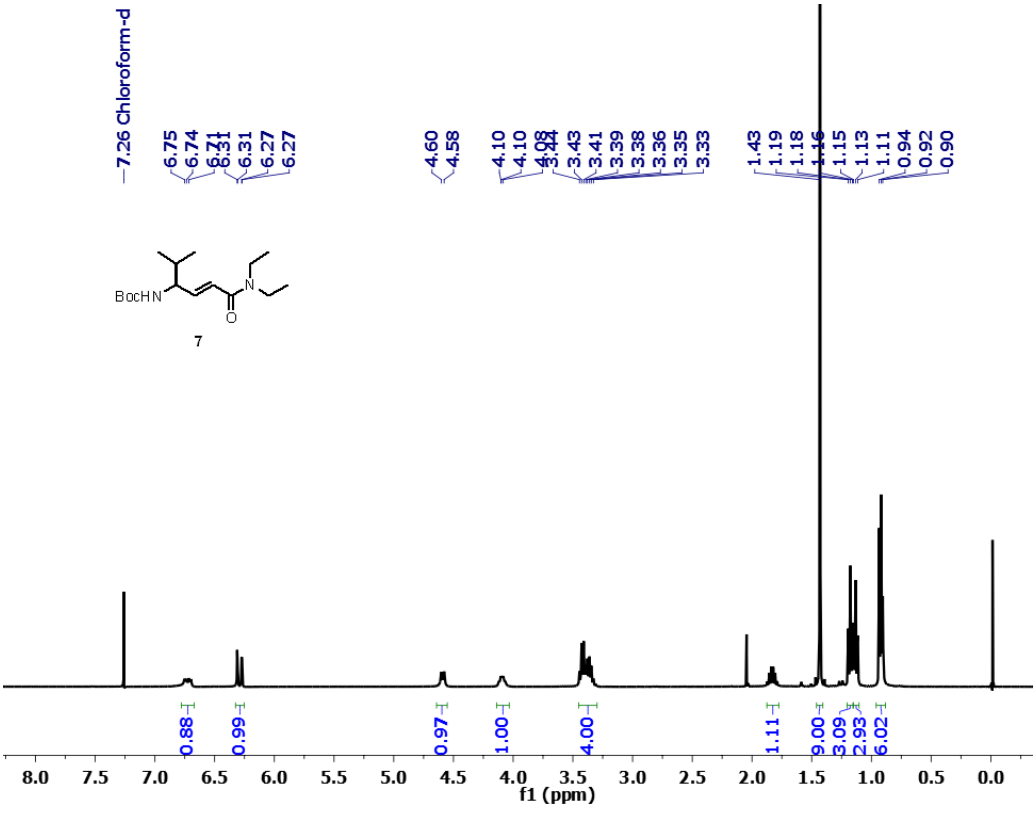
7.26 Chloroform-d
6.75
6.74
6.31
6.27
4.60
4.58
4.10
3.43
3.41
3.39
3.38
3.36
3.35
3.33
1.43
1.19
1.18
1.15
1.13
1.11
0.94
0.92
0.90
BocHN
7
0.88
0.99
0.97
1.00
4.00
1.11
9.00
3.09
2.93
6.02
f1 (ppm)

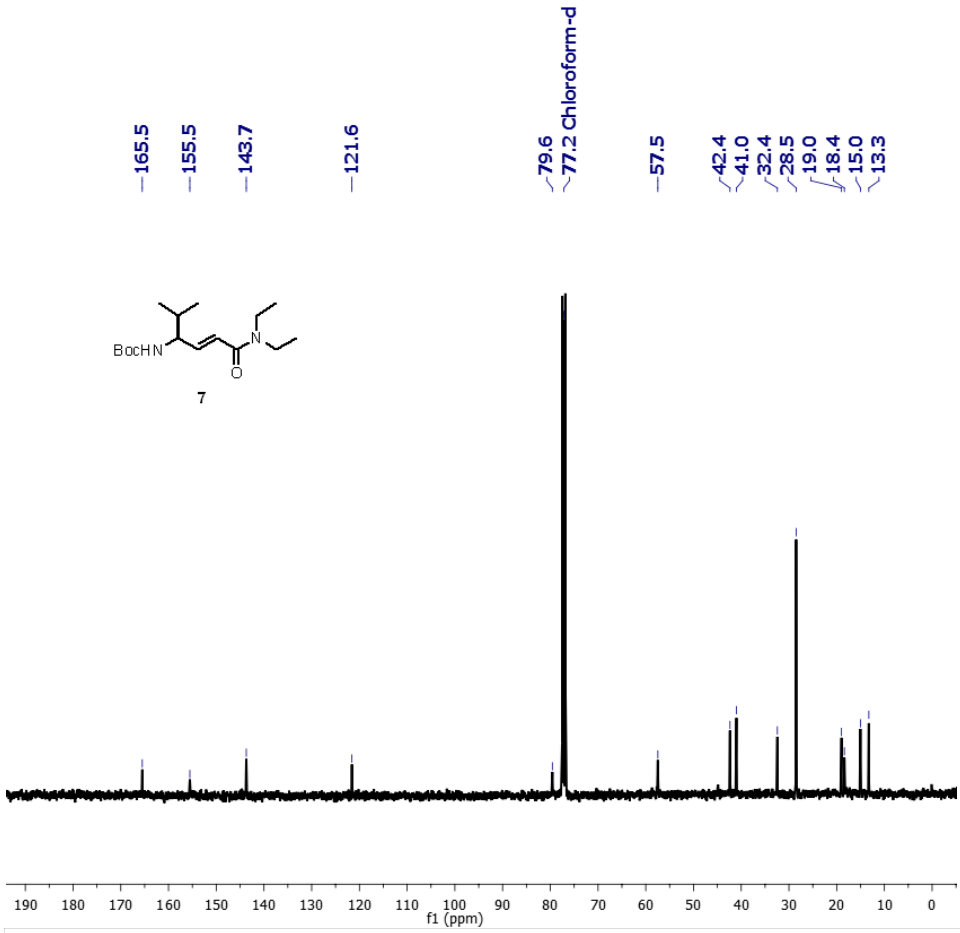
165.5
155.5
143.7
121.6
79.6
77.2 Chloroform-d
57.5
42.4
41.0
32.4
28.5
19.0
18.4
15.0
13.3
BocHN
N
O
7
f1 (ppm)

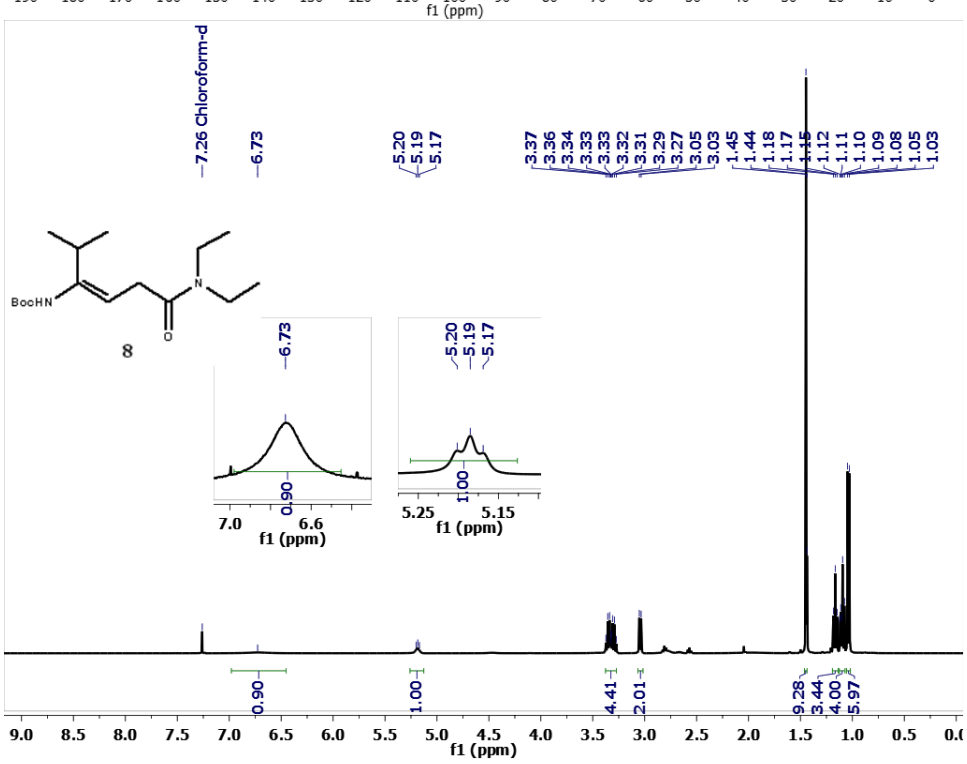
7.26 Chloroform-d
6.73
5.20
5.19
5.17
3.37
3.36
3.34
3.33
3.33
3.32
3.31
3.29
3.27
3.05
3.03
1.45
1.44
1.18
1.17
1.15
1.12
1.11
1.10
1.09
1.08
1.05
1.03
BocHN
N
O
8
0.90
1.00
4.41
2.01
9.28
3.44
4.00
5.97
f1 (ppm)

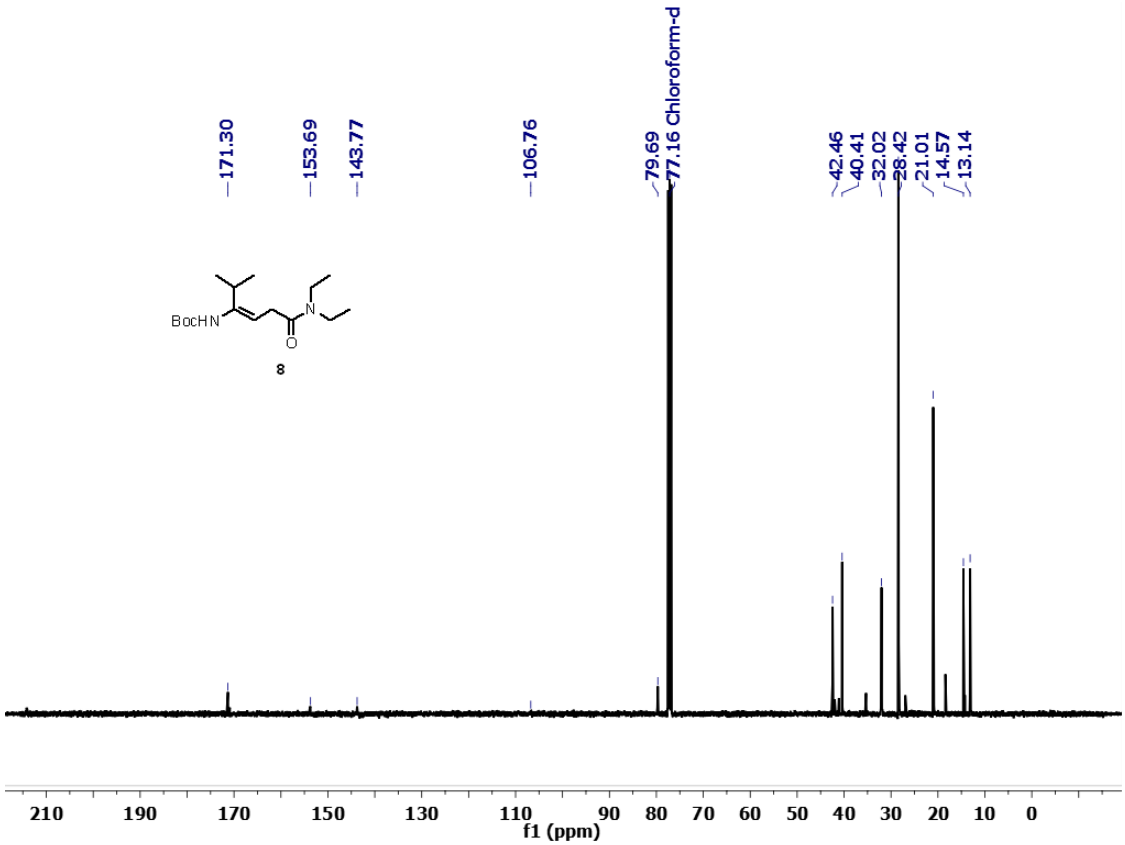
171.30
153.69
143.77
106.76
79.69
77.16 Chloroform-d
42.46
40.41
32.02
28.42
21.01
14.57
13.14
BocHN
N
O
8
210
190
170
150
130
110
90
80
70
60
50
40
30
20
10
0
f1 (ppm)

Direct Transformation of N-Protected α,β-Unsaturated γ-Amino Amides into γ-Lactams through a Base-Mediated Molecular Rearrangement

Author: Mothukuri Ganesh Kumar, Kuruva Veeresh, Sachin A. Nalawade, et al

Publication: The Journal of Organic Chemistry

Publisher: American Chemical Society

Date: Dec 1, 2019

PERMISSION/LICENSE IS GRANTED FOR YOUR ORDER AT NO CHARGE

This type of permission/license, instead of the standard Terms & Conditions, is sent to you because no fee is being charged for your order. Please note the following:

- Permission is granted for your request in both print and electronic formats, and translations.
- If figures and/or tables were requested, they may be adapted or used in part.
- Please print this page for your records and send a copy of it to your publisher/graduate school.
- Appropriate credit for the requested material should be given as follows: "Reprinted (adapted) with permission from (COMPLETE REFERENCE CITATION). Copyright (YEAR) American Chemical Society." Insert appropriate information in place of the capitalized words.
- One-time permission is granted only for the use specified in your request. No additional uses are granted (such as derivative works or other editions). For any other uses, please submit a new request.

BACK CLOSE WINDOW

CHAPTER 4

Design of β-Sheet Mimetic and β-Double Helix from (*E*)-Vinylogous Amino Acid Oligomers

The original work of this chapter has been published in the "Organic & Biomolecular Chemistry" journal. Here, we adopted the text from Ref. Veeresh, K.; Manjeet, S.; Gopi, H. N. *Org. Biomol. Chem.* **2019**, ***17***, 9226. with permission from the Royal Society of Chemistry. An E-mail copy of permission attached at the end of the chapter.

1. Introduction

β-Sheets are common structural motifs found in proteins and these structures are stabilized by the *inter*-strand hydrogen-bonds.[1] Even though not common in proteins and peptides, the structure of β-double helix is also stabilized by the *inter*-strand hydrogen bonds.[2] The natural gramicidin A is a lone example representing the structure of β-double helix in polypeptides and proteins.[2] Gramicidin A is an ionophore of fifteen amino acids containing linear peptide synthesized by *Bacillus brevis,* that forms a β-helical dimer in biological membranes and acts as cation channels. In organic solvents, this β-helical structure of gramicidin A transforms into a β-double helix structure. The β-double helix structure of gramicidin A is shown in Figure **1A**. But, the double-helical secondary structure is a common and most important structural motif found in nucleic acid, DNA[3] where two nucleotide strands get connected with systematic hydrogen bonding between nucleotide bases and form a double-helical structure. The structure of DNA double helix is shown in Figure **1B**. Inspired by the double-helical structure and function of nucleic acids and gramicidin A, synthetic chemists have been tried extensively to design double-helical structures using various types of natural and synthetic building blocks and allow them to fold into double-helical structures through supramolecular assembly facilitated by hydrogen bonds,[4] metal ionic interactions,[5] ion coordination,[6] aromatic π-π staking[7] or the different combinations of these forces.[8] Structures of synthetic double helices are shown in Figure **2**.

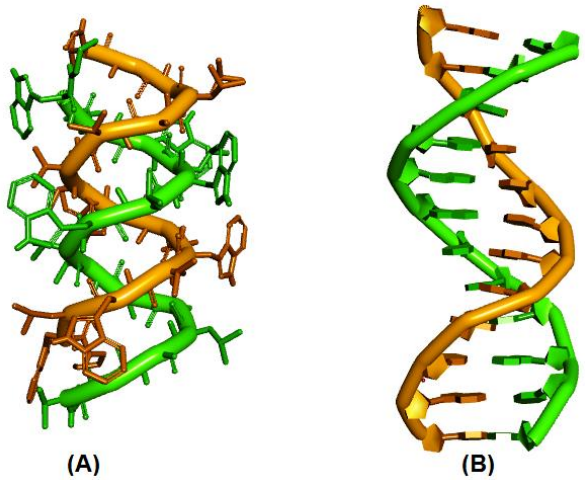

Figure 1: Natural double helical structures (A) Gramicidin A peptide Double helical structure (PDB: 1AV2). (B) DNA double-helical structure (PDB: 1BNA).

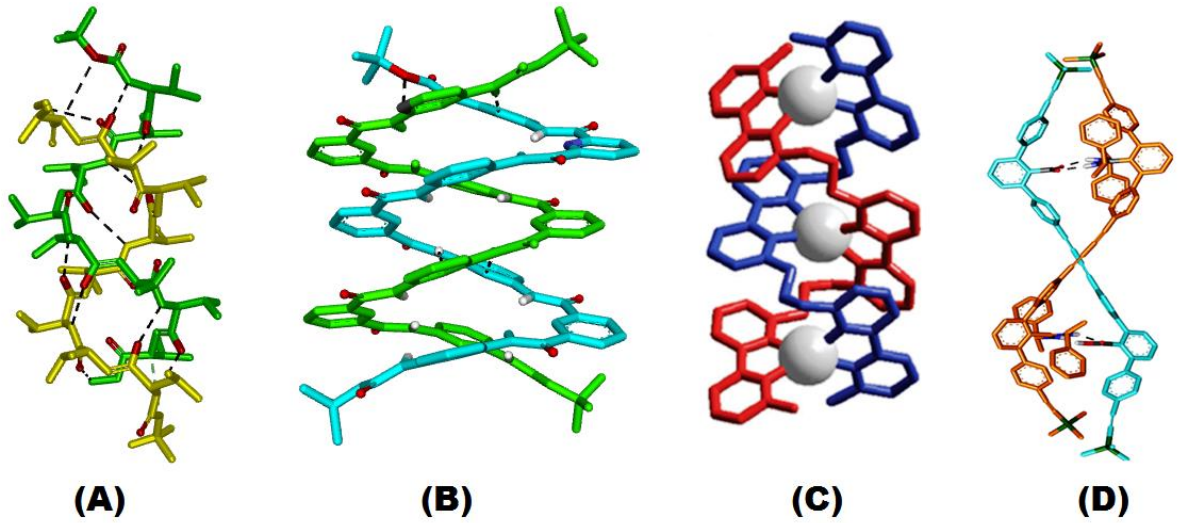

Figure 2: Synthetic double-helical structures. (A) Crystal of alternative L- and D-valine containing polypeptide. (B) Crystal structure of aromatic oligomides (C) Crystal structure of Cu coordination of bipyridine ligand (D) Crystal structure meta-terphenyl derivatives through salt bridge interaction.

In proteins and peptides, β-sheets and β-double-helical structures are constructed from different types of building blocks. In proteins, β-pleated sheet structures are always predominated by β-branched amino acid residues.[9] β-sheets can also be designed from the oligomers of either L- or D-amino acid residues (D is only synthetic peptides).[10] In addition, Pauling and Corey's great insight into the β-sheets structures suggested that a better β-sheet can be constructed by a combination of alternative L- and D-polypeptide β-stands.[11] As observed in gramicidin A, peptides composed of alternating L- and D-amino acids adopts a β-double helix structure in organic solvents and separates to β-helical structure in the lipid bilayer surroundings.[12] Though both β-double helical and β-sheet structures are stabilized by the *inter*molecular hydrogen bonds between the β-strands, there are not many examples in the literature showing the conformational difference between the β-double helices and β-sheet structures.

2. Aim and rationale of the present work

We have been working in the area of foldamers composed of γ-amino acids and proved the spontaneous self-association of oligomers of (*E*)-vinylogous $\gamma^{4,4}$-amino acid ((*E*)-$d^{2,3}\gamma$Aic) into β-double-helical structures.[13] Previously, Schreiber and co-workers showed

antiparallel β-sheet structure from the dipeptide composed of (*E*)-vinylogous γ^4-amino acid residues.[14] Herein, we wanted to study the substituent effect, that transforming a β-sheet type structure into a β-double helix using (*E*)-vinylogous γ-amino acids.

3. Results and discussion

3.1. Design and synthesis

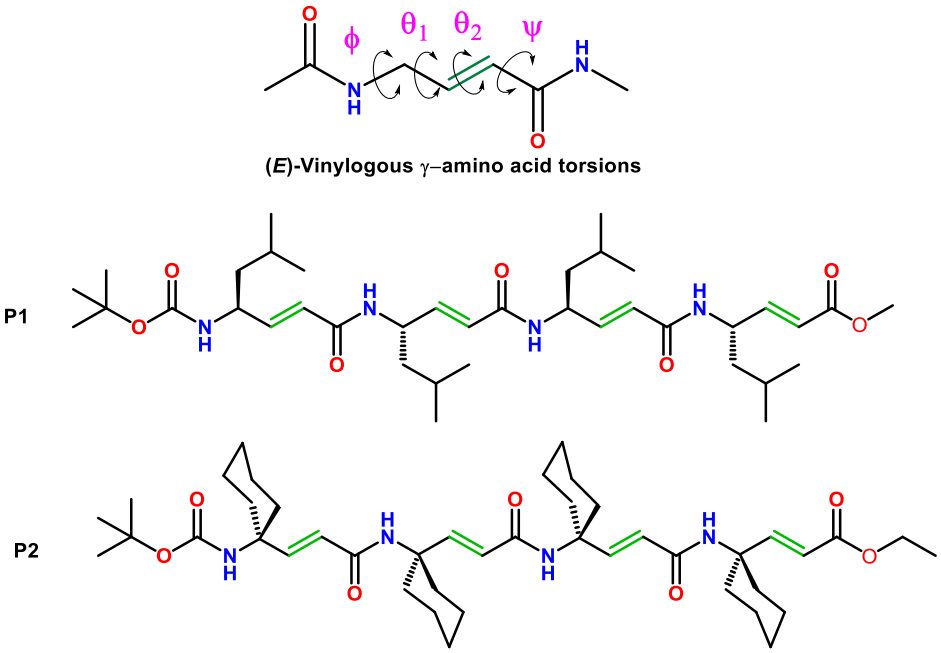

Scheme 1: Sequences of peptides P1 and P2. Peptide P1 is a homooligomer of (*E*)-α,β-unsaturated γ^4-amino acids and P2 is a homooligomer of (*E*)-α,β-unsaturated $\gamma^{4,4}$-amino acids.

To understand the effect of substituents on the conformation of (*E*)-vinylogous γ-amino acid homooligomers, we have designed two peptides **P1** and **P2**. The sequences of these homooligomers are shown in Scheme **1**. Peptide **P1** consists of amino acids with mono-alkyl substitution at γ-position (γ^4) and **P2** consists of a gem-dialkyl substitution at γ-position ($\gamma^{4,4}$). Synthesis these tetrapeptides were carried out through the conventional solution-phase method. The *tert*-butyloxycarbonyl group was used for *N*-terminus protection and the *C*-terminus was protected with the ester group. Deprotections were carried out with trifluoroacetic acid and aqueous *1N* sodium hydroxide solution for N- and C-termini, respectively. Couplings were mediated by HBTU. The α,β-unsaturated γ-amino acids BocHN-*E*-$d^{2,3}$γLeu-OMe and BocHN-*E*-$d^{2,3}\gamma Ac_6c$-OEt were synthesized starting from the *N*-Boc-Amino aldehyde through Wittig reaction as reported earlier.[15] The dipeptide of **P1** was prepared by a coupling reaction between *N*-terminal BocHN-*E*-

d^{2,3}γLeu-OH (**1a**) and H$_2$N-*E*-d^{2,3}γLeu-OMe (**1b**). The tetrapeptide of **P1** was prepared by [2+2] condensation involving *N*-terminal dipeptide acid BocHN-*E*-d^{2,3}γLeu-*E*-d^{2,3}γLeu-COOH (**1d**) and H$_2$N-*E*-d^{2,3}γLeu-*E*-d^{2,3}γLeu-COOMe (**1f**). The synthetic strategy for this peptide **P1** is given in Scheme **2.** Similar strategy was used for the synthesisof peptide **P2**, using BocHN-*E*-d^{2,3}γAc$_6$c-OEt monomer. The final crude peptides of **P1** and **P2** were purified through column chromatography.

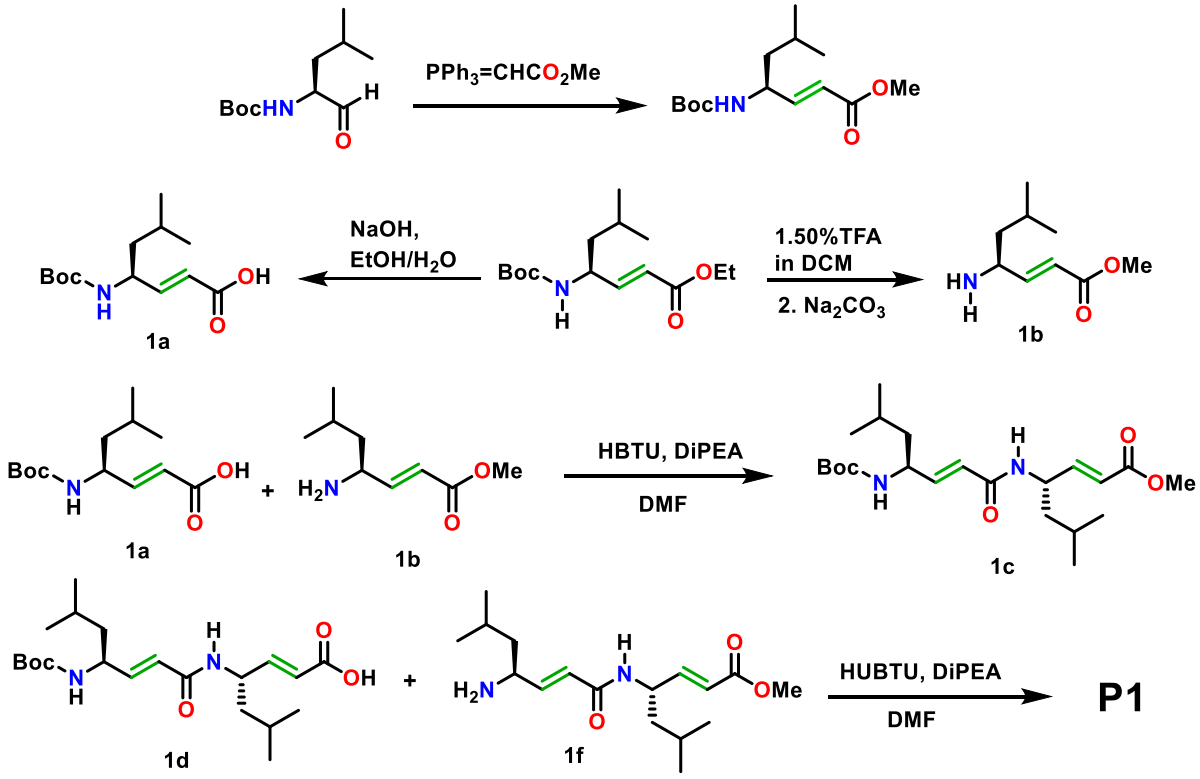

Scheme 2: Schematic representation of synthetic strategy for the peptide **P1.** Similar strategy was used for the synthesis of peptide **P2**.

3.2. Single-crystal analysis of P1

To study their conformations in solid-state, we subjected both peptides for crystallization in different organic solvent combinations. Both **P1** and **P2** gave good quality single crystals on the slow evaporation of peptides solution in ethyl acetate/n-hexane solvent system.

The X-ray diffracted single crystal structure of peptide **P1** is depicted in Figure **3**. The crystal structure analysis revealed that peptide **P1** adopted a parallel β-sheet-type structure. The self-assembled parallel β-sheets are stabilized through four 16-membered

between the β-strands. The amide NH of an (*E*)-vinylogous γ-amino acid residue (*i*) is involved in the hydrogen bonding with the amide CO group of previous (*i-1*) residue of the other strand in the parallel β-sheet stack (see Figure **3**). In contrast, the natural parallel β-sheet structures of α-peptides are stabilized by the 12-membered intermolecular hydrogen bond pseudo-cycles.[1b] Along with these hydrogen bondings between two strands we have also found that the parallel β-sheet structure is also stabilized by the *inter*-strand C-H···O hydrogen bond interactions. The presence of C-H···O hydrogen bonding interactions in peptides and protein structures has been

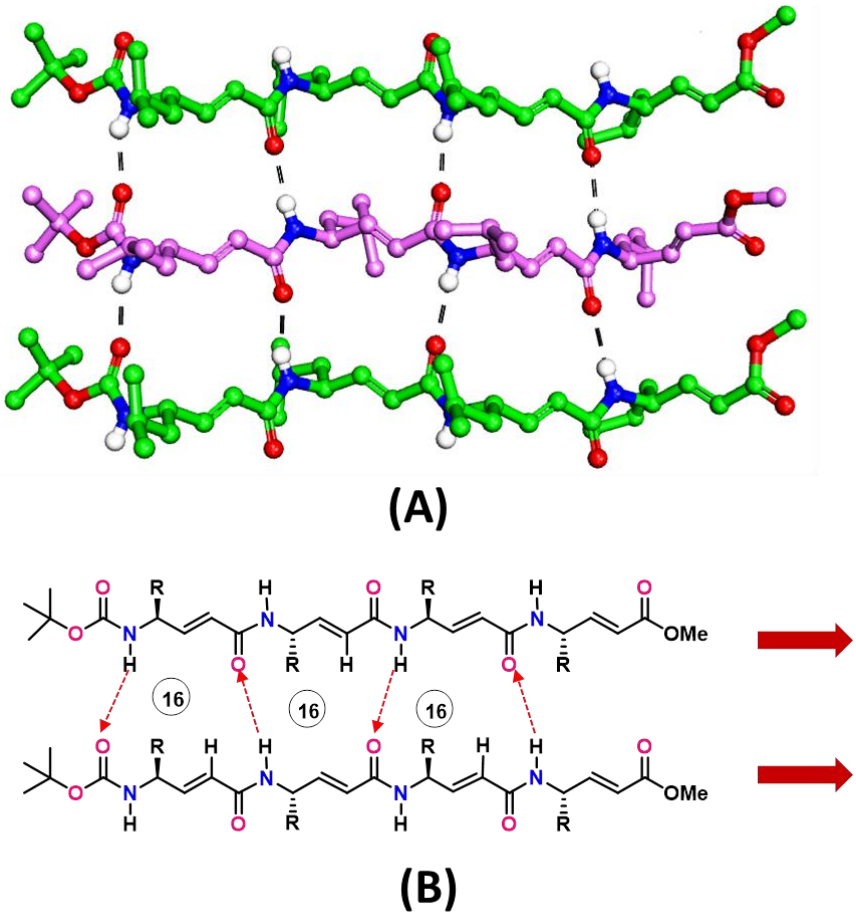

Figure 3: A) Single-crystal structures of Peptide **P1** adopted parallel β-sheet type conformation B) The hydrogen bonding pattern observed in the crystal structures of **P1** is stabilized by 16-membered inter-strand hydrogen bond pseudocycles.

Extensively studied.[16] The C=O···H-N hydrogen bond and the C-H···O hydrogen bond forms a network called the bifurcated hydrogen bond where the O atom is common to two

hydrogen bonds. Similar types of C-H···O hydrogen bonds have also been observed in the parallel β-sheet structures of γ-peptides constructed from the *trans*-cyclopropane γ-amino acid building blocks.[17] The C=O···H-N hydrogen bond parameters are tabulated in Table **2** and C-H···O hydrogen bond parameters are tabulated in Table **3**. The local conformation of the (*E*)-vinylogous γ-amino acid residues can be analyzed through the torsion variables ϕ (N-C^{γ}), θ_1 (C^{γ}-C^{β}), θ_2 (C^{β}-C^{α}) and ψ (C^{α}-C(O)) similar to the other γ-residues, however θ_2 attained ±180° due to double bonds (Scheme **1**). The torsion values of the parallel β-sheet structures are tabulated in Table **1**. Except C-terminal residues, ϕ and θ_1 in all (*E*)-vinylogous γ-amino acid residues in **P1** displayed -109±9° and 114±3° similar to the natural β-sheet structures of α-peptides. In addition, the torsion angle ψ adopted fully extended conformation (*s-cis*) with the value ± 180° in all the residues, except the C-terminal residue of the strand **b**. Further, θ_1 of the C-terminal residue in strand **a** of the β-sheets showed the values close to 0° (C-N eclipsed with C-C double bond). Except for the C-terminal (*E*)-vinylogous esters, the other three residues ((*E*)-vinylogous amides) in the β-strands of the parallel β-sheet follow the same pattern of the torsion angles (Table **1**).

Table 1: Backbone torsion angles of (*E*)-vinylogous γ-residues of the peptides **P1**.

	Residue	$\boldsymbol{\phi}$ °	$\boldsymbol{\theta}_1$°	$\boldsymbol{\theta}_2$°	$\boldsymbol{\psi}$°
Strand **a**	(*S,E*)d^{2,3}γLeu (1)	-96.16	114.35	179.15	172.76
	(*S,E*)d^{2,3}γLeu (2)	-109.18	115.34	-178.54	169.27
	(*S,E*)d^{2,3}γLeu (3)	-118.00	112.22	179.03	175.33
	(*S,E*)d^{2,3}γLeu (4)	-112.40	116.90	-179.64	-10.97
Strand **b**	(*S,E*)d^{2,3}γLeu (1)	-100.88	112.67	-177.95	169.06
	(*S,E*)d^{2,3}γLeu (2)	-104.01	111.86	177.63	172.30
	(*S,E*)d^{2,3}γLeu (3)	-108.51	114.93	179.27	166.99
	(*S,E*)d^{2,3}γLeu (4)	137.20	-15.24	176.76	178.77

Table 2: Hydrogen bond parameters of **P1**

Donor (D)	Acceptor (A)	DH….A (Å)	D….A (Å)	NH….O (deg)
N1	O9	2.073	2.854	150.68
N3	O11	2.086	2.882	153.77
N6	O3	2.040	2.881	165.33
N8	O5	2.15	2.996	167.37

Table 3: C-H···O H-bond parameters **P1**

Donor (D)	Acceptor (A)	DH….A (Å)	D….A (Å)	CH….O (deg)
C66	O5	2.825	3.561	136.88
C23	O11	2.783	3.482	129.61
C53	O3	2.740	3.489	134.47

3.3. Single crystal analysis of P2

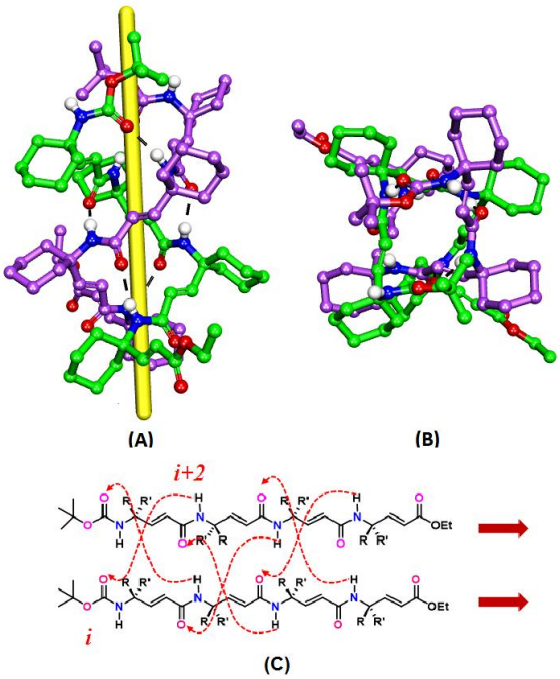

Figure 4: A) Single-crystal structures of peptide **P2** showing parallel β-double helix. B) Top view of β-double helical crystal structure C) The hydrogen bonding pattern observed in the crystal structures is stabilized by the *inter*-strand hydrogen bonding between residues *i* and *i+2*.

Even though both **P1** and **P2** containing (*E*)-vinylogous γ-residues, the crystal structure analysis of the **P2** revealed that it adopted a completely different type of conformation. The peptide adopted parallel β-double helix conformation in single crystals. The structure of **P2** is similar to the β-double helix reported earlier from the homooligomers of the $\gamma^{4,4}$-dimethyl substituted α,β-unsaturated γ-amino acids.[12] Crystal structure analysis revealed that two **P2** peptides intertwined into a β-double helix conformation. Being constructed from achiral amino acids, two different double helices with opposite handedness (*P* and *M*) in the asymmetric unit were observed. The β-double helix structure of **P2** is stabilized by six *inter*-strand hydrogen bonds. The amide CO group of *i* residue of one strand is involved in the hydrogen bonding with amide NH of the *i+2* residue in the other strand. The schematic representation of the pattern of hydrogen bonding in the β-double helix structure is shown in Figure **4.** The hydrogen bond parameters are tabulated in Table 4. Except for the N-terminal Boc-NH and the C-terminal ester carbonyl group all other amide CO and NH groups are involved in the *inter*-strand hydrogen bonding ($i \rightarrow i+2$). In comparison, each β-strand in peptide **P1** is involved in hydrogen bonding with two other adjacent parallel β-strands. However**,** each β-strand in **P2** is involved in hydrogen bonding with only one adjacent β-strand. Moreover, the N-terminal Boc-NH groups of **P2** are involved in the intermolecular hydrogen bonding with the C-terminal CO group of the β-strands of other double helices. This type of head-to-tail hydrogen bonding is observed in the α-peptide helices. Thus, the β-double helix consists of both types of hydrogen bonding patterns. Similar to peptide **P1**, we have also observed bifurcated C-H···O hydrogen bond in the parallel β-double helix **P2**. The C-H···O hydrogen bond parameters are tabulated in Table **6**. Akin to **P1**, the backbone conformation of γ-residues in **P2** can be described using torsion variables as shown in Scheme **1**. The average torsion angle parameters of γ-residues involved in the (*P*) β-double helix formation are given the Table **4.** The crystal structure analysis reveals that similar to **P1**, the both θ_2 (C^{β}-C^{α}) and ψ (C^{α}-C') adopted fully extended conformation. However, the torsion angles of ϕ and θ_1 were found to be different than the β-sheets structures observed in the peptide **P1**. The torsion angle ϕ attained an average value -72±8° which is nearly equal or little higher than the α-helix. The θ_1 displayed the values -15±3°. As **P2** achiral, similar torsion angles with

opposite signs are observed for the other double helical ((*M*) β-double helix) molecule in the asymmetric unit. The torsion angles ϕ, θ_1, θ_2 and ψ of **P2** displayed characteristic sign as +,+,+ and – (or –, –, – and +), respectively. These values are again nearly close or little lower than the average ψ values observed in the helices composed of gem-dialkyl substituted α-amino acids such as Aib and Ac_6c.[18] The structural analysis reveals that the amino group in all amino acid residues in **P2** adopted axial orientation, similar to its α-peptide analogues containing Ac_6c residues. Same trend is also observed in the β- and γ-peptides (gabapentin) composed of Ac_6c analogues.[19]

Table 4: Backbone torsion angles of (*E*)-vinylogous γ-residues of the peptides **P2.**

	Residue	$\boldsymbol{\phi}$ °	$\boldsymbol{\theta}_1$°	$\boldsymbol{\theta}_2$°	$\boldsymbol{\psi}$°
Strand **a**	*E*-$d^{2,3}\gamma Ac_6c$ (1)	72.41	5.81	173.97	-167.10
	E-$d^{2,3}\gamma Ac_6c$ (2)	65.25	27.69	172.38	-172.65
	E-$d^{2,3}\gamma Ac_6c$ (3)	68.42	21.02	172.86	-174.16
	E-$d^{2,3}\gamma Ac_6c$ (4)	-65.76	-15.31	-176.50	168.39
Strand **b**	(*E*)-$d^{2,3}\gamma Ac_6c$ (1)	65.50	17.72	169.10	-167.56
	(*E*)-$d^{2,3}\gamma Ac_6c$(2)	79.61	15.46	173.89	-170.96
	(*E*)-$d^{2,3}\gamma Ac_6c$(3)	66.11	14.26	173.05	-173.77
	E-$d^{2,3}\gamma Ac_6c$ (4)	-62.58	-17.43	177.65	175.34

Table 5: Hydrogen bond parameters of **P2.**

Donor (D)	**Acceptor (A)**	**DH….A (Å)**	**D….A (Å)**	**NH….O (deg)**
N2	O9	2.041	2.879	172.21
N3	O10	2.13	2.819	155.59
N4	O11	2.11	2.857	145.60
N6	O2	2.073	2.930	175.03
N7	O3	2.059	2.883	160.22
N8	O4	2.130	2.995	160.80

Table 6: C-H···O H-bond parameters **P2**

Donor (D)	**Acceptor (A)**	**DH….A (Å)**	**D….A (Å)**	**NH….O (deg)**
C19	O9	2.257	3.357	143.59
C59	O6	2.702	3.392	128.56
C71	O5	2.684	3.372	128.29
C22	O10	2.678	3.404	135.50
C31	O11	2.642	3.371	135.22
C80	O4	2.662	3.384	131.52

3.4. Conformational difference between the β-sheets and β-double helices.

As θ_2 and ψ attained the similar values in both **P1** and **P2**, only the difference was observed in the values of ϕ and θ_1. In order to understand the conformational difference between the β-sheets and β-double helices, we plotted a Ramachandran type two dimensional map using the values ϕ and θ_1 as shown in Figure **5**. A clear distinction between the two types of structures has been observed in the 2-dimensional torsion angle map. The torsion angles ϕ and θ_1 of **P1** occupy the space very similar to the α-peptides β-sheets, whereas the same torsion angles of **P2** (*P*) β-double helix falls in the region close to the α-helices. Further, careful analysis revealed that the double bond nearly eclipsed with C-N bond in β-double helices, while the double bond is eclipsed with C-H in β-sheet structures (Figure **6**). Overall, the torsion parameters ϕ and θ_1 are responsible for the β-sheet and β-double helix conformations in (*E*)-vinylogous γ-amino acid homooligomers. The γ-disubstitution restricts the rotational freedom of ϕ and θ_1 which enforce the peptides to adopt β-double helix (**P2**) conformation. However, this steric restriction can be released through a single substitution at γ-position, which leads the β-sheet (**P1**) conformation. Overall these results suggested homooligomers of $\gamma^{4,4}$-dialkyl substituted (*E*)-vinylogousγ-amino acids promote the β-double helix conformation.

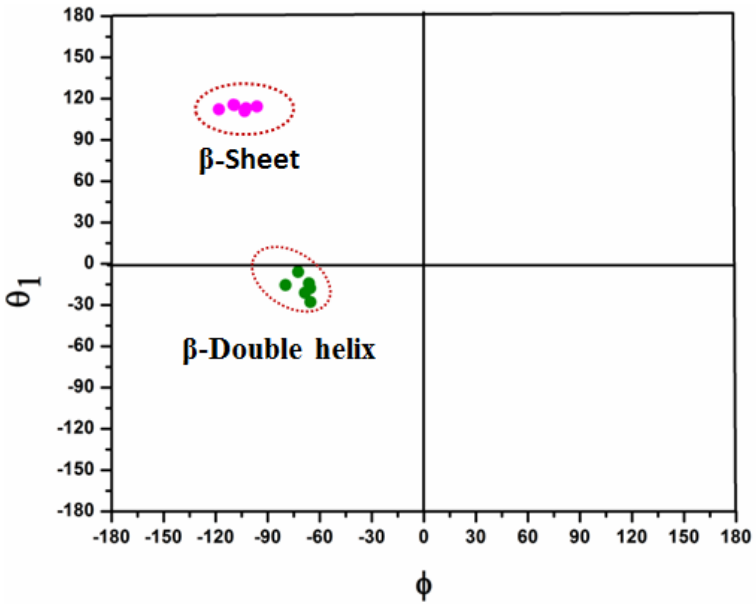

Figure 5: Two-dimensional ϕ and θ_1 plot of *E*-vinylogous γ-residues of **P1** and **P2**. The other two torsion variables θ_2 and ψ are always attained values close to 180°

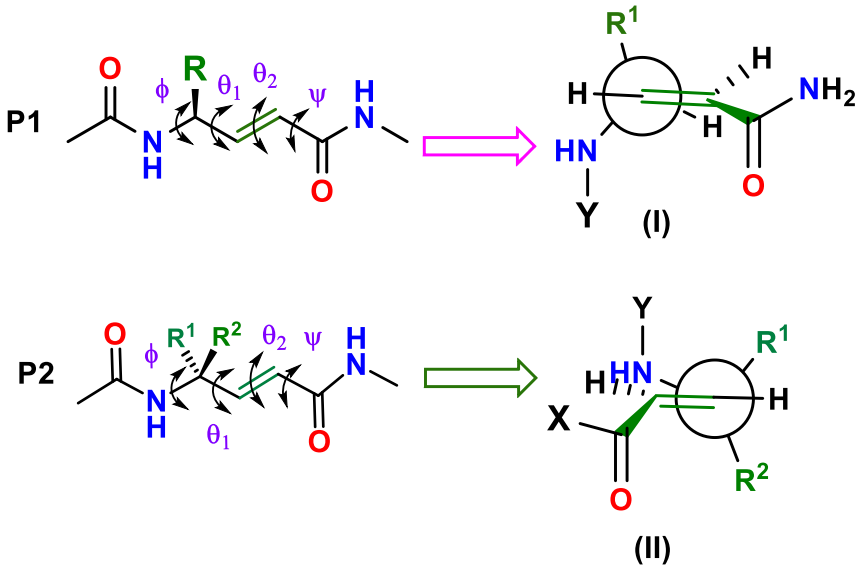

Figure 6: Local conformation of (*E*)-vinylogous γ-residues along the C^{γ}-C^{β} bonds of **P1** and **P2**. The C^{γ}-Hand C=C bonds are eclipsed in β-sheet (**P1**) structure (**I**), the C^{γ}-N and C=C are eclipsed in (*P*) β-double helix (**P2**) structure (**II**).

4. Conclusions

In conclusion, we have shown the single-crystal conformation of β-sheets and β-double helix generated from homooligomers of (*E*)-vinylogous amino γ-acids. It is clear from the

results that homooligomers of γ^4-alkyl substituted (*E*)-vinylogous γ-amino acids favors the β-sheets structure, while homooligomers of $\gamma^{4,4}$-dialkyl substituted (*E*)-vinylogous γ-amino acids preferred to adopt β-double helix structure. The double helix structure is stabilized by the intermolecular hydrogen bonds between the residues *i* (*CO*) of one strand and *i+2* (*NH*) of the other. Along with the inter-strand, the structures also displayed head-to-tail hydrogen bonding similar to the α-helices. The results reported suggested double helices can be constructed from the oligomers of $\gamma^{4,4}$-dialkyl substituted (*E*)-vinylogous γ-amino acids. In addition, this work also suggests the alternative way to construct β-double helices other than alternating L-and D-peptides.

5. Experimental

Synthetic procedure for BocHN-(*S,E*)$d^{2,3}$γLeu-OH (1a): BocHN-(*S,E*)$d^{2,3}\gamma^4$Leu-OMe[15] (2.71 g, 10 mmol) was dissolved in methanol (60 mL), to this solution aqueous sodium hydroxide (1*N* NaOH, 20 mL) was added. The reaction mixture was stirred for 6 h. After completion of the reaction (monitored with TLC) methanol was evaporated, remained basic solution was acidified with 5% HCl. The organic product was extracted from the acidified solution with ethyl acetate (3 × 60 mL). The combined ethyl acetate layer was washed with brine solution (60 mL) and dried over anhydrous sodium sulfate The ethyl acetate solution was concentrated under reduced pressure, the obtained BocHN-(*S,E*)$d^{2,3}$γLeu-OH (**1a**) was further used for coupling reaction without any purification.

Synthetic procedure for TFA.H_2N-(*S,E*)$d^{2,3}$γLeu-OMe (1b): BocHN-(*S,E*)$d^{2,3}$γLeu-OMe[15](2.71 g, 10 mmol) was dissolved in a mixture of DCM:TFA (1:1, 10 mL), this solution was stirred at room temperature about 1 h. The reaction progress was monitored by TLC. After the completion of the reaction, DCM:TFA solvent mixture was evaporated. To remove the traces of TFA the compound was co-evaporated with DCM solvent a couple of times. The obtained viscous oily product (1b) was used for coupling.

Synthetic procedure for dipeptide (1c): Compound 1a (2.06 g, 8 mmol) was dissolved in DMF (10 mL), to this solution HBTU (3.033 g, 8 mmol) and DIPEA (4.18 mL, 24 mmol) were added. This reaction mixture was stirred for 5 min and added to compound 1b (2.82 g, 10 mmol) under ice-cooled condition. The reaction mixture was further stirred at room temperature about 6 h. After completion of the reaction (monitored with TLC), the

reaction mixture was diluted with 5% HCl (60 mL). Organic product was extracted with ethyl acetate (3 × 60 mL). Combined ethyl acetate layer was washed successively with 10% Na_2CO_3 (3 × 60 mL), 10% HCl (3 × 60 mL) and brine solution (60 mL) and dried over anhydrous sodium sulfate. Ethyl acetate was evaporated under reduced pressure to get dipeptide (1c). The crude compound 1c was used for next step without any purification.

Synthetic procedure for dipeptide acid (1d): Methyl ester group of 1c (1.24 g, 3 mmol) was deprotected by following the above mentioned synthetic procedure for 1a and obtained product (1d) was used for next coupling.

Synthetic procedure for dipeptide amine (1f): Boc group of **1c** (1.02 g, 2.5 mmol) was deprotected by following the above mentioned synthetic procedure for 1b and obtained viscous oily product (**1f**) was used for next coupling.

Synthetic procedure for P1: Coupling between 1d (0.991 g, 2.5 mmol) and 1f (1.05 g, 2.5mmol) was done by following the above mentioned synthetic procedure for dipeptide 1c. Obtained crude peptide P1 was purified by precipitation method. Precipitation of crude compound (P1) in ethyl acetate solvent was carried out by increasing the n-hexane percentage. The obtained white solid precipitate was filtered through Whatman filter paper and dried at room temperature.

Characterization of peptide P1: White crystalline solid; Yield 1.17 g (68%); ^{1}H NMR (400 MHz, $CDCl_3$) δ 8.09 (brs, 2H), 7.81 (brs, 1H), 7.04 – 6.70 (m, 4H), 6.08 – 5.84 (m, 2H), 5.64 – 5.37 (m, 2H), 4.77 (m, 2H), 4.51 (m, 2H), 4.20 (m, 1H), 3.70 (s, 3H), 1.83 – 1.21 (m, 30H), 1.0 – 0.75 (m, 25H); ^{13}C NMR (101 MHz, $CDCl_3$) δ 167.5, 167.0, 165.5, 165.3, 156.7, 148.9, 148.6, 146.4, 145.8, 145.0, 120.7, 120.2, 120.0, 81.1, 77.5, 77.4, 77.2, 76.8, 70.4, 65.3, 63.5, 60.2, 51.5, 50.7, 49.9, 48.7, 48.4, 44.0, 43.9, 43.8, 42.9, 32.1, 29.9, 28.7, 25.5, 25.1, 23.3, 23.2, 23.0, 23.0, 22.8, 22.7, 22.7, 22.2, 21.7, 21.6, 14.5; MALDI/TOF-TOF mass $[M+Na]^+$ calculated *m/z* 711.467 found 711.494.

Synthesis of peptide P2

Synthesis of BocHN-*E*-d^{2,3}γAc$_6$c-OEt (I): *tert*-butyl (1-formylcyclohexyl)carbamate (2.77 g, 10 mmol) was dissolved in THF (50 mL). To this solution, Wittig ylide (Ph_3P=CH-COOEt) (5.220 g, 15 mmol) was added. The reaction mixture was stirred at 60 °C, about 24 h. After completion of the reaction (monitored by TLC), the THF solvent was

evaporated and the product was purified through column chromatography using ethyl acetate/ n-hexane solvent system.

Characterization of compound (I): White solid, Yield = 2.526 g (85%); m. p. 212-216 °C; ^{1}H NMR (400 MHz, $CDCl_3$) δ 6.94 (d, *J* = 15.9 Hz, 1H), 5.85 (d, *J* = 15.9 Hz, 1H), 4.52 (s, 1H), 4.18 (q, *J* = 7.1 Hz, 2H), 1.67 – 1.44 (m, 9H), 1.42 (s, 9H), 1.28 (t, *J* = 7.1 Hz, 4H); ^{13}C NMR (101 MHz, $CDCl_3$) δ 167.0, 153.5, 149.69, 118.9, 77.5, 77.4, 77.2, 76.8, 60.4, 55.3, 34.7, 28.5, 25.4, 21.7, 14.4.; HRMS *m/z* calculated $[M+Na]^+$ is 320.1838 found 320.1839.

Synthetic procedure for peptide P2: Peptide **P2** was synthesized by following a similar procedure as mentioned for the peptide **P1**, using the BocHN-*E*-$d^{2,3}\gamma Ac_6c$-OEt (**I**) monomer. The final crude compound was purified through silica gel column chromatography using ethyl acetate and n-hexane.

Characterization of peptide P2: White crystalline solid; Yield 1.37 g (73%); ^{1}H NMR (400 MHz, $CDCl_3$) δ 8.21 (s, 1H), 7.78 (s, 2H), 7.37 (s, 1H), 7.08 (d, *J* = 15.9 Hz, 2H), 6.83 (d, *J* = 15.1 Hz, 2H), 6.75 (d, *J* = 15.2 Hz, 2H), 6.67 (d, *J* = 15.3 Hz, 2H), 4.60 (s, 1H), 4.14 (q, *J* = 7.1 Hz, 2H), 1.84 – 0.95 (m, 52H); ^{13}C NMR (101 MHz, $CDCl_3$) δ 167.6, 165.7, 165.6, 164.8, 154.7, 148.2, 147.7, 121.6, 121.1, 120.8, 118.9, 80.0, 77.5, 77.4, 77.2, 77.2, 76.8, 65.3, 60.2, 57.2, 57.1, 56.3, 56.26, 56.0, 34.3, 32.0, 31.1, 29.8, 29.8, 28.8, 25.8, 25.7, 25.5, 25.3, 25.06, 22.8, 22.1, 22.0, 21.8, 21.8, 21.6, 14.5, 14.3. MALDI/TOF-TOF mass $[M+Na]^+$ calculated *m/z* 773.482 found 773.448.

6. References

1. Creighton, T. E. *Proteins: structure and molecular properties*, 2nd Ed., Freeman, W. H. and Co., New York, **1993**.
2. (a) Langes, D. A. *Science*, **1988**, *241*, 188. (b) Langs, D. A.; Smith, G. D.; Courseille, C.; Precigoux, G. *Proc. Nat. Acad. Sci. U. S. A.* **1991**, *88*, 5345. (c) Wallace, B. A.; Ravikumar, K. *Science* **1988**, *241*, 182. (d) Sychev, S. V.; Barsukov L. I.; Ivanov, V. T. *J. Pept. Sci.*, **2013**, *19*, 452.
3. (a) Watson, J. D.; Crick, F. H. C. *Nature* **1953**, *171*, 964. (b) Watson, J. D.; Crick, F. H. C. *Nature* **1953**, *171*, 737.

4. (a) Benedetti, E.; DiBlasio, B.; Pedone, C.; Lorenzi, G. P.; Tomasic, L.; Gramlich, V. *Nature* **1979**, *282*, 630. (b) DiBlasio, B.; Benedetti, E.; Pavone, V.; Pedone, C.; Gerber, C.; Lorenzi, G. P. *Biopolymers* **1989**, *28*, 203. (c) Sastry, M.; Brown, C.; Wagner, G.; Clark, T. D. *J. Am. Chem. Soc.* **2006**, *128*, 10650. (d) Szczypińskia, F. T.; Hunter, C. A.; *Chem. Sci.* **2019**, *10*, 2444. (f) Chakraborty, T. K.; Koley, D.; Ravi, R.; Kunwar, A. C. *Org. Biomol. Chem.* **2007**, *5*, 3713.
5. (a) Tanaka, Y.; Katagiri, H.; Furusho, Y.; Yashima, E. *Angew. Chem. Int. Ed.* **2005**, *44*, 3867. (b) Yamada, H.; Wu, Z.-Q.; Furusho, Y.; Yashima, E. *J. Am. Chem. Soc.* **2012**, *134*, 9506.
6. Krämer, R.; Lehn. J.-M.; Marquis-Rigault, A. *Proc. Natl. Acad. Sci. U. S. A.* **1993**, *90*, 5394.
7. (a) Berl, V.; Huc, I.; Khoury, R. G.; Krische, M. J.; Lehn, J.-M. *Nature* **2000**, *407*, 720. (b) Gan, Q.; Wang, X.; Kauffmann, B.; Rosu, F.; Ferrand, Y.; Huc, I.; *Nat. Nanotechnol.* **2017**, *12*, 447. (c) Wang, X.; Wicher, B.; Ferrandand, Y.; Huc, I. *J. Am. Chem. Soc.* **2017**, *139*, 9350. (d) Li, X.; Markandeya, N.; Jonusauskas, G.; McClenaghan, N. D.; Maurizot, V.; Denisov, S. A.; Huc, I. *J. Am. Chem. Soc.* **2016**, *138*, 13568.
8. Liu, C. Z.; Koppireddi, S.; Wang, H.; Zhang, D. W.; Li, Z. T. *Angew. Chem. Int. Ed.*, **2019**, *131*, 232.
9. (a) Janin, J.; Wodak, S.; Levitt, M.; Maigret, B. *J. Mol. Biol.* **1978**, *125*, 357. (b) Joo, H.; Tsai, J. *Proteins* **2014**, *82*, 2128. (c) Nowick, J. S. *Acc. Chem. Res.* **2008**, *41*, 1319. (d) Kung, V. M.; Cornilescu, G.; Gellman, S. H. *Angew. Chem. Int. Ed.* **2015**, *54*, 14336.
10. (a) Smith, C. K.; Regan, L. *Acc. Chem. Res.* **1997**, *30*, 153. (b) Hecht, M. H. *Proc. Natl. Acad. Sci. U. S. A.* **1994**, *91*, 8729. (c) Marcos, E.; Chidyausiku, T. M.; McShan, A. C.; Evangelidis, T.; Nerli, S.; Carter, L.; Nivón, L.G.; Davis, A.; Oberdorfer, G.; Tripsianes, K.; Sgourakis, N. G.; *Nat. Struct. Biol.* **2018**, *25*, 1028. (d) Loughlin, W. A.; Tyndall, J. D. A.; Glenn M. P.; Fairlie, D. P.; *Chem. Rev.* **2004**, *104*, 6085.

11. (a) Pauling, L.; Corey, R. B. *Proc. Natl. Acad. Sci. U. S. A.* **1953**, *39*, 253. (b) Pauling, L.; Corey, R. B. *Proc. Natl. Acad. Sci. U. S. A.* **1951**, *37*, 251. (c) Pauling, L.; Corey, R. B. *Proc. Natl. Acad. Sci. U. S. A.* **1951**, *37*, 256.
12. (a) Ketchem, R. R.; Hu, W.; Cross, T. A. *Science* **1993**. *261*, 1457. (b) Bamberg, E.; Apell. H. J.; Alpes, H. *Proc. Natl. Acad. Sci. U. S. A.* **1977**, *74*, 2402.
13. Misra, R.; Dey, S.; Reja, R. M.; Gopi, H. N. *Angew. Chem. Int. Ed.* **2018**, *57*, 1057.
14. Hagihara, M.; Anthony, N. J.; Stout, T. J.; Clardy, J.; Schreiber, S. L. *J. Am. Chem. Soc.* **1992**, *114*, 6568.
15. Hintermann, T.; Gademann, K.; Jaun, B.; Seebach, D. *Helv. Chim. Acta.* **1998**, *81*, 983.
16. (a) Ho, B. K.; Curmi, P. M. *J. Mol. Biol.* **2002**, *317*, 291. (b) Derewenda, Z. S.; Lee, L.; Derewenda, U. *J. Mol. Biol.* **1995**, *252*, 248. (c) Vargas, R.; Garza, J.; Dixon, D. A.; Hay, B. P. *J. Am. Chem. Soc.* **2000**, *122*, 4750. (d) Senes, A.; Ubarretxena-Belandia, I.; Engelman, D. M. *Proc. Natl. Acad. Sci. U. S. A.* **2001**, *98*, 9056. (e) Ramesh, M.; Bharatam, P. V.; Venugopalan, P.; Kishore, R. *Cryst. Growth Des*. **2013**, *13*, 2004.
17. Qureshi, M. K. N.; Smith, M. D. *Chem. Commun.* **2006**, 5006.
18. (a) Karle, I. L.; Balaram, P. *Biochemistry* **1990**, *29*, 6747. (b) Crisma, M.; Formaggio, F.; Moretto, A. Toniolo, R. *Biopolymers* **2006**, *84*, 3. (c) Basuroy, K.; Rajagopal, A.; Ragothama, S.; Shamala, N.; Balaram, P. *Chem. Asian J.* **2012**, *7*, 1671.
19. (a) Wani, N. A.; Raghothama, S.; Singh, U. P.; Rai, R. *Chem. Eur. J.* **2017**, *23*, 8364. (b) Balaram, P. *Pept. Sci.* **2010**, *94*, 733.

7. Appendix

1. Crystallographic Information of Peptides

The X-ray data of **P1** and **P2** was collected at 100 K on diffractometer using Mo K_α radiation (λ = 0.71073 Å). The structures were obtained by direct methods using the SHELXS-97 program.

Table 1: Crystallographic information of peptides **P1** and **P2.**

	P1	**P2**[(a)]
Chemical formula	C_{38} H_{64} N_4 O_7	C_{43} H_{66} N_4 O_7
Molecular weight	688.9510	751.022
Crystal habit	Clear	Clear
Crystal size (nm)	0.2× 0.2× 0.3	0.3× 0.3× 0.4
Crystallization solvent	ethyl acetate/n-hexane	ethyl acetate/n-hexane
Space group	P 1	P -1
a (Å)	10.0311(19)	15.8190(9)
b (Å)	13.762(3)	15.8231(10)
c (Å)	14.965(3)	21.9625(13)
α (dge)	92.146(5)	71.776(4)
β (dge)	95.340(5)	84.613(4)
γ (dge)	97.624(5)	63.813(4)
Volume $(Å)^3$	2036.1(7)	4679.4(5)
Z	2	2
Molecules/asym.unit	2	2
Density (g/cm^3)(cal)	1.124	1.163
F (000)	1752.33	751.0
Radiation	Mo K_α	Mo K_α
2θ Max. (^{o})	56.924	155.702
μ mm^{-1}	0.077	0.656
Reflections (cal)	20574	19967
Parameters	907	1065
R (reflections)	0.1362(6570)	0.1122(7584)
wR2 (Reflections)	0.3810(20311)	0.3551(19967)
Goodness-of- fit (S)	0.977	1.031

[(a)]Option SQUEEZE of PLATON program was used to remove disordered solvent molecules.

2. ^{1}H, and ^{13}C spectra of compounds

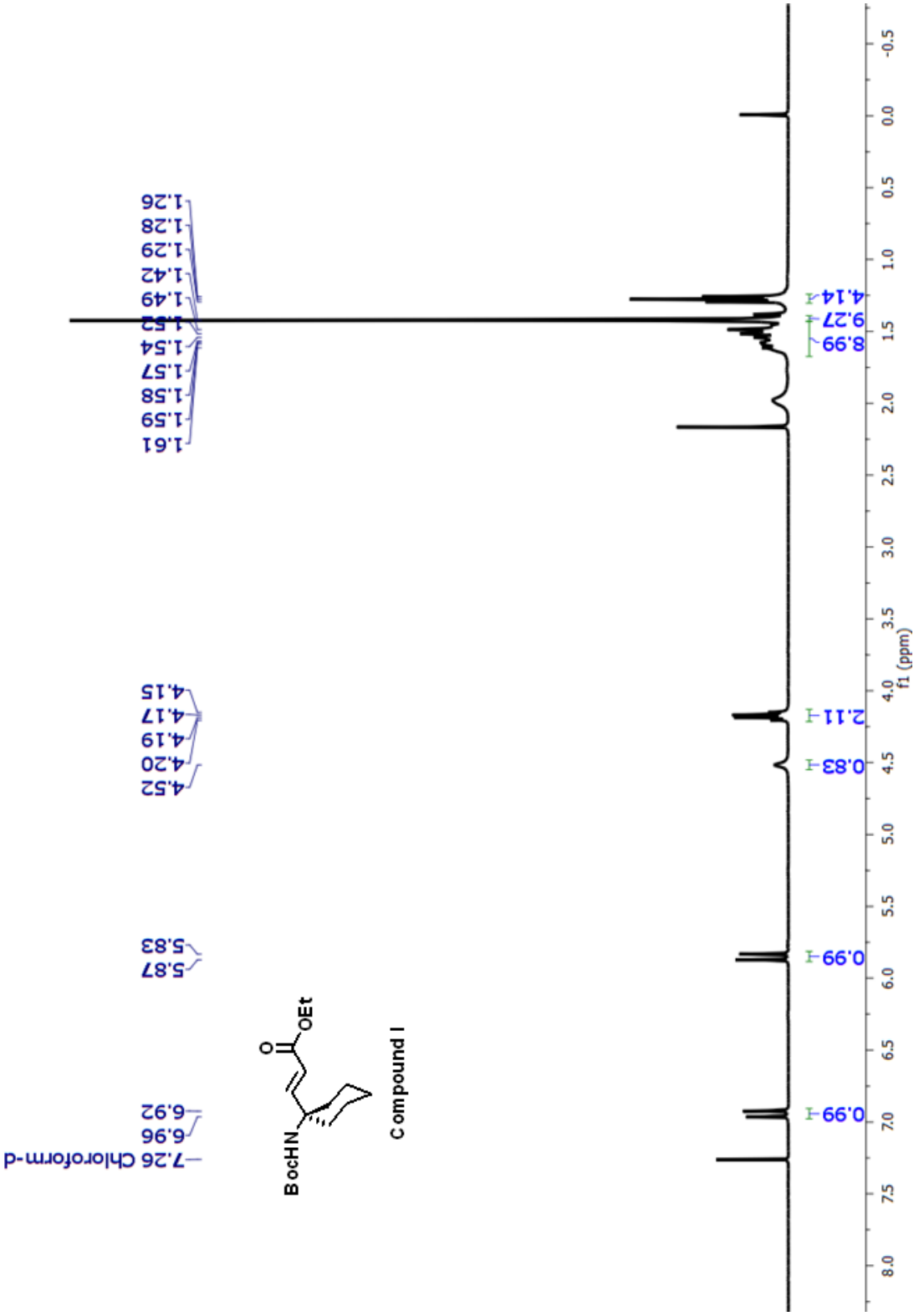

14.40
21.41
25.41
28.53
34.86
55.33
60.45
76.84
77.16
77.36
77.48
149.62
153.55
166.93
BocHN
O
OEt
Compound I
f1 (ppm)

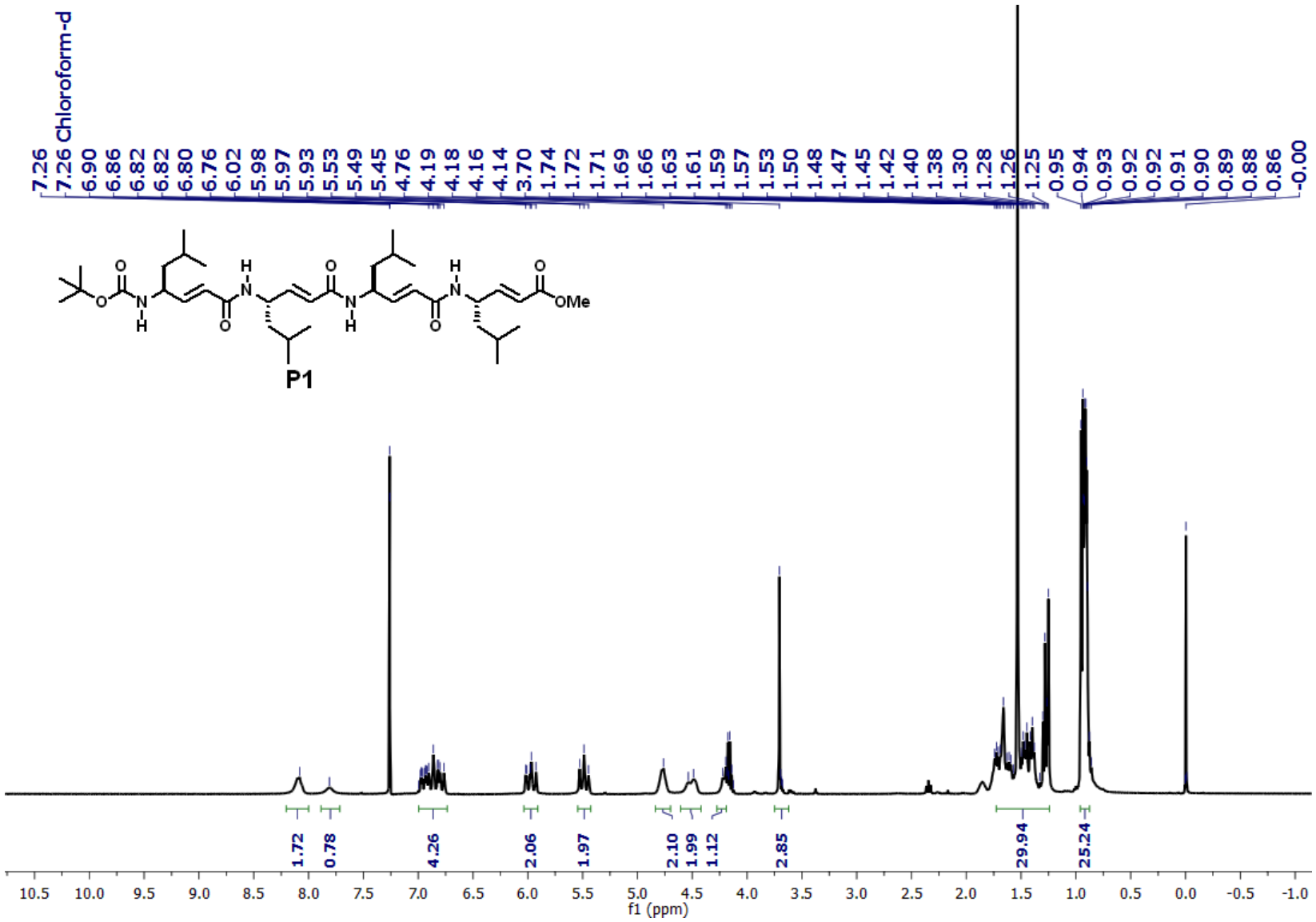
7.26 Chloroform-d
7.26 6.90 6.86 6.82 6.82 6.80 6.76 6.02 5.98 5.97 5.93 5.53 5.49 5.45 4.76 4.19 4.18 4.16 4.14 3.70 1.74 1.72 1.71 1.69 1.66 1.63 1.61 1.59 1.57 1.53 1.50 1.48 1.47 1.45 1.42 1.40 1.38 1.30 1.28 1.26 1.25 0.95 0.94 0.93 0.92 0.92 0.91 0.90 0.89 0.88 0.86 -0.00
OMe
P1
1.72 0.78 4.26 2.06 1.97 2.10 1.99 1.12 2.85 29.94 25.24
10.5 10.0 9.5 9.0 8.5 8.0 7.5 7.0 6.5 6.0 5.5 5.0 4.5 4.0 3.5 3.0 2.5 2.0 1.5 1.0 0.5 0.0 -0.5 -1.0
f1 (ppm)

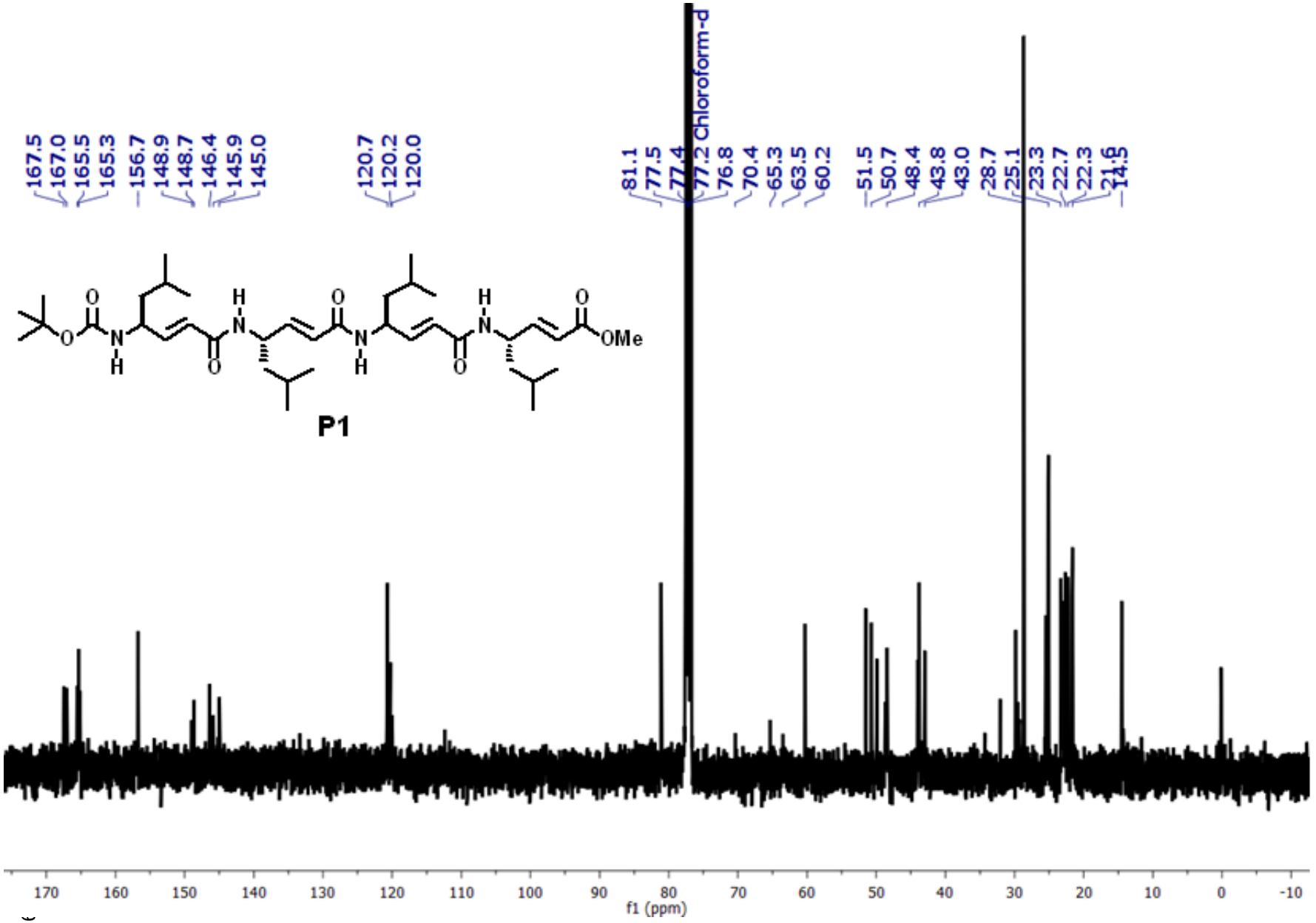
167.5
167.0
165.5
165.3
156.7
148.9
148.7
146.4
145.9
145.0
120.7
120.2
120.0
81.1
77.5
77.4
77.2 Chloroform-d
76.8
70.4
65.3
63.5
60.2
51.5
50.7
48.4
43.8
43.0
28.7
25.1
23.3
22.7
22.3
21.6
14.5
OMe
P1
170
160
150
140
130
120
110
100
90
80
70
60
50
40
30
20
10
0
-10
f1 (ppm)

P2
1.24
1.26
1.28
1.42
1.51
1.66
4.11
4.13
4.15
4.17
4.59
5.73
5.75
5.77
5.79
5.89
5.93
6.05
6.09
6.64
6.68
6.74
6.78
6.81
7.06
7.10
7.26 Chloroform-d
7.85
8.31
51.42
2.14
0.93
2.02
1.03
1.01
5.22
1.00
0.64
0.67
0.65
f1 (ppm)

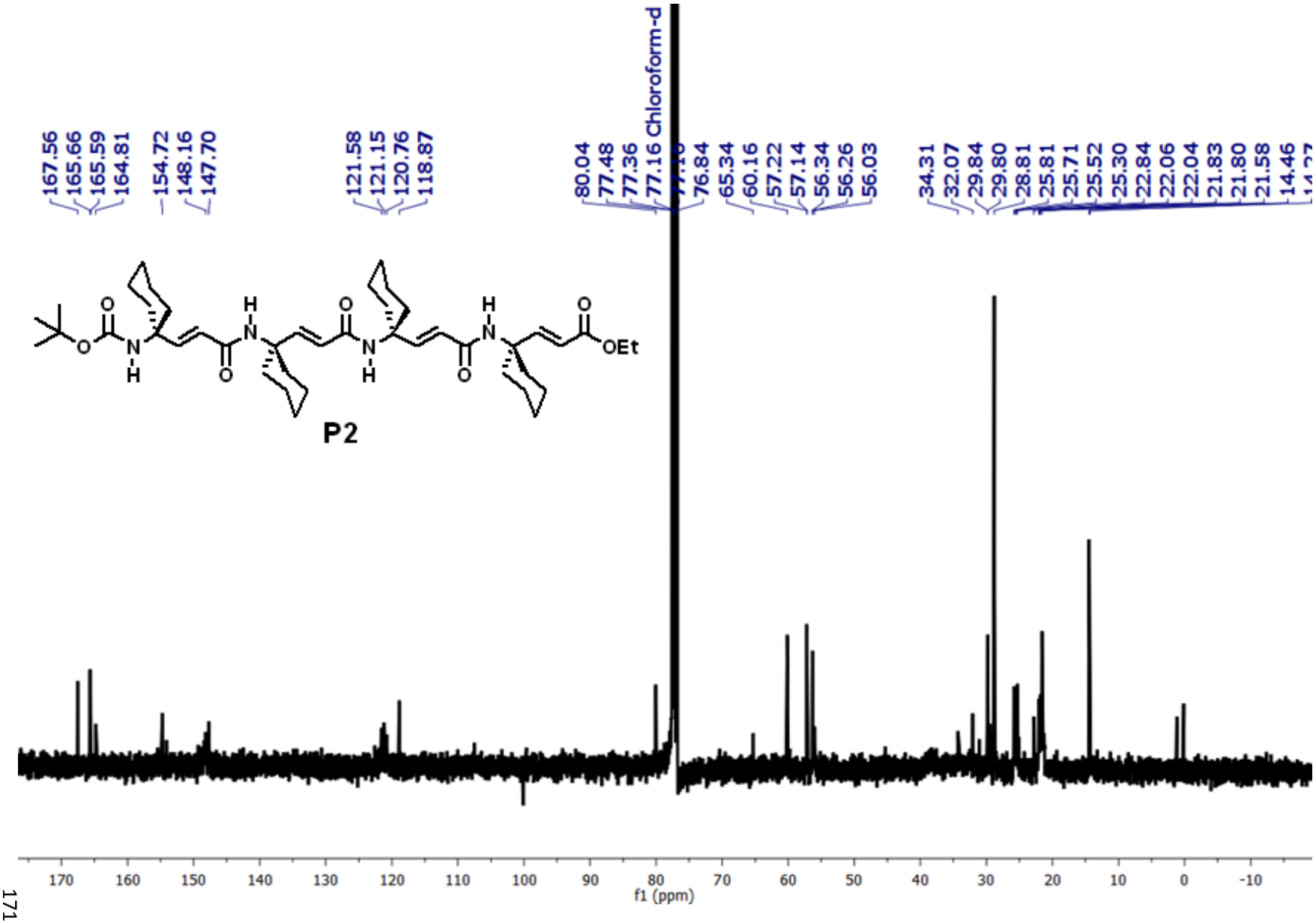
167.56
165.66
165.59
164.81
154.72
148.16
147.70
121.58
121.15
120.76
118.87
80.04
77.48
77.36
77.16 Chloroform-d
76.84
65.34
60.16
57.22
57.14
56.34
56.26
56.03
34.31
32.07
29.84
29.80
28.81
25.81
25.71
25.52
25.30
22.84
22.06
22.04
21.83
21.80
21.58
14.46
OEt
P2
170
160
150
140
130
120
110
100
90
80
70
60
50
40
30
20
10
0
-10
f1 (ppm)

3. Mass spectra of compounds

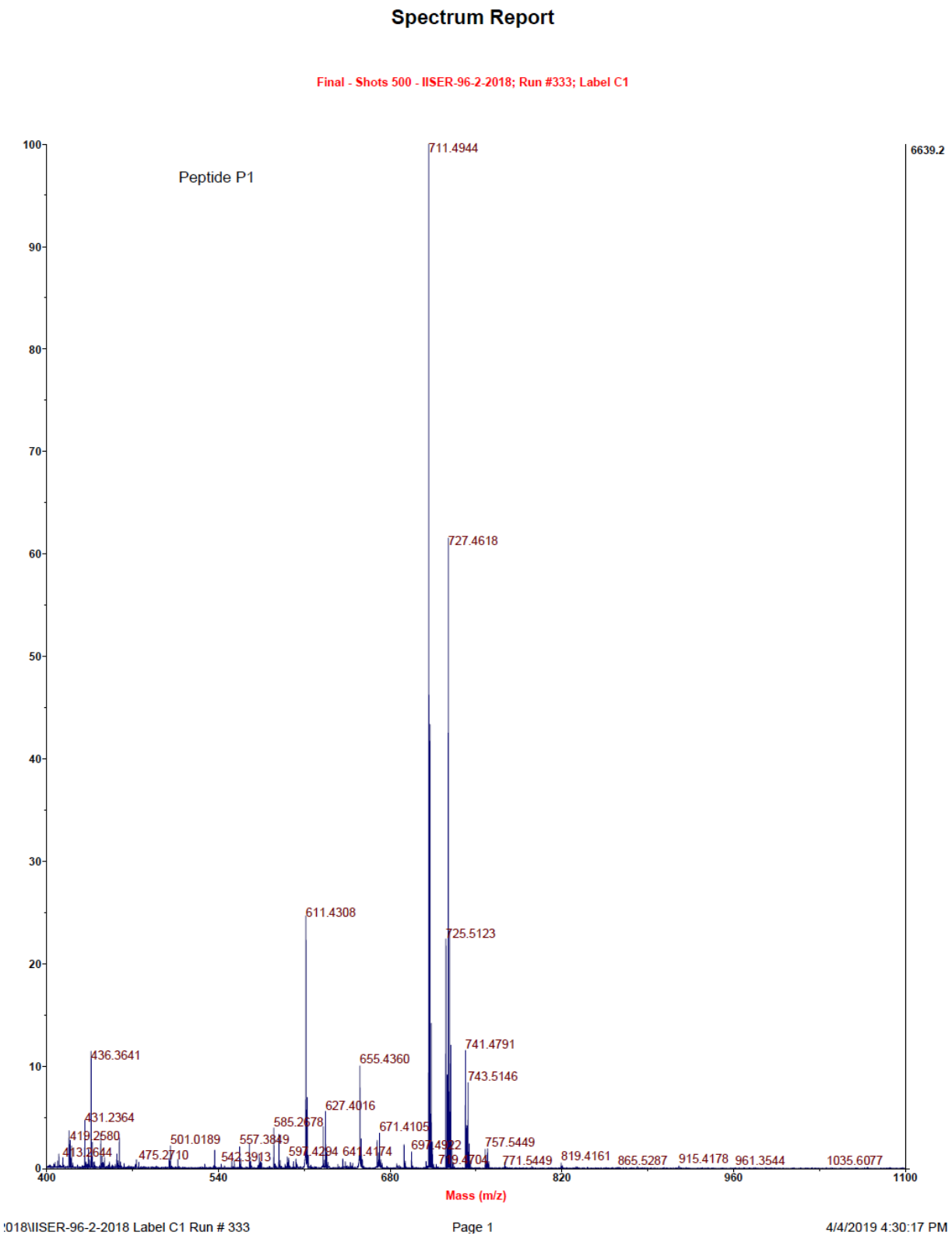

Spectrum Report

Final - Shots 400 - IISER-96-2-2019; Label B6

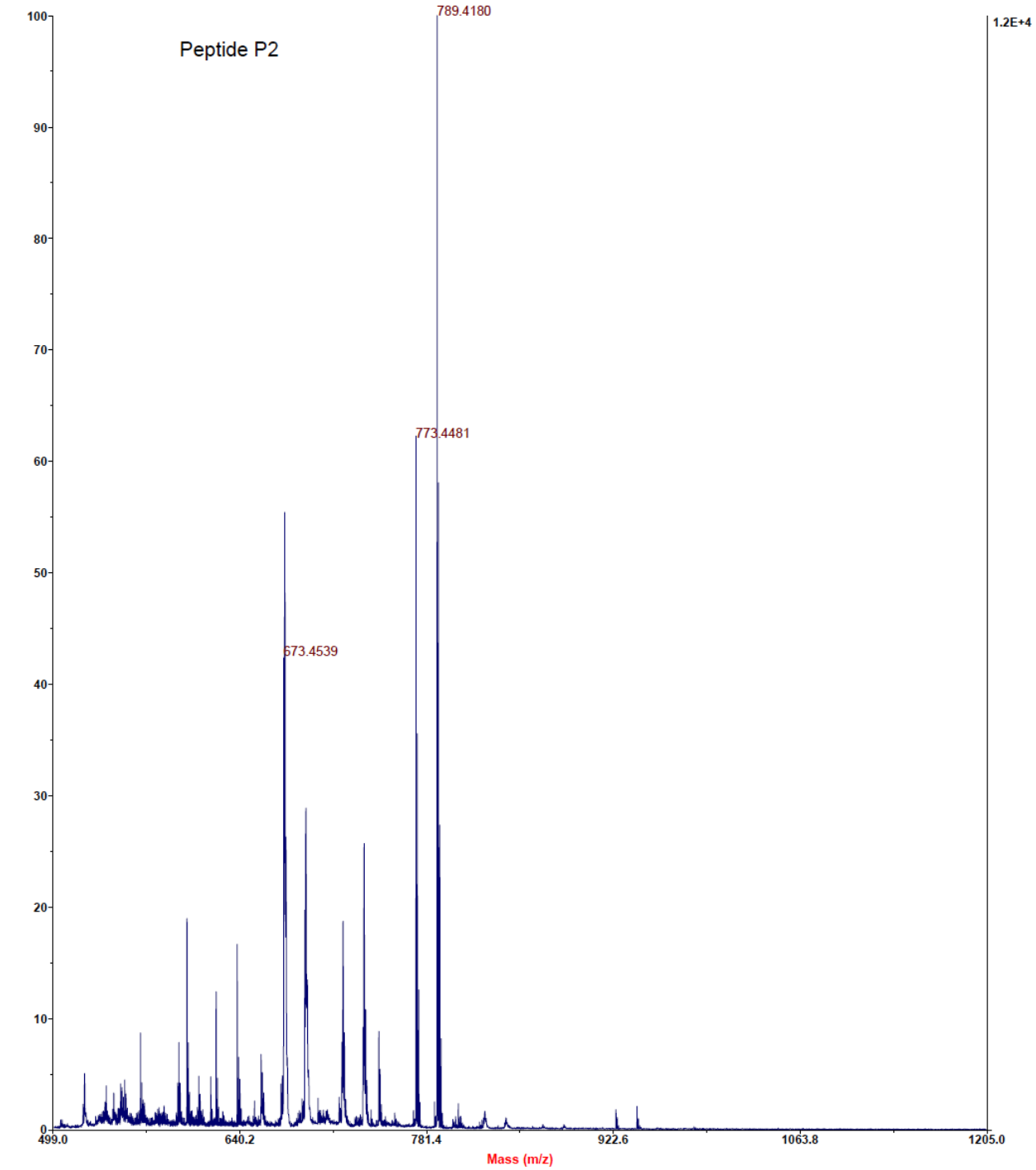

2019\IISER-96-2-2019 Label B6 Run # 102 Page 1 4/4/2019 3:50:23 PM

IISER PUNE

K. Veeresh <k.veeresh@students.iiserpune.ac.in>

FW: Permission Request Form: Kuruva Veeresh

1 message

CONTRACTS-COPYRIGHT (shared) <Contracts-Copyright@rsc.org> Mon, Jan 6, 2020 at 7:18 PM
To: "k.veeresh@students.iiserpune.ac.in" <k.veeresh@students.iiserpune.ac.in>

Dear Kuruva

The Royal Society of Chemistry (RSC) hereby grants permission for the use of your paper(s) specified below in the printed and microfilm version of your thesis. You may also make available the PDF version of your paper(s) that the RSC sent to the corresponding author(s) of your paper(s) upon publication of the paper(s) in the following ways: in your thesis via any website that your university may have for the deposition of theses, via your university's Intranet or via your own personal website. We are however unable to grant you permission to include the PDF version of the paper(s) on its own in your institutional repository. The Royal Society of Chemistry is a signatory to the STM Guidelines on Permissions (available on request).

Please note that if the material specified below or any part of it appears with credit or acknowledgement to a third party then you must also secure permission from that third party before reproducing that material.

Please ensure that the thesis includes the correct acknowledgement (see http://rsc.li/permissions for details) and a link is included to the paper on the Royal Society of Chemistry's website.

Please also ensure that your co-authors are aware that you are including the paper in your thesis.

Regards

Gill Cockhead

Contracts & Copyright Executive

CHAPTER 5

Design of Crown Ether Embedded γαα-Hybrid Peptide Foldamer Ion Channels

1. Introduction

Ion channels are the complex protein molecules, which are responsible for the regulated passage of ions through the cell membrane. In the biological system, ion channels perform extensive roles such as conduction of nerve impulse, salt and water balance, muscle contractions, absorption of nutrients and ions, and hormonal secretion.[1] Dysfunction of the ion channels leads to channelopathies such as cystic fibrosis, epilepsy, diabetes, cardiac arrhythmia, asthma and cancer.[2] Due to their widespread biological applications, extensive efforts have been made in the literature to mimic the activity of ion channels using various synthetic molecules.[3,4] The ability of crown ethers in selective complexation of cations has served as an attractive strategy to use them as ion channels. Voyer and colleagues have designed the unimolecular transmembrane channels by placing crown ether derived phenylalanine amino acid ionophores at (*i*, *i+4*, *i+7*, *i+11*,….) positions in the oligo-leucine α-helix scaffolds.[5] This placing keeps the crown ether rings on top of others to form a crown ether nano-pore which was expected to act like an ion transporter. The structure of this peptide ion channel is represented in Scheme **1A**. Inspired by this, a variety of crown ether functionalized scaffolds were synthesized and utilized as transmembrane ion channels, including hydraphiles,[6] (see Scheme **1B**) polyisocyanates,[7] 2,6-pyridylene ethynylene polymer,[8] oligo(p-phenylene) rods,[9] (see Scheme **1C**) etc.[10] In continuation, we sought to investigate whether the hybrid peptide foldamers can be used to construction of artificial ion channels.

2. Aim and rationale of the present work

Extensive work by the groups of Gellman, Seebach, and others revealed that peptides composed of β-, γ- and higher homologated amino acids can fold into definite structures similar to α-peptides.[11] In addition to the homo-oligomers of β- and higher homologues, mixed $(\alpha\beta)_n$,[12] $(\alpha\gamma)_n$,[13] $(\beta\gamma)_n$[14] and $(\alpha\delta)_n$[15] sequences have attracted considerable attention due to their different H-bonding patterns. Among the hybrid peptides, the αγ-hybrid peptides have preferred fold into C_{12}-helical structures even in short peptides sequences.[16] These short helices have been utilized as templates to construct metal-helix frameworks[17] and peptide nanotubes.[18] Further, we previously demonstrated the stable $C_{10/12}$-helical structures from ααγ-hybrid peptides in single crystals.[19] The stable helical structures of hybrid peptides composed of α- and γ-amino acids motivated us to design a crown ether

functionalized γαα-hybrid peptides to study the cation conducting properties. In this chapter, we sought to investigate whether the γαα-hybrid peptides foldamers can be used to construction of artificial ion channels.

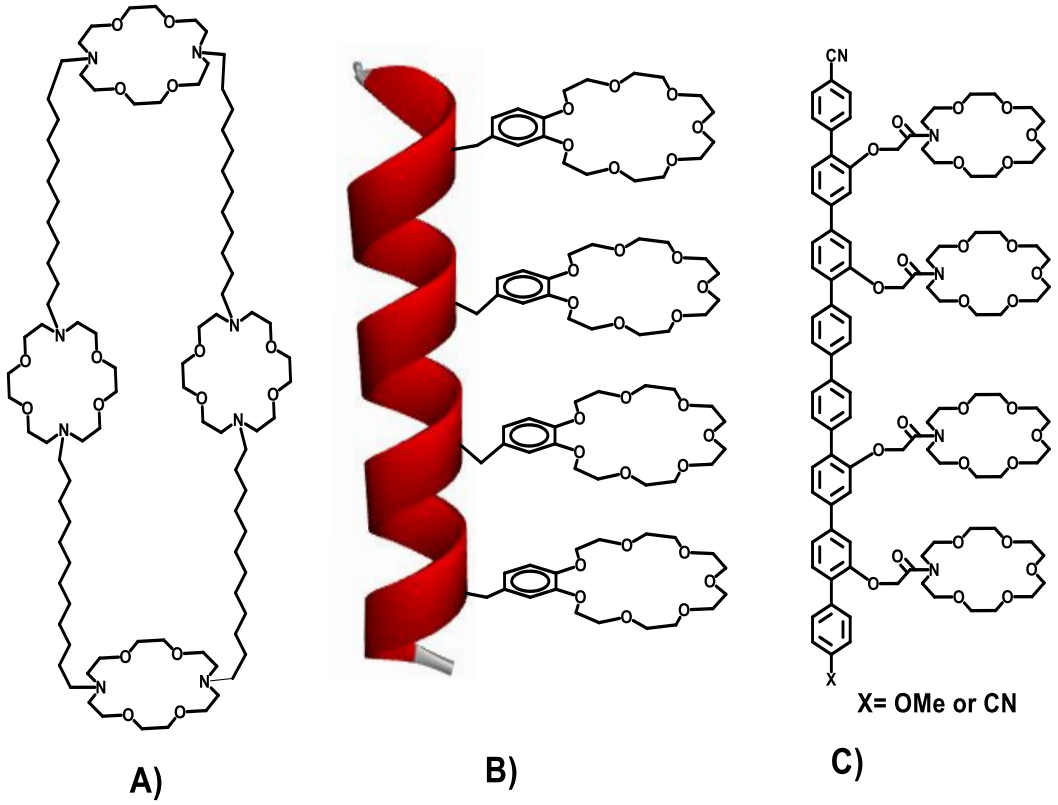

Scheme 1: Unimolecular crown ether based transmembrane ion channels. A) Hydrophiles B) α-helix-crown ether ion channels C) Oligo (p-phenylene)-crown ether ion channels.

3. Design and synthesis

Prelude to designing the crown ether functionalized $(\gamma\alpha\alpha)_n$-hybrid peptide ion channels, we have elucidated the conformation and side-chain projection of new $(\gamma\alpha\alpha)_n$-hybrid peptide foldamers by crystallizing the $(\gamma\alpha\alpha)_3$-hybrid peptide **P1** (see Schem **2**). The crystal structure and amino acid sequence of the peptide **P1** is shown in Figure **1**. The crystal analysis revealed that the peptide **P1** is stabilized by C_{12} and C_{10} intramolecular hydrogen bonding pseudocycles formed between *i* and *i+3* residues of the backbone. The H-bonding parameters of the **P1** helix are given in Table **2**. One of the potential C_{12} H-bonding cycles between Ala (5) and Ala (8) has been dirapted by a water molecule. These types of solvent interfearences have been found in the literature.[20] The backbone conformation of α and γ hybrid helices are generally defined by introducing additional

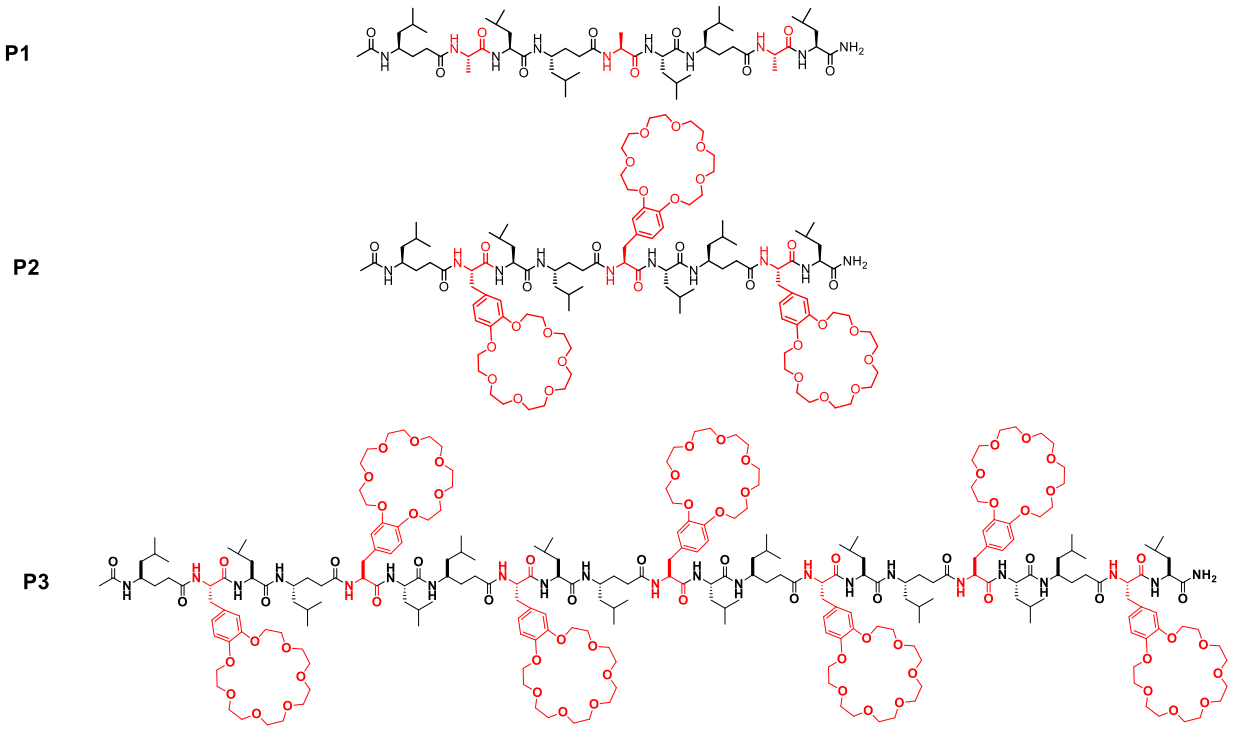

Scheme 2: Chemical structure of γαα-hybrid peptide **P1** and crown ether embedded γαα-hybrid peptide **P2** and **P3**

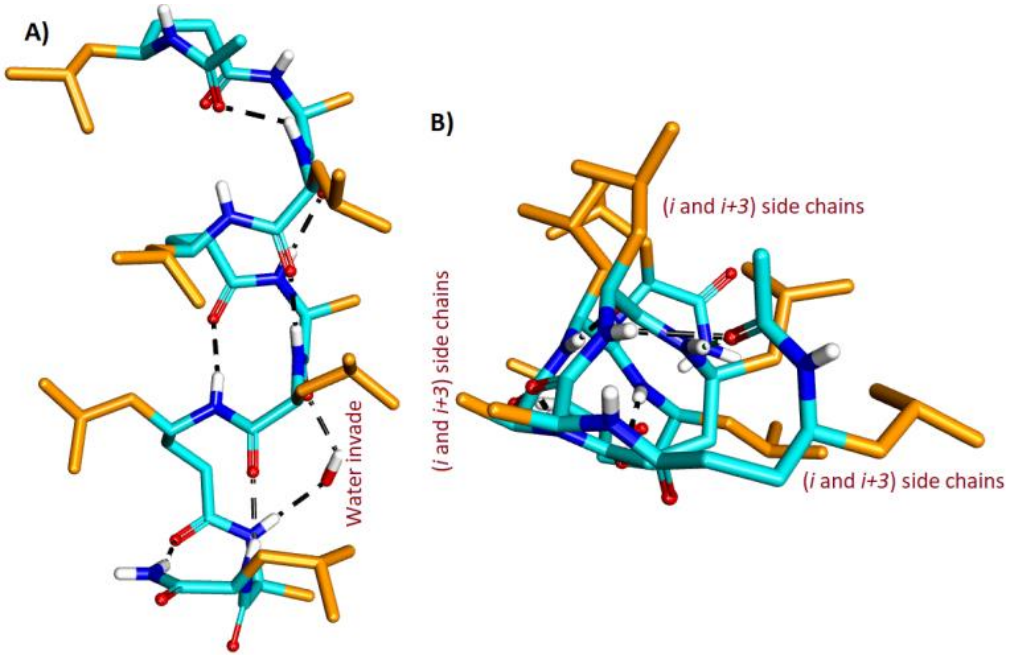

Figure 1: Crystal structure of peptide Ac-(γL-A-L)$_3$-NH$_2$ (**P1**). (A) Side view of the helix, showing $C_{12/10}$-helical structure. (B) Top view of the helix, showing *i* and *i+3* amino acid side chains stacking on top of each other.

torsion variables θ_1 and θ_2 along with ϕ and ψ at γ-residues. The torsion angles of the helical backbone are tabulated in Table **1**. Conformational analysis of **P1** revealed that the γ^4-residues adopted *gauche*$^+$, *gauche*$^+$ (g^+, g^+, $\theta_1 \approx \theta_2 \approx 60°$) conformation at the C_β–C_γ (θ_1) and C_α–C_β (θ_2) bonds. The average backbone torsion angles for the three γ^4-residues are: $\phi = (-105.7 \pm 6)°$, $\theta_1 = (52.9 \pm 2)°$, $\theta_2 = (65.9 \pm 2)°$, $\psi = (-146.6 \pm 13)°$. Interestingly, the top view of the peptide **P1** showed the projection of side chains at three faces of the helical cylinder and side chains of all the *i* and *i+3* residues stack on top of each other along the helical axis as shown in Figure. **1B**.

Table 1 Torsion angles of peptide **P1** backbone

Residue	$\boldsymbol{\phi}$ °	$\boldsymbol{\theta}_1$°	$\boldsymbol{\theta}_2$°	$\boldsymbol{\psi}$°
γ-Lue (1)	-104.41	51.85	65.42	-153.16
Ala (2)	-95.60			-16.96
Leu (3)	-73.93			-44.53
γ-Leu (4)	-112.17	52.26	64.42	-133.05
Ala (5)	-57.66			-35.63
Leu (6)	-68.87			-21.47
γ-Leu (7)	-100.58	54.71	68.00	-153.51
Ala (8)	-60.52			-29.15
Leu (9)	-81.89			0.5

Table 2: Hydrogen bond parameters of **P1**

Donor (D)	**Acceptor (A)**	**DH….A (Å)**	**D….A (Å)**	**NH….O (deg)**
N3	O1	2.217	2.855	130.86
N5	O3	2.033	2.893	178.76
N6	O4	2.037	2.888	169.99
N7	O5	2.280	3.068	152.44
N9	O7	2.064	2.859	153.45
N10	O8	2.147	2.983	163.97

Based on the side chain projection of **P1,** we have selectively replaced alanine residues (i.e. *i* and *i+3* residues) of **P1** with 21-crown-7-phenylalanine to construct peptides **P2** and **P3**. The selective replacement of alanine with 21-crown-7-phenylalanine projects the crown ether rings to one face of the helix and stacks them on top of each other (Scheme **3C**). We speculate that these crown ether stack provides a pore for translocation of ions through the membrane. The design of γαα-hybrid peptide foldamer ion channels and sequences of designed peptides **P2** and **P3** are schematically represented in Scheme **3** and Scheme **1**, respectively. The crown ethers are introduced into the sequences using FmocHN-21-crown-7-phenylalanine amino acid.[5a] Both peptides **P2** and **P3** were synthesized through the solid-phase method. The 9-mer peptide **P2** consisting of three 21-crown-7-phenylalanine ion carriers, while the 21-mer peptide **P3**, the extended version of **P2**, consisting of seven 21-crown-7-phenylalanines ion carriers.

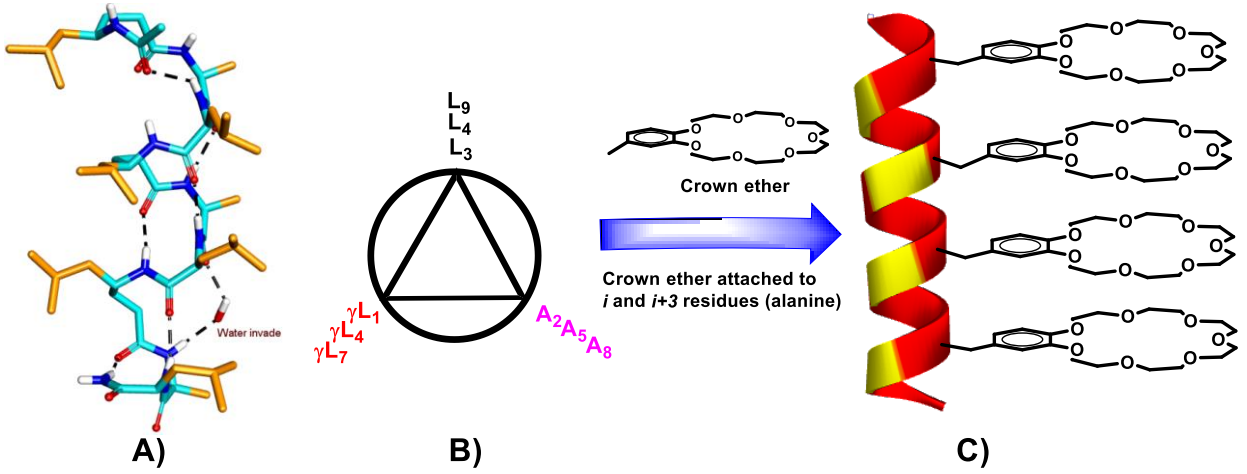

Scheme 3: Schematic representation (γαα)-hybrid peptide ion channels design. A) Crystal structure of γαα-hybrid peptide **P1** (Ac-HN-(γLAL)$_3$-CONH$_2$). B) Helical wheel diagram of γαα-hybrid peptide **P1,** showing the *i* and *i+3* Side-chain aggregation into three corners of helical cylinder. C) Crown ethers attached (i.e., to alanine residues) γαα-hybrid peptide ion channel, showing crown ether rings stacking to form a nanopore.

4. Conformational studies of ion channel peptides

To validate the conformational properties of γαα-peptides after the crown ether attachments, we subjected peptide **P2** to the 2D NMR studies in $CDCl_3$ solvent. Well dispersed chemical shifts of all amide NH protons in ^{1}H NMR spectrum hint a definite

structure of the peptide **P2** in solution at room temperature. The amino acids in the peptide sequences were identified using the TOCSY spectrum. A partial TOCSY spectrum of Peptide P2 is shown in Figure **2**.

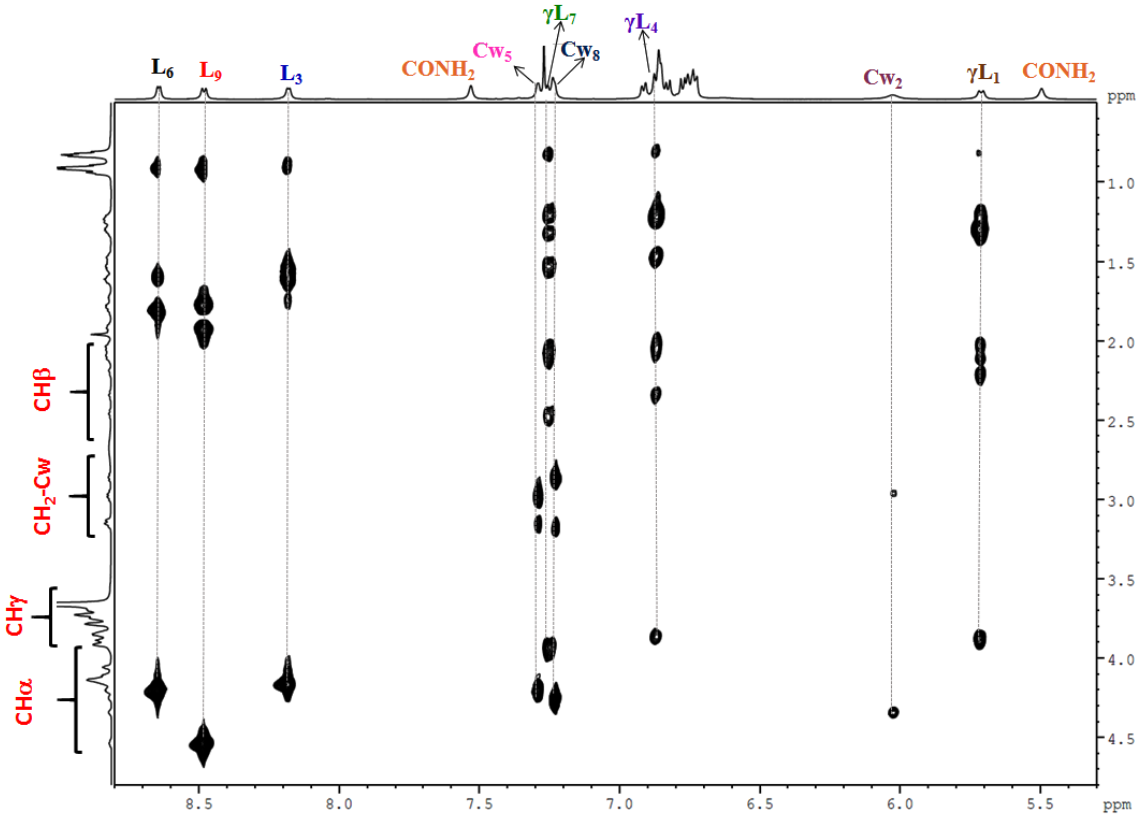

Figure 2: Partial TOCSY spectra of Peptide **P2**. **(**Sequence of NH protons were assigned by ROESY)

The ROESY spectrum reveals the characteristic sequential NOEs of helical structure between NH(*i*)↔NH(*i+1*) residues.[21] Fully assigned ROESY spectrum with all unambiguous NH↔CH*α*and NH↔CHγ NOEs is shown in Figure **3**. In a sharp contrast to the NH(α-residue, *i*)↔NH(α-residue, *i+1*) and NH(α-residue, *i*)↔NH(γ-residue, *i+1*)NOEs, we did not observed the NOEs between the NH(γ-residue, *i*)↔NH(α-residue, *i+1*). This is probably due to the relatively long distance between the two residues.[21] ROESY spectrum with all unambiguous NH(*i*)↔NH(*i+1*) NOEs is shown in Figure **4**. Further, the DMSO-d_6 titration experiment reveals the change in the chemical shift values of N-terminal amide NH groups γ-Leu (1) NH and α-Phe (2) NH increasing concentration of DMSO-d_6, suggesting NH group of these residues were exposed to the solvent. No considerable change in the chemical shift values were observed for

the other residues (Leu 3 to Leu 9) in the sequence, indicating that the amide protons of these residues are not exposed to the solvent and probably involved in the intramolecular H-bonding with amide CO groups in the sequences. Solvent dependence of NH chemical shifts of the peptide **P2**, at varying concentrations of $(CD_3)_2SO$ is shown in Figure **5**.

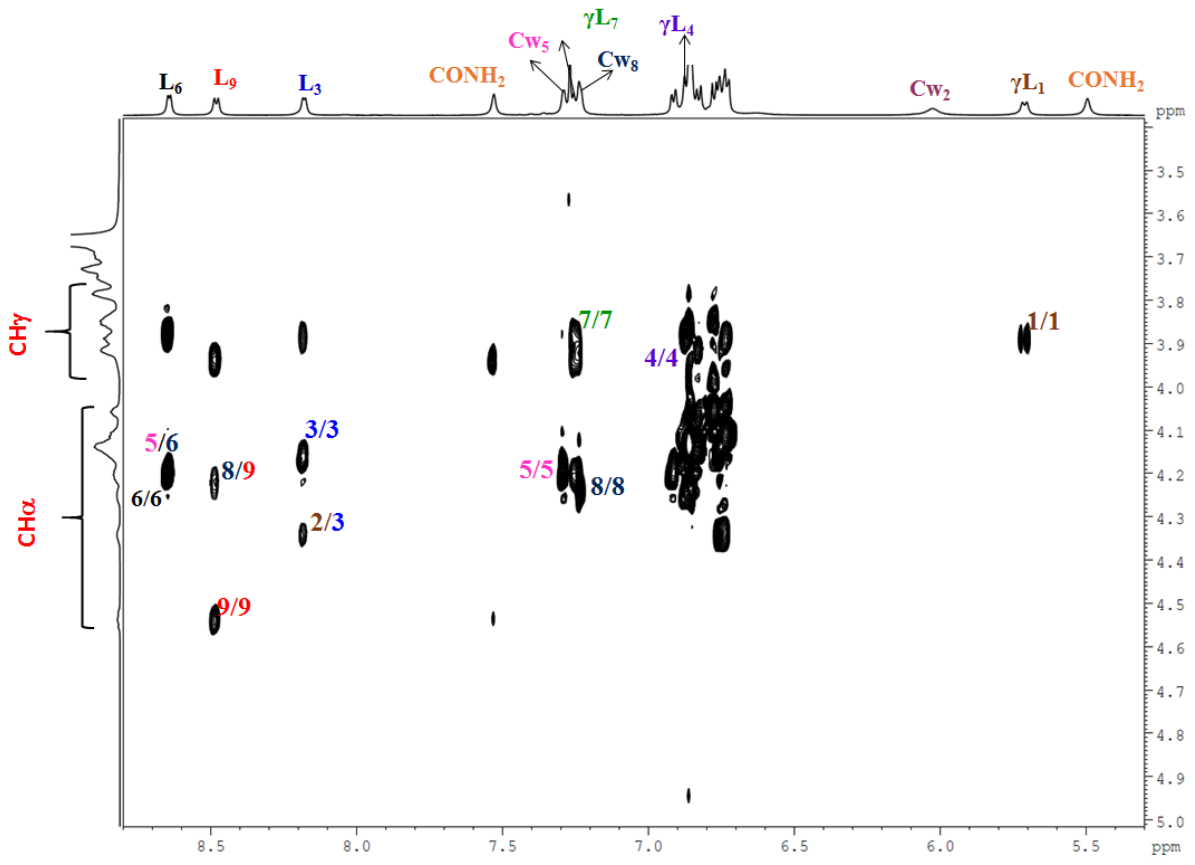

Figure 3: Partial ROESY spectrum of **P2** in CDCl3 showing NH↔α and γ CH_2 NOEs.

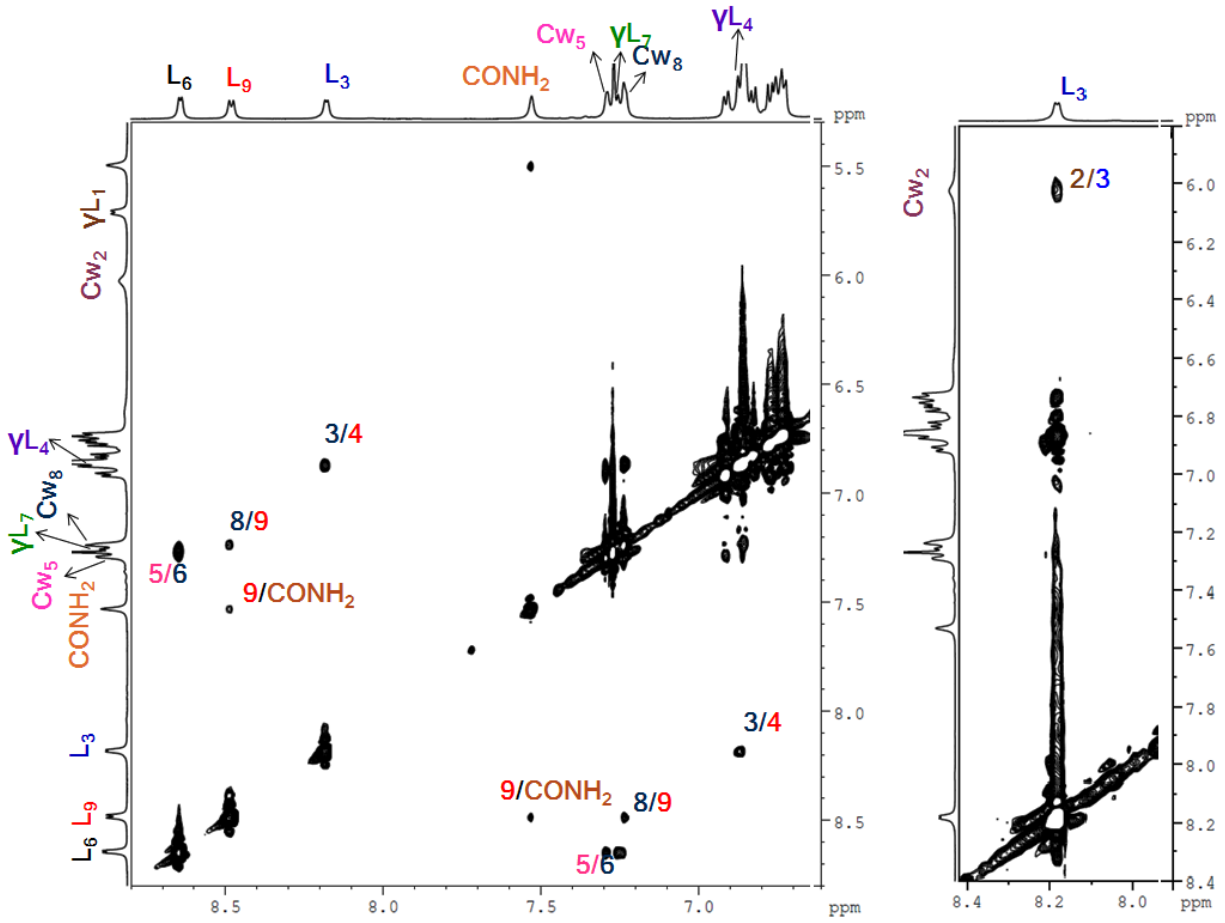

Figure 4: Partial ROESY spectrum of **P2** in CDCl3 showing NH↔NH NOEs.

Using the unambiguous NOEs (Table **3**) and hydrogen bonding constraints, molecular dynamic simulations were performed to get the energy minimized structure of **P2**.[22] The energy minimized solution structure of **P2** is shown in Figure **6**. The structure revealed that the peptide **P2** adopted helical conformation in solution and the structure is stabilized by the seven intramolecular hydrogen bonds (C_{12} and C_{10}). More importantly, no influence of side-chain crown ethers on structures of the peptides was observed. The top view of the NMR structure showed the orientation of crown ethers at one side of the $C_{12/10}$-helix. The stable helical conformation and the projection of side chains provide greater scope to examine their ion transporting activity.

Table 3: List of unambiguous NOEs constraints used for molecular dynamic simulations

Residue	**H-atom**	**Residue**	**H-atom**	**NOE($CDCl_3$)**
Cw(2)	NH	Leu(3)	NH	Weak
Leu(3)	NH	γLeu(4)	NH	Strong
Cw(5)	NH	Leu(6)	NH	Strong
Cw(8)	NH	Leu (9)	NH	Medium
Leu(9)	NH	$CONH_2$(9)	NH	Medium
γLeu (1)	NH	γLeu(1)	Hγ (backbone)	Medium
Leu(3)	NH	Leu(3)	CαH(backbone)	Strong
γLeu (4)	NH	γLeu(4)	CγH(backbone)	Medium
Cw(5)	NH	Cw(5)	CαH(backbone)	Strong
Leu(6)	NH	Leu(6)	CαH(backbone)	Strong
γLeu (7)	NH	γLeu(7)	CγH(backbone)	Medium
Cw(8)	NH	Cw(8)	CαH(backbone)	Strong
Leu(9)	NH	Leu(9)	CαH(backbone)	Medium
Leu(3)	NH	Cw(2)	CαH (backbone	Medium
Leu(6)	NH	Cw(5)	CαH(backbone)	Strong
Leu(9)	NH	Cw(8)	C^{α}H(backbone)	Medium

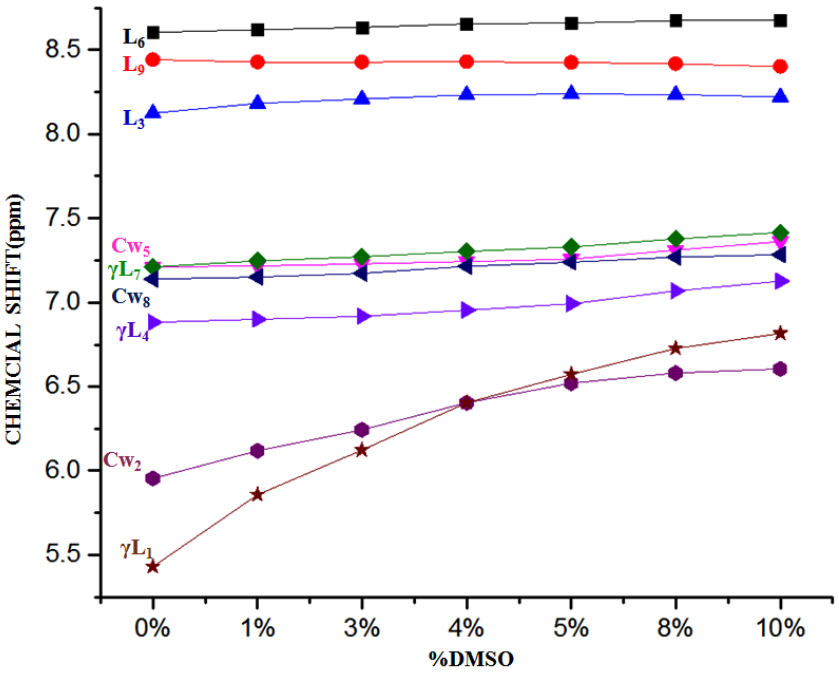

Figure 5: Solvent dependence of NH chemical shifts of the peptide **P2**, at varying concentrations of$(CD_3)_2SO$

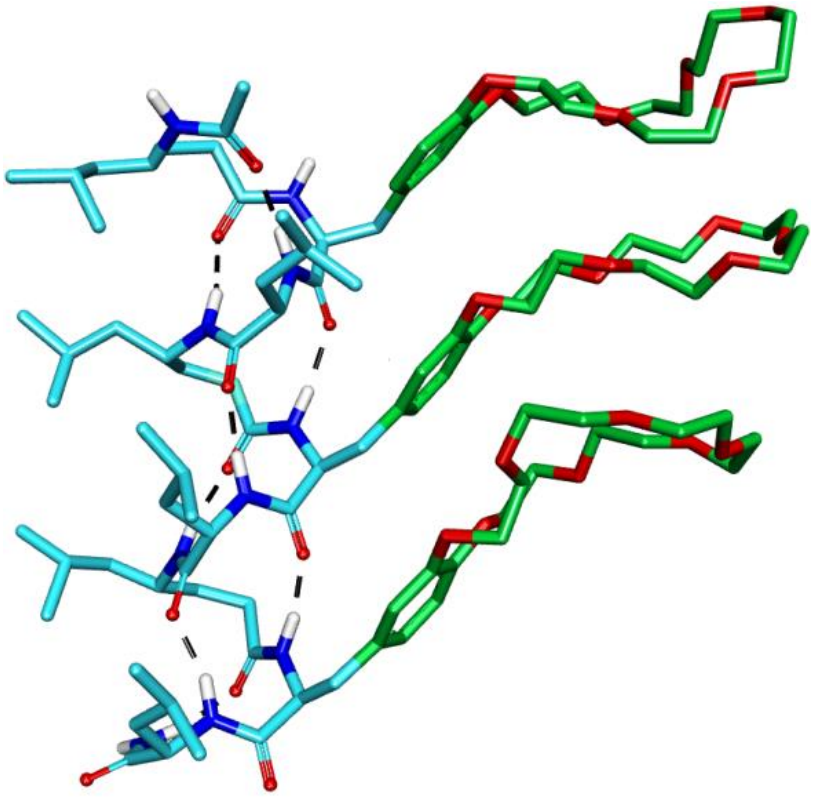

Figure 6: Solution state conformation of peptide **P2**, showing crown ethers orientation to form a pore along the helix to pass cations.

5. Ion transporting activity

a. HPTS based fluorescence assay

Ion transporting activity of peptide **P2** and **P3** were tested using synthetic liposomes.[23] A pH-sensitive fluorescent dye, pyranine (8-hydroxypyrene-1,3,6-trisulfonic acid (HPTS)) was used as a marker. The dye was entrapped in liposomes with the internal pH = 6.4 and these liposomes were diluted with cationic (Na^+, K^+ or Cs^+) solution of pH = 7.2. The addition of the capable ion transporter destroys the proton gradient across the lipid bilayer by exporting the protons from liposome to outside solution, simultaneously importing the cations into liposome from outside to maintain the ionic equilibrium. The decrease in proton gradient of inside solution of liposome was measured by recording the change in fluorescence of HPTS, which is proportional to the number of ions transported. We monitored the ion channel activity up to 450 seconds, where 100% of ions transport was achieved by disrupting the liposomes by treating with Triton X-100.

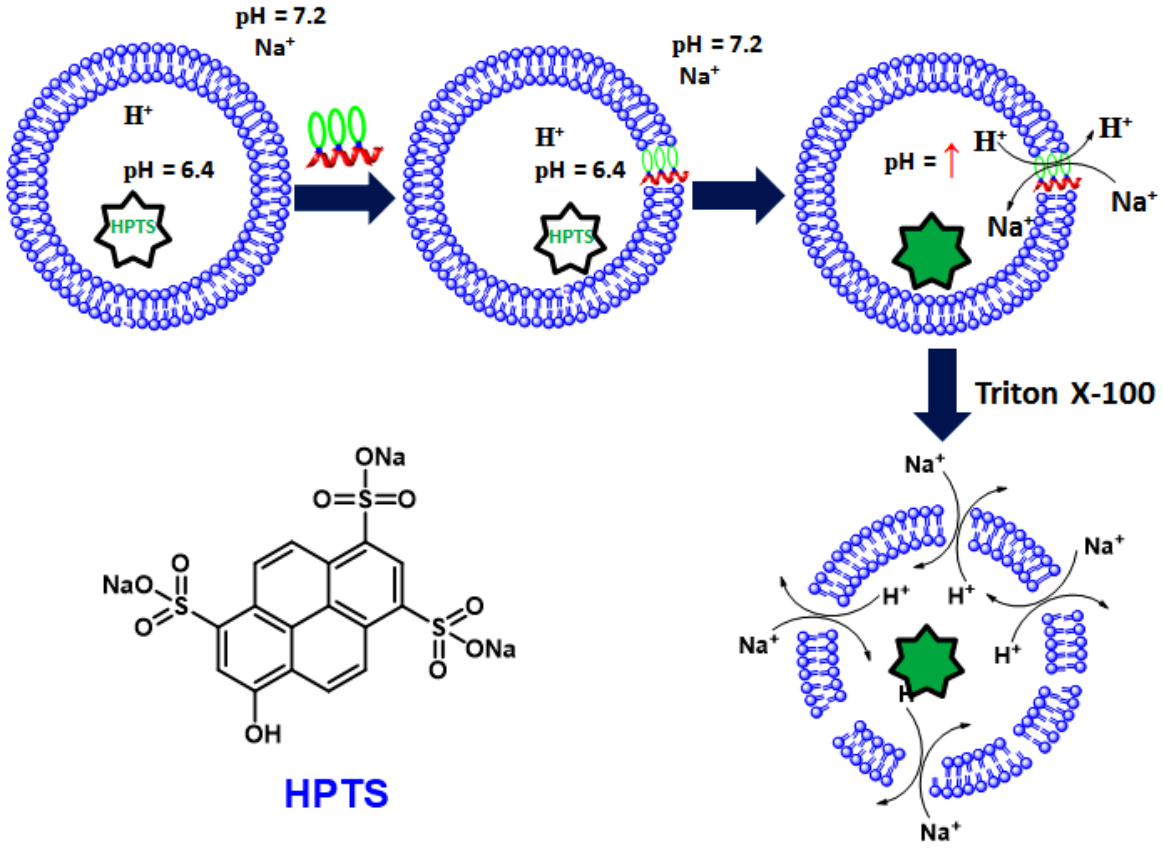

Figure 7: Schematic representation of HPTS based liposome assay and chemical structure HPTS

The experimental results of peptide **P1** and **P2** are shown in Figure **8**. Both the peptides were dissolved in methanol and their ion transporting activity was tested using three different cations (Na^+, K^+ and Cs^+). After the addition of **P2** to the solution containing liposomes, a sudden increase in fluorescence intensity (i.e. rapid transport of ions) was observed and immediately reached to the saturation. In sharp contrast to peptide **P2**, peptide **P3** showed a gradual increase in the fluorescence intensity and reached saturation. Both peptides show the ion transporting activity, however, we observed rapid cation transport in the case of peptide **P1**.

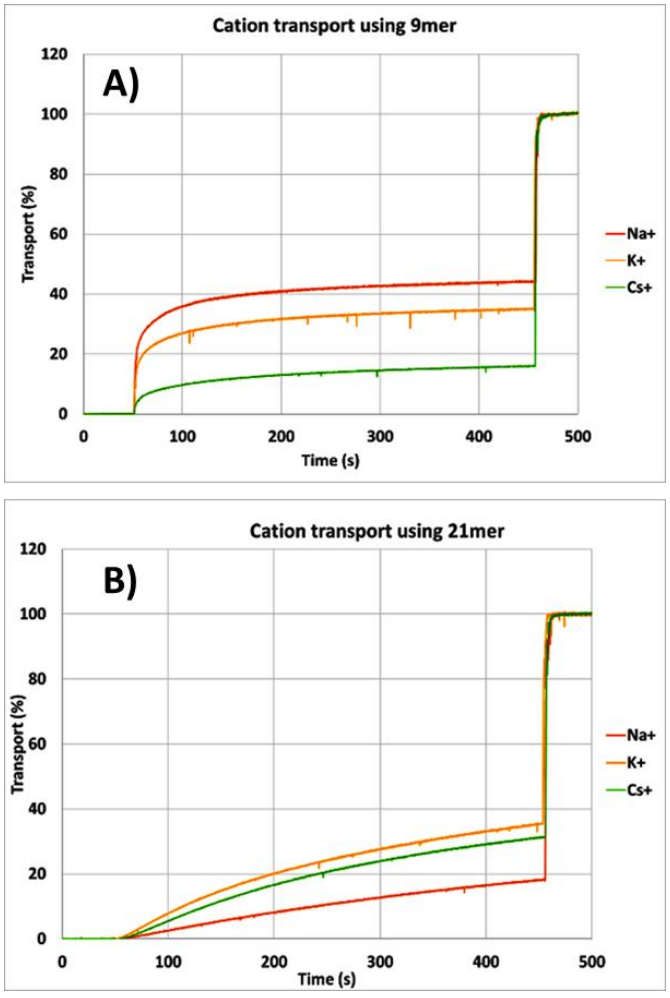

Figure 8: Ion channel activity measurement through liposome assay of peptide (A) **P2** and **(B) P3**, showing the ion channel activity against Na^+, K^+ or Cs^+ cations. The addition of peptide to the liposome solution was done at 50 s and recorded the ion transport activity up to 450 s where the complete lysis of liposomes was done by treating with Triton X-100.

b. Calcein leakage assay

In order to understand whether the transport of ions is due to membrane perturbation or through the channels, we have performed vesicle leakage assays using a fluorescent self-quenching dye calcein.[5a,24] It is expected that at lower concentration the dye gives measurable fluorescence due to poor self-quenching. Calcein leakage assay is schematically represented in Figure **9**. Both the peptides **P2** and **P3** were examined for the vesicle leakage and the resultant graph was shown in Figure **10**. A sudden increase in fluorescence was observed immediately after the addition of peptide **P2**. In contrast to **P2,** no increase in the fluorescence was observed after the addition of peptide **P3.** These results suggested that peptide **P2** perturb the vesicle membrane and lysis vesicles. The longer the length of the peptide **P3** probably accommodate into the vesicle and serve as ion transporter without perturbing the vesicle membrane. This type of ion transportation is only possible due to the orientation of the crown ether side chains at side of the helical cylinder.

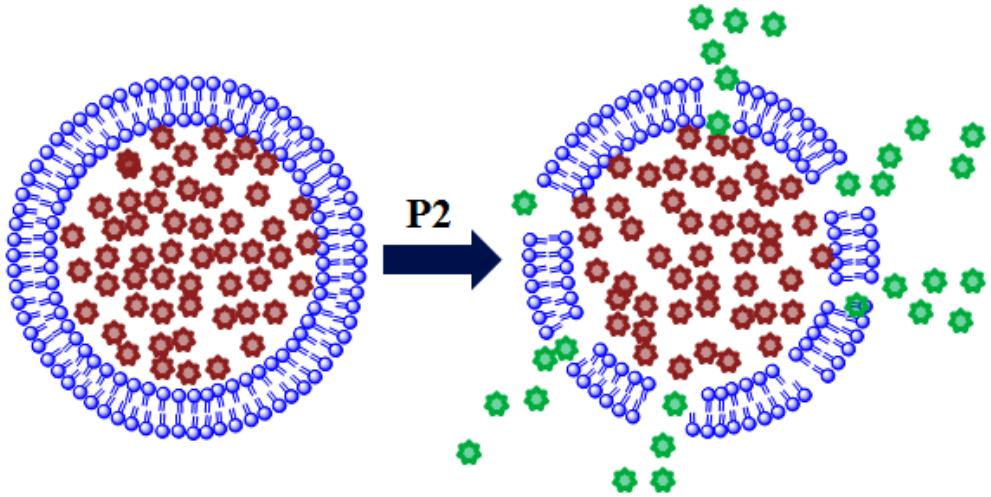

Figure 9: Schematic representation calcein leakage assay of peptide **P2,** showing the perturbation of the vesicle membrane and calcein leakage.

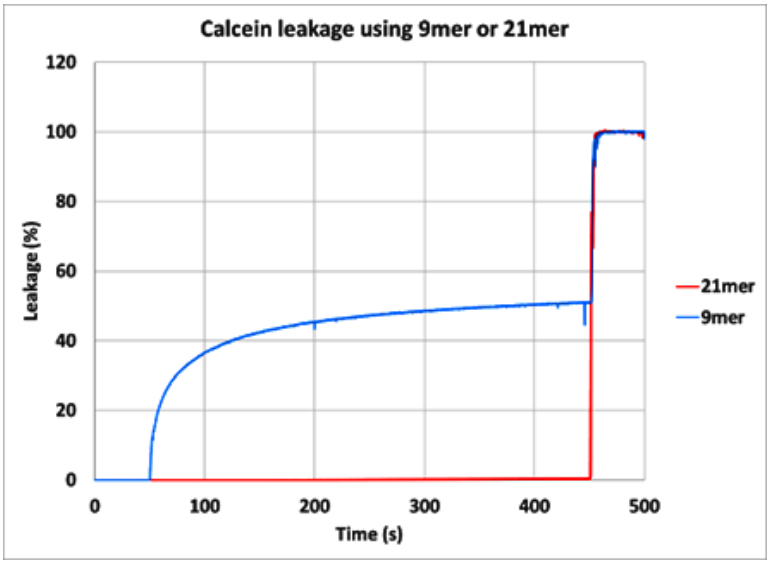

Figure **8**: Calcein leakage measurement of peptide **P2** and **P3.** The addition of peptide to the liposome solution was done at 50 s and recorded the ion transport activity up to 450 s where the complete lysis of liposomes was done by treating with Triton X-100.

6. Conclusions

In conclusion, we studied the conformations of γαα-hybrid peptides. These peptides have shown to adopt a new $C_{12/10}$-helical conformation. In addition, the structure analysis revealed the orientation of the side chains along three faces of the helix. No interference of crown ether side chains on the conformation of the peptide was observed. The stable helical conformation and the projection of side chains provide greater scope to examine their ion transporting activity. Though both designed peptides **P2** and **P3** showed the ion transporting activity, the mechanism of action is different. The shorter peptide **P2** transport cation by perturbing the membrane, while the longer peptide **P3** transport the ions without perturbing membrane, probably by incorporating into the membranes of the vesicles, similar to the previously reported α-helix. These results reported here suggested hybrid peptide foldamers can be used to design synthetic ion transport channels. These results may open new avenues to explore the hybrid peptide foldamers as new functional materials in nanobiotechnology.

7. Experimental details

7.1. Crystallographic information of peptide P1

Crystals of **P1** were grown by slow evaporation of aqueous methanol solution. A single crystal (0.18 × 0.18 × 0.18 mm) was mounted on a loop with a small amount of the paraffin oil. The X-ray data were collected at 100K temperature on a Bruker APEX(II) DUO CCD diffractometer using Mo K_α radiation (λ = 0.71073 Å), ω-scans (2θ = 56.272), for a total of 15855independent reflections. Space group $P\,2_1\,2_1\,2_1$, a = 10.576(3), b = 18.302(5), c = 33.488(9), $\alpha=\beta=\gamma$= 90, V = 6482 (3) $Å^3$, orthorhombic, Z = 4 for chemical formula C53 H98 N10 O10, with one molecule in asymmetric unit; ρcalcd = 1.145gcm^{-3}, μ = 0.081 mm^{-1}, F (000) = 2448. The structure was obtained by intrinsic methods using SHELXS-97.The final R value was 0.0703 (wR2 = 0.1936) 15763 observed reflections ($F_0 \geq 4\sigma$ ($|F_0|$)) and 2449 variables, S = 1.040. (CCDC no.1952614)

7.2. General experimental details

All the chemicals were purchased from commercially available sources. Column chromatography was performed on silica gel (100-200 mesh). Final peptides were purified on reverse phase HPLC (C8 columns, MeOH/H2O 70:30-95:5 as a gradient with a flow rate of 3.00 mL/min). **2DNMR spectroscopy:** All NMR studies were carried out by using a Bruker AVANCE III -400 and 600 MHz spectrometers. Resonance assignments were obtained by TOCSY and ROESY analysis. All two-dimensional data were collected in phase-sensitive mode, by using the time proportional phase incrimination (TPPI) method. Sets of 1024 and 512 data points were used in the t2 and t1 dimensions, respectively. For TOCSY and ROESY analysis, 32 and 72 transients were collected, respectively. A spectral width of 6007 Hz was used in both dimensions. A spinlock time of 256 ms was used to obtain ROESY spectra. Zero-filling was carried out to finally yield a data set of 2 K × 1 K. A shifted square-sine-bell window was used before processing. **Ion channel activity:** Egg yolk L-α-phosphatidylcholine was purchased from Avanti Polar Lipids (Alabaster, AL, USA) and used without further purification. All solvents were Reagent, Spectro, or HPLC grade quality, purchased commercially and used without any further purification. Water used throughout the studies was distilled and deionized using a Barnstead NANOpurII system (Boston, MA) with four purification columns. All other reagents were purchased from Sigma Aldrich Co. (Milwauke, WI). Fluorescence vesicles experiments were performed on a Varian Cary Eclipse spectrofluorometer.

7.3. Synthesis of FmocHN-Phe-21-crown-7-OH

The synthesis of this compound was reported previously [5]. We described briefly here. BocHN-Phe-21-Crown-7-OH (5.436 g, 10 mmol) was treated with a 1:1 (v/v) mixture of DCM/TFA (20 mL, 2mL/mmol) for 30 min. followed by the addition of DCM and concentration of the mixture under reduced pressure. In order to remove excess TFA, the mixture was co-evaporated with DCM thrice. The obtained compound was dissolved in1:1 (v/v) mixture of 10% aqueous Na_2CO_3/ THF (40 mL) and added Fmoc-OSu (10 mmol), the reaction mixture was stirred for 12 h. After completion of the reaction (monitored by TLC) THF was evaporated using vacuum and acidified with 10% aqueous HCl. The compound was extracted with Ethyl acetate (3 × 50 mL), the combined organic layer was washed with Brine solution (3 × 50 mL) and dried over anhydrous sodium sulfate. Ethyl acetate was evaporated to get a crude compound. Crude was dissolved in a minimal amount of Ethyl acetate and precipitated with Petroleum ether. The process was repeated twice to get a white precipitate of FmocHN-Phe-21-crown-7-OH. The compound was confirmed by ^{1}H-NMR and MALDI TOF/TOF.

White solid; yield 82% (5.4 g); ^{1}H NMR (400 MHz, $CDCl_3$) δ 7.74 (d, *J* = 7.5 Hz, 2H), 7.56 (t, *J* = 7.3 Hz, 2H), 7.37 (t, *J* = 7.3 Hz, 2H), 7.28 (t, *J* = 7.4 Hz, 4H), 6.84 – 6.51 (m, 3H), 4.63 - 4.55 (m, 1H), 4.54 – 4.35 (m, 7H), 4.25 – 4.14 (m, 1H), 4.15 - 4.05 (m, 3H), 3.88 - 3.79 (m, 2H), 3.75 – 3.50 (m, 17H).

7.4. Synthesis of peptides P1, P2 and P3

Peptides were synthesized by following the classical sold phase Fmoc-chemistry, using Knorr-Amide resin (0.2 mmol scale) as solid support. HBTU/HOBT was used as a coupling agent and 30 min and 1 h reaction times were used for deprotections and couplings, respectively. The final amine was acetylated using Ac_2O/Py. After completion of the synthesis, peptides were cleaved from the resin using 5 mL of TFA/TIPS/Phenol/H_2O (88:2:5:5) mixture. After completion of cleavage, the resin was removed by filtration. The cleavage mixture was evaporated under reduced pressure to get the gummy peptide product. Peptides were purified through reverse-phase C8 columns using MeOH/H_2O gradient. Further Purity of peptides was confirmed by the analytical C8 column in MeOH/H_2O gradient system and identified by MALDI TOF/TOF.

7.5. Molecular dynamics (MD) Structure calculation of peptide P2

Structure calculation was done using a simulated annealing protocol in vacuum using DESMOND and OPLS 2005 force field with NOE and hydrogen bonding constraints. A peptide molecule was kept in an orthorhombic simulation cell of dimensions 36.73 * 43.81 * 62.68 Å. The upper limit for distance was kept at 3.0 Å, 3.5 Å and 5 Å for strong, medium and weak NOEs respectively. All the lower distance limits were taken to be 1.8 Å. For Hydrogen bonding constraints, an upper bound of 2.5 Å and a lower bound of 1.8 Å was used. A force constant of 1 Kcal/Molwas used for all the constraints used. NOE potentials (appropriate for treating ambiguous NOE assignments) used are having the following form,

E_{NOE} = **fc** * (**lower** - *d*)^2, if *d* <**lower**;
E_{NOE} = 0, if **lower** <= *d* <= **upper**;
E_{NOE} = **fc** * (**upper** - *d*)^2, if **upper** <*d* <= **upper** + **sigma**;
E_{NOE} = **fc** * (a + **beta** * (*d* - **upper**) + c / (*d* - **upper**)), if *d* >**upper** + **sigma**;
Where *d* is the distance and fc is the force constant.

Values of sigma and beta used in the calculation are 0.5 and 1.5 respectively. The values a and c are determined automatically such that potential is continuous and differential everywhere.

Before production run simulation, a default NVT relaxation was done as implemented in DESMOND. NVT ensemble was used for the production run simulation. Berendsen thermostat with a relaxation time of 1ps was used. A RESPA integrator was used in which for all the bonded interactions, near nonbonded interactions and far nonbonded interaction time step of 1 fs was used. A cutoff of 9 Å was used for short range electrostatic interactions. A smooth particle mesh ewald method was used for treating long range electrostatic interactions. Simulated annealing was done in 6 stages. First stage consist simulation for 30 ps at 10 K. In the second stage, temperature was linearly increased to 100 K till 100 ps. In the third stage, temperature was linearly increased to 300 K till 200 ps. In the fourth stage, temperature was linearly increased to 400 K till 300 ps. In the fifth stage, the temperature was maintained at 400 k till 500 ps. In the sixth stage, the temperature was linearly decreased to 300 K till 1000 ps and maintained at 300 k till 1200 ps. 20 minimum energy structures were taken from the trajectory between 1000 ps and

1200 ps. The lowest energy structure from the trajectory between 1000 ps and 1200 ps was taken and minimized using the steepest descent method using a convergence gradient threshold of 0.05 kcal/mol/Å

7.6. Ion transport assays of P2 and P3

a. Vesicle preparation

For sodium transport experiments, vesicles were prepared by drying 0.64 mL of L-α-phosphatidylcholine (20 mg/mL solution in $CHCl_3$) and 3.1 mg of cholesterol under reduced pressure for 2 hours. Lipids were suspended in an internal buffer (15 mM HEPES, 2 mM pyranine, pH 6.2), and vortexed. The suspension was subjected to 5 freeze/thaw cycles, extruded on 0.2 µM filter using a Mini-extruder for 15 passes, and then purified through a Sephadex^{TM} G-25 column (1 X 40 cm) to remove pyranine outside vesicles using the external buffer (15 mM HEPES, 200 mM MCl, pH 6.2) as eluent. MCl design NaCl, KCl or CsCl, depending of the cation tested. The pH of the external buffer is kept at 6.2 to prevent disturbing the vesicles during purification. The pyranine loaded vesicle solution was added to the external buffer at pH 7.2 only at the beginning of the assay. The lipid concentration was obtained with the Barlett method for the quantification of phosphates.

b. Fluorescence assay

Fluorescence was measured at the emission wavelength of 520 nm with excitation at 460 nm. The slit was set to 5 nm and the temperature controlled at 298 K. For each assay, sensitivity was adjusted to obtain a signal near 900 a.u. after the lysis of vesicles by Triton X-100. Solutions of peptide were prepared in methanol at a concentration near 1 mM. In a typical experiment, 182 µL of pyranine loaded vesicle solution was added to 3 mL of external buffer in a 1 cm path-length cuvette equipped with a stir bar. After stabilization of the signal for 50 s, 10 µL of channel solution was added to reach a peptide/lipid ratio of 1/60. Fluorescence intensity was measured and, at 450 s, 10 µL of a 10% aqueous solution of Triton X-100 were incorporated to completely lyse vesicles for the determination of maximum fluorescence signal. A control assay was performed using only methanol.

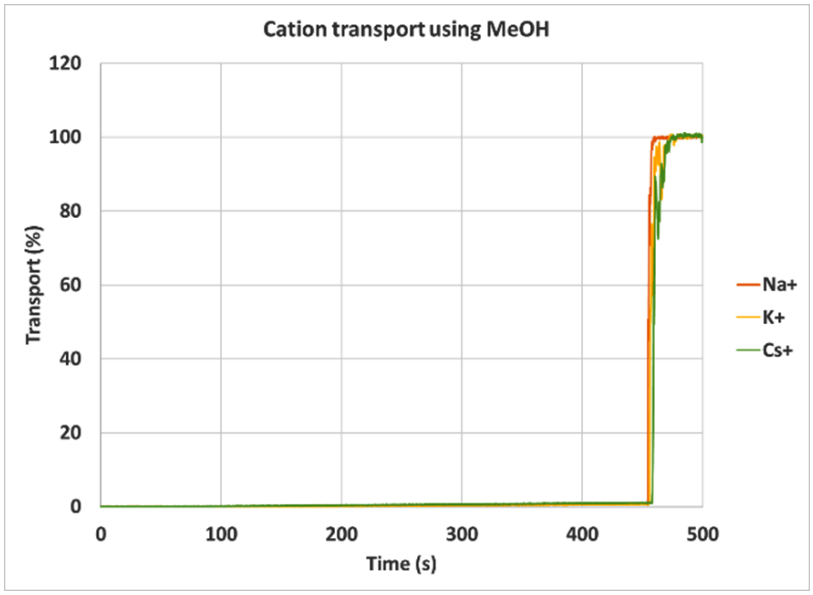

Figure **7**: A control Fluorescence assay, performed using only methanol solvent.

c. Calcein leakage assay

Vesicles were prepared as for transport assays by using calcein internal buffer (15 mM HEPES, 80 mM calcein, pH 7.2) and the external buffer (15 mM HEPES, 200 mM MCl, pH 7.2). Fluorescence was measured at the emission wavelength of 513 nm with excitation at 490 nm. The slit was set to 5 nm and the temperature-controlled at 298 K. For each assay, sensitivity was adjusted to obtain a signal near 900 a.u. after the lysis of vesicles by Triton X-100. Solutions of peptide were prepared in methanol at a concentration near 1 mM. In a typical experiment, 172 µL of calcein loaded vesicle solution was added to 3 mL of external buffer in a 1 cm pathlength cuvette equipped with a stir bar. After stabilization of the signal for 50 s, 10 µL of channel solution was added to reach a peptide/lipid ratio of 1/60. Fluorescence intensity was measured and, at 450 s, 10 µL of a 10% aqueous solution of Triton X-100 were incorporated to completely lyse vesicles for the determination of maximum fluorescence signal.

8. References

1. Hille, B. *Ion Channels of Excitable Membranes*, Sinauer, Sunderland MA, **2001**.
2. (a) Riordan, J. R.; Rommens, J. M.; Kerem, B.; Alon, N.; Rozmahel, R.; Grzelczak, Z.; Zielenski, J.; Lok, S.; Plavsic, N.; Chou, J. L.; et al. *Science* **1989**, *245*, 1066. (b) Valverde, M. A.; Cantero-Recasens, G.; Garcia-Elias, A.; Jung, C.; Carreras-Sureda A.; Vicente, R. *J. Biol. Chem.* **2011**, *286*, 32877. (c) Ashcroft, F. M. *Nature* **2006**, *440*, 440.
3. Tabushi, I.; Kuroda, Y.; okota, K. Y. *Tetrahedron Lett.* **1982**, *23*, 4601.
4. (a) Lear, J. D.; Wasserman, Z. R.; DeGrado, W. F. *Science* **1988**, *240*, 1177. (b) Voyer, N.; Robitaille, M. A.; *J. Am. Chem.* **1995**, *117*, 6599. (c) Ghadiri, M. R.; Granja, J. R.; Buehler, L. K. *Nature* **1994**, *369*, 301. (d) Doyle, D. A.; Cabral, J. M.; Pfuetzner, R. A.; Kuo, A. L.; Gulbis, J. M.; Cohen, S. L.; Chait, B. T.; MacKinnon, R. *Science* **1998**, *280*, 69. (e) Yoshii, M.; Yamamura, M.; Satake, A.; Kobuke, Y. *Org. Biomol. Chem.* **2004**, *2*, 2619. (f) Fyles, T. M.; Hu, C. W.; Luong, H. *J. Org. Chem.* **2006**, *71*, 8545 (g) Gokel, G. W.; Daschbach, M. M. *Coord. Chem. Rev.* **2008**, *252*, 886. (h) Ma, L.; Harrell, W. A. J. Davis, T. *Org. Lett.* **2009**, *11*, 1599. (i) García-Fandiño, R.; Amorín, M.; Castedo, L.; Granja, J. R. *Chem. Sci.* **2012**, ***3***, 3280.
5. (a) Otis, F.; Racine-Berthiaume, C.; Voyer, N. *J. Am. Chem. Soc.* **2011**, *133*, 6481. (b) Voyer, N. *J. Am. Chem. Soc.* **1991**, *113*, 51818. (c) Otis, F.; Auger, M.; Voyer, N. *Acc. Chem. Res.* **2013**, *46*, 2934.
6. (a) Gokel, G. W. *Chem. Commun*. **2000**, 1. (b) Murray, C. L.; Gokel, G. W. *J. Supramol. Chem.* **2001**, *1*, 23.
7. Neevel, J. G. Nolte, R. *Tetrahedron Lett.* **1984**, *25*, 2263.
8. Abe, H.; Takashima, S.; Yamamoto, T.; Inouye, M. *Chem. Commun.* **2009**, *16*, 2121.
9. Winum, J.-Y.; Matile, S. *J. Am. Chem. Soc.* **1999**, *121*, 7961.
10. (a) Chen, S.; Wang, Y.; Nie, T.; Bao, C.; Wang, C.; Xu, T.; Lin, Q.; Qu, D.-H.; Gong, X.; Yang, Y.; Zhu, L.; Tian, H. *J. Am. Chem. Soc.* **2018**, *140*, 17992. (b) Ye, R.; Ren, C.; Shen, J.; Li, N.; Chen, F.; Roy, A.; Zeng, H. *J. Am. Chem. Soc.* **2019**, *141*, 9788 (c) Gilles, A.; Barboiu, M. *J. Am. Chem. Soc.* **2016**, *138*, 426. (d) Moyer, B. A. in *Molecular Recognition: receptors for cationic guests*, ed. Gokel, G. W. *Comprehensive Supramolecular Chemistry*, Elsevier Science Ltd., Oxford, **1996**, vol. 1, pp. 377–416.

11. (a) Seebach, D.; Beck, A. K.; Bierbaum, D. J. *Chem. Biodiversity* **2004**, *1*, 1111. (b) Seebach, D.; Gardiner, J. *Acc. Chem. Res.* **2008**, *41*, 1366. (c) Gellman, S. H. *Acc. Chem. Res.* **1998**, *31*, 173. (d) Cheng, R. P.; Gellman, S. H.; De Grado, W. F. *Chem. Rev.* **2001**, *101*, 3219. (e) Horne, W. S.; Gellman, S. H. *Acc. Chem. Res.* **2008**, *41*, 1399. (f) Venkatraman, J.; Shankaramma, S. C.; Balaram, P. *Chem. Rev.* **2001**, *101*, 3131. (g) Goodman, C. M.; Choi, S.; Shandler, S.; DeGrado, W. F. *Nat. Chem. Biol.* **2007**, ***3***, 252. (h) Fülöp, F.; Martinek, T. A.; Tóth, G. K. *Chem. Soc. Rev.* **2006**, *35*, 323.
12. (a) De Pol, S.; Zorn, C.; Klein, C. D.; Zerbe, O.; Reiser, O. *Angew. Chem. Int. Ed.* **2004**, *43*, 511. (b) Hayen, A.; Schmitt, M. A.; Ngassa, F. N.; Thomasson, K. A.; Gellman, S. H. *Angew. Chem. Int. Ed.* **2004**, *43*, 505. (c) Sharma, G. V. M.; Nagendar, P.; Jayaprakash, P.; Krishna, P. R.; Ramakrishn, K. V. S.; Kunwar, A. C. *Angew. Chem. Int. Ed.* **2005**, *44*, 5878. (d) Schmitt, M. A.; Choi, S. H.; Guzei, I. A. Gellman, S. H. *J. Am. Chem. Soc.* **2006**, *128*, 4538.
13. (a) Baldauf, C.; Günther, R.; Hofmann, H. -J. *J. Org. Chem.* **2006**, ***71***, 1200. (b) Vasudev, P. G.; Ananda, K.; Chatterjee, S.; Aravinda, S.; Shamala, N.; Balaram, P. *J. Am. Chem. Soc.* **2007**, *129*, 4039. (c) Sharma, G. V. M.; Chandramouli, N.; Choudhary, M.; Nagendar, P.; Ramakrishna, K. V. S.; Kunwar, A. C.; Schramm, P.; Hofmann, H. -J. *J. Am. Chem. Soc.* **2009**, *131*, 17335.
14. (a) Grison, C. M.; Robin, S.; Aitken, D. J. *Chem. Commun.* **2016**, *52*, 7802. (b) Guo, L.; Almeida, A. M.; Zhang, W.; Reidenbach, A. G.; Choi, S. H.; Guzei, I. A.; Gellman, S. H. *J. Am. Chem. Soc.* **2010**, *132*, 7868.
15. Sharma, G. V. M.; Babu, B. S.; Ramakrishna, K. V. S.; Nagendar, P.; Kunwar, A. C.; Schramm, P.; Baldauf, C.; Hofmann, H.-J. *Chem. Eur. J.* **2009**, *15*, 5552.
16. Jadhav, S. V.; Bandyopadhyay, A.; Gopi, H. N. *Org. Biomol. Chem.* **2013**, *11*, 509.
17. Misra, R.; Saseendran, A.; Dey, S.; Gopi, H. N. *Angew. Chem., Int. Ed.* **2019**, *58*, 2251.
18. Jadhav, S. V.; Misra, R.; Gopi, H. N. *Chem. Eur. J.* **2017**, ***23***, 3764.
19. Ganesh Kumar,M.; Benke, S. N.; Raja, K. M. P.; Gopi, H. N. *Chem. Commun.* **2015**, *51*, 13397.
20. (a) Basuroy, K.; Dinesh, B.; Shamala, N.; Balaram, P. *Angew. Chem., Int. Ed.* **2013**, *52*, 3136. (b) Karle, I. L.; Flippen-Anderson, J. L.; Uma, K.; Balaram, P. *Int. J. Pept. Protein*

Res. **1994**, *44*, 491. (c) Karle, I. L.; Flippen-Anderson, J. L.; Uma, K.; Balaram, P. *Biopolymers* **1993**, *33*, 827.

21. Sonti, R.; Dinesh, B.; Basuroy, K.; Raghothama, S.; Shamala, N.; Balaram, P. *Org. Lett.*, **2014**, *16*, 1656.
22. Shankaramma, S. C.; Kumar Singh, S.; Sathyamurthy, A.; Balaram, P. *J. Am. Chem. Soc.***1999**, *121*, 5360.
23. (a) Clement, N. R.; Gould, J. M. *Biochemistry* **1981**, *20*, 1534. (b) Aguedo, M.; Wache, Y.; Belin, J. M. *FEMS Microbiol. Lett.* **2001**, *200*, 185.
24. Benachir, T.; Lafleur, M. *Biophys. J.* **1996**, *70*, 831.

9. Appendix

^{1}H-NMR of compound 1

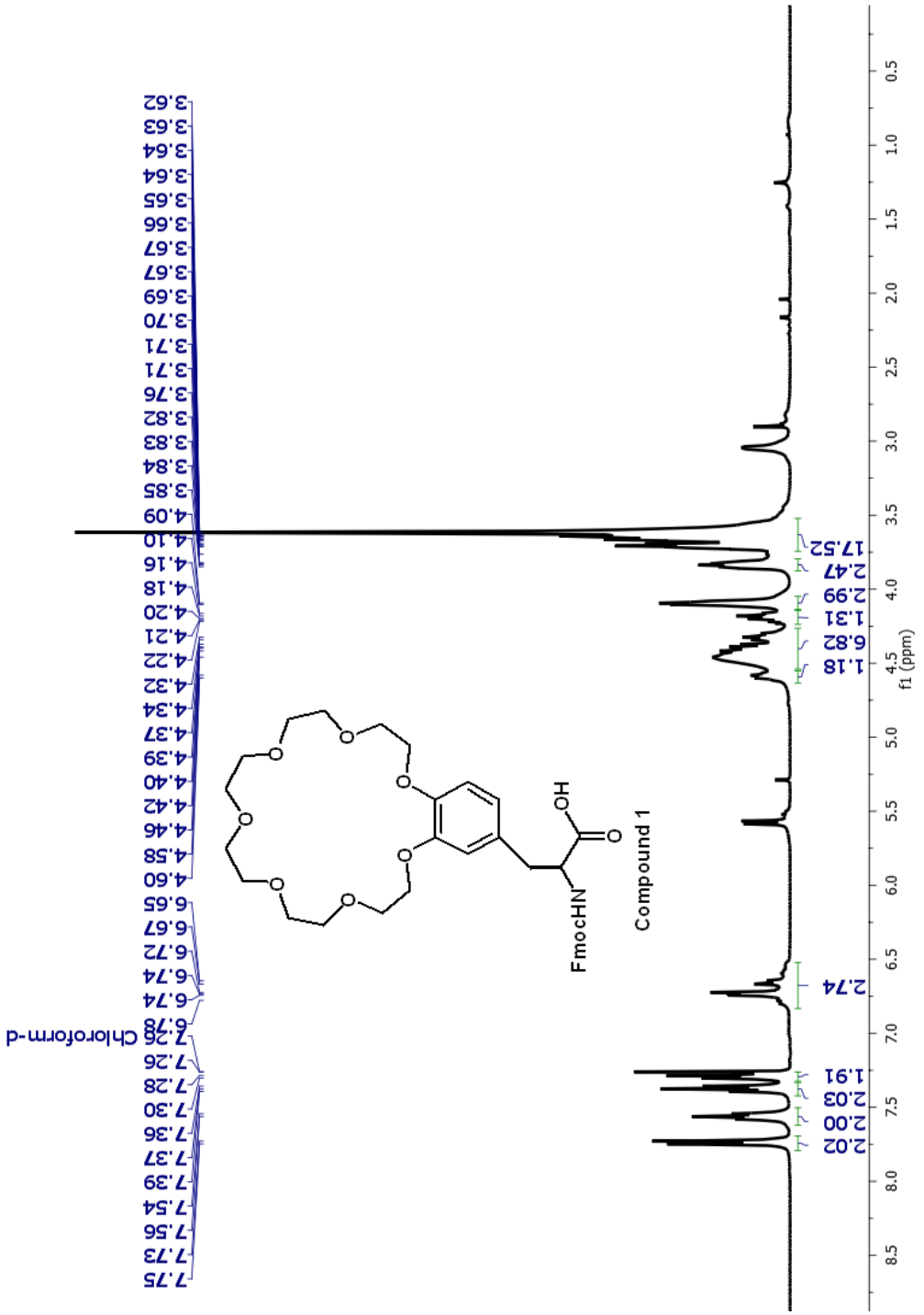

[1]H-NMR of Peptide P2. (Sequence of NH protons were assigned based on the NOEs of ROESY)

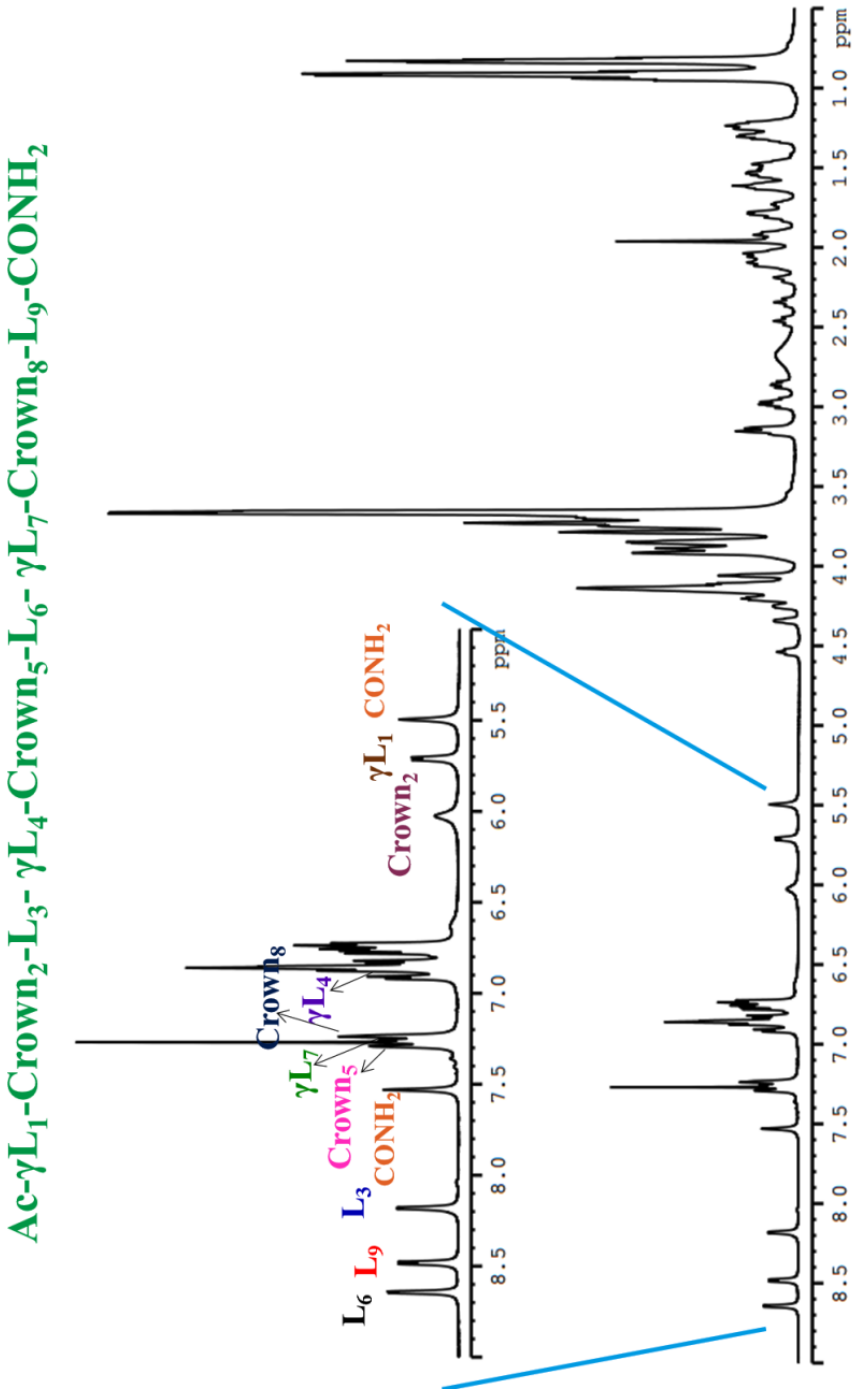

^{1}H-NMR of peptide P2, at varying concentrations of $(CD_3)_2SO$

.

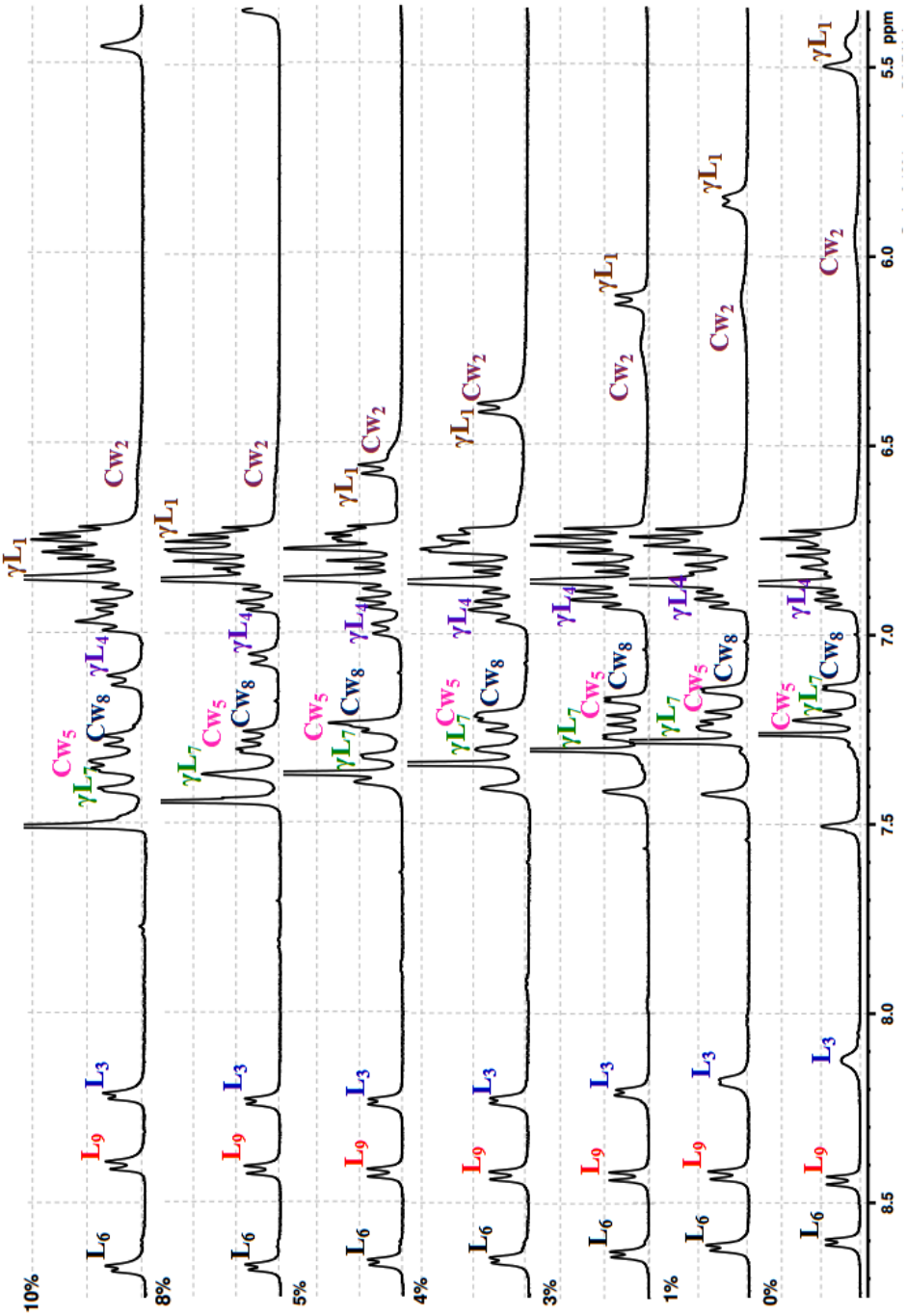

HPLC trace of peptides

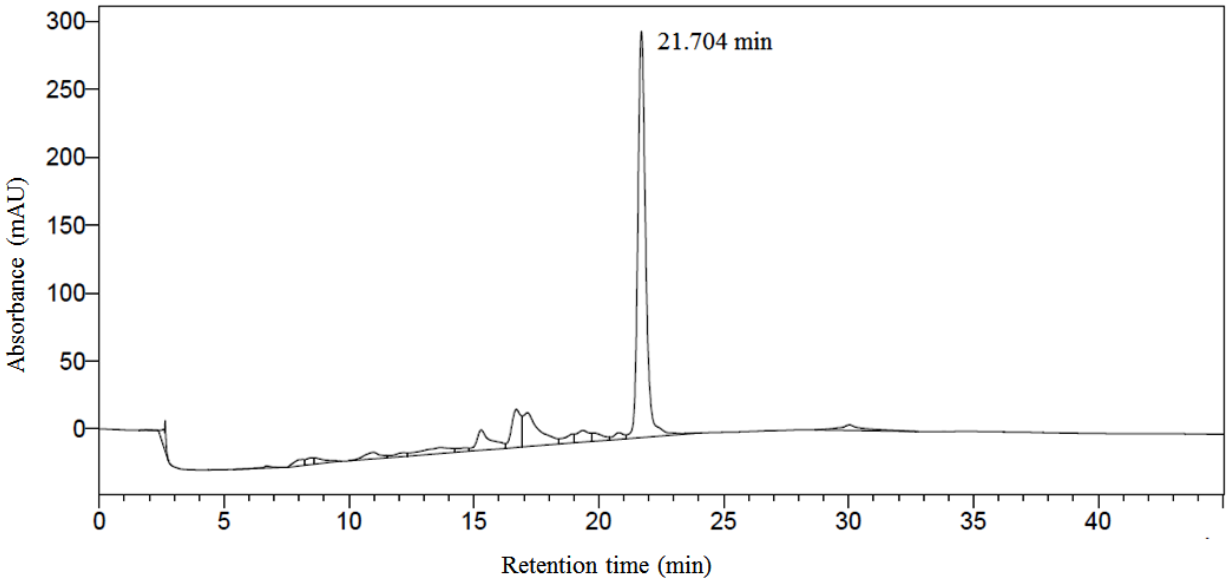

Figure 9: HPLC Trace of Peptide **P2**

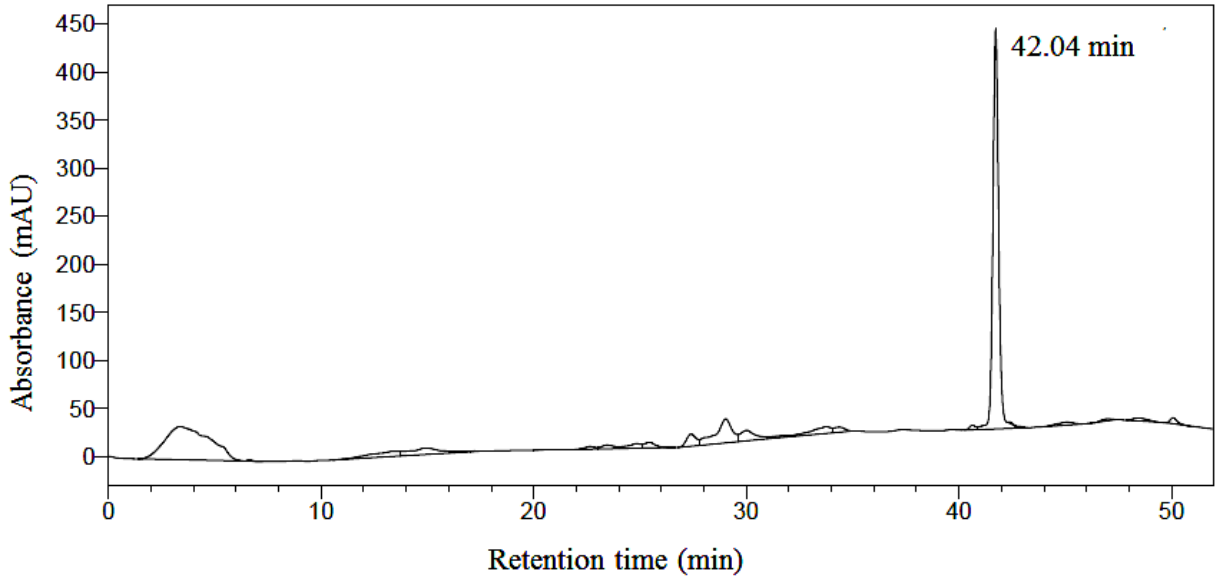

Figure 10: HPLC Trace of Peptide **P3**

1. Mass spectrum of peptides

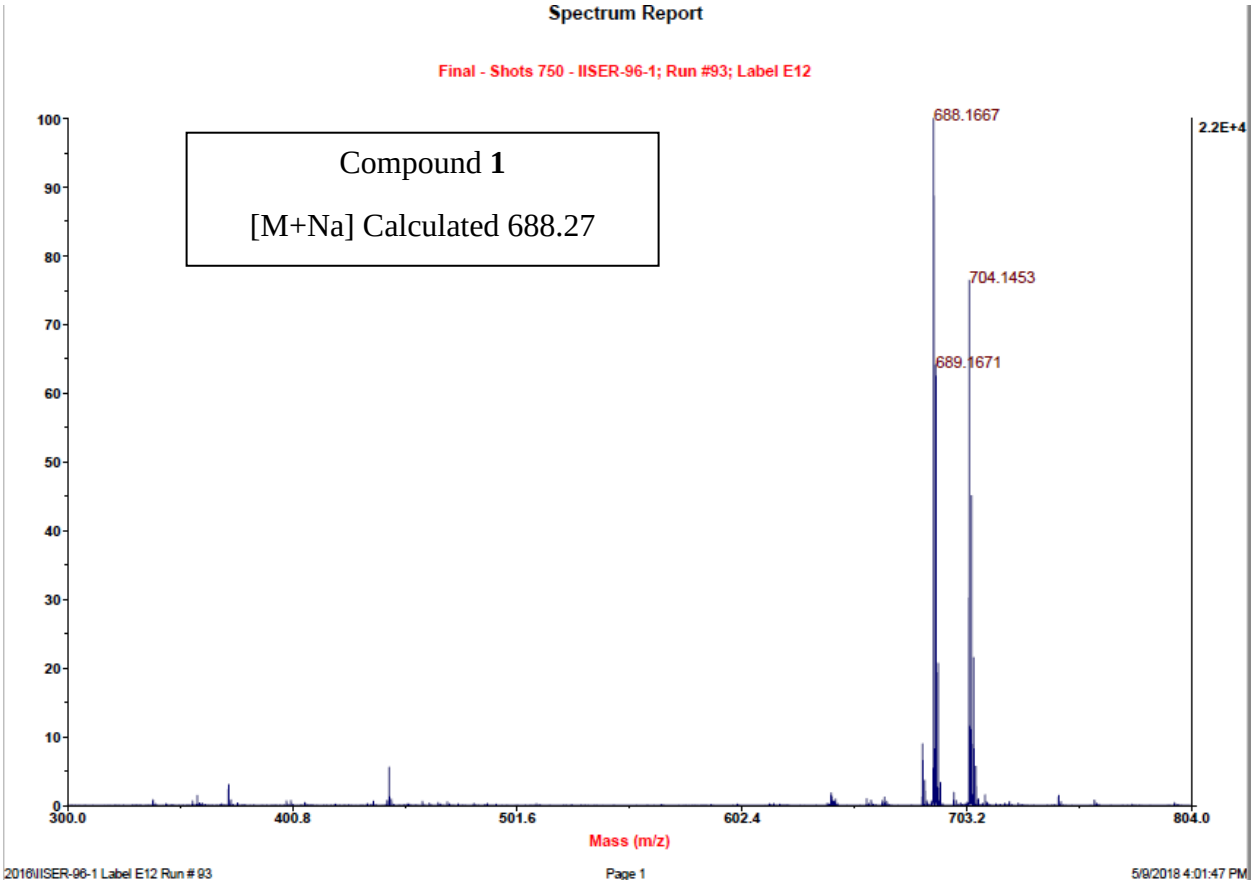

Spectrum Report

Final - Shots 400 - IISER-96-2-2019; Label A4

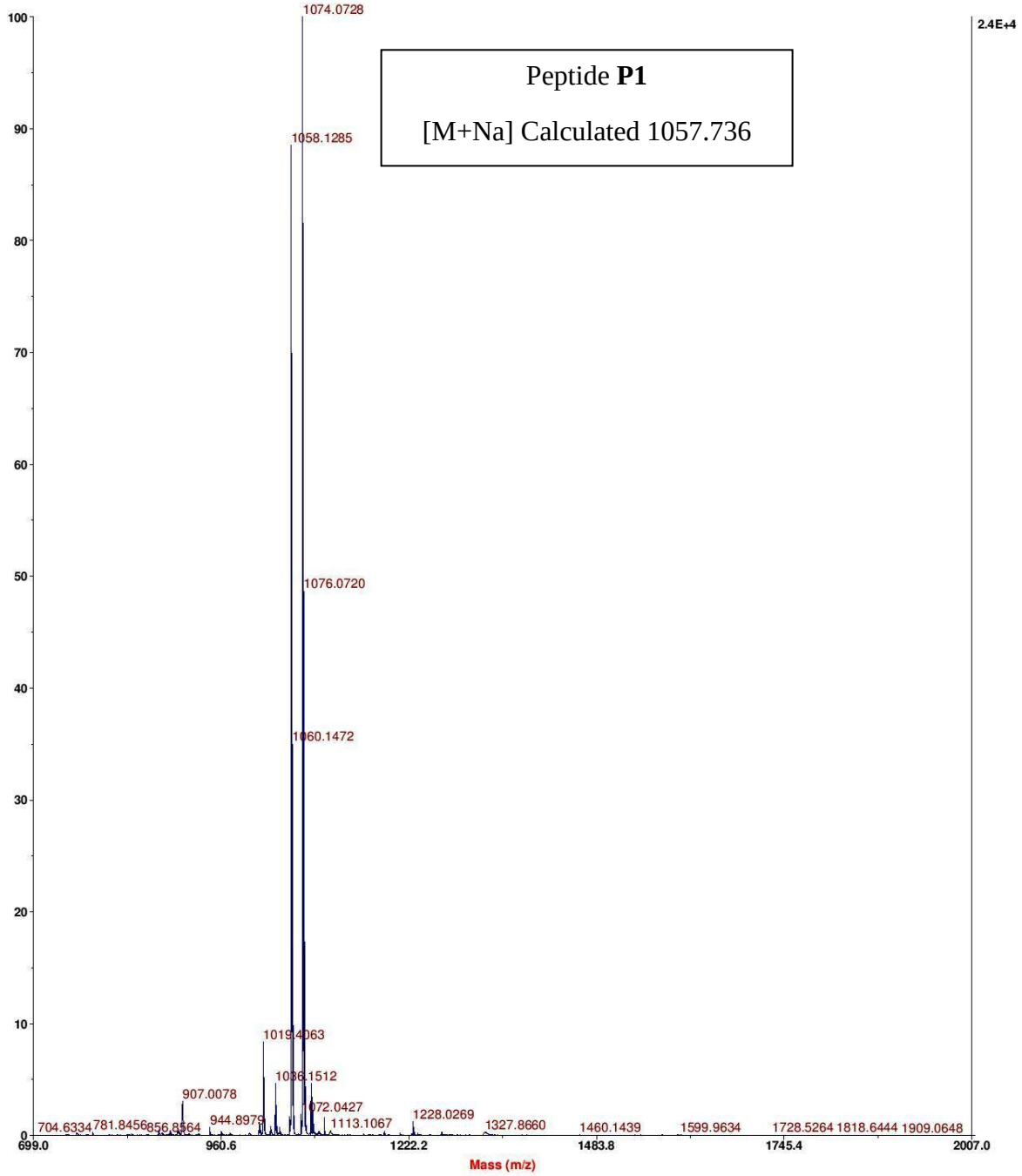

2019\IISER-96-2-2019 Label A4 Run # 227 Page 1 8/19/2019 4:08:46 PM

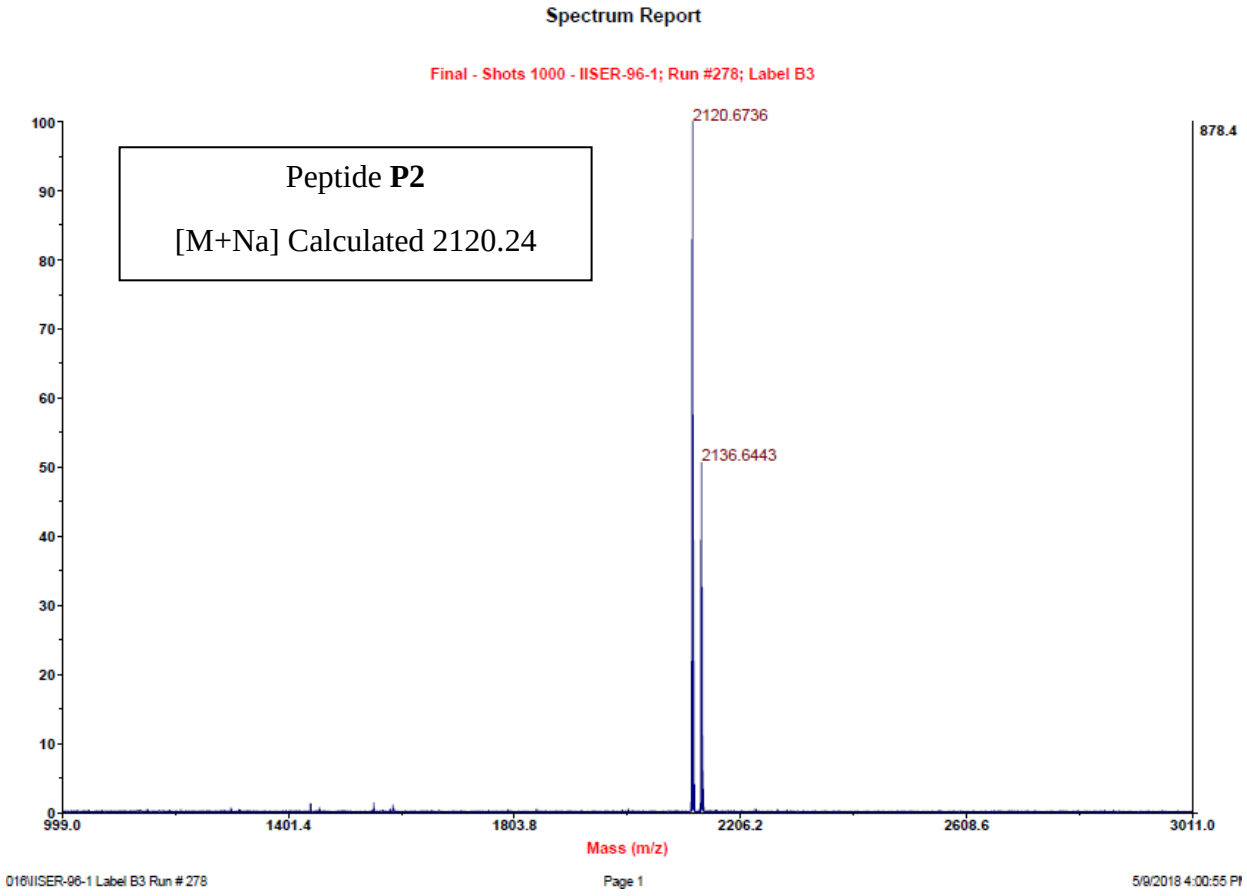
Spectrum Report
Final - Shots 1000 - IISER-96-1; Run #278; Label B3
Peptide P2
[M+Na] Calculated 2120.24
2120.6736
2136.6443
878.4
100
90
80
70
60
50
40
30
20
10
0
999.0
1401.4
1803.8
2206.2
2608.6
3011.0
Mass (m/z)
016IISER-96-1 Label B3 Run # 278
Page 1
5/9/2018 4:00:55 PM

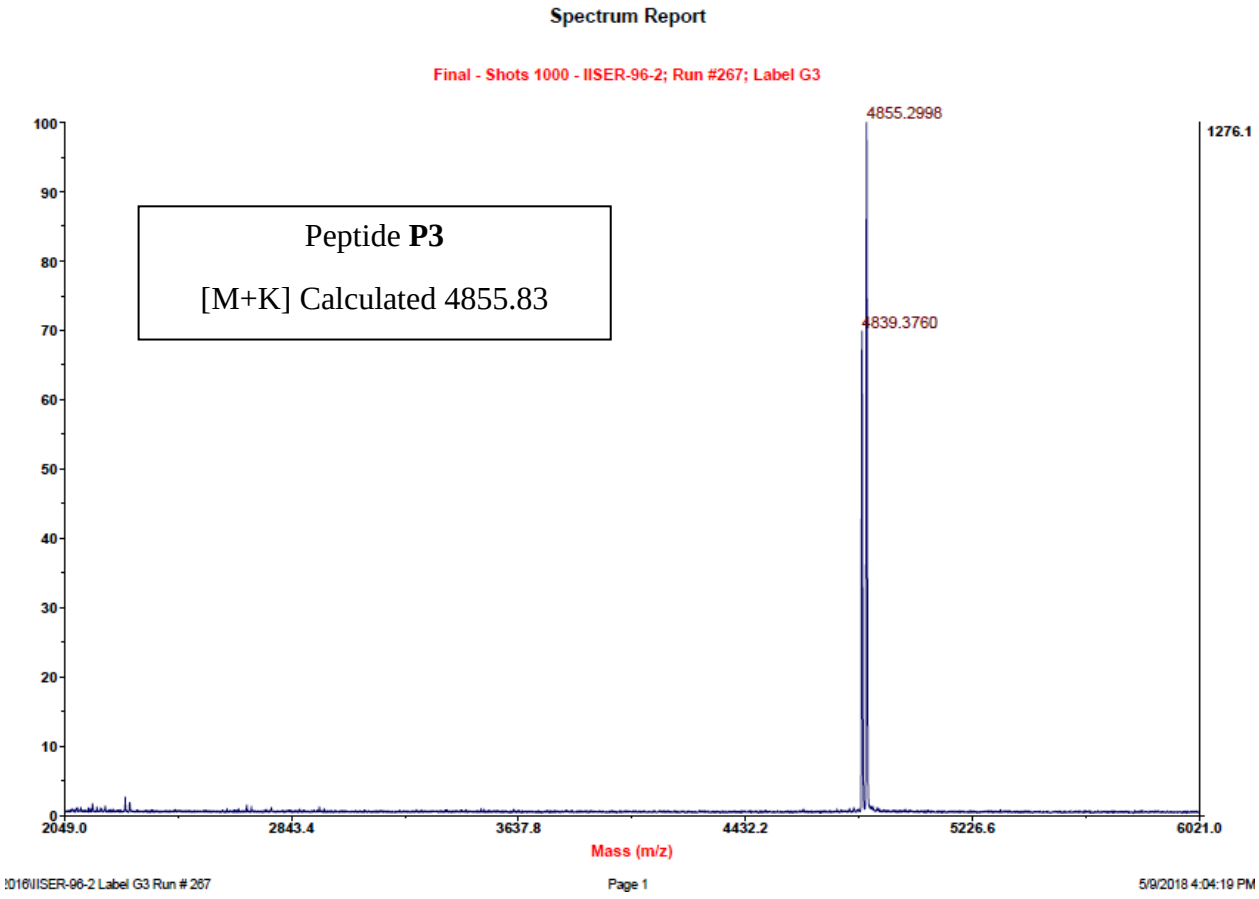
Spectrum Report
Final - Shots 1000 - IISER-96-2; Run #267; Label G3
Peptide P3
[M+K] Calculated 4855.83
4855.2998
4839.3760
1276.1
100
90
80
70
60
50
40
30
20
10
0
2049.0
2843.4
3637.8
4432.2
5226.6
6021.0
Mass (m/z)
!016\IISER-96-2 Label G3 Run # 267
Page 1
5/9/2018 4:04:19 PM